

The copyright of this thesis rests with the University of Cape Town. No quotation from it or information derived from it is to be published without full acknowledgement of the source. The thesis is to be used for private study or non-commercial research purposes only.

**A FORENSIC ANTHROPOLOGICAL
INVESTIGATION OF SKELETAL REMAINS
RECOVERED FROM A 1000 YEAR OLD
ARCHAEOLOGICAL SITE IN NORTH-WESTERN
NAMIBIA**

by

LACHÉ ZOLYN ROSSOUW

RSSLAC001

SUBMITTED TO THE UNIVERSITY OF CAPE TOWN

In fulfilment of the requirements for the degree

M Sc Applied Anatomy

Faculty of Health Science

UNIVERSITY OF CAPE TOWN

January 2010

Supervisor: Prof Alan G. Morris

Department of Human Biology, University of Cape Town

DECLARATION

I, hereby declare that the work on which this dissertation/thesis is based is my original work (except where acknowledgements indicate otherwise) and that neither the whole work nor any part of it has been, is being, or is to be submitted for another degree in this or any other university.

I empower the university to reproduce for the purpose of research either the whole or any portion of the contents in any manner whatsoever.

Signature:

Date:

University Of Cape Town

DEDICATION

Philippians 4:13 “I can do all things, through Him who gives me strength.”

This thesis is dedicated to my parents, Ps. Howard and Lynn Rossouw. Thank you for always believing in me. I Love You Both.

Not forgetting the individuals of Khoraxa-ams without whom this project would never have been possible.

University Of Cape Town

ACKNOWLEDGEMENTS

It takes many hands to build a nation, completing a thesis is no different.

To my supervisor, Professor Alan G. Morris, words fall short in expressing how thankful I am for ALL that you have taught me. You have not only been a source of infinite knowledge during this project, but your patience, guidance, unwavering support, endless encouragement and generosity (the loan of your 'baby' laptop) has led to the completion of this thesis - a major feat - that at times seemed insurmountable. Your light-hearted and humorous disposition helped make the impossible seem 'do-able' at the best of times. Thank you for never giving up on me and for going above and beyond the call of duty. For this, I will forever be truly grateful.

Dr. John Kinahan, without you this project would never have been a reality. Thank you for all your unending support, encouragement and the sacrifice of your time throughout this project. Your hospitality while Prof Morris and I were in Windhoek, and the time I spent with your family will always be remembered fondly. Thank you too for liaising with the museum curator in Windhoek and the National Heritage Council of Namibia for the release of the remains. Though, the biggest Thank You is reserved for not only transporting the remains to Cape Town at the commencement of my project, but for making the trip for the second time to collect the remains and return them to Namibia.

To the curator of the State Museum in Windhoek, Ms Moombolah-Goagoses thank you for allowing me the opportunity to analyse (and loan) the remains from Khoraxa-ams. In addition, I would like to thank the staff at the museum, who not only stored the remains and painstakingly labelled each bone and bone fragment, but prepared the remains for transportation to Cape Town. To the director of the National Heritage Council of Namibia, Mr Aribeb succeeded by Ms Ndalikokule, thank you for granting permission to export the remains to South African for the purpose of analysis.

A special thank you to the NRF as well as the UCT, Postgraduate Funding Office (PGFO) for their financial assistance during my masters degree. From the NRF, courtesy of my supervisor, thank you for awarding the Masters Grant Linked Student Award for two consecutive years. From the PGFO, specifically the trustees of the Marcus Rubin Scholarship and the KW Johnstone Research Scholars thank you for your support. Without funding, research remains just an interesting idea.

I would like to acknowledge the following laboratories and departments for their assistance in generating the necessary data without which this project would not have succeeded: The QUADRU laboratory, CSIR Pretoria for radiocarbon dating and the Groningen Laboratory in

Germany for AMS dating. The Archaeology Department, UCT for stable light isotope analysis and Prof Judy Sealy for her advice and guidance in interpreting the results. The Department of Geological Sciences, UCT for trace elemental analysis and Prof Anton Le Roex for being willing to run my samples despite his lack of confidence in the accuracy of bone material. A special thank you to Anneil Hardy at the Statistical Consultancy Unit, Department of Statistical Science UCT, for assisting with principal component analysis and for all your patience with my lack of statistical knowledge. Also, to the staff at the Health Sciences library, thank you for all your willingness to assist throughout the writing of this thesis.

Caroline Powrie, thank you for the use of the Bone Museum and Anatomy Workshop laboratory as well as the equipment. Your patience during my lengthy stay in the lab is greatly appreciated. To the wonderful staff and fellow postgraduate students at the Department of Human Biology (HUB north), thank you for all your support and kindness during my masters degree, especially the FUN TIMES at conferences. UP's 'Anatomy 30 Seconds,' who can forget?

To my colleagues and 'awesome-oh' friends within the Department of Human Biology, Kundisai Dembetembe, Belinda Roff, Nonhlanhla Dlamini, Rip Da Silva, Dr. Jacqui Friedling, Thabang Maanyapelo, Victoria Van Kets, not forgetting Maya Krein and Emma Makin. I am truly blessed! Thank you all so much for your support and encouragement throughout my masters 'Drama.' And a special THANK YOU for being a pillar of strength when I lost my laptop and most of my masters work of three years. Your belief in me to complete my thesis and come through the most traumatic experience of my life triumphant will be appreciated for years and years to come. I love you all dearly.

To the most amazing family (cousins, aunts, uncles, grandparents) and friends that have become like family over the years, words cannot express the gratitude and love I feel towards you. Your unconditional love, support, guidance, words of encouragement and unwavering belief in me throughout my masters and more especially during my most challenging trial has been an experience that will stay with me forever. I am truly, truly blessed! Ma, Pa and Aunty Gloria, THANK YOU, THANK YOU, THANK YOU...

I trust that this project has in some way honoured the lives of the people of Khoraxa-ams and that despite the time depth, their 'story' has been told. To the men and women, young and old who were deposited on the floor of a sinkhole in Khoraxa-ams, north-western Namibia, Thank you! Thank you! Thank you! My knowledge of investigating unknown, co-mingled human remains would never have been what it is to date, if it were not for you. May your souls forever rest in peace!

TABLE OF CONTENTS

ACKNOWLEDGEMENTS.....	iv
ABBREVIATIONS.....	xii
LIST OF TABLES.....	xiv
LIST OF FIGURES.....	xix
ABSTRACT.....	xxiii

Chapter 1 INTRODUCTION	1
1.1 The site	2
1.1.1 Cave formation geology	3
1.1.2 Physical geography of Namibia	5
1.1.3 Geological survey	7
1.2 The challenges faced in this study	7
1.2.1 Location and topography of site	7
1.2.2 Presence of six-eyed crab spiders	9
1.3 Importance of the study	11
1.3.1 Forensic vs. Anthropological approach	11
1.4 Previous work on Khoraxa-ams remains	13
1.5 The purpose of this study	13
1.5.1 Aim	13
1.5.2 Objectives	13
Chapter 2 BACKGROUND	15
2.1 Historical background to the inhabitants of Namibia	15
2.1.1 The Bantu-speakers	15
2.1.1.1 The Ovambo	16
2.1.1.2 The Herero-Himba	16
2.1.2 The Nama-speaking groups	18
2.1.2.1 The Nama	18
2.1.2.2 The Dama	19
2.1.3 The San	20

2.2	Namibian burial practices	20
2.2.1	The Ovambo	21
2.2.2	The Herero-Himba	21
2.2.3	The Nama	22
2.2.4	The Dama	22
2.2.5	The San	23
2.3	Comparing similar studies of mass deposition	23
2.3.1	Group deposition and mass burials	24
2.3.1.1	Iroquoian ossuaries	24
2.3.1.2	Prehistoric cannibalism at Mancos 5MTUMR-23	25
2.3.2	Victims of violence	26
2.3.2.1	Vilnius and the Grande Armée	26
2.3.2.2	Croatian War	27
Chapter 3	MATERIALS	29
3.1	The Khoraxa-ams remains	29
3.2	Skeletal inventory	30
3.3	In summary	36
Chapter 4	METHODS	37
4.1	Sorting into individuals and MNI	37
4.1.1	Standard sorting techniques	38
4.2	Recording preservation of bone elements	38
4.2.1	The Anatomical Preservation Index	38
4.2.2	The Bone Representation Index	39
4.2.3	The Qualitative Bone Index	39
4.3	Skeletal analysis	40
4.3.1	Sex estimation	40
4.3.1.1	Standard macroscopic analysis	40
4.3.1.2	Distal humerus method	41
4.3.1.3	Femoral neck method	44
4.3.2	Estimation of age at death	46
4.3.2.1	Age categories	46

4.3.2.2 Morphological methods	48
4.3.2.2.1 Sub-adults	48
4.3.2.2.2 Adults	51
4.3.3 Identification of Ancestry	54
4.3.4 Identification of Pathology	57
4.3.4. Skeletal pathologies	57
4.3.5 Trauma	61
4.4 Skeletal measurements	64
4.4.1 Cranial and mandibular measurements	66
4.4.2 Post-cranial measurements	71
4.4.2.1 Stature estimation	78
4.4.3 Standardization of measurements and observations	80
4.5 Activity patterns	81
4.5.1 Squatting facets	81
4.6 Radiography	82
4.6.1 Harris lines	82
4.7 Dental analysis	83
4.7.1 Dental condition and inventory	84
4.7.2 Dental wear	84
4.7.3 Dental disease processes	85
4.7.3.1 Linear enamel hypoplasia	87
4.7.3.2 Dental caries	88
4.7.3.3 Ante-mortem tooth loss	89
4.7.3.4 Dental abscesses	89
4.7.3.5 Periodontal disease	90
4.7.4 Dental modification	91
4.8 Physio-chemical analysis	91
4.8.1 Radiocarbon dating	92
4.8.2 Stable light isotopic analysis	93
4.8.2.1 Sampling	94
4.8.3 Trace elemental analysis	95
4.8.3.1 Sampling	95
4.9 Statistical methods	96

Chapter 5 RESULTS	99
5.1 Total number of individuals	99
5.1.1 Sorting into individuals	99
5.1.2 Minimum number of individuals	103
5.2 Sex distribution	107
5.2.1 Sex distribution – Distal humerus method	107
5.2.2 Sex distribution – Femoral neck method	107
5.2.3 Sex distribution – Summary of various methods	111
5.3 Distribution of age at death	111
5.3.1 Age distribution – Radiographic method	116
5.3.2 Age distribution – Epiphyseal closure	116
5.3.3 Age distribution – Summary of various methods	119
5.4 Morphological features	124
5.4.1 Body size and stature	124
5.4.2 Squatting facets	125
5.5 Ante-mortem features	129
5.5.1 Dental features	129
5.5.1.1 Dental health	129
5.5.1.2 Ante-mortem tooth loss	134
5.5.1.3 Dental anomalies and modification	138
5.5.2 Physio-chemical analysis	144
5.5.2.1 Stable light isotope analysis	144
5.5.2.2 Trace elemental analysis	144
5.5.3 Stress indicators	149
5.5.3.1 Harris lines	149
5.5.4 Skeletal pathology	149
5.5.4.1 Non-specific pathologies	149
5.5.4.2 Joint disease	151
5.5.4.3 Other skeletal pathological processes	155
5.5.4.4 Skeletal anomalies	157
5.5.4.5 Summary of skeletal pathologies	160
5.5.5 Cranial morphology	163

5.6 Peri- and Post-mortem features	177
5.6.1 Breakage patterns	177
5.6.2 Preservation states	186
5.6.2.1 Completeness	186
5.6.2.2 Fragmentation	187
5.6.2.3 Bone quality	191
5.7 ¹⁴ C radiocarbon dating	193
Chapter 6 DISCUSSION	195
6.1 How many people are present in the Khoraxa-ams sample?	195
6.1.1 Mortality profile	196
6.1.2 Does the MNI reflect the real number of people at the site?	198
6.1.3 Challenges with excavation	200
6.1.3.1 Problems with recovery of remains	200
6.1.3.2 Impact of storage on the remains	201
6.1.4 Problems confronted in sorting individuals	201
6.1.4.1 Incomplete recovery of the remains	201
6.1.4.2 Trace elemental analysis	202
6.1.5 Summary	203
6.2 Identifying ethnicity	203
6.2.1 Who could the people of Khoraxa-ams be historically?	204
6.2.1.1 Differences based on biological markers	206
6.2.1.2 Differences based on lifestyle habits	208
6.2.2 Summary of lifestyle observations and possible ethnic identity	221
6.3 How did they die and how did they get into the cave?	223
6.3.1 How did they end up in the cave?	224
6.3.1.1 Were they alive when they entered the cave?	224
6.3.1.2 Burial style	225
6.3.2 How were they killed?	226
6.3.2.1 Absence of ante-mortem fractures	226
6.3.2.2 Peri-mortem fractures caused by blunt force trauma	226
6.3.2.3 Peri-mortem fractures caused by 30 metre drop	228

6.3.2.4 Summary	231
6.3.3 What could the events at death have been?	232
Chapter 7 CONCLUSION	236
REFERENCES	239
APPENDICES	

University Of Cape Town

ABBREVIATIONS

AD	Anno Domini
AMS	Accelerator Mass Spectrometry
AMTL	Ante-mortem Tooth Loss
API*	Anatomical Preservation Index
BP	Before Present
BRI*	Bone Representative Index
CAM	Crassulacean Acid Metabolism
CO	Cribra Orbitalia
CSIR	Council for Scientific and Industrial Research
DIC	Disseminated Intravascular Coagulation
DJD	Degenerative Joint Disease
DMI	Disease Missing Index
DNA	Deoxyribonucleic acid
GSH	Groote Schuur Hospital
HL	Harris Lines
ICP-ES	Inductively Coupled Plasma Emission Spectroscopy
ICP-MS	Inductively Coupled Plasma Mass Spectroscopy
LEH	Linear Enamel Hypoplasia
LIMS	Light Isotope Mass Spectrometry Laboratory, UCT
LODOX	Low Dose X-ray
LSA	Later Stone Age
MNI	Minimum Number of Individuals
n	Number
NHCN	National Heritage Council of Namibia
PC	Principle Components
PCA	Principle Component Analysis
PDB	Peedee Belemnite
PH	Porotic Hyperostosis

PMC	Percent Modern Carbon
ppm	parts per million
QBI/QBI*	Qualitative Bone Index
QUADRU	Quaternary Dating Research Unit
RSD	Relative Standard Deviation
SA	South African
SI	Sacro-iliac joint
SID	Supero-inferior diameter of the femoral neck
SWA	South West Africa
TEA	Trace Element Analysis
TMJ	Temporomandibular Joint Disease
UCT	University of Cape Town

University Of Cape Town

LIST OF TABLES

		Page number
Table 3.01	Inventory of the complete sample set B4108 with accession numbers, initial sorting and identification of each bone element	31
Table 3.02	Summary of skeletal elements recovered from the cave site in Khoraxa-ams (B4108), north-western Namibia	36
Table 4.01	Radiographic standards for age determination: Proximal femur	56
Table 4.02	Numerical classification and description of tooth wear categories	86
Table 5.01	Summary of the total number of skeletal elements recovered from a cave site in Khoraxa-ams (B4108), north-western Namibia	100
Table 5.02	Fitting individuals based on cranial and mandibular skeletal elements	101
Table 5.03	Fitting individuals based on post-cranial skeletal elements	104
Table 5.04	The minimum number of individuals represented by crania	105
Table 5.05	The minimum number of individuals represented by post-cranial bones	106
Table 5.06	Sex distribution for Khoraxa-ams site based on cranial regions	108
Table 5.07	Sex estimation using the distal humeri method	109
Table 5.08	Sex distribution using the distal humeri method in comparison with standard visual methods	109
Table 5.09	Estimation of sex based on femora present in study sample, comparing standard morphological traits to the femoral neck method	110
Table 5.10	Summary of sex distribution using femoral neck method (SID)	110
Table 5.11	Summary of sex identification of skeletal remains based on various methods	110
Table 5.12	Age at death estimation from crania recovered from Khoraxa-ams using cranial suture fusion	113
Table 5.13	Age at death estimation for crania recovered from Khoraxa-ams using dental eruption	114

Table 5.14	Estimation of age at death using relative tooth wear (attrition) as a means to separate adult individuals within the sample	114
Table 5.15	Summary of estimating age at death based on cranial suture closure, dental eruption of M3 and occlusal tooth wear	115
Table 5.16	Estimation of age at death using the femoral radiographic method compared to epiphyseal union	117
Table 5.17	Estimation of age based on the fusion of epiphyses of the post-cranial skeleton in sub-adult individuals	117
Table 5.18	Summary of estimated age at death of sub-adult and young adult cranial and post-cranial bones using the union of epiphyseal ends method	118
Table 5.19	Age at death estimation of adult skeletal remains based on various methods	121
Table 5.20	Age at death estimation of juvenile/sub-adult skeletal remains based on various methods	121
Table 5.21	Summary of age at death estimation and distribution of sex among skeletal remains from the sample based on five age categories	121
Table 5.22	Possible linkages of cranial and post-cranial elements	123
Table 5.23	Estimated skeletal height calculated from the long bones of the upper limbs	126
Table 5.24	Estimated skeletal height calculated from the long bones of the lower limbs	127
Table 5.25	Estimated stature using maximum femur length and the sum of the lower limb bones, comparing three methods developed for the estimation of stature	127
Table 5.26	Squatting facets observed on the tibia of samples from Khoraxa-ams	128
Table 5.27	Occurrence of squatting facets in the study sample	128
Table 5.28	Average stage of occlusal attrition on adult dentition	130
Table 5.29	Tooth types affected by carious lesions in adult individuals	132
Table 5.30	Incidence of Linear Enamel Hypoplasia in the sample per tooth type	132

Table 5.31	Dental abscesses observed in individuals from Khoraxa-ams sample	135
Table 5.32	Occurrence of dental abscesses in adult individuals	135
Table 5.33	Location of periodontal disease observed in the sample	135
Table 5.34	Periodontal disease observed per socket in adult individuals	136
Table 5.35	Occurrence of periodontitis in adult individuals	136
Table 5.36	Occurrence of ante-mortem tooth loss in adult individuals	139
Table 5.37	Summary of ante-mortem tooth loss percentage per tooth type in the sample	139
Table 5.38	Individuals presenting with dental anomalies in the sample	142
Table 5.39	Individuals presenting with dental modification in the sample	142
Table 5.40	$\delta^{13}\text{C}/^{14}\text{C}$ results from bone collagen of cranial samples sent for stable light isotope analysis	146
Table 5.41	Mean trace elemental concentrations (in ppm) of cranial samples from the Khoraxa-ams site	147
Table 5.42	Interpreting relative standard deviation (% RSD) to determine reliable trace elemental concentrations in biological material	148
Table 5.43	Elements with reliable mean % RSD	148
Table 5.44	Individual long bones specifically the tibia, exhibiting Harris lines in the sample	150
Table 5.45	Summary of Harris line formation in the study sample	150
Table 5.46	Occurrence and state of Cribra Orbitalia and Porotic Hyperostosis	152
Table 5.47	Anatomical location of synovial joint arthritis in the Khoraxa-ams sample per individual	154
Table 5.48	Incidence of observed osteoarthritis of the intervertebral disc and articular (synovial and non-synovial) joints	156
Table 5.49	Incidence of other non-synovial degenerative joint disease observed on the post-crania	159

Table 5.50	Incidence of other skeletal pathologies observed on the crania and post-crania	159
Table 5.51	Observed skeletal anomalies in the post-crania of the Khoraxa-ams sample	162
Table 5.52	Occurrence of flared metaphysis and septal apertures in study sample	162
Table 5.53	Total variance explained for vault measurements for males and females	167
Table 5.54	Selected vault measurements in rank order of computed components for males and females using Principle Component Analysis (PCA)	167
Table 5.55	Total variance explained for face measurements for males and females	171
Table 5.56	Selected face measurements in rank order of computed components for males and females using Principle Component Analysis (PCA)	171
Table 5.57	Total variance explained for mandible measurements for males and females	175
Table 5.58	Selected mandible measurements in rank order of computed components for male and females using Principle Component Analysis (PCA)	175
Table 5.59	Incidence of skeletal trauma and fracture patterns as visible on the crania	178
Table 5.60	Incidence of skeletal trauma and fracture patterns on the post-cranial remains	181
Table 5.61	Individuals from Khoraxa-ams with observed peri-mortem injuries	182
Table 5.62	The Bone Representative Index (BRI*) scored for all elements represented in the study sample	188
Table 5.63	The relative frequency of individual skeletal elements recovered from the sinkhole in Khoraxa-ams within the total sample	189
Table 5.64	Summary of cranial bone frequency ranked from the most frequent to the least frequent cranial bone elements recovered	190
Table 5.65	Summary of post-cranial bone frequency ranked from the most frequent to the least frequent post-cranial bone elements recovered	190
Table 5.66	The Anatomical Preservation Index (API*) ranked per bone element for the Khoraxa-ams remains	192

Table 5.67	The Qualitative Bone Index (QBI*) ranked per bone element for the Khoraxa-ams remains	192
Table 5.68	Initial ¹⁴ C radiocarbon date for sample B4108 H4:1 as prepared by the QUADRU laboratory, South Africa	194
Table 5.69	Amended AMS date for sample B4108 H4:6 as prepared by the Groningen laboratory, Germany	194
Table 6.01	Summary of sex and age at death estimates for individuals from Khoraxa-ams	196
Table 6.02	Comparison of sex and age at death ratios for ‘normal’ cemetery burials	197
Table 6.03	Comparison of relative frequency of MNI per bone element	198
Table 6.04	A comparison of adult stature with other samples for males	209
Table 6.05	A comparison of adult stature with other samples for females	209
Table 6.06	Comparison of occlusal attrition scores in adult dentition	212
Table 6.07	Frequency of squatting in Khoraxa-ams compared to Later Stone Age foragers from South Africa	220
Table 6.08	Summary showing the features used to differentiate between historic ethnic groups of Namibia	222

LIST OF FIGURES

	Page number
Figure 1.01 Khoraxa-ams and its location in Namibia; Latitude: 19° 31' 0S and Longitude: 13° 58' 0E	3
Figure 1.02 Stages of karstic cave formation	4
Figure 1.03 Map of Namibia showing the four main types of geography of the country	6
Figure 1.04 A geological map of northern Namibia which encompasses rocks of Palaeo-, Meso- and Neoproterozoic and Palaeozoic to Cenozoic age	8
Figure 1.05 <i>Sicarius hahnii</i> , from the Northern Cape and Namibia is extremely toxic and regarded as possibly the most lethal spider in the world	10
Figure 2.01 Historic map of Namibia (South West Africa) during 1820-1880 illustrating the regions of Central and Northern Namibia and the distribution of various ethnic groups as well as Khoraxa-ams in the northwest	17
Figure 3.01 Collection (B4108) of disarticulated bone elements analysed in this study from Khoraxa-ams, north-western Namibia	29
Figure 4.01 Sex estimation from the pubic symphysis	42
Figure 4.02 Sex estimation from the sciatic notch	42
Figure 4.03 Cranial regions used for estimating sex	43
Figure 4.04 Estimating sex using the trochlear outline	45
Figure 4.05 Estimating sex using trochlear symmetry and olecranon fossa shape	45
Figure 4.06 Estimating sex using the medial epicondyle	45
Figure 4.07 The supero-inferior femoral neck diameter measurement (SID), used for the estimation of sex	47
Figure 4.08 Estimation of age – times of epiphyseal union of various parts of the skeleton in sub-adults	49
Figure 4.09 Estimation of age from epiphyseal union	50

Figure 4.10	Sequence of tooth formation and eruption among Native Americans, useful in the estimation of age at death	52
Figure 4.11	Estimation of age from ectocranial suture closure	53
Figure 4.12	Radiographic standards for seriation of the proximal femur	55
Figure 4.13	Fractures caused by direct trauma	65
Figure 4.14	Fractures caused by indirect trauma	65
Figure 4.15	Anatomical landmarks of the skull, anterior view	68
Figure 4.16	Anatomical landmarks on the lateral view of the skull	68
Figure 4.17	Anatomical landmarks on the base of the skull	70
Figure 4.18	Anatomical landmarks on the anterior view of the mandible	72
Figure 4.19	Anatomical landmarks on the lateral aspect of the mandible	72
Figure 4.20	Clavicle measurements, superior view of left clavicle	74
Figure 4.21	Scapular measurements, dorsal view of left scapular	74
Figure 4.22	Measurements of the left humerus, anterior view	74
Figure 4.23	Measurements of the left radius, anterior view	76
Figure 4.24	Measurements of the left ulna, anterior view	76
Figure 4.25	Measurements of the sacrum	76
Figure 4.26	Measurements of the left femur, posterior view	79
Figure 4.27	Measurements of the left tibia, anterior view	79
Figure 4.28	Measurements of the left fibula, lateral view	79
Figure 4.29	Measurements of both the left and right calcaneus	79
Figure 5.01	UCT1C – Mandible showing heavy occlusal wear	130
Figure 5.02	UCT1D – Abscess at maxillary incisor and premolar positions showing infection surrounding the abscess	133

Figure 5.03	UCT1K – Abscess on maxillary palate at position of right central Incisors	133
Figure 5.04	UCT1D – Severe maxillary periodontal disease affecting all the sockets and resulting in a partially edentulous maxilla	137
Figure 5.05	UCT1C – Periodontal disease affecting the maxillary dentition, shows resorbtion of the sockets	137
Figure 5.06	UCT1A – Unilateral torus maxillaries on the lingual surface below the left molars	141
Figure 5.07	UCT1F – Malformation of maxillary anterior tooth	141
Figure 5.08	UCT1I – Extra cusp on buccal side of right maxillary M2	143
Figure 5.09	UCT1E – Mandibular ablation of both central incisors	143
Figure 5.10	UCT1F – Porotic Hyperostosis – inactive	152
Figure 5.11	UCT2C – Schmorl’s nodes	158
Figure 5.12	UCT1C – Periostitis observed on the base of the occipital bone - unhealed	158
Figure 5.13	UCT2A – Atlas and axis vertebrae showing cleft vertebrae (Spina bifida) and malformed bificated spinous process	161
Figure 5.14	UCT4D – Flared distal metaphysis with septal aperture	161
Figure 5.15	Scatter plots based on factor scores for vault measurements for males and females	168
Figure 5.16	Scatter plots based on factor score for facial measurements for males and females	172
Figure 5.17	Scatter plots based on factor scores for mandibular measurements for males and females	176
Figure 5.18	UCT1K – Le Forts’ fracture with resultant radial fractures due to blunt force trauma to the face	183
Figure 5.19	UCT1B – Depression fracture at Bregma with concentric and radial fractures	183
Figure 5.20	UCT1E – Trauma on right parietal bone resulting in delamination	184

and bone loss

Figure 5.21	UCT1E – Complete separation of the frontal bone to the parietals along the coronal suture, resulting in plastic deformation of the cranial vault	184
Figure 5.22	UCT1J – Fractures to skull causing extensive bone loss	185
Figure 5.23	UCT1I – Trauma to the left facial region resulting in bone loss to most of the left facial bones	185
Figure 6.01	LeFort I, II, III fractures are directed by areas of buttressing	229

University Of Cape Town

ABSTRACT

Human and faunal skeletal remains were found scattered around the base of a talus cone at the bottom of a 30 metre sinkhole at Khoraxa-ams northwest of the Central Namib Desert. Subsequent dating of the site indicated that the remains had been deposited in the cavern in the order of a thousand years ago. The aim of this study was to examine skeletal remains recovered from the site and draw possible conclusions as to who they were and the circumstances surrounding their deposition in the cave.

A forensic analytical approach was utilized to uncover the evidence, allowing us to manage the site as a 'crime scene.' This approach included determining the MNI, constructing a demographic profile and analysing post-mortem preservation as well as posing questions vital to forensic investigations including ante-mortem features that could lead to the ethnic identification of unknown individuals and the peri-mortem circumstances surrounding the deposition of the remains.

Sixteen individuals, based on cranial bone representation were identified in the sample, consisting of only adult individuals with the exception of one sub-adult, and a male to female ratio of roughly 1:1. The people of Khoraxa-ams were of Negroid ancestry, consumed a mixed diet of gathered and agricultural foods, were in fairly good health at the time of their death, showed signs of involvement in low-impact labour and practiced dental modification. Their most likely identity, based on these biological markers, lifestyle observations and cultural practices, is a group similar or ancestral to the modern Herero of Namibia.

The exact nature and circumstance surrounding the cause of death is unknown. Based on the extent of skeletal injuries, it is likely that they received peri-mortem blunt force trauma and post-mortem trauma after death by being dropped into the 30 metre cave. It is speculated, given the demographic profile of women and children presenting with more severe blunt force trauma, the lack of defence wounds and the fact the individuals were dead before being dropped in the cave, that the site at Khoraxa-ams represents an execution location, though no secure evidence exists to support this theory.

The forensic approach to this study has enabled the identification of otherwise unknown archaeological remains, and has also provided insight into a period of Namibian history where relatively little is known.

INTRODUCTION

Human skeletons form the most direct evidence of the life history of past humans because features such as growth, disease and activity patterns are stored in bones. According to Weiss (1976), the study of birth, death and growth rates, of population size and dispersion, and of mating and migration, have all been advanced through the science of anthropology. The information gained by researching the physical record of bones, provides anthropologists with the solid theoretical foundation they require. A foundation expressed in terms of variables which can be observed and from which significant indirect inferences can be made (Weiss, 1976). Thus, the information we learn from the past is important for interpreting the present human condition (Larsen, 2000).

In addition, bones provide evidence of events that took place at death, a factor essential in the identification of skeletal remains in forensic medicine, forensic science and forensic anthropology. The field of forensic medicine covers the investigation of pathological changes caused by acts of violence or medical negligence. Forensic science is the application of scientific methods used in a legal context, and forensic anthropology, as defined by Cattaneo (2007:185), is the “application of physical anthropology to a forensic context”.

The past two decades have seen a rapid rise in the field of forensic anthropology. İşcan (1988) and Dirkmaat *et al.*, (2008) have discussed the current and future state of forensic anthropology, the development of DNA analysis techniques and its enhancement of victim identification as well as the establishment of the *Daubert*¹ criteria with regards to admissibility of scientific evidence in the courtroom (Dirkmaat *et al.*, 2008). These advances in forensic anthropological and scientific knowledge and techniques, and their increasing application in forensic contexts have influenced the

¹ The Supreme Court decision in *Daubert vs Merrell Dow Pharmaceuticals* drastically changed approaches to research, evidence, analysis and expert witness testimony in forensic anthropology (Dirkmaat *et al.*, 2008).

approach of this study significantly. The current study focused on the investigation of a potential historic „crime scene’, in which the identification and circumstances surrounding the deposition of skeletal remains within a cave were examined.

1.1 The Site

In September 1995 a sinkhole cavern at a depth of 30 metres was discovered at a site northwest of the Central Namib Desert. The remains of both human and faunal skeletons were found co-mingled within the cave. The site is situated approximately 700 km north of Windhoek in the Kaokoland/Damaraland region of north-western Namibia (Malan, 1980; Jacobsohn, 1990; Miescher and Henrichsen, 2000), and positioned at the following co-ordinates: Latitude: 19° 31` 0 S and Longitude: 13° 58` 0 E (GoogleEarth) (Figure 1.01). The site is known as Khoraxa-ams (Figure 1.01), and roughly translated from Khoekhoegowab (a Khoekhoe language), means a natural hole, hollow or small depression that contains water, used by man and animals alike, especially in arid regions (Nienaber and Raper, 1983; Miescher and Henrichsen, 2000; Raper, 2004).

The skeletal remains within the cave were found scattered along the base of a talus cone directly under the cave opening. The skeletons that were recovered from the cave were all disarticulated and displaced along the length of the talus cone. From the condition of the remains, it was evident that the bone elements had not been buried but rather deposited on the cave floor. According to Simmons (2002), remains deposited within vertical caves are generally isolated from surface taphonomic processes such as weathering and scavengers, but subject to subsurface, geological taphonomy. These variables provide limits and challenges to the interpretation of post-mortem intervals, co-mingling and evidence of the cause of death, as well as the technical issues of scene processing and recovery of remains.

With regards to the preservation and taphonomic process of the remains due to subsurface influences within the cave at Khoraxa-ams, the evidence of bat guano

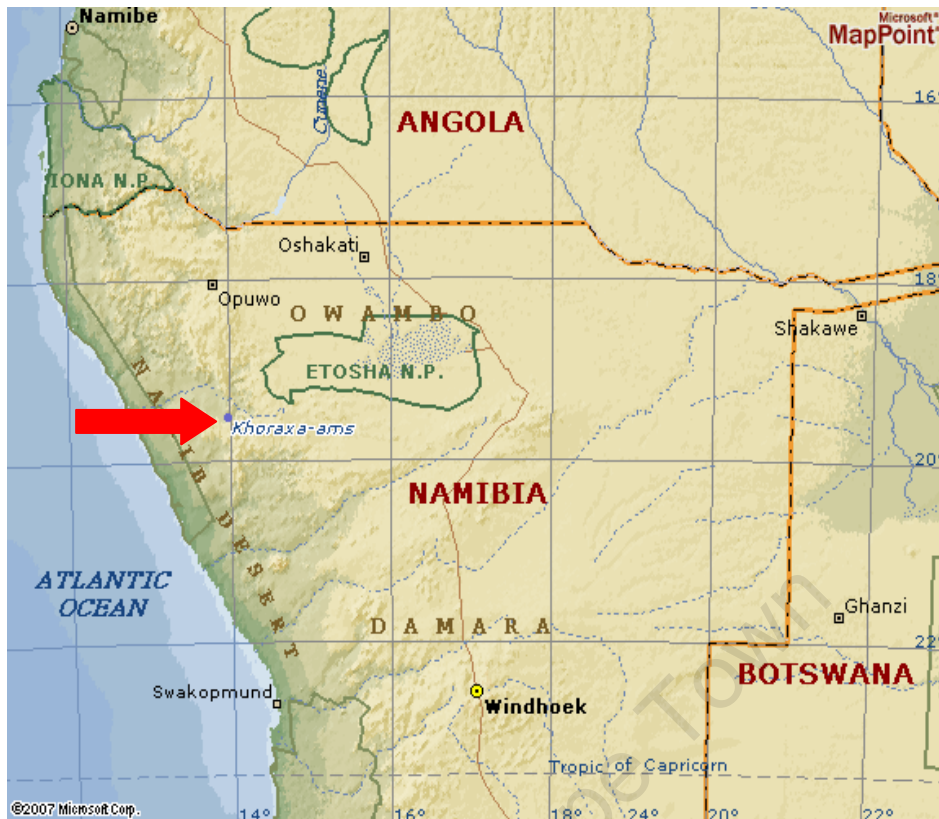


Figure 1.01 Khoraxa-ams and its location in Namibia (red arrow); Latitude: 19° 31' 0S and Longitude: 13° 58' 0E. (Microsoft MapPoint, 2007 Microsoft Corp.).

adhering to the cortical surface of the skeletal remains was of some interest. Shahack-Gross and colleagues (2004) have shown that bat guano affects the preservation of archaeological remains in cave sites because it contains large amounts of mineral phosphate which is highly acidic. Since minerals are the major component of bone, substantial loss of minerals results in the reduction of bone preservation. Another factor that influences bone dissolution is pH. The reduction in pH occurs when organic matter is oxidised and leads to bone dissolution or reduced preservation. Differential bone preservation can take the form of uneven distribution in caves, or biases in skeletal element representation relative to the complete skeleton (Stiner *et al.*, 2001).

1.1.1 Cave formation geology

The cave geology, including the cave type, the depth and width of the shaft and the existence of the talus cone beneath the aven (cave opening) is key to understanding the taphonomy of the human remains deposited within it (Simmons, 2002). The northwest region of Namibia has large areas of karst topography, with an abundance of both caves

and actively forming sinkholes (Vedder, 1938; Malan, 1980). The cave at Khoraxa-ams is typical of karst topography in that the rock is dolomitic and erodes slowly but easily in water. Such a region has many underground caves which are frequently linked to the surface by sinkhole developments.

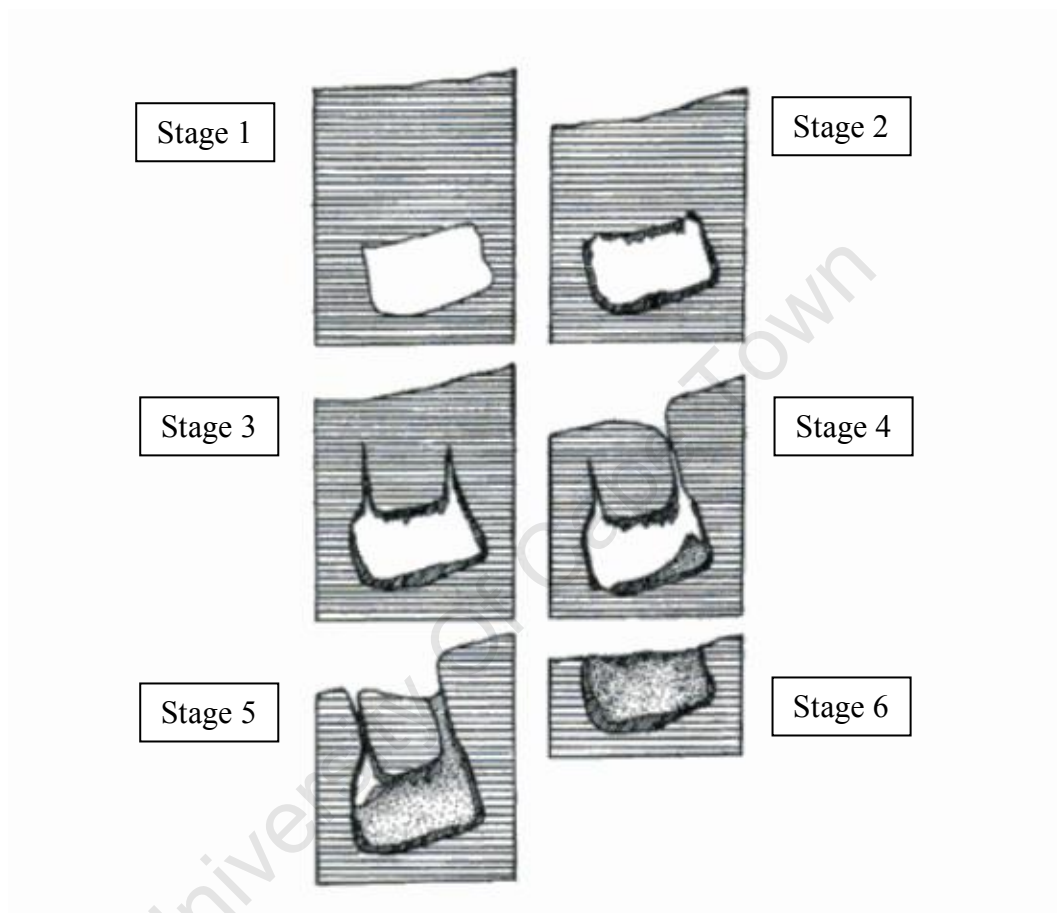


Figure 1.02 Stages of karstic cave formation, beginning from upper left: horizontal lines = dolomite; vertical lines = travertine; stippling = breccias (adapted from Brain, 1981).

Karstic cave systems are part of limestone or dolomite rock formations (Simmons, 2002). As Brain (1981) describes, their formations proceed in an ordered sequence with six separate stages of formation (Figure 1.02). In Stage 1, a solution cavity is formed inside the rock strata. During Stage 2, the water level drops and the cavern becomes filled with air, which may be ventilated to the surface by distant and indirect means. Stalactites and stalagmites may begin to form during this period. The development of the aven (or vertical shaft to the surface) is the hallmark of Stage 3 and is caused by

rainwater enlarging fissures in the rock. Stage 4 witnesses the break-through of the aven to the surface, thus opening the cavern to the external environment. It is during Stages 3 and 4 that a depression may develop in the ground above the forming aven. Trees are often plentiful in and around these depressions due to the abundance of water. The Stage 4 cavern begins to fill with debris from the surface and accumulating deposits form a talus cone on the floor beneath the aven (Brain, 1981; Simmons, 2002).

1.1.2 Physical geography of Namibia

The name Namibia means “place of great arid plains,” it is a Khoekhoe name derived from Nama-speaking people, as half of the land is either desert or semi-desert (IDAF, 1989; Room, 2006). Thus, Namibia has the direst climate in sub-Saharan African and as a result is sparsely populated. The geography of Namibia can roughly be divided into four areas (Figure 1.03) (IDAF, 1989). In the east lies the western edge of the Kalahari Desert, a vast area of semi-desert that supports some plant and animal life, but few people. The Kalahari is characterised by thick layers of terrestrial sand and limestone and a near absence of surface water. More centrally, there are high plateaus ranging from around 1000 m high up to 1700 m in height, as well as a mountainous escarpment that runs virtually the length of the country. The Central Plateau constitutes more than half of Namibia and the diverse landscape includes rugged mountains, rocky outcrops, sand-filled valleys and plains. In the coastal region lies the harsh Namib Desert comprising about a fifth of the total area of Namibia. This desolate strip of sand desert stretches along the entire Namibian coastline as is characterised by huge sand dunes in the central areas, with massive gravel fields to the north and south (Serfontein, 1976; IDAF, 1989).

The Khoraxa-ams site falls within the semi-desert region of the country. According to Figure 1.03, the semi-desert region of Namibia is characterised by scarce vegetation with goat and sheep breeding (IDAF, 1989). Dr. Kinahan (*pers. comm.*, 01 March 2007) suggested that the cave at Khoraxa-ams is a sinkhole. According to the IDAF 1989, the north of the country, apart from isolated pockets, is the only region where there is sufficient water for growing crops. Namibia has a sub-tropical desert climate, where there is little rainfall and large fluctuations between day and night temperatures.

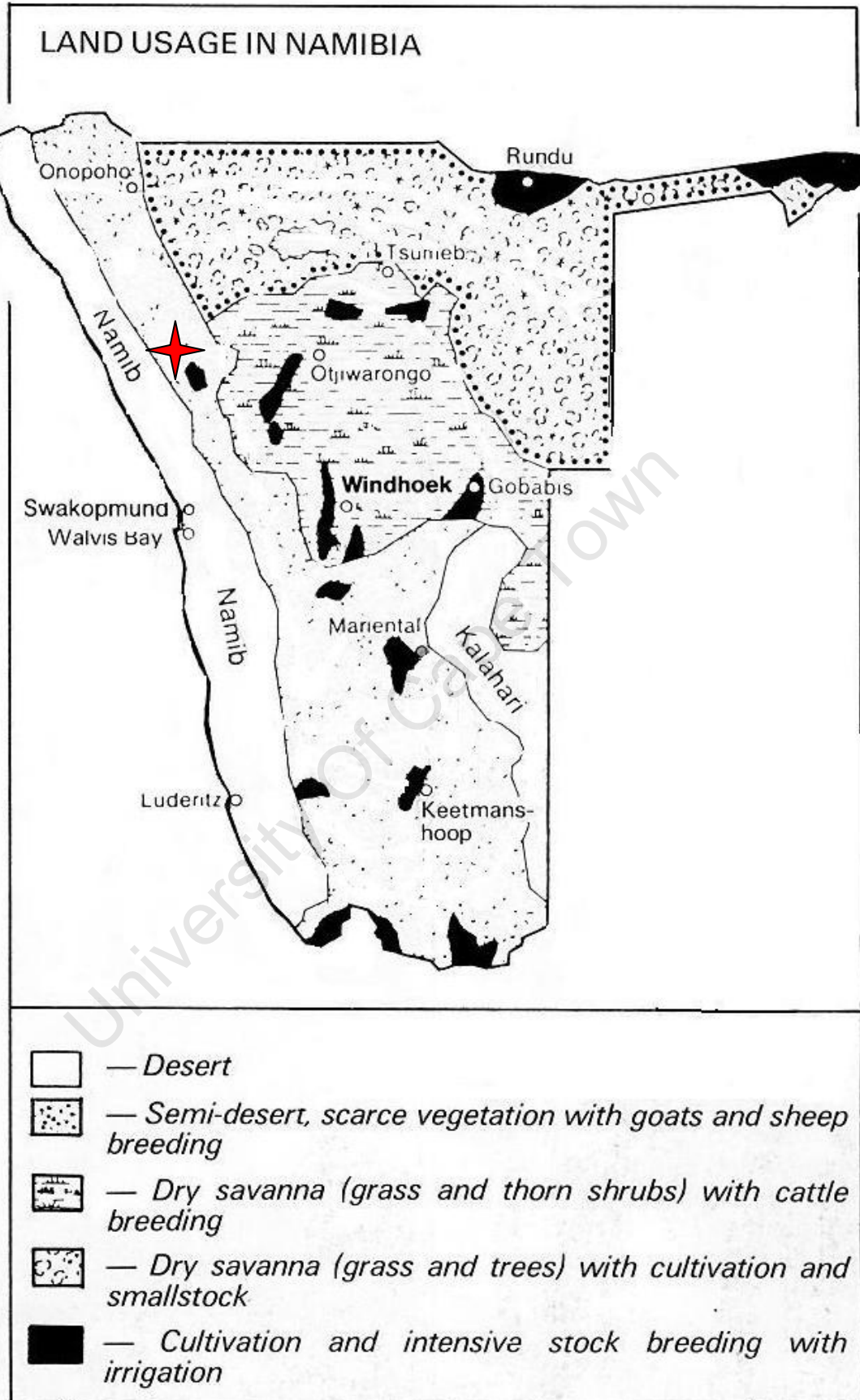


Figure 1.03 Map of Namibia showing the four main types of geography of the country. The study site Khoraxa-ams (red cross) is situated in the Semi-desert region of north-western Namibia (IDAF, 1989).

1.1.3 Geological survey

Namibia's geology encompasses rocks of Palaeo-, Meso- and Neoproterozoic and Palaeozoic to Cenozoic age (Mendelsohn *et al.*, 2002). Nearly half (46%) of the country's surface area are bedrock exposure, while the remainder is covered by the young superficial sediments of the Kalahari and Namib Desert (Martin, 1965; Mendelsohn *et al.*, 2002). According to Bierman and Caffee (2001), the geology of west-central Namibia is varied and influenced by ancient orogenies, many of the older rocks were metamorphosed during the Precambrian, and many of the granite rocks were introduced during the Cambrian.

Khoraxa-ams, in the northwest of Namibia, is situated within the Khoabendus and Haib Groups comprising karst rock belonging to the Palaeoproterozoic Vaalian (>2000 Ma) to lower Mokolian (2000-1800 Ma) Precambrian Metamorphic Complex (Figure 1.04) (Mendelsohn *et al.*, 2002). According to Martin (1965), metamorphic inliers (basement rocks) consisting of highly deformed metasediments and intrusive rocks occur in the northern parts of the country and represent the oldest rocks of Palaeoproterozoic age in Namibia. Therefore, the karst rock where Khoraxa-ams is located belongs to the oldest geotectonic and lithologic domain and consists mainly of limestone and dolomite rock types which are readily penetrated and dissolved by water, typically forming caves and sinkholes (Irish. 1991).

1.2 The Challenges faced in this Study

1.2.1 Location and topography of site

Dr. John Kinahan an archaeologist and Dr. Eugene Marais an expert on caves and an entomologist with the State Museum of Namibia excavated the site. The remains were taken to the State Museum in Windhoek, where they are currently being housed. According to Dr. Kinahan (*pers. comm.*, 01 March 2007) no formal archaeological excavation was carried out at the site due to the topography of the cave and the enormous difficulty experienced in recovering the remains. In addition, it should be noted that this particular recovery was more of an emergency excavation than a planned

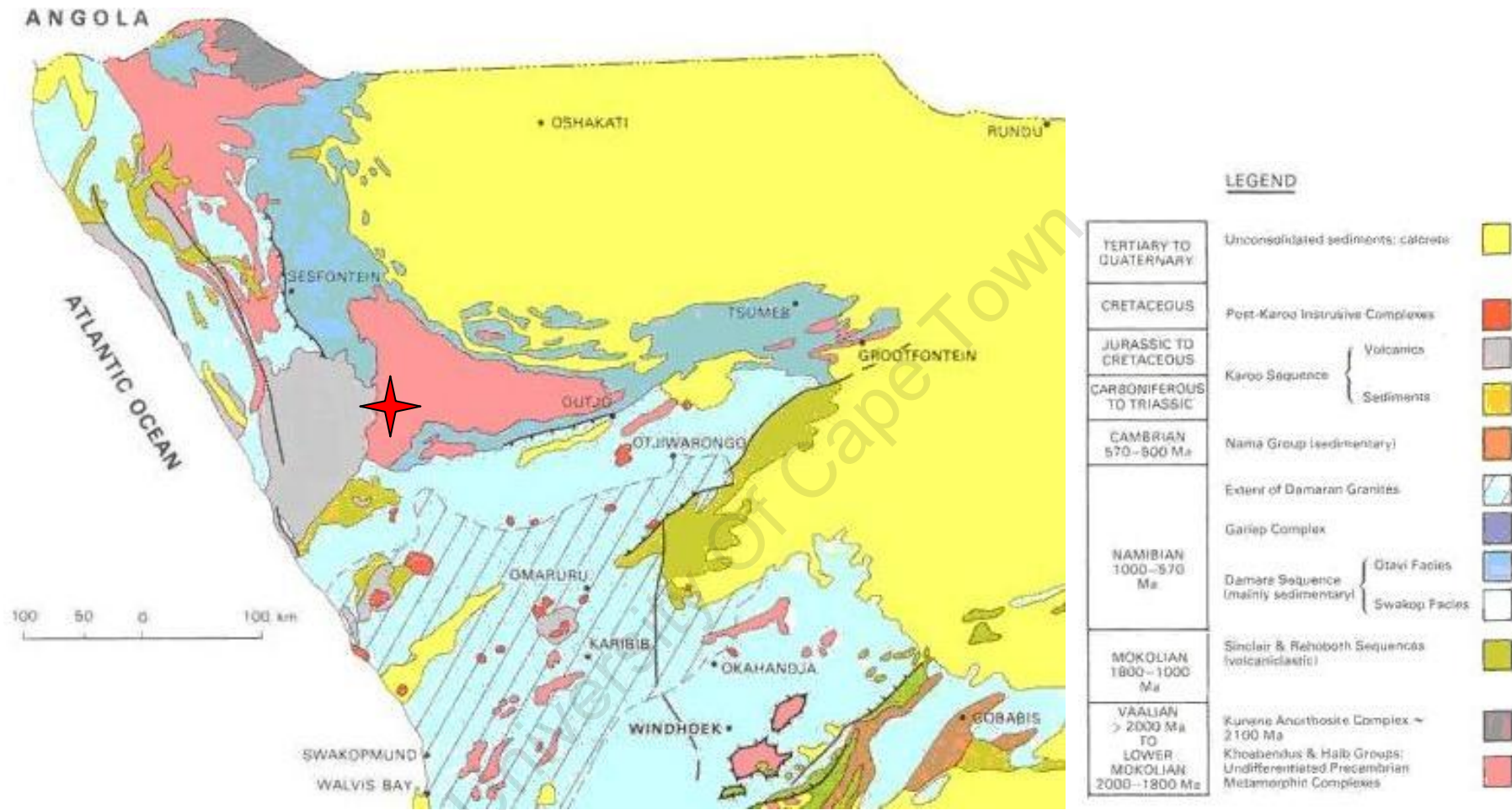


Figure 1.04 A geological map of northern Namibia, which encompasses rocks of Palaeo-, Meso- and Neoproterozoic and Palaeozoic to Cenozoic age. The site at Khoraxa-ams (red cross) is located within the undifferentiated Precambrian Metamorphic Complex (adapted from John Mendelsohn, *et al.*, 2002).

and pre-documented archaeological excavation. Therefore no site report or field notes exist, nor any cave sketches or site photographs to document the excavation.

According to Dr Kinahan (*pers. comm.*, 01 March 2007) the cave is a classic karst bell chamber with a small entrance via the top of the large cavern, thus making it a difficult site to enter. In order to reach the base of the cave, the excavation team had to abseil approximately 30 metres into the cave and climb out again with the use of a rope. Dr Kinahan constructed a gantry to hoist the material recovered from the base, as it was impossible to carry anything out of the cave by hand. The environment inside the cave was extremely adverse, with poor lighting, extreme humidity and claustrophobic conditions adding to the challenge of excavation. As a result of these challenges, only material from a surface collection on and around the talus cone at the base of the bell chamber was recovered (J. Kinahan, *pers. comm.*, 01 March 2007). Thus, the recovery of human remains from within the cave was incomplete.

Considering the practical difficulty experienced in removing skeletal elements from the cave, the enormous size and depth of the cave, and the geographical location of the site, there was strong reluctance to return to the site. This had adverse consequences for the investigation of this site, as an incomplete recovery limits the accuracy and thoroughness for identification of unknown human remains as well as the circumstances surrounding their deposition.

1.2.2 Presence of six-eyed crab spiders

Considering the practical difficulties experienced in excavating skeletal elements from the cave, the enormous size and depth of the cave, and the geographical location of the site, there was strong reluctance to return to the site as mentioned above. In addition to the physical challenges, a more convincing factor, such as the presence of six-eyed crab spiders within the cave increased the reluctance to return to the site to complete the excavation.

The *Sicarius* spider of the family Sicariidae inhabits regions of southern Africa, Central America, and western and southern parts of South America (van Aswegen *et al.*, 1997; Richardson-Boedler, 1999). The species *Sicarius hahnii* occurs in parts of Namibia and

north-western South Africa, and together with *Sicarius albospinosus*, are two of the most toxic species of the six-eyed crab spider family and are regarded as potentially lethal (Newlands and de Meillon, 1987; Richardson-Boedler, 1999). According to Richardson-Boedler (1999) *S. hahnii* is possibly the most lethal spider in the world (Figure 1.05). To date, *S. albospinosus* is the only species from which venom has been tested (van Aswegen *et al.*, 1997; Richardson-Boedler, 1999). The *Sicarius* spider causes symptoms of envenomation very similar to those of Ebola haemorrhagic fever (Richardson-Boedler, 1999).



Figure 1.05 *Sicarius hahnii*, from the Northern Cape and Namibia is extremely toxic and regarded as possibly the most lethal spider in the world. (<http://www.biodiversityexplorer.org/arachnids/spiders/sicariidae/sicarius.htm>, last accessed on 25 January 2010)

According to experiments conducted on animals, specifically rabbits, the venom of *Sicarius* causes massive tissue destruction (necrosis) at the location of the bite site, severe haemorrhaging locally and systemically, as well as disseminated intravascular coagulation (DIC) (van Aswegen *et al.*, 1997; Richardson-Boedler, 1999). The venom also acts systematically, resulting in petechial bleeding of viscera, thrombocytopenia and elevated fibrogen levels (van Aswegen *et al.*, 1997). Ultimately the venom affects clotting factor VIII (platelet cofactor) of the blood and results in a pathological blood-clotting defect (Newlands and de Meillon, 1987; van Aswegen *et al.*, 1997; Richardson-

Boedler, 1999). At present, no specific antivenom is available, neither are any antivenoms effective.

Consequently, due to the presence of six-eyed crab spiders living within the cave and the lethal threat they pose, there will be no further excavation at this site. Thus, the current sample must suffice for the investigation of the Khoraxa-ams remains.

1.3 Importance of this Study

Relatively little has been published about the history of Namibia. Little can be said with any certainty about the early history of the pastoral Herero-speakers and Nama-speakers, or of the agriculturalists in the north (Saunders, 1983). According to Vedder (1938) the history of Namibia of earlier times had been collected haphazardly, chiefly from old notes, letters, reports, and diaries as well as from information given by word of mouth by invading Europeans and locals. Due to the irregular methods of recording the Namibian past, little attention has been paid to the country's heritage.

The evidence from Khoraxa-ams will therefore shed light on the events that led to the deposition of these skeletons. The identification of the origin of these people may help to link them to living groups and the information gleaned from the analysis of the bones may shed some light on the particular event or events that led to their deaths.

1.3.1 Forensic vs. Anthropological approach

Khoraxa-ams is an archaeological site that falls into the context of physical anthropology, however it is apparent that the best approach in dealing with the investigation of this site is to make use of forensic analysis as a tool to uncover the evidence. A forensic approach allows one to view the site as a „crime scene‘, posing questions that are similar to those used in a criminal investigation. These questions revolve around ante-mortem information that could lead to the identification of individuals (in this case ethnic rather than unique identity), and the events at death especially with regards to the peri-mortem circumstances surrounding deposition of the remains.

The sample size of human skeletal remains analysed in this study is far too small in number to deduce any assumptions or speculations as to the cultural traditions and historical lifestyle patterns of the people involved. Anthropological behaviour of the group of human remains, if at all related, could therefore not be used to describe the historical past of the group. When investigating the anthropological behaviour of past populations, a suitable sample size is required for analysis, so that the data obtained is statistically significant and the number of outliers reduced. This results in decreasing the error rate and generates more accurate and plausible data.

Another factor that needs to be considered is the use of the total sample of skeletal remains rather than individuals for analysis. In 'anthropology', it is commonly believed that analysis is based on as complete a population as is possible to obtain. Anthropologists therefore determine the demographic profile, as well as document the pattern of injuries sustained by the population sample as a whole (Baraybar and Gasior, 2006). Individual features and categories are pooled and the data analysed in its totality and in comparison to other population groups.

Forensic anthropology however, is principally based on the identification of an individual, using a combination of features and tools, such as forensic bioarchaeology and forensic science, to increase the probability of positive identification and manner of death. Forensic anthropology has a primary role in recording skeletal injuries of known mechanisms and etiology (i.e. gunshot wounds) in individual skeletal remains, which may lead to establishing the cause and determine the manner of death (Baraybar and Gasior, 2006). Not only is this discipline involved in the study of the dead, but also anthropological expertise are requested in the identification and aging of living individuals (Cattaneo, 2007).

It should be noted that if indeed a crime has been committed, in this case an ancient crime, there is no chance of identifying neither catching the perpetrators responsible. Therefore, this study has no legal obligation usually associated with forensic casework.

1.4 Previous work on Khoraxa-ams Remains

The only work previously carried out on the remains recovered from the cave involved the estimation of a date surrounding the time period for the deposition of faunal and human remains, as well as associated artefacts within the cave. This was achieved by dating archaeological artefacts, i.e., a wooden vessel and copper bracelets used as adornments that were found among the remains recovered from the cave floor. Dr's Kinahan and Marais, along with the staff at the National Museum of Namibia used archaeological dating techniques to place the artefacts in historical context. A date of ca 1000 AD was achieved using this form of dating. Upon their findings, they assumed that this date could shed light on the dating of the cave goods as well as the period in which the events took place at the site.

1.5 The Purpose of this Study

1.5.1 Aim

The primary aim is to examine skeletal remains recovered from a site in Khoraxa-ams, north-western Namibia so that their identity and the circumstances surrounding their deposition in the cave can be determined.

1.5.2 Objectives

- **The number of people (MNI) and their demographics:**
Identify specific bone and bone sides of complete and fragmentary human skeletal elements, in order to 'join' disarticulated remains.
Determine chronological age, sex and adult stature of skeletal remains.
- **Post-mortem preservation:**
Identify modification of bones due to various taphonomic agents, including decomposition, heat alteration, preservation and burial factors.
- **The ante-mortem characteristics of the people:**
Examine life-style habits and practices, dietary preferences, as well as signs of disease processes and life-style stress present on and within the bones.

- **The biological and ethnic affinity of the remains:**

Determine the bio-ethnic (ancestral) grouping to which the remains are associated with. Provide background information on the bio-history of the remains.

- **Events at death (peri-mortem):**

Establish whether this was a violent episode by providing biomechanical interpretations for traumatic force. Attempt to reconstruct plausible events at death as well as the circumstances surrounding the deposition of the remains in the cave.

University Of Cape Town

BACKGROUND

The ethnographic and biological identity of the individuals recovered from the cave at Khoraxa-ams is not known. The only available comparative information is from modern groups who occupied the area surrounding the location of the site historically. This chapter therefore serves as a background on the inhabitants of northern Namibia.

Namibia, or South West Africa (SWA) as it was previously known, is a sparsely populated, vast country spanning 824 269 square kilometres (Serfontein, 1976; Malan, 1980; IDAF, 1989). Prior to colonial conquest the inhabitants of central Namibia herded cattle and lived a nomadic life (Vedder, 1938). In the south where vegetation is drier, sheep and goats were kept, while in the flood plains of the north and in better-watered parts of the north-east, inhabitants grew millet and other crops (IDAF, 1989).

2.1 Historical Background to the Inhabitants of Namibia

In southern Africa, linguistics plays an important role in identifying ethnicity, as linguistic data provides a valuable measure of population movement in periods without recorded history (Nurse *et al.*, 1985). Namibia is no different, with three major linguistic families, Bantu, Khoesan and Germanic, and over 28 languages and dialects belonging to these three linguistic families spoken in modern day Namibia (Fourie, 1997). Thus, when discussing the historical inhabitants of Namibia (Figure 2.01), it is best to separate the various ethnic groups based on the language they spoke.

2.1.1 The Bantu-speakers

The languages of a great majority of the inhabitants of southern Africa fall into the large family known as Bantu. All the Bantu languages are so closely related that it appears highly improbable that the depth of their historical divergence can be very great

(Nurse *et al.*, 1985). Thus, the Bantu-speakers are a cultural and linguistic delimitation of people who share many common features within their cultural traditions and chosen language (Malan, 1980). Numerous studies have proposed that Bantu-speaking people had their origins in central Africa and migrated into southern Africa, including Namibia during the first millennium AD (Hammond-Tooke, 1974; Malan, 1980; Nurse *et al.*, 1985; Van Reenen, 1986). For the most part, modern Bantu-speakers share a Negroid biological ancestry (Malan, 1980) and their appearance in the region coincides with the earliest evidence of cattle pastoralism and metallurgy in Namibia (Tobias 1974; Nurse *et al.*, 1985; Denbow, 1986). Of the modern Bantu-speaking populations in Namibia, the most numerous are the Ovambo and Herero-Himba.

2.1.1.1 The Ovambo

The Ovambo is a collective name for a group of tribes living in northern Namibia and southern parts of Angola. The Ovambo people constitute the majority of the Namibian population and comprise of roughly fourteen autonomous tribes living in southern Angola and Namibia (Serfontein, 1976). Of these, seven live in Ovamboland (Figure 2.01), six tribes live in Angola and two live on the northern boundary of Namibia and Angola (Van Reenen, 1986). They are a branch of the south-western Bantu group, but are culturally related to the matrilineal agriculturalists of Central Africa (Malan, 1980). It is suggested that the Ovambo migrated southwards from the upper end of the Zambezi at the same time as the Herero. However, on reaching „Ovamboland’ in central northern Namibia, the Herero are said to have continued in a westerly direction in search of suitable pastures for their cattle (Hahn *et al.*, 1928). The Ovambo, being an agricultural people remained and settled on the Great Plains north of the Etosha Pan where conditions were more suitable to their agricultural economic mode (Hahn *et al.*, 1928; Vedder, 1938; Malan, 1980). According to Vedder (1938) the Ovambo are known to produce millet and for cattle farming and are divided into broad kinship groups based on the matrilineal system.

2.1.1.2 The Herero-Himba

The Herero are thought to have migrated from Central Africa in a westerly direction through southern Angola, across the Kunene River temporarily settling in Kaokoland until reaching historic Hereroland (Figure 2.01) (Hahn *et al.*, 1928; Vedder, 1938). There are approximately nine groups of Herero-speaking people in Namibia. Their

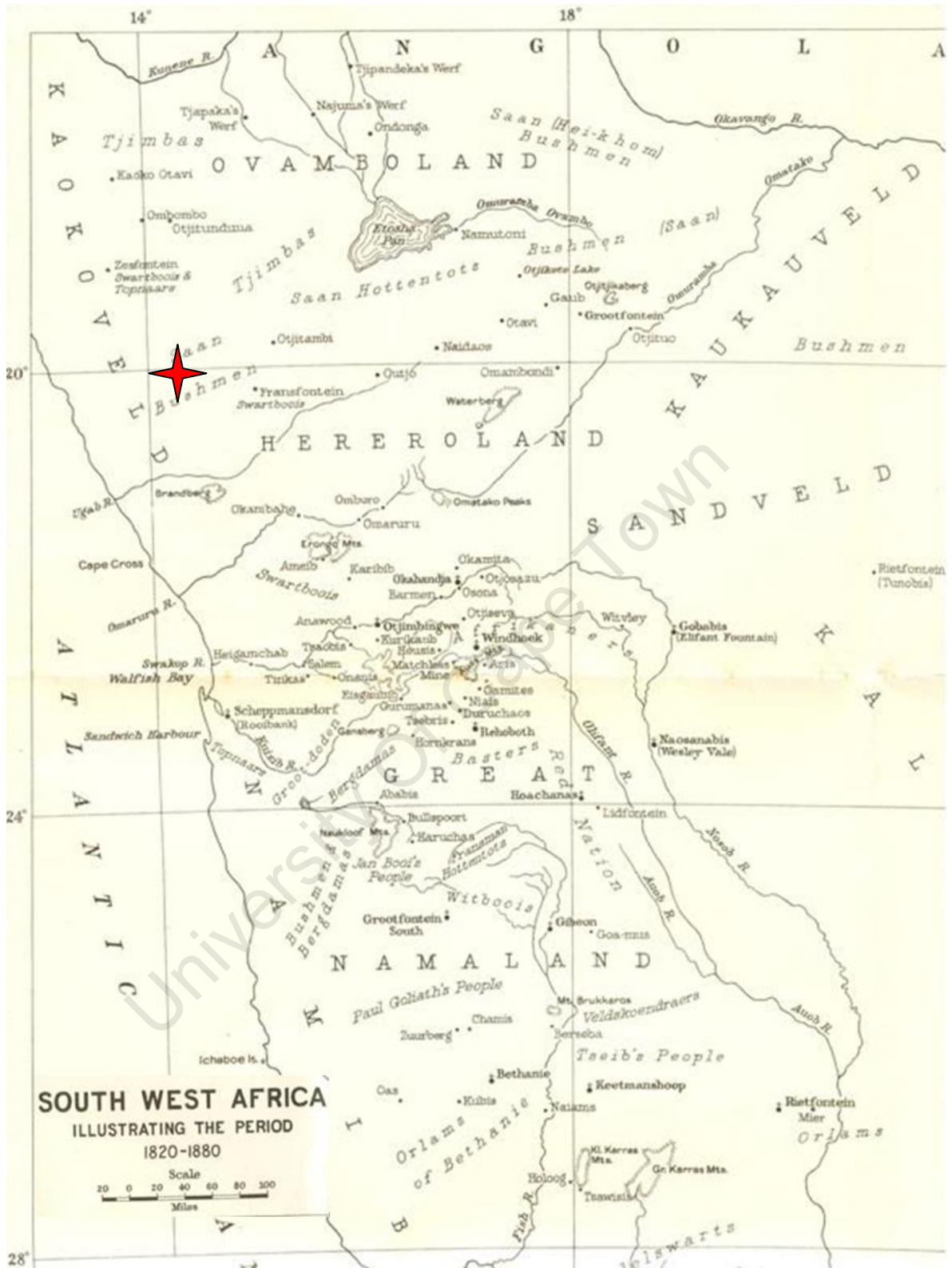


Figure 2.01 Historic map of Namibia (South West Africa) during 1820-1880 illustrating the regions of Central and Northern Namibia and the distribution of various ethnic groups as well as Khoraxa-ams in the northwest (red cross). Groups present in Ovamboland, Kaokoveld and Hereroland include the Himba, San and Nama. (adapted from Vedder, 1938).

Legend: Tjimbas = Himba; Saan Bushmen = San; Saan Hottentots = Nama.

language, although Bantu in origin, differs considerably from other ethnic groups in Namibia (Serfontein, 1976; Van Reenen, 1986).

Of the nine sub-groups of Herero, the Himba are of particular interest as they occupy the north-western parts of Namibia, present day Kaokoland (Figure 2.01). The Himba share the same origin, culture and language with the Herero but they are semi-nomadic pastoralists who spread wherever conditions were suitable for their herds (Jacobsohn, 1990; Kinahan, 2001; 2004), whereas the other Herero-speaking groups are pastoralists who settled in the central and eastern parts of Namibia with their cattle (Kinahan, 2001).

The traditional social structure of the Himba consists of a dual system with patrilineal and matrilineal groups, both playing a part in their religious and economic philosophy (Serfontein, 1976). In the middle of the 1800's the Himba were impoverished by the Nama cattle raiders and were forced to rely on hunter-gathering as a means of access to food (Vedder, 1938; Malan, 1980; Jacobsohn, 1990). Though, they regained their cattle wealth by raiding other groups in southern Angola (Jacobsohn, 1990). At present the Himba still occupy the north-western parts of Namibia.

2.1.2 The Nama-speaking groups

There are two Nama-speaking groups present in the region, the Nama and Dama, though they have different origins and are physically distinct from one another (Hahn *et al.*, 1928).

2.1.2.1 The Nama

The Nama are recognised as a Khoesan group, while the name „Nama’ refers to people of Khoe origin (Hahn *et al.*, 1928). Traditionally, the Nama are pastoral nomads who herd small stock such as cattle, sheep and goats, though they rely on hunting and gathering to a lesser extent as well (Vedder, 1938). Much has been written about their origins (Hahn *et al.*, 1928; Fauvelle-Aymar and Sadr, 2008; Smith, 2008) and they are said to be ethnically similar to the Dama as both groups are Nama-speaking and practice pastoralism. The Nama are said to be the only true relatives of the Khoekhoe group, once a nomad people consisting of numerous tribes who roamed over the great plains of southern Africa (Hahn *et al.*, 1928; Vedder, 1938).

Ehret (2008) stated that there is reasonable agreement among researchers (Denbow, 1986; Barnard, 2008; Smith, 2008) that the Khoe were herders who introduced sheep into southern Africa approximately 2000 years ago, however different views concerning the specific migration associated with the spread of the Khoe exists. Current studies by Nurse *et al.*, (1985), Denbow (1986), Haacke (2008), Sadr (2008) and Smith (2008) have suggested a central Kalahari origin. This is based on strong linguistic affinities between the languages of the Khoe and some extant hunter-gatherers of Central Botswana (Nurse *et al.*, 1985). According to Ehret (2008), Khoekhoe societies organized themselves around patrilineages and patrilans, to which people belonged by birth and from which responsibilities and social identities stemmed.

2.1.2.2 The Dama

The Dama are said to speak central Khoe (Khoekhoegowab), a dialect of the Nama language, though they are physically distinct from other Nama-speaking tribes (Hahn *et al.*, 1928; Vedder, 1938; Nurse *et al.*, 1985; Lau, 1987). The Dama are also distinctly different in their mode of living to the Herero living to the north, despite sharing a Negroid ancestry (Malan, 1980). Therefore, culturally and linguistically the Dama do not reveal any similarities to the neighbouring Bantu-speaking groups. They are the most southerly Negroid tribe in historic Namibia, and were said to be present in Namibia before the Herero's migrated into the country (Nurse *et al.*, 1985; Van Reenen, 1986). The ancestors of the Negro inhabitants of Southern Africa were hypothesised to have come from Western Africa and all of the living groups, with the exception of the Dama, have definite and fairly dateable traditions of immigration. Thus, the true origin and descent of the Dama remains unknown. It is thought however, that the earliest Negroes to enter Southern Africa may have come through the flood-plains of the upper reaches of the Zambezi and its tributaries (Nurse *et al.*, 1985). Their subsistence economy was reliant mainly on pastoralism, though they were also known to cultivate maize and vegetables, for hunting as well as collecting wild fruits from the veld (,veldkos') (Hahn *et al.*, 1928; Vedder, 1938). According to Lau (1987), unlike the nomadic Nama, the Dama settlements were reported to have been permanent.

2.1.3 The San

The San are believed to be the earliest aboriginal group in southern Africa and were scattered across a vast area of the region (Hahn *et al.*, 1928; Smith *et al.*, 2000). The Nama, Hereros and Ovambos state that on their arrival in South West Africa (Namibia) the San were found in occupation and that “they must have been living there ever since the creation of man” (Hahn *et al.*, 1928:82). They are best known as the first hunter-gatherers in southern Africa and have been extensively studied in the east of Namibia and the Kalahari Desert in Botswana (Nurse *et al.*, 1985; Gordon, 1992). Nurse *et al.*, (1985) states that more than half of the San population live in Botswana, across which they are widely distributed. In addition, Schapera (1930) identified several San groups living in the general area of north-western Namibia at the beginning of the 20th century (Figure 2.01).

There are five relatively large San populations, the !Kung or Zhu/oasi, the Hei//om, the G!oakx'ate as well as the Nharo and the Strandlopers or Beachroamers known to be present in Namibia and are spread throughout the north-east, the Etosha area, in the southern part of the country, as well as along the southern half of the border with Botswana (Nurse *et al.*, 1985). The San are divided into these separate groups based on their languages. The San or „Bush’ languages were originally classified by Bleek (1927) into three main groups, the Northern, Central and Southern (courtesy of Nurse *et al.*, 1985). Ethnographic evidence indicates that the San were hunter-gatherers until very recently but only a few living groups still practice this as a mode of subsistence (Lee and DeVore, 1976; Barnard, 1983; Myers, 1988)

2.2. Namibian Burial Practices

In order to establish the context as well as circumstances surrounding the deposition of human remains in a cave in north-western Namibia it is necessary to understand the burial customs and traditions followed by the various ethnic groups discussed above. Burial practices, as a material means of culture, can provide a variety of different insights into the nature of society and the relationships between the living and the dead.

Burials may also show the interaction among individual members in the living society, who used particular burial practices to construct their own social reality (Peleg, 2002).

Hahn *et al.*, (1928) noted that burial rites and customs varied a great deal among the Ovambo, Herero, the Nama and Dama as well as the San.

2.2.1 The Ovambo

Burial practices and traditions differed greatly among the different Ovambo tribes (Hahn *et al.*, 1928). In the Ondonga area after the death of a Chief no one was permitted to be buried until the Chief's grave had been washed clean by the seasonal rains. Therefore, the bodies of people who died during this period were dragged out into the bush and burnt. The bodies of people who committed suicide or had died from disease were never buried but simply left for wild animals in the bush. Similarly, in the Ukuambi area the dead, with the exception of the Chief, were not buried but the bodies thrown out on the veld. In tribes where burial was a common practice, headmen and the heads of kraals were buried in the cattle kraals, their wives in the vicinity of the area for stamping corn and their children in the enclosure for the calves. Common people were buried in a sitting posture in a grave, but the corpse was not wrapped in the skin of a freshly-slaughtered animal (Hahn *et al.*, 1928).

2.2.2 The Herero-Himba

Ancestral Himba graves are situated mostly at dry season camps along the banks of the Kunene and its tributaries, and are therefore not in the immediate vicinity of the settlements (Hahn *et al.*, 1928; Kinahan, 2004). A possible reason being that people are most likely to die at these sites or that the elderly people will remain here throughout the year. Himba graves are regarded as the residences of the deceased, i.e., where they stay and can be consulted (Hahn *et al.*, 1928). The graves are also tangible evidence of land ownership where no other records exist and they mark the place of the lineage (Kinahan, 2004). The patriarch and the ancestral graves form a powerful link between the living and the dead of this nomadic society (Kinahan, 2004).

According to Hahn *et al.*, (1928) the burial of a poor Himba is as insignificant as his life was. No one ever discusses his death or funeral, whereas the burial of the rich is in

stark contrast to that of the poor. When an elder or village-head dies his body is wrapped in the hide of the freshly-slaughtered ‚holy’ ox. The corpse is tied in a crouching position and lowered on a bier made of branches and buried facing towards the east in a deep round grave dug on a lonely spot (Kinahan, 2004). The grave is then filled with earth and heavy stones are placed on the grave. All the meat from the ‚holy’ cattle is eaten at the burial feast and the skulls with their horns are placed on stakes at the grave (Hahn *et al.*, 1928; Malan, 1980; Kinahan, 2004). The elder will therefore enter the spirit world accompanied by the ‚holy’ cattle.

2.2.3 The Nama

The Nama never laid out graves conjointly, but buried their dead somewhere in a solitary place and secured the grave with heavy stones (Hahn *et al.*, 1928). This was not only done because they wanted to protect the corpse against scavenging by wild animals, but more importantly to prohibit the dead from rising up again. It was believed that anyone who trod on a grave, past one unawares, or pointed at a grave with his finger had disturbed the rest of the dead and would therefore receive his revenge (Hahn *et al.*, 1928).

2.2.4 The Dama

Funeral rites among the Dama are observed to a limited extent and the burial of the corpse frequently takes place on the same day (Hahn *et al.*, 1928). The corpse is buried according to old customs which involves being tied up with rope in a squatting posture and covered with a sleeping-skin. The grave is then dug in a lonely veld at a depth of 1 to 1.5 metres and covered with heavy stones. The dead are treated with great distrust and are said to be able to return under certain circumstances where they can take a beloved or hated person with them. Therefore, to prevent the resurrection and return of the dead, the corpse is tied up and the grave is covered with stones. In addition, the place where the deceased lay has to be avoided so as to escape the returning dead, because it is believed that the soul of the dead lives in the grave (Hahn *et al.*, 1928).

2.2.5 The San

Hahn *et al.*, (1928) noted that the burial of the dead was carried out universally among the San at the time of their observations; though no detail as to the rituals and customs practiced by the San were recorded. More recent research by Inskeep (1986) and Morris (1992) has suggested that there has been a wide range of burial practices of San hunter-gatherers. Typically, the body was buried in or near the residential hut shortly after death, and then the band moved away from the location. San graves are therefore mostly single interments with shallow grave depth.

Overall, none of the historic Namibian populations were known to use caves as burial locations.

2.3 Comparing Similar Studies of Mass Deposition

The primary characteristic of the Khoraxa-ams site is that it contains the remains of a number of individuals whose remains are scattered on the floor of the cave and are not formally buried. It is not known what the circumstances surrounding the deposition of human remains in the cave at Khoraxa-ams was. Thus, it is important to compare the 'site' at Khoraxa-ams with similar sites recorded in the literature in order to possibly establish the context of the site.

Co-mingling of human remains commonly follows mass fatalities including plane crashes, war, explosions and genocide (Budimlija *et al.*, 2003; Andelinovic *et al.*, 2005; L'Abbé, 2005; Adams and Byrd, 2006; Schaefer and Black, 2007; Komar, 2008). Failure to recognise that two or more individuals are represented in one assemblage can result in both misidentification and a primary lack of identification (Schaefer and Black, 2007). Therefore, the investigation and analysis of mass graves are of utter importance to both human rights groups as well as to law enforcement officials.

Numerous studies of similar mass depositions are currently available (White, 1992; Pfeiffer and Fairgrieve, 1994; Brkic *et al.*, 1997; Budimlija *et al.*, 2003; L'Abbé, 2005). In particular, case studies of mass deposition and mass burials are often the result of

vicious intent to cause bodily harm or based on war and genocide causalities. Another form of mass deposition is based on cultural practices, where humans are often buried in secondary graves resulting in co-mingled human remains. Therefore, we can divide the comparative cases into those that involve the mass disposal of the dead (both primary and secondary) and the remains of victims of violence.

2.3.1 Group deposition and mass burials

Mass graves and multiple burials are not only confined to and the result of heinous crimes against humanity or war casualties, but can be as a result of cultural practices and historic traditions. More often than not, mass graves are the consequence of secondary burials. According to Ubelaker (1989), secondary inhumations consist of non-articulated collections of bones. Most secondary burials represent interment of the bones after natural decomposition of the flesh. They present a complicated method of treatment of the dead involving two or more stages of burial (Ubelaker, 1989).

2.3.1.1 Iroquoian ossuaries

Fragmentary skeletal remains are a significant problem for osteologists attempting to reconstruct individuals or populations. This problem is further aggravated by the discovery of sites yielding co-mingled remains, such as were recovered from the large protohistoric and historic ossuaries from southern Ontario, where two Iroquoian societies, the Huron and the Neutral lived during the first half of the seventeenth century (Hirschfelder, 1891; Jackes, 1996; Hoppa and Gruspier, 1996).

In an ossuary-style burial, the individuals' remains were defleshed, disarticulated and reburied in a single communal pit outside of the main village (Weslager, 1942; Churcher and Kenyon, 1960; Bathurst and Barta, 2004). Ossuaries are therefore considered secondary burials as the remains have undergone natural decomposition before being interred into a mass pit, a two-stage process (Katzenberg and White, 1979; Peleg, 2002). Ethnographic and archaeological evidence indicates that the remains were thoroughly mixed and tightly packed during the burial process (Kidd, 1953; Hickerson, 1960).

This type of communal burial practice provides a number of limitations for archaeologists and physical anthropologists due to the often brittle and disarticulated nature of the assemblage, which can make the collection of standard osteological data and diagnosis of pathological conditions difficult (Bathurst and Barta, 2004). The physical mixing of elements within an ossuary necessitates an approach in which data must be collected on a bone-by-bone basis. However, most single elements do not yield accurate indicators of sex and age at death, so data often must be interpreted without individual characteristics (Pfeiffer and Fairgrieve, 1994).

Despite the apparent limitations described above, ossuaries include the remains of a culturally and temporally defined cohort with considerable genetic commonality (Pfeiffer *et al.*, 1985), because they include most members of a community who died during a given period, roughly one decade. All bones and teeth were therefore interred in a small space, thus in principle minimizing differential preservation (Pfeiffer and Fairgrieve, 1994).

2.3.1.2 Prehistoric cannibalism at Mancos 5MTUMR-2346

A special case of mass burial of human remains is that of cannibalism. Although economic cannibalism (using human beings as a food source) is rare, there are several examples where this has happened (White, 2001). The Mancos assemblage of human remains is one such example. It was excavated from a small settlement in South West Colorado as part of a routine mitigation project on the Ute Mountain Indian Reservation. The pueblo comprised a score of rooms located at the foot of the Mesa Verde, and dates to ca. 1100 A.C. and was occupied at two different periods (Wesolowsky, 1993).

According to the original analysis conducted by Larry Nordby in 1974 and Paul Nickens in 1975 (White, 1992), human remains were found in two contexts: several conventional inhumations within the confines of the pueblo, and “bone beds,” deposits of unarticulated human remains blanketing the floor of several rooms. The original report concluded that the bones were smashed and extremely fragmented in ways that were congruent with the treatment of faunal remains from other Anasazi sites (Wesolowsky, 1993).

The human remains at Mancos were typified by their extreme fragmentation at the site. Of the 2106 bone pieces sorted, 551 specimens participated in joins that resulted in 185 total conjoining sets. Thus 26.2% of the Mancos assemblage was found to conjoin mechanically across peri-mortem fracture surfaces (White, 1992). White's analysis confirmed the original observation by Wesolowsky that the human remains were treated in a very similar manner to other animal bone that was processed for food at the site.

2.3.2 Victims of violence

Identification of victims in mass graves as a result of war as well as genocide is of humanitarian, human rights violation and political concern (Stover *et al.*, 2003; Djurić *et al.*, 2007; Komar, 2008; Ubelaker, 2008). Numerous studies based on the investigation and analysis of war casualties and the identification of often-innocent individuals are reported in the literature. Adams and Byrd (2006) investigated the resolution of small-scale co-mingling in a case report on the Vietnam War. Djurić *et al.*, (2007) critically evaluated the classical markers of co-mingling identification on victims from two mass-graves in Serbia as a result of war crimes. Two examples are presented below; one demonstrating the mass deposition of war mortality, and the second being a clandestine burial of mass murder victims.

2.3.2.1 Vilnius and the Grande Armée

In December 2001, Lithuanian construction workers made a bizarre discovery on the site of the former barracks of the Soviet Army, north of Vilnius (Thomas, 2007; Signoli *et al.*, 2004). The remains of a multitude of skeletons were piled chaotically in a communal pit. The remains of the dislocated corpses lying in the Vilnius pit were those of the French Emperor's soldiers, soldiers of the Grande Armée (Bahn, 2003). It has been said that this was by far the biggest historic grave ever discovered of Napoleonic soldiers who died during the retreat from Russia in December 1812 (Bahn, 2003; Signoli *et al.*, 2004).

In March 2002, an extensive excavation was carried out on the first part of the mass grave under the direction of the Vilnius Department of Archaeology (Thomas, 2007). The mass grave was located in a trench about 40 metres long, up to 10 metres wide and

starting 2 metres below ground level (Signoli *et al.*, 2004). This size along with the depth of the trench and the obvious high density of skeletons were, with the climatic conditions, the main difficulties experienced by the recovery team. It was decided that the excavation would benefit further from the collaboration of both Lithuanian and French anthropologists, reinforcing the anthropological team in the field (Signoli *et al.*, 2004). A second excavation of another trench in September of the same year (2002) completed the salvage excavation of the entire mass grave.

2.3.2.2 Croatian War

The process of recovering and identifying human remains from individual and mass graves has proven to be the most effective method of resolving the fate of missing individuals in the former Yugoslavia (Brkic *et al.*, 1997; Rainio *et al.*, 2001; Djurić, 2004; Šlaus *et al.*, 2006; Baraybar and Gasior, 2006). The primary objective of these efforts included identification and possible determination of manner of death of the recovered individuals, as well as bringing closure to the living relatives (Šlaus *et al.*, 2006).

The 1991 war between Croatia and Serbia that followed the dissolution of the former Yugoslavia caused extensive material destruction and loss of life (Brkic *et al.*, 1997). Executions and mass burials of civilians and military personnel, extensive destruction of private and government property, and the intentional destruction of schools, hospitals, museums and cultural objects characterized the conflict. All together, from 1991 to 1995, there were more than 14 000 war related deaths in Croatia. To deal with this humanitarian crisis, the Croatian Government formed the Committee for Imprisoned and Missing Individuals (Šlaus *et al.*, 2006).

Following the reintegration of occupied territories in 1995, the Committee recovered the remains of 3398 individuals. Some of the victims were partially or completely incinerated, a small number were recovered from septic tanks, several were recovered from fishponds, and 61 individuals were recovered from wells. By 2006, the remains of 3459 previously missing individuals were recovered, of which 2878 were positively identified (Šlaus *et al.*, 2006).

The identification of the maximum possible number of exhumed victims in Croatia was attempted by an interdisciplinary approach involving forensic odontostomatologists, forensic pathologists, and forensic anthropologists (Gunby, 1994; Primorac *et al.*, 1996; Šlaus *et al.*, 2006; Brkic *et al.*, 1997; Djurić *et al.*, 2007).

With regards to taphonomic processes observed on the skeletal remains recovered from the site of the Grande Armée in Vilnius as well as the mass graves of Croatia, it is evident that both sites were represented by fairly complete skeletons. Since mass graves were discovered at both sites, the mode of burial is indicative of a ‚hasty’ burial or disposal of human remains together with a lack of grave preparation leading to the construction of a mass grave. Where co-mingling did occur in the grave, this could have been due to the close proximity of the bodies at the time of burial. Thus, disarticulated skeletal elements were located in the immediate vicinity of its primary burial position.

MATERIALS

3.1 The Khoraxa-ams Remains

The source of the skeletal material examined in this study is from a collection of remains recovered from a site in Khoraxa-ams, north-western Namibia. The remains are accessioned to the State Museum of Namibia, Windhoek and permission to borrow the skeletal collection was obtained from Esther Moombolah-Goagoses, Director of the museum (Appendix 1A). In addition, a temporary export permit was acquired from Karl Aribeh, Director of the National Heritage Council of Namibia (NHCN) in order to



Figure 3.01 Collection (B4108) of disarticulated bone elements analysed in this study from Khoraxa-ams, north-western Namibia.

A total of 11 boxes, containing disarticulated individuals were analysed in this study (Figure 3.01). Each box housed similar bone elements, e.g. BOX 1: three cranial vaults, one with face; BOX 2: three mandibles, four cranial vaults, etc. Museum staff in Windhoek had cleaned the remains, removing as much soil and bat guano as they could without any damage to the bones. Each individual bone element or fragment was given

a National Museum of Namibia accession registration number starting with the letter “H”, which was used in this study to identify each bone element or bone fragment.

List of Accession Numbering by Museum Staff:

H1:	<i>Crania and Mandible</i>	64 labelled pieces
H2:	<i>Vertebrae, including Sacrum</i>	62 labelled pieces
H3:	<i>Ribs and Sternum</i>	49 labelled pieces
H4:	<i>Scapula and Clavicle</i>	15 labelled pieces
H5:	<i>Upper limb long bones</i>	23 labelled pieces
H6:	<i>Pelvic bones</i>	6 labelled pieces
H7:	<i>Lower limb long bones</i>	31 labelled pieces
H8:	<i>co-mingled hand bones</i>	un-catalogued
H9:	<i>Calcaneus</i>	1 labelled piece

New identity numbers were given to individual skeletons if re-articulation of remains was achieved. For the purpose of this investigation, the site number given by the National Museum of Namibia ,**B4108**’ was used.

3.2 Skeletal Inventory

Table 3.01 represents the initial inventory performed once the skeletal remains arrived at the bone laboratory at UCT. Data recorded in the initial inventory included listing the bone accession numbers as aforementioned, preliminary sorting by means of fitting and the identification and siding of each bone element represented.

A complete summary of the sample set was also recorded using sorting techniques proposed by L’Abbé (2005). This sorting method involves assessing the number of skeletal elements present, visual pair matching by which similarities in morphology are used to match right and left sides of a particular skeletal element, articulation of skeletal joints from which a close fit can be approximated, process of elimination where by the duplication of bones or additional bones on either the right or left side are used to

indicate another individual, and taphonomic appearance based on the examination of variation in preservation of bones such as, colour, staining, desiccated tissue, mold and odour (L'Abbé, 2005). A total count and „siding’ was performed for each bone element present in the sample, and recorded as such in Table 3.02.

Table 3.01 Inventory of the complete sample set from the cave in Khoraxa-ams B4108, initial sorting and identification of each bone element

B4108 Sample no.	Bone Name	Notes
<u>Cranial bones</u>		
H1: 1, 60	Cranium and mandible	Right maxilla
H1: 2, 40, 41	Cranium and mandible	Lower half of face missing
H1: 3	Cranium	Complete
H1: 4, 43, 55, 61	Cranium and mandible	Left half of Cranium missing
H1: 5, 30	Cranium and mandible	Complete
H1: 6, 14, 29	Cranium and mandible	Complete
H1: 7, 37	Cranium and mandible	Right half of mandible
H1: 8, 15, 31	Cranium, maxilla and mandible	Right half of face missing, Mandible fragmentary
H1: 9, 54	Cranium, face and mandible	Fragmentary
H1: 10, 20	Cranium and mandible	Complete
H1: 11, 12, 16, 28	Cranium	Roof of cranium, facial cranium. Left and right mastoid process
H1: 44, 63	Cranium and face	Base of cranium and face, with right zygomatic arch and floor or orbit present
H1: 22, 24, 25, 26, 34, 35, 36	Cranium	Fragments of roof of cranium and left temporal bone
H1: 23, 39, 49, 50, 51	Cranium	Roof of cranium fragmentary
H1: 13	Cranium	Fragment of right parietal bone
H1: 17	Cranium	Fragment
H1: 18	Cranium	Fragment of frontal bone
H1: 19	Cranium	Fragment of right parietal bone
H1: 21	Cranium	Frontal bone with groove and margin of orbital socket
H1: 27	Cranium	Right fragment of temporal bone with mastoid process
H1: 32	Maxilla	Right half of maxilla, edentulous
H1: 33	Cranium	Right temporal bone at superior orbital margin
H1: 38	Cranium	Right fragment with half mastoid process, superior part of external auditory meatus and zygomatic arch
H1: 42	Maxilla	Right fragment of maxilla
H1: 45	Cranium	Fragment
H1: 46	Cranium	Fragment of tympanic bone
H1: 47	Cranium	Fragment of tympanic bone
H1: 48	Cranium	fragment
H1: 52	Cranium	Cranium fragment and bag of dentition
H1: 53	Mandible	Left mandibular condyle
H1: 57	Dentition	Molar
H1: 58	Cranium	Fragment of zygomatic arch
H1: 59	Cranium	Fragment of maxilla
H1: 62	Cranium	Foramen magnum
H1: 64	Face	Left half of zygomatic arch and floor of orbit

B4108 Sample no.	Bone Name	Vertebral no.	Notes
<u>Post-cranial bones</u>			
Vertebrae			
H2: 1	Lumbar	-	Vertebral body
H2: 2	Thoracic	-	Vertebral body
H2: 3, 29, 35, 37	Lumbar	Vertebral body of L1/L2	H2: 29 robust vertebral body
H2: 18	Cervical	C4	H2: 37 robust
H2: 19, 22, 25, 26, 39	Thoracic	Vertebral body of T1, T5	H2: 25, 26 spinous process
H2: 4	Sacrum	-	Complete
H2: 5, 34, 36	Thoracic	T7, T8, T9	
H2: 6	Thoracic	T2	
H2: 7, 13, 18, 31	Cervical	C6, C3, C4, C5	
H2: 8, 14, 20	Cervical	C1	Incomplete fusion of posterior arch of atlas
		C7, C2	Robust with malformed bifurcated spinous process
H2: 9, 12, 38	Sacrum	S1 and S2	Fragments
H2: 10	Thoracic	-	Epiphysis of vertebral body
H2: 11, 23	Thoracic	T3, T4	
H2: 15	Lumbar	-	Fragment of spinous process
H2: 16	Lumbar	-	
H2: 17, 30, 32, 40	Thoracic	T6, T5, T7, T4	
H2: 21	Lumbar	-	Vertebral body
H2: 24	Cervical	C4/C5	Gracile, deformed bifurcated spinous process
H2: 27, 41	Thoracic	T9, T10	
H2: 28	Lumbar	-	
H2: 33	Thoracic	-	Fragment
H2: 34	Thoracic	T7	
H2: 42	Cervical	C2	Gracile
H2: 43	Cervical	-	Fragment
H2: 44	Lumbar	-	Spinous process
H2: 45	Cervical	C2	Fragment with dens of axis
H2: 46	Thoracic	T1	Spinous process
H2: 47	-	-	Vertebral body fragment
H2: 48	Thoracic	-	Vertebral body and partial transverse process
H2: 49	Thoracic	-	Vertebral body
H2: 50	Thoracic	-	Fragment
H2: 51	Cervical	-	Fragment
H2: 52	-	-	Vertebral fragments
H2: 53	-	-	Vertebral fragments
H2: 54	Cervical	-	
H2: 55	-	-	Vertebral fragments
H2: 56	Cervical	-	Fragment
H2: 57	Thoracic	-	Vertebral body
H2: 58	Thoracic	-	Vertebral body
H2: 59	Cervical	-	Vertebral body and left transverse process
H2: 60	Thoracic	-	Transverse and spinous process, and half vertebral body
H2: 61	Thoracic	T1	Vertebral body
H2: 62	Thoracic	-	Vertebral body

B4108 Sample No.	Bone Name	Side	Notes
Ribs and Sterna			
H3: 1	Sternum		
H3: 2, 4	Sternum		Fragment
H3: 3	Sternum		Fragment
H3: 5	Rib	L	
H3: 6	Rib 2	R	
H3: 7	Rib	L	
H3: 8	Rib	R	
H3: 9	Rib	R	
H3: 10	Rib 1	R	
H3: 11	Rib	-	Fragment
H3: 12	Rib	L	Sternal end present
H3: 13	Rib	R	
H3: 14	Rib	L	
H3: 15	Rib	R	
H3: 16	Rib	L	
H3: 17	Rib	L	
H3: 18	Rib	R	
H3: 19	Rib	L	
H3: 20	Rib	L	Fragment
H3: 21	Rib	-	Fragment
H3: 22	Rib	L	Fragment
H3: 23	Rib	L	
H3: 24	Rib 2 or 3	R	Fragment
H3: 25	Rib 1	L	
H3: 26	Rib	R	
H3: 27	Rib	L	
H3: 28	Rib	L	Fragment
H3: 29	Rib	R	
H3: 30	Rib	-	Fragment with sternal end present
H3: 31	Rib	L	
H3: 32	Rib 1 or 2	L	
H3: 33	Rib	R	Fragment
H3: 34	Rib	L	Poorly preserved sternal end
H3: 35	Rib	R	
H3: 36	Rib	R	
H3: 37	Rib 2	L	
H3: 38	Rib	R	
H3: 39	Rib	L	
H3: 40	Rib	L	
H3: 41	Rib	L	
H3: 42	Rib	R	
H3: 43	Rib	R	
H3: 44	Rib	R	
H3: 45	Rib	L	
H3: 46	Rib	R	
H3: 47	Rib	R	
H3: 48	Rib	R	
H3: 49	Rib	R	

B4108 Sample No.	Bone Name	Side	Notes
Scapulae and Clavicae			
H4: 5, 2	Clavicle	R & L	Complete clavicae
H4: 14, 12	Scapulae		Fragmented scapulae
H4: 3, 8	Clavicle	R & L	Pair
H4: 13, 11	Scapulae		Fragmented scapulae
H4: 6, 7	Clavicle	R & L	Fragmented left clavicle, right clavicle sent for radiocarbon dating
H4: 16, 15	Scapulae		Robust fragmented scapulae
H4: 1, 4	Clavicle	R & L	H4:1 sent for radiocarbon dating
H4: 9, 10	Scapulae		Complete and robust scapulae

Bone Accession no.	Bone Name	Side	Notes
Upper limbs			
H5: 19, 23	Humerus	R & L	Right humerus missing distal epiphysis
H5: 1, 8, 2	Radius	L	Fractures proximal head and shaft fragment of left radius
H5: 18, 22	Humerus	R & L	Robust individual
H5: 5, 10	Radius		
H5: 11, 12	Ulna		
H5: 17, 16	Humerus	R & L	Robust individual
H5: 9; H7: 17	Radius		Left ulna fragmented
H5: 14, 3, 4	Ulna		
H5: 20, 15	Humerus	R & L	Fair sized individual
H5: 6, 7	Radius		Only left ulna present
H5: 13	Ulna		
H5: 21	Humerus	L	Septal aperture present

Bone Accession no.	Bone Name	Side	Notes
Lower limbs			
H7: 9, 8	Femur	R & L	Robust individual
H7: 16, 23	Tibia		
H7: 28, 25	Fibula		
H7: 1, 10	Femur	R & L	Robust individual
H7: 12, 15	Tibia		
H7: 26	Fibula		
H7: 4, 7	Femur	R & L	
H7: 13, 18, 21	Tibia		
H7: 3, 2, 6	Femur	R & L	Left femur reconstructed
H7: 20, 14, 22	Tibia		Left tibia reconstructed
H7: 24, 27	Fibula		
H7: 5, 19	Femur	R	Fragmented. H7: 5 distal end with lateral and medial condyles present
H7: 11	Femur	L	
H7: 29	Patella	R	Complete
H7: 30	Patella	R	Complete
H7: 31	Patella	L	Complete

Bone Accession no.	Bone Name	Side	Notes
Pelvis			
H6: 1	Iliac crest	-	Fragment
H6: 2	Iliac crest	L	Billowed and fused
H6: 3	Pelvic bone	-	Fragment
H6: 4	Iliac crest	R	Billowed and fused
H6: 5	Pelvic bone	-	Fragment
H6: 6	Acetabulum, auricular surface, sciatic notch and anterior part of iliac crest	R	Fused, male pelvic bone – less than 90% greater sciatic notch

Bone Accession no.	Bone Name	Side	Notes
Co-mingled hand and foot bones			
H8: 34	Carpal	L	Capitate
H8: 1	Metacarpal	L	Digit 2
H8: 2	Proximal Phalanx	L	Digit 3
H8: 3	Proximal Phalanx	L	Digit 3
H8: 4	Metacarpal	L	Digit 3
H8: 5	Proximal Phalanx	L	Digit 4
H8: 6	Metacarpal	R	Digit 1
H8: 7	Metacarpal	L	Digit 3
H8: 8	Proximal Phalanx	L	Digit 1
H8: 9	Metacarpal	L	Digit 4
H8: 10	Metacarpal	R	Digit 5
H8: 11	Metacarpal	L	Digit 2
H8: 12	Metacarpal	R	Digit 5
H8: 13	Proximal Phalanx	R	Digit 2
H8: 14	Proximal Phalanx of foot	L	Digit 1
H8: 15	Proximal Phalanx	L	Digit 1
H8: 16	Proximal Phalanx	R	Digit 1
H8: 17	Metacarpal	R	Digit 3
H8: 18	Metacarpal	R	Digit 3
H8: 19	Metacarpal	L	Digit 2
H8: 20	Metacarpal	R	Digit 2
H8: 21	Metacarpal	L	Digit 3
H8: 22	Metacarpal	L	Digit 3
H8: 23	Metacarpal	L	Digit 1
H8: 24	Proximal Phalanx	L	Digit 4
H8: 25	Proximal Phalanx	L	Digit 3
H8: 26	Metacarpal	L	Digit 4
H8: 27	Proximal Phalanx	-	Digit 2 – fragmentary
H8: 28	Distal Phalanx	-	Unobservable
H8: 29	Distal Phalanx	-	Digit 1 – fragmentary
H8: 30	Distal Phalanx	R	Digit 4
H8: 32	Distal Phalanx	-	Digit 1 – fragmentary
H8: 33	Distal Phalanx	-	Digit 5 – fragmentary
H9: 1	Calcaneus	L	Complete

3.3 In Summary

Table 3.02 illustrates the complete inventory of bone elements present in the sample set. A total of 254 individual bone elements were recovered from the sinkhole in Khoraxa-ams, Namibia, however this was not a complete recovery. It should be noted that due to the sample being co-mingled, standard inventory techniques were adapted to suit this study.

Table 3.02 Summary of skeletal elements recovered from the cave site in Khoraxa-ams (B4108), north-western Namibia.

Skeletal element		Right side	Left side	Un-sided	Total
Cranial					
	Cranium	-	-	-	16
	Mandible	-	-	-	8
Post-cranial					
	Clavicle	4	4	-	8
	Scapula	4	4	-	8
	Sternum	-	-	-	3
	Ribs	21	21	3	45
	Cervical vertebra	-	-	-	16
	Thoracic vertebra	-	-	-	29
	Lumbar vertebra	-	-	-	9
	Humerus	4	5	-	9
	Radius	3	5	-	8
	Ulna	2	3	-	5
	Carpal	-	1	-	1
	Metacarpal	6	10	-	16
	Phalanx	3	7	5	15
	Pelvis	2	1	3	6
	Sacrum	-	-	-	2
	Femur	5	5	-	10
	Patella	2	1	-	3
	Tibia	4	4	-	8
	Fibula	3	2	-	5
	Tarsal	-	1	-	1
	Metatarsal	-	-	-	-
	Phalanx	-	1	-	1
	Miscellaneous	-	-	-	22
TOTAL No. of Elements		254			

METHODS

This is the first major study involving these remains, therefore a wide variety of both analytical and morphological techniques were carried out on the skeletal material in order to compile a broad set of data that could be thoroughly analysed for this research. Standard methods proposed by Buikstra and Ubelaker (1994) formed the basis for the analyses, however various osteological methods developed by İşcan (2001, 2005), Rösing *et al.*, (2007), Rogers (1999), Feldesman and Fountain (1996) and Lovell (1997) were used to construct a demographic profile. These osteological techniques were employed to increase the accuracy of the analysis and when greater depth of observation was required. This allowed a better understanding of the circumstances surrounding the skeletal remains and their deposition on the cave floor.

4.1 Sorting into Individuals and Establishing MNI

The initial step was to create an inventory to record the co-mingled remains of the study sample. This included identification and „siding’ the skeletal elements individually. Standard methods set out for inventorying co-mingled remains as outlined by Buikstra and Ubelaker (1994) were employed. The minimum number of individuals was determined for the study sample by examining the number of repeated elements by side and age. Fragments were identified as precisely as possible using suitable osteological features and matched where possible to larger known elements. In order to achieve this, every fragment must share a unique landmark to ensure that fragments of the same element of the same individual are not counted as two distinct individuals (Adams and Konigsberg, 2004). The basic principle of establishing an MNI is to avoid counting the same individual twice (Adams and Konigsberg, 2004).

4.1.1 Standard sorting techniques

After completing the skeletal inventory, the remains were sorted into individuals where possible, employing standard sorting techniques as proposed by Snow (1948), Byrd and Adams (2003) and L'Abbé (2005). These techniques include fitting and re-articulation of bone elements, visual pair matching (Left or Right) of relevant bone elements, determining age and sex of skeletal remains, establishing distinct preservation and bone taphonomy, and osteometric comparisons (Adams and Byrd, 2006). These techniques, when used in conjunction with each other, provide a solid basis for the individualization of most skeletal elements.

Table 3.02 in the materials chapter indicates the total count of bone elements present in the study sample, where the skeletal remains were identified and „sided“. The sorting techniques aforementioned were then applied to the skeletal inventory in order to pair the co-mingled remains and assign skeletal elements to „individuals“. Thus, the minimum number of individuals represented in the sample was determined

4.2 Recording Preservation of Bone Elements

The preservation of each skeletal element in the sample was recorded. The cranial and post-cranial remains were recorded separately. A scoring system or quantification of preservation states was employed according to Bello *et al.*, (2006). Each bone element was analysed separately using three preservation indexes: the anatomical preservation index (API*), the bone representation index (BRI*), and the qualitative bone index (QBI*) (Bello *et al.*, 2006).

4.2.1 The Anatomical Preservation Index (API*)

The anatomical preservation index is a preservation score assessing the quantity of osseous material present in the sample (Bello *et al.*, 2006). The API* expresses the ratio between the score of preservation (i.e., the percentage of bone preserved) for each single bone and the skeleton's total anatomical number of bones. The scores of preservation were recorded as follows:

- Class 1 = Bone not preserved (0% of the bone preserved);
- Class 2 = 1-24% of bone preserved;
- Class 3 = 25-49% of bone preserved;
- Class 4 = 50-74% of bone preserved;
- Class 5 = 75-99% of bone preserved; and
- Class 6 = Bone completely preserved (100% of bone preserved).

A score of preservation of >50% for each bone element was considered well-preserved.

4.2.2 The Bone Representation Index (BRI*)

The bone representation index measures the frequency of each bone in the sample. It is the ratio between the actual number of bones removed during excavation and the total number of elements of the skeleton that should be present (Bello *et al.*, 2006).

The bone representation index was calculated as follows:

$$\text{BRI}^* = \frac{100 \times \sum \text{Number of observations}}{\text{Number of theories}}$$

Where *Number of observations* = the recorded number of bone elements present in the sample; *Number of theories* = the total number of bone elements expected in the sample. For the BRI*, a score of > 50% is considered well-represented.

The hand and foot bones present in the sample were included in the analysis as single entities. The vertebral column was divided into cervical, thoracic and lumbar vertebrae, however the sacrum was analysed as a single element. The coccyx was not included in the analysis, as it was not represented in the sample.

4.2.3 The Qualitative Bone Index (QBI*)

The state of preservation of the cortical surface of bone was evaluated by the qualitative bone index, which is the ratio between the sound cortical surface and the damaged cortical surface of each bone element (Bello *et al.*, 2006). The scores of preservation of cortical surfaces were recorded as follows:

- Class 1 = 0% of sound cortical surface;
- Class 2 = 1-24% of sound cortical surface;
- Class 3 = 25-49% of sound cortical surface;
- Class 4 = 50-74% of sound cortical surface;
- Class 5 = 75-99% of sound cortical surface; and
- Class 6 = Cortical surface completely sound.

Qualitatively well-preserved bones were considered to have a score of preservation of cortical surface >50%.

4.3 Skeletal Analysis

4.3.1 Sex estimation

Standard techniques set out by Buikstra and Ubelaker (1994) formed the basis for sexing the skeletal material present in the sample, however several other methods optimized for the estimation of sex were also used and are listed below (Seidemann *et al.*, 1998; Rogers, 1999). These methods were employed due to sample preservation and co-mingling. Bone elements were therefore analysed individually, rather than as a complete skeleton and sex was assigned to individual bone elements where possible.

4.3.1.1 Standard macroscopic analysis

Sex determination involved the employment of multiple morphological criteria, such as shape, robusticity and size variables. Thus, various features of the pelvis, cranium and post-cranial bones were used to assess the sex of individual bone elements.

The pelvis is one of the most sexually dimorphic areas in the human skeleton and is therefore one of the most reliable regions for sexing human skeletal remains. The most common features used to assess sex are the ventral arc, the sub-pubic concavity, the pubic symphysis and the ischio-pubic ramus (Figure 4.01), obturator foramen shape and the size of the acetabulum (Buikstra and Ubelaker, 1994). In addition, the sciatic notch appears broader in females and narrower (< 90°) in males (Figure 4.02). Scarring of the pre-auricular surface, which can be caused by parturition, has been recognized as a

typical marker indicating a female. Thus, the general morphology of the pelvis as well as the pre-auricular sulcus was used to estimate sexual dimorphism.

The cranium and mandible were used as supporting elements to the pelvis or used solely when the pelvis was destroyed or missing, in estimating sex. In general, males tend to have larger, more robust crania than females. The nuchal crest, mastoid process, supra-orbital margin, supra-orbital ridge and the mental eminence were observed for signs of sexual dimorphism. The emphasis was based on gracile features for the female with a score of 1, and more robust, well-developed features on the male cranium with a score of 5 (Figure 4.03).

Long bones also play an important role in the determination of sex (İşcan and Miller-Shavitz, 1984), and are of great use in the absence and fragmentation of pelvic and cranial bones. The primary assumption when using long bones for sexual dimorphism is that males are larger in size than females. In this study the size of the femoral head when intact and well preserved (Seidemann *et al.*, 1998), and the sexual dimorphism of the distal humerus (Rogers, 1999; Vance, 2007), as well as the general robusticity of the long bones were employed to assist in the estimation of sex.

4.3.1.2 Distal humerus method

The most successful sexually diagnostic elements used for the determination of sex are the cranium and pelvis, as previously mentioned. However, if these elements are lacking, the ability to estimate sex becomes more complex. The method initially developed by Rogers (1999) and modified by Wanek (2002), makes use of the distal humerus to determine sex and has claimed approximately 92% accuracy based on four characters of the distal humerus (White, 2000a). These characters are based on the carrying angle of the arm. The carrying angle refers to the lateral deviation of the human forearm from the humeral axis. It is approximately 10-15 degrees in males and 20-25 degrees in females (Grabiner, 1989). A similar study by Vance (2007) on the age related changes in the human skeleton and its implication for the determination of sex made use of Rogers' (1999) method. According to these studies the distal humerus trait is sexually dimorphic (Rogers, 1999; Vance, 2007).

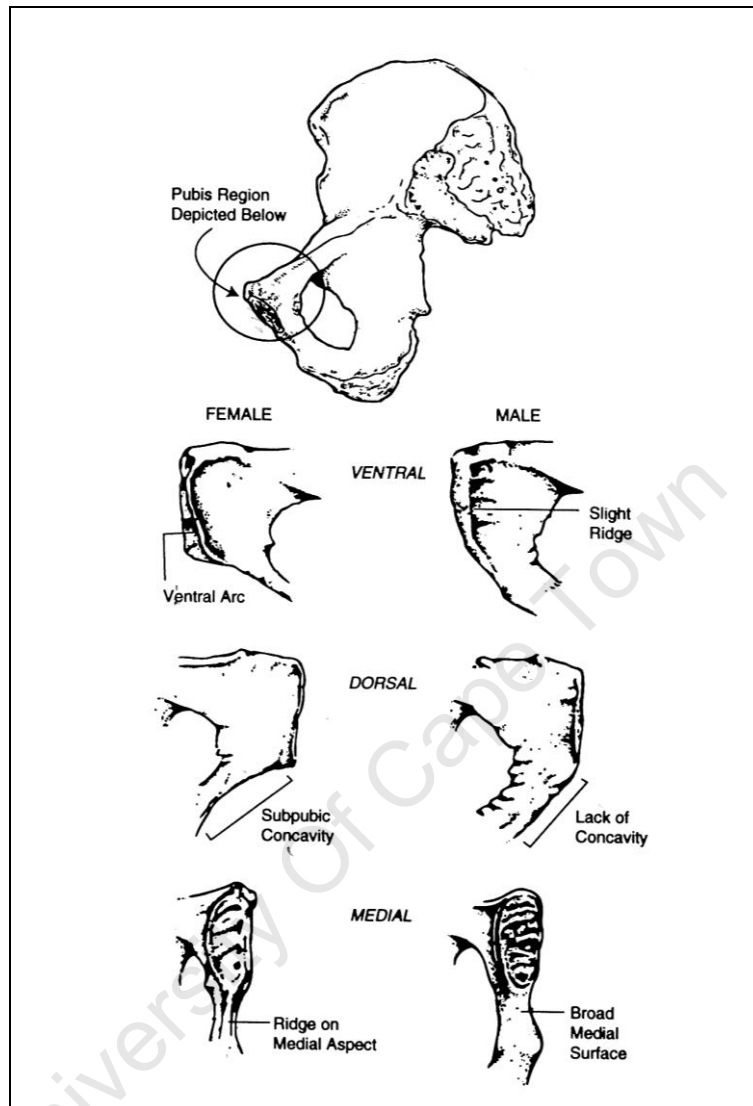


Figure 4.01 Sex estimation from the pubic symphysis (after Buikstra and Ubelaker, 1994)

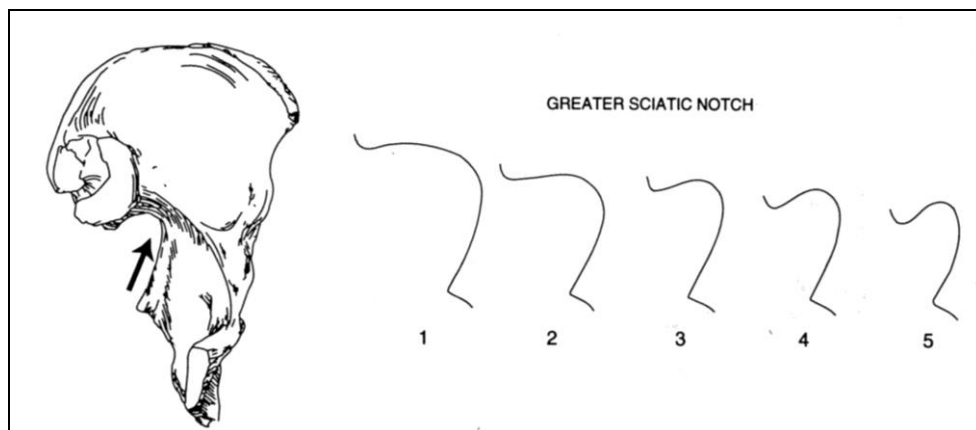


Figure 4.02 Sex estimation from the sciatic notch (after Buikstra and Ubelaker, 1994)

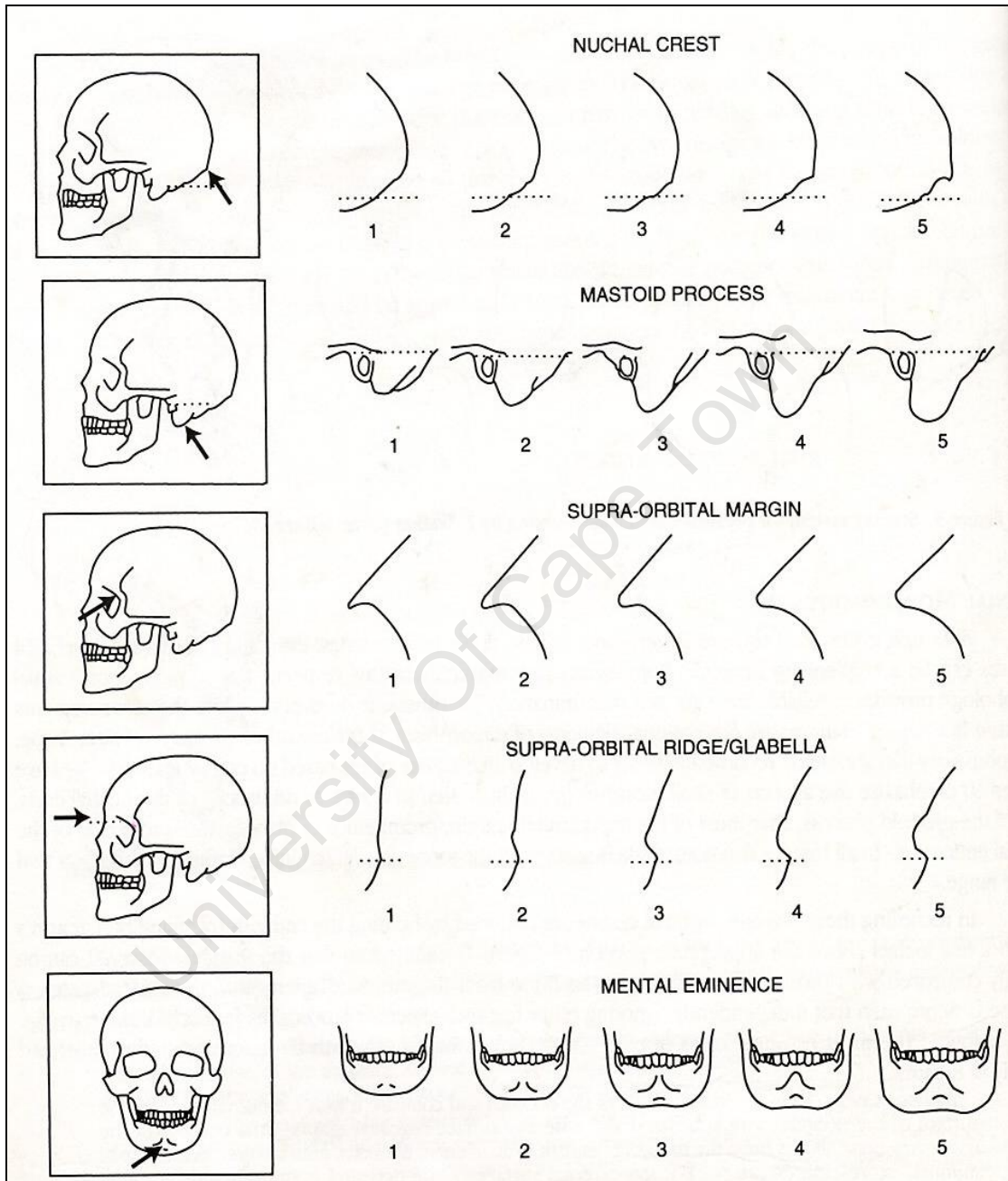


Figure 4.03 Cranial regions used for estimating sex (after Buikstra and Ubelaker, 1994: 20). The Five Point Scale recommended by the Workshop of European Anthropologists and later in Standards for Data Collection from Human Skeletal Remains, was applied in scoring each trait (Walrath *et al.*, 2004; Djurić *et al.*, 2007).

The Rogers (1999) method is based on five traits examined on the distal humerus:

1. The orientation of the medial aspect of the trochlear relative to the humeral shaft – it runs parallel to the shaft in males and angles across the shaft in females (Figure 4.04).
2. Trochlear constriction – less constricted in males than in females where it is spool-shaped (Figure 4.04).
3. Trochlear symmetry – asymmetrical in males and more symmetrical in females (Figure 4.05).
4. Olecranon fossa shape – triangular in males and oval in females (Figure 4.05).
5. Angle of the medial epicondyle – flat in males and slightly raised in females (Figure 4.06).

As adapted from Friedling, 2007

This technique relies on the differences in shape rather than size of the distal humerus. Therefore, the prediction is that this method should be at least 80% accurate in establishing sexual dimorphism between unknown individuals and should complement existing procedures (Rogers, 1999). Sexual dimorphism based on the distal humerus was ranked as 1 / 2 = male and 3 / 4 = female according to Figures 4.04 to 4.06.

4.3.1.3 Femoral neck method

The femoral neck is a flattened region of bone that serves to unite the head of the femur with the shaft. Unlike other anatomical landmarks of the proximal end of the femur, the neck is not the result of epiphyseal ossification (Seidemann *et al.*, 1998). Instead it is considered to be an upward growth of the shaft and actually develops from the diaphyseal centre (Paterson, 1929).

Whereas conventional methods of sexing typically rely on the crania and pelvic regions, which are susceptible to considerable deterioration, the femoral neck has a high rate of intact preservation (Seidemann *et al.*, 1998). The supero-inferior diameter (SID) is measured with sliding callipers across the narrowest part of the femoral neck (Figure 4.07). The measurement is then placed into various equations calculated for ancestral groups. Scores above zero indicate males and therefore scores below zero indicate females. The equation for individuals of unknown ancestry, as is the case with the Khoraxa-ams samples is:

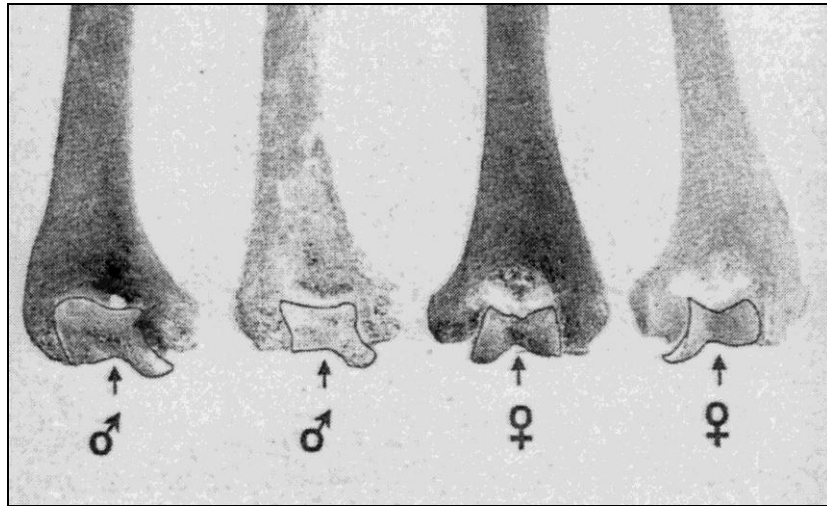


Figure 4.04 Estimating sex using the trochlear outline (after Rogers, 1999).



Figure 4.05 Estimating sex using the trochlear symmetry and olecranon fossa shape (after Rogers, 1999).

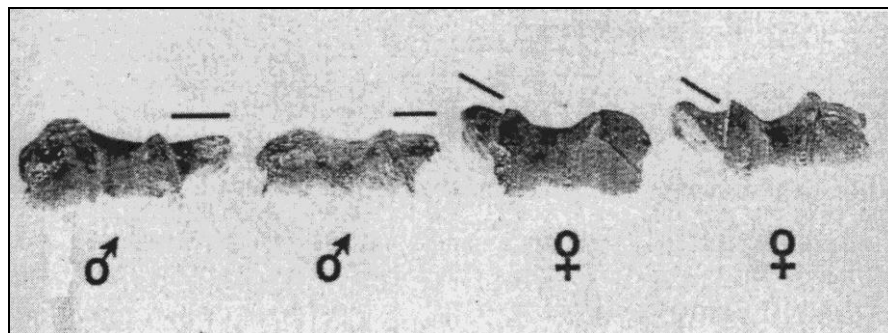


Figure 4.06 Estimating sex using the medial epicondyle (after Rogers, 1999).

$$\text{Sex} = 0.510 \times \text{SID} - 15.356;$$

Where $\text{Sex} < 0$ indicates a female and $\text{Sex} > 0$ indicates a male. This equation is said to be 90% accurate (Seidemann *et al.*, 1998).

According to the study done by Seidemann *et al.*, (1998), statistically the SID is a reliable sex predictor. Percent accuracies ranged from 87% to 92% in their study as the technique relies on the differences in size of the femoral neck and should complement existing methods.

4.3.2 Estimation of age at death

Estimation of age at death for the study sample was determined for each individual bone element rather than for a complete skeleton. This being the case due to the fact that the remains were co-mingled and individual skeletons was not identifiable.

Age estimation was therefore achieved by evaluating morphological and macroscopic biological changes in the skeletal remains using various bone elements (Figure 4.08) and teeth (Figure 4.10) where appropriate. The union of epiphyseal ends was examined for each bone element according to Brothwell (1981), and Buikstra and Ubelaker (1994) (Figure 4.08 and Figure 4.09).

4.3.2.1 Age categories

Since none of the skeletons in the sample were complete and age at death needed to be assessed from isolated bones using methods of varying degrees of accuracy, it was decided not to attempt to identify exact ages at death, but rather broader age categories. For comparative purposes, this study employed four of the five age categories as presented by Peckmann (2002) who utilized those presented by Morris (1984). Due to the absence of infants in the sample set, it was decided that the category “Infants – birth to 5 years of age” was not applicable and therefore not included. As a result of rapid age changes in the skeleton during the growth phase of life, a 5 to 10 year interval period was used to characterize and emphasize this in juveniles and sub-adults. Adult age is assumed from 20.1 years of age. This age category allows for the average age of complete fusion of long bones to be taken into account (Figure 4.09) (Buikstra and Ubelaker, 1994).

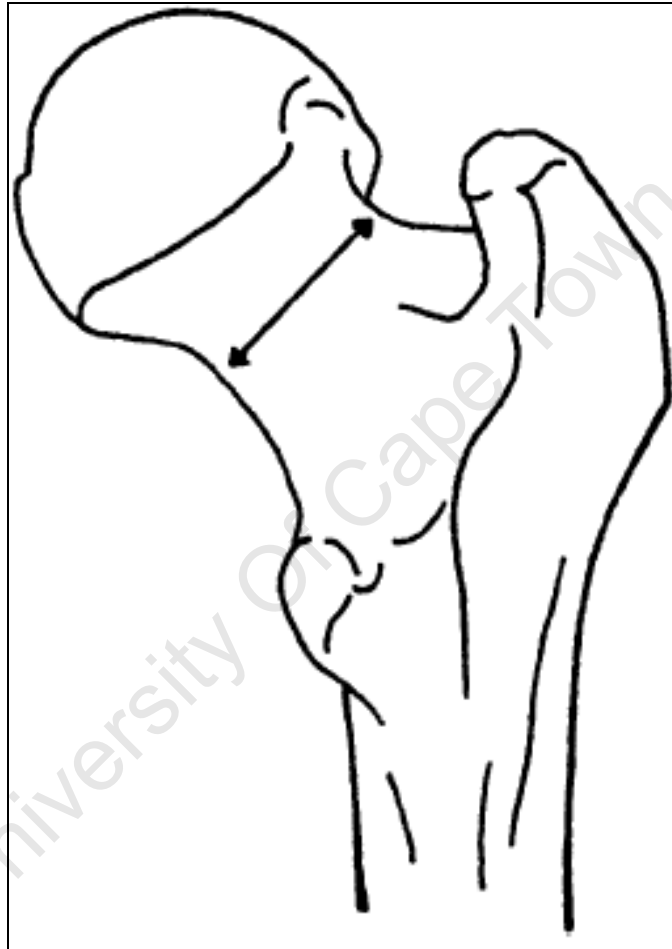


Figure 4.07 The supero-inferior femoral neck diameter measurement (SID), used for the estimation of sex (after Seidemann *et al.*, 1998).

The categories are:

- Juvenile – 5.1 to 15 years of age
- Sub-adult – 15.1 to 20 years of age
- Young adult – 20.1 to 40 years of age
- Old adult – 40.1+ years of age

4.3.2.2 Morphological methods

The estimation of age at death involved observing macroscopic morphological features in the skeletal remains. During infancy, most changes involve the ossification and growth of bones and the eruption and growth of deciduous teeth. During childhood and through adolescence, bone growth, dental eruption and calcification of permanent dentition continue. In addition, the epiphyses on the post-cranial skeleton develop and unite. Between 18 and 20 years of age, most growth is complete, almost all the teeth have erupted and are fully calcified, and most of the epiphyses are united. After 20 years of age, landmarks are provided by the progressive union of cranial sutures (Figure 4.11), and changes in the symphyseal face of the pubis (Ubelaker, 1978; Gillett, 1991; Buikstra and Ubelaker, 1994; White, 2000a; Friedling, 2007).

Morphological techniques have the advantage of being the easiest and also the least destructive, as compared with microscopic analysis. However, microscopic methods have the advantage of being more accurate (Friedling, 2007).

4.3.2.2.1 Sub-adults

Timing of epiphyseal union is an important means to estimate the age at death of adolescent and young adult skeletons (Figure 4.08 and Figure 4.09). It is based on the known period of time and order in which the various epiphyses fuse, so that age at death of unidentified skeletal remains can be established by comparing the maturational state of the bone with the chronological age-based reference standard (Cardoso, 2008).

Dental age assessments have long been considered the best indicators of age at death in immature skeletal remains (Thevissen *et al.*, 2009). Both the formation and eruption of dentition provide objective methods of age estimation in immature skeletal remains (Cardoso, 2007) and were used in this study (Figure 4.10). In addition, the stage of

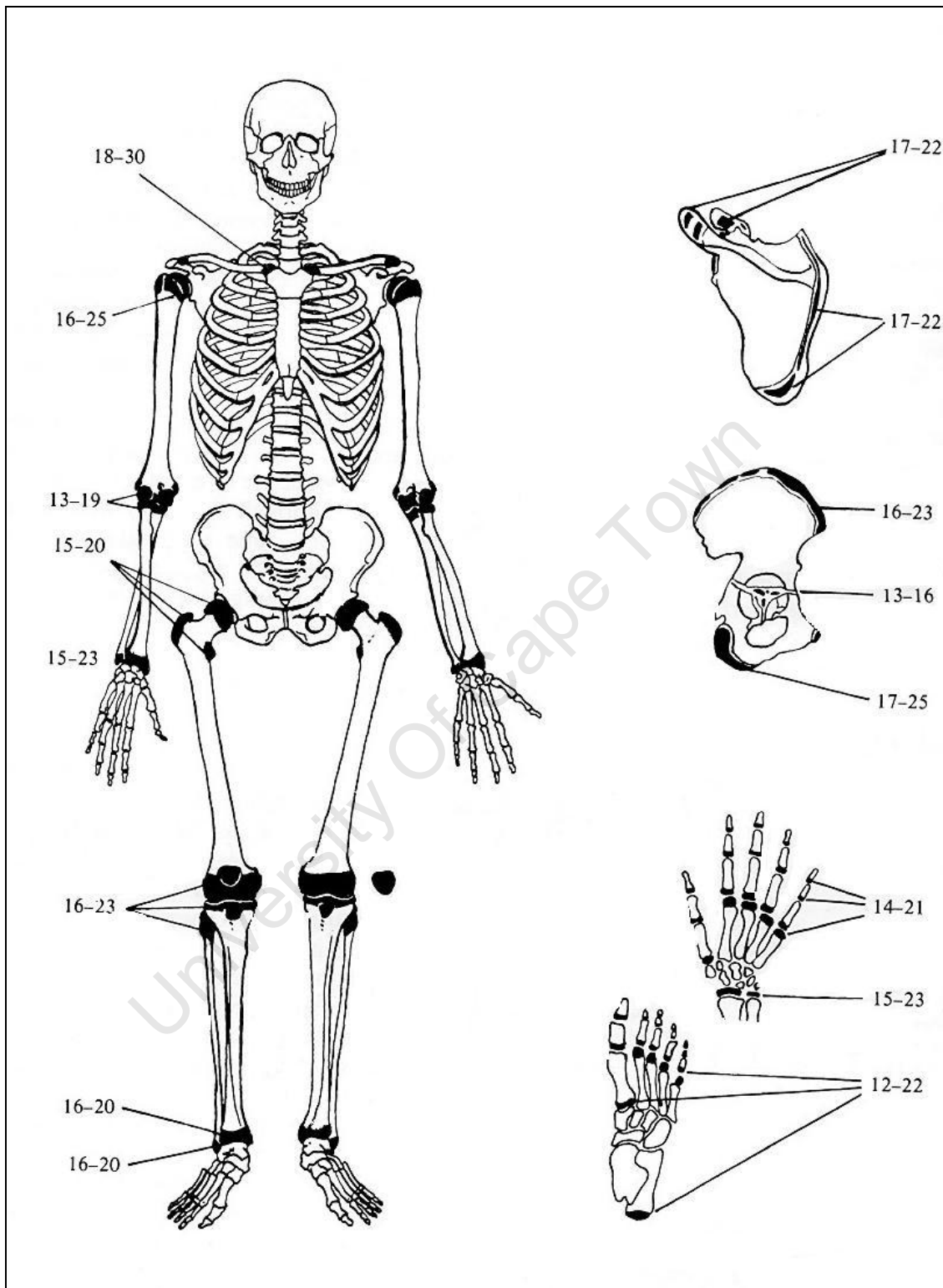


Figure 4.08 Estimation of age - times of epiphyseal union of various parts of the skeleton in sub-adults. All numbers represent years, the difference between each pair showing the time span within which the particular epiphyses unite (after Brothwell, 1981: 60).

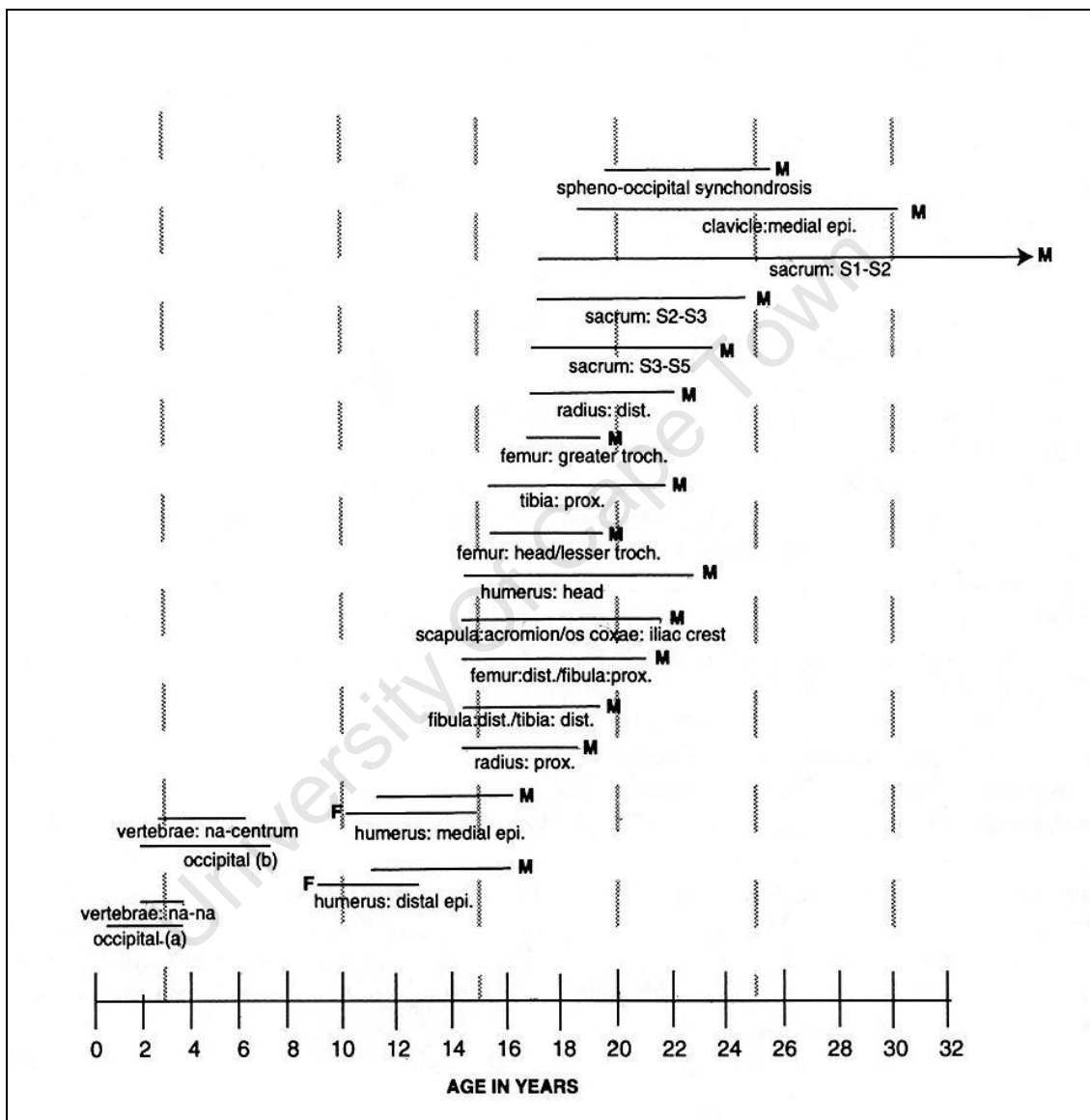


Figure 4.09 Estimation of age from epiphyseal union. M – Males, F – Females (after Buikstra and Ubelaker, 1994: 43).

fusion of epiphyseal ends (Figure 4.08 and 4.09) was used to determine the age at death of individual skeletal elements, as no complete skeleton was available.

4.3.2.2.2 Adults

The more common morphological methods used for estimating adult age (Meindl *et al.*, 1985; Brooks and Suchey, 1990; İşcan *et al.*, 1992; Loth, 1995) could not be used in this study because of the absence of pelvic bones and the fragmentary state of the ribs. For this reason, the age of adult skeletal remains was estimated using the stages of cranial suture fusion/closure and the radiographic examination of spongy bone in the proximal femur, along with the relative state of dental wear on the surviving maxillae and mandibulae.

Cranial suture closure

The study of cranial sutures was one of the first lines of research and was based on the initial hypothesis that suture closure is part of an age-related physiological process (Singer, 1953; Brooks, 1955; Meindl and Lovejoy, 1985). Closure of cranial sutures is still frequently used to estimate the age at death of adults from both an anthropological and forensic viewpoint, despite considerable variability in closure rates (Buikstra and Ubelaker, 1994). This is probably due to the fact that the cranium is often a well-preserved bone, sometimes even the only bone found, also the principle of macroscopic observations in most instances does not require any specific equipment (Dorandeu *et al.*, 2008).

The Degree of closure for all suture segments (Figure 4.11) was recorded according to the following stages as proposed by Buikstra and Ubelaker (1994). The left side of the cranium was used in instances of bilateral segments:

- **blank = Unobservable**
- **0 = Open.** There is no evidence of any ectocranial closure at the site.
- **1 = Minimal Closure.** Some closure has occurred. Score is assigned to any minimal to moderate closure, i.e. from a single bony bridge across the suture to about 50% synostosis at the site. (*< 40 years of age*)
- **2 = Significant Closure.** There is marked degree of closure but some portion of the site is still not completely fused. (*± 40 years of age*)

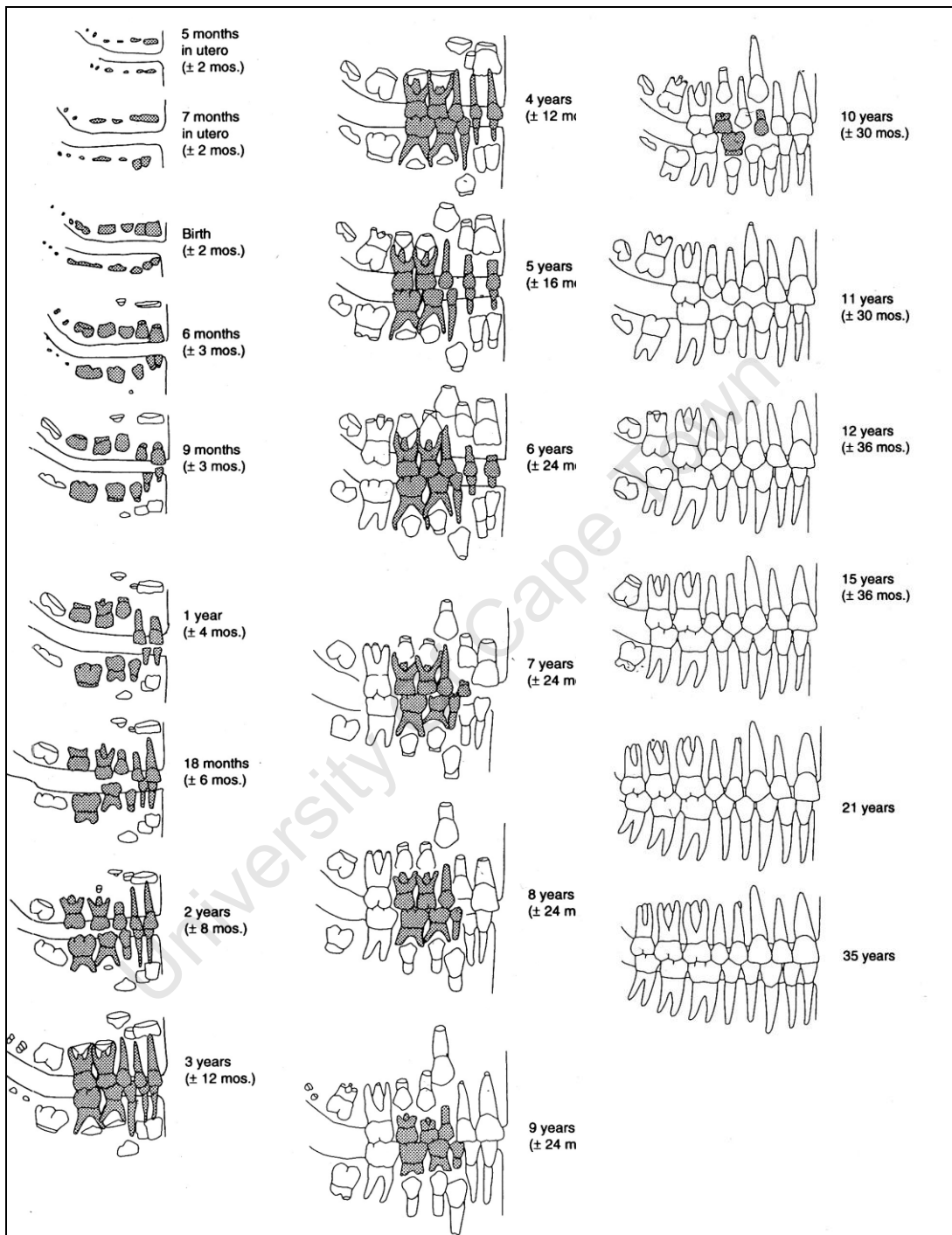


Figure 4.10 Sequence of tooth formation and eruption among Native Americans, useful in the estimation of age at death of infants and juveniles (after Buikstra and Ubelaker, 1994: 51).

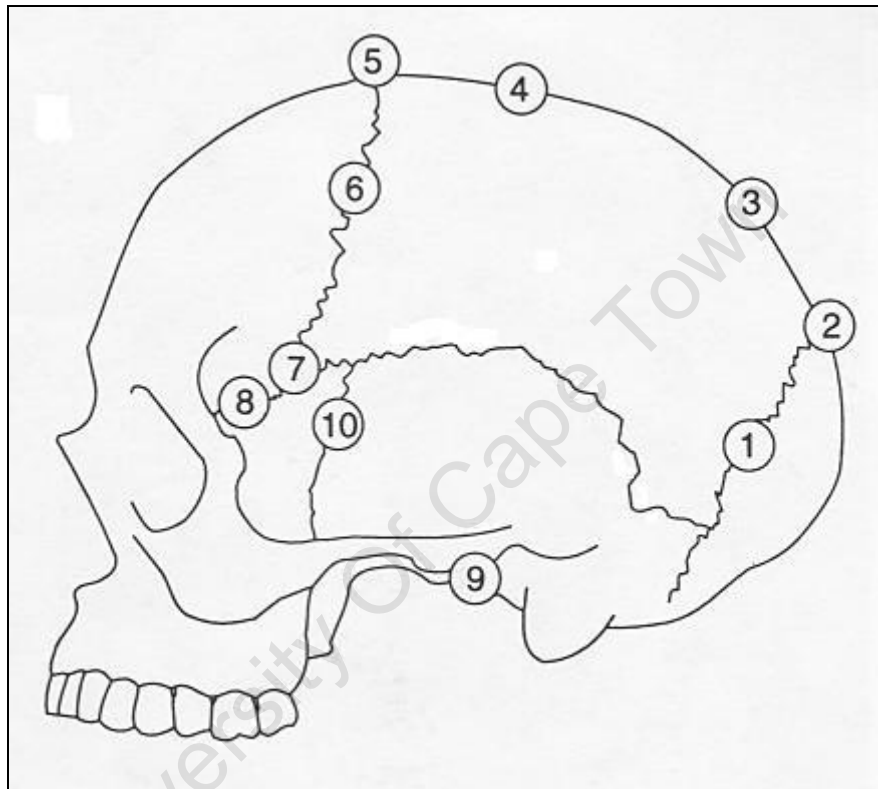


Figure 4.11 Estimation of age from ectocranial suture closure (after Buikstra and Ubelaker, 1994: 71).

- **3 = Complete Obliteration.** The site is completely fused. (*> 40 years of age*)

Suture closure was quite difficult to quantify in some cases as many sutures were only partially closed. Thus, the results were treated with caution.

Radiographic analysis of long bones

Radiographic imaging was also employed to estimate age at death by x-raying the proximal femur (Walker and Lovejoy, 1985). A total of ten femora were x-rayed using the LODOX² (Low Dose X-ray) machine housed at Groote Schuur Hospital's (GSH) Trauma Centre. A trained LODOX technician and operator, Mr Stefan Steiner from the Bio-medical Engineering unit within the Department of Human Biology at UCT, administered the scans and prepared them using Statscan software in dicom format. The radiographic image was then converted to a jpeg file for the purpose of this study. Each femoral radiograph was assessed and aged based on the stage of trabecular involution and seriation as illustrated in Figure 4.12 and assigned an appropriate age-range phase according to Table 4.01. The standards proposed by Walker and Lovejoy (1985), are presented in 5-year increments, but are only used as guidelines in the seriation of individuals.

4.3.3 Identification of ancestry

The purpose of determining 'race' of the skeletal material was not aimed at establishing their identification; rather it was used to compare the present sample to the skeletons of known populations who might have been present in Namibia in the prehistoric period. More specifically, the issue is, are the Khoraxa-ams remains more similar to Khoesan populations who were present as hunters and herders in the late prehistoric period, or to modern Bantu-speakers who were present as herders and low-intensity agriculturalists in the same time frame. Therefore, the unknown crania of Khoraxa-ams were compared to a reference data set of Khoesan and Southern African Negro groups from Morris (1984; 1992). The statistical method used to compare the data was principle component analysis³.

² A more detailed description of the LODOX machine can be found under the sub-heading **4.5 Radiography**, Harris Lines.

³ A more detailed description of principle component analysis can be found under the sub-heading **4.8 Statistical methods**.

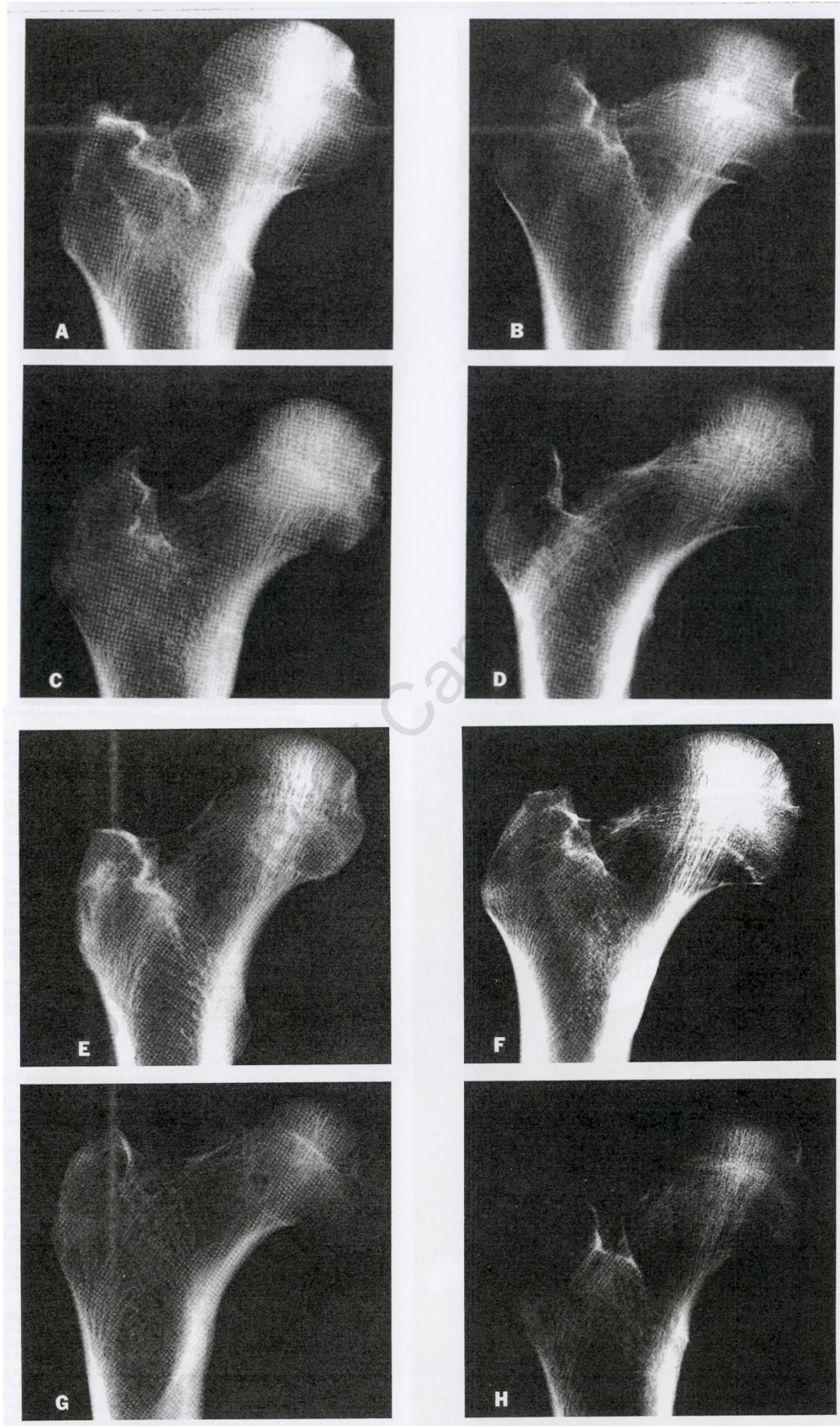


Figure 4.12 Radiographic standards for seriation of the proximal femur. A) phase 1; B) phase 2; C) phase 3; D) phase 4; E) phase 5; F) phase 6; G) phase 7; H) phase 8. For descriptions see Table 4.01 (after Walker and Lovejoy, 1985).

Table 4.01 Radiographic standards for age determination: Proximal femur (adapted from Walker and Lovejoy, 1985)

Phase 1	Cortical areas are well-defined with sharp boundaries. Trabeculae are fine-meshed and completely fill femoral head. Secondary trabeculae are almost as dense as primary systems (“compressive” and “transverse arcing” groups) so that distinguishing the two is difficult. Secondary trabeculae fill the proximal end of medullary cavity as well. Extremely dense and thick cortex, most prominent medially. <i>18-24 years</i>
Phase 2	Similar to phase 1 in most respects, but with slightly reduced density and localized bone loss (especially in Ward’s triangle). Translucency in the greater trochanter is more marked and some small areas of increased translucency appear in secondary trabeculae of both head and neck. Primary trabeculae are equivalent to phase 1. <i>25-29 years</i>
Phase 3	There is considerable reduction in general translucency especially in secondary trabeculae of head and neck. Principle supporting trabeculae are still strong and fine-meshed. Medial cortex is strong, but there is some loss of lateral cortex. Ward’s triangle is clearly defined by increased translucency. General resorption of secondary trabeculae allows clearer definition of classic primary groups. <i>30-34 years</i>
Phase 4	Similar to previous phase, but with greater translucency of all trabecular groups. Trabeculae of head are slightly more coarse than in previous phase with thickening of individual trabeculae. This is difficult to judge because no singular pronounced features separate it from phase 3. <i>35-39 years</i>
Phase 5	Greater trochanter shows marked resorption. Trabecular patterns are less dense in all areas, and individual trabeculae show strong tendency toward coarseness. Inferior portion of the head shows significant loss of secondary trabeculae. A similar loss is seen in medullary cavity. Ward’s triangle is virtually void of significant trabeculation. <i>40-44 years</i>
Phase 6	There is continued loss of secondary bone in femoral head, including superior portion; increased loss of secondary trabeculae in medullary canal and neck; and significant reduction in primary trabeculae. Cortex continues to be strong and shows greater contrast in translucency with trabeculated bone than in preceding phase. Slight scalloping of lateral cortex is seen. <i>45-49 years</i>
Phase 7	Primary trabeculae are coarse and greatly reduced in number. Secondary trabeculae patterns are almost totally absent. Transverse primary group is still present, but coarse and weak. There is significant general cortical loss. This phase is easily recognizable by significant increase in general translucency of the specimen. <i>50-59 years</i>
Phase 8	No secondary trabeculation is evident. Transverse group is also resorbed. Only primary supporting trabeculae (in markedly coarsened condition) remain in femoral head. There is marked cortical scalloping of both medial and lateral cortex. Medullary cavity is practically void. <i>60+ years</i>

4.3.4 Identification of pathology

4.3.4.1 Skeletal pathologies

Macroscopic analysis of non-specific pathological conditions and signs of abnormality were observed and recorded on all available skeletal elements. The signs of some of these conditions affect all age groups, e.g. cribra orbitalia, porotic hyperostosis and periostitis, while other conditions are more commonly found in older individuals, e.g. osteoarthritis and temporomandibular joint disease (Katzenberg and Saunders, 2000). In addition to the aforementioned conditions, non-specific pathologies also observed in the sample include growth arrest lines affecting the teeth, linear enamel hypoplasia and the long bones, Harris lines. These pathologies will be described in more detail below, under **4.7 Dental analysis** and **4.6 Radiography** respectively.

A. Cribra orbitalia and Porotic hyperostosis

Cribra orbitalia and porotic hyperostosis exhibit lesions that can be identified as spongy, porous regions located on the roofs of the eye orbits and on the ectocranial surface of the cranium, primarily on the frontal and parietal bones. Previously many authors (Hengen, 1971; El-Najjar *et al.*, 1976; Stuart-Macadam, 1992; Gruspier, 1999; White, 2000b) were in agreement that these lesions appeared to be caused by anaemia-associated hypertrophy of the diploë between the inner and outer tables, resulting in thickening and thinning of the outer surface of the bone. It is for this reason that both cribra orbitalia and porotic hyperostosis were usually associated with iron-deficiency anaemia as the most likely cause of marrow hypertrophy (Stuart-Macadam, 1985; Stuart-Macadam, 1992; Sullivan, 2005). However, recent studies have suggested that other pathological processes such as those associated with chronic scalp infections and scurvy can also produce porosities in the external surface of the cranial vault (Ortner, 2003; Walker *et al.*, 2009). Haematological evidence presented by Walker and colleagues (2009) suggests that a vitamin-B₁₂-deficient diet is much more likely to be the key nutritional component in the set of interacting variables responsible for both porotic hyperostosis and cribra orbitalia. All individuals with intact orbits and/or cranial vaults were examined for the presence and severity of cribra orbitalia and porotic hyperostosis.

Scoring system for the presence and severity of cribra orbitalia (Stuart-Macadam, 1985; Peckmann, 2002):

- 0 = none
- 1 = Light: scattered fine formation
- 2 = Medium: large and small isolated foramina that have linked to form a trabecular structure
- 3 = Severe: outgrowth in trabecular structure from the normal contour of the outer bone table

Status at time of death was observed; however this may be difficult to interpret as a number of pathological conditions can affect bone modelling and remodelling (Friedling, 2007):

- Remodelled = healed at time of death, bone is smooth to the touch but pitting is still visible
- Unremodelled = active at time of death, bone is rough to the touch

Lesions that are active at death display very sharp, defined edges regardless if the foramina are coalescing or not. Lesions categorized as healed at the time of death display smoother edges around the porous holes, with many holes no longer appearing circular (Aufderheide and Rodriguez-Martin, 1998).

B. Periostitis

Periosteal bone lesions are non-specific skeletal lesions most frequently found on the shafts of long bones, but can also occur on the orbital, endo- and ecto-cranial tables of the cranium (Mensforth *et al.*, 1978; Larsen, 1997). Periostitis is characterized as osseous plaques with demarcated margins, swollen shafts, or irregular elevations of bone surfaces (Steckel *et al.*, 2002). These lesions represent a non-specific, basic inflammatory response that may result from bacterial infection or injury, sufficient to stimulate osteoblastic activity of the periosteum (Mensforth *et al.*, 1978; Larsen, 1997). According to Mensforth *et al.*, (1978) periosteal reactions commonly occur in a number of disease conditions such as rheumatoid and psoriatic arthritis, widespread osteomyelitis, scurvy and rubella to name a few.

The skeletal tissue in the unhealed form is loosely organized woven bone. In the healed form, the tissue is incorporated into the normal cortical bone and the surface is often smooth, undulating and somewhat inflated (Larsen, 1997; Katzenberg and Saunders, 2000). Observations were recorded according to the site of infection and whether the spread was localized or widespread, and whether the status at the time of death was healed or unhealed.

The lesions were scored as follows (Friedling, 2007):

- 0 = none
- 1 = slight to moderate (pits and striations on bone surfaces with slight elevation of the bone surface)
- 2 = severe (sheaths of new bone with proliferation of endosteal and periosteal surfaces)

C. Joint disease

Synovial Joints

Degenerative joint disease (DJD) is a non-inflammatory, chronic, progressive pathological condition characterised by the loss of joint cartilage (Aufderheide and Rodriguez-Martin, 1998). DJD is the most common form of joint pathology and is evidenced by the destruction of the articular cartilage in a joint, and the formation of adjacent bone in the form of bony lipping and osteophyte formation around the edges of the joint (Aufderheide and Rodriguez-Martin, 1998; White, 2000b). The causes of joint disease are mainly due to mechanical or occupational stress; however whether this is an accurate etiology of DJD has long been a focus of debate among skeletal biologists (Brown *et al.*, 2008).

Rojas-Sepúlveda *et al.*, (2008) reported that DJD could be related to many variables: age, sex, trauma, genetic predisposition (metabolic and endocrine factors), as well as biomechanical stress or physical activity. Aufderheide and Rodriguez-Martin, (1998) sub-classify DJD as either primary or idiopathic in which no cause is evident, and secondary in which the joint has been altered by some other disease or event. The latter may be physical (trauma, congenital hip dislocation), infectious, metabolic (rickets, ochronosis), vascular (ostechondritis dissecans); neurotrophic (peripheral neuropathy)

or other arthritis type (rheumatoid) in addition to extra-articular causes (obesity, occupational stress, congenital deformities, diaphyseal angulations or limb asymmetry). Osteoarthritis is a non-infective form of arthritis and is one of the more common pathological conditions which occur in synovial joints (Ubelaker, 1978; Peckmann, 2002). The causes of osteoarthritis are mostly mechanical and the disease occurs mostly in load-bearing joints, particularly in the spine, the hip and the knees (White, 2000b). Osteoarthritis is classified as either primary, resulting from a combination of factors that include age, sex, hormones, mechanical stress, and genetic predisposition, or secondary, initiated by trauma or another cause such as the invasion of the joint by bacteria (White, 2000b).

Non-synovial Joints

Non-synovial osteoarthritis is a common degenerative disease affecting the vertebral column. Intervertebral disk degeneration often results in bone remodelling producing osteophytes commonly located on the rim (margin) of vertebral bodies. Irritation from bony contact at the vertebral margins stimulates the periosteum to form nodules of new bone or osteophytes (Peckmann, 2002). The vertebral locations that are the most frequently flexed are generally involved, including: C5-C6, T8-T9, and L4-L5 (Aufderheide and Rodriguez-Martin, 1998). The incidence of vertebral osteophytosis therefore increases with advancing age.

Joint disease was observed on the following post-cranial joints were available, adapted from Buikstra and Ubelaker, (1994):

1. Temporo-mandibular joint
2. Vertebral column (amphiarthrodial joints found at intervertebral discs)
3. Shoulder (glenoid fossa, humeral head, distal clavicle)
4. Elbow (distal humerus, proximal ulna and radius)
5. Radii-carpal (distal radius, proximal ends of first row of carpals)
6. Sacro-iliac, anterior (articulation between the sacrum and ilium)
7. Hip joint (head of femur)
8. Knee joint (distal femur and proximal tibia)
9. Tibia-calcaneal (distal tibia, articular surface of calcaneus)

Osteoarthritis was analysed occurring in either the upper or lower body: above and below the sacro-iliac (SI) articulation. The SI joint is functionally part of the upper body as it is involved in transmitting weight from the vertebral column to the lower limbs (Peckmann, 2002).

The above observations were made visually. The visual diagnostic criterions used include (Peckmann, 2002; Friedling, 2007):

- 0 = none
- 1 = slight lipping (osteophytes: process of bone remodelling producing focal nodules of new bone formation at the bone margins)
- 2 = marked lipping (alteration of joint surface contours: e.g. DJD of the hip may reveal a ‚mushroom’ type deformation of the femoral head)
- 3 = eburnation (smooth, shiny, polished surface produced by bone-to-bone contact in cartilage-free areas during joint movement)

4.3.5. Trauma

The skeletal remains were examined for the presence of ante-, peri- and post-mortem breakage. The identification of ante-mortem injuries was based on observed healed or healing bone fractures that occurred prior to death (Steckel *et al.*, 2002; White, 2000c). Bone healing, or bone remodelling is characterised by abnormal bone growth, callus formation, abnormal bone shape, necrotic tissue or characteristics associated with infection (Kimmerle and Pablo, 2008). According to Lovell (1997), fractures begin to heal immediately after the bone is broken when the bone is still living. Healing of bone is commonly described in three phases: inflammatory, reparative and remodelling phases. Though many variables affect these sequential phases of healing such as location of the fracture on the bone, which bone is fractured, age and sex of the individual (Symes, 2005a).

Without signs of bone healing, fractures are often identified as peri-mortem, implying that it is not possible to ascertain whether the fracture occurred just before, during, or after death (White, 2000c). Thus, peri-mortem fractures is the term given to injuries which may have occurred in the recent ante-mortem period (i.e., up to three weeks before death) and are therefore unhealed (Lovell, 1997).

Post-mortem damage refers to remains that have undergone modification by a wide range of taphonomic agents after death, such as carnivores or transport by flowing water. Post-mortem trauma is therefore differentiated from peri-mortem trauma by noting the patterns of bone breakage in relation to moisture and fat loss, differential staining on fracture margins and signature modification of scavengers, plants or geological processes (White, 2000c). According to Buikstra and Ubelaker (1994), breaks that occur long after death (post-mortem), in tissues of low collagen content, typically have squared edges at right angles to the bone surface, while peri-mortem fractures tend to form oblique angles.

The rate at which bone loses its organic component and becomes ‚dry’ as opposed to ‚green’ or ‚fresh’ varies widely, depending on the environment of deposition. Despite the variations in rate of change, it is possible to distinguish between peri-mortem fracture of bones that still retained much organic component when broken, and recent fractures of dry bones occurring post-mortem during excavation and transport (White, 2000c). Peri-mortem longitudinal or spiral fractures of the shaft are usually straight, with sharp, linear edges. Since the fracture surface had already formed at the time of burial, this surface is usually the same colour as the rest of the bone surface. Dry or fossilized bones that have been recently broken (post-mortem) usually have rougher, more jagged fractures, and the fracture surface is usually a different colour (lighter in most unfossilized bone) than the adjacent unbroken surfaces (White, 2000c).

Differentiating between ante-mortem/peri-mortem trauma and that which clearly occurred after death, as previously mentioned is predicated upon the different properties associated with bone that retains its viscoelastic nature and bone that does not, and upon the different appearances of bone surfaces after various post-mortem intervals (Buikstra and Ubelaker, 1994). **Ante-mortem** or **peri-mortem fractures** can thus be identified by 1) any evidence of healing or inflammation; 2) the uniform presence of stains from water, soil or vegetation on broken and adjacent bone surfaces; 3) the presence of greenstick fractures, incomplete fractures, spiral fractures, and depressed or compressed fractures; 4) oblique angles on fracture edges; and/or 5) a pattern of concentric circular, radiating, or stellate fracture lines. **Post-mortem fractures**, in contrast, tend to be characterised by 1) smaller fragments; 2) non-uniform colouration of the surface, especially light-coloured edges; 3) squared fracture edges;

and 4) absence of fracture patterning due to the increased tendency of dry, brittle bone to shatter on impact (Lovell, 1997).

In addition, Symes (2005a) characterised distinguishing features that differentiate between post-mortem carnivore trauma and peri-mortem blunt force trauma. Based on the mechanism of force and the analysis of contact surfaces, **post-mortem carnivore trauma** involves:

- 1) Low energy, vice-like crushing which creates tooth punctures in cortical bone, pits, scores or furrows, splintering or frayed edges as well as an increase in longitudinal fractures, and
- 2) Low energy prying which causes delamination, tear tags, flaking, and rounded or frayed fracture lines (slow load).

The mechanical features and bone surface of **peri-mortem blunt trauma** involves:

- 1) Low to high energy blunt impact which causes radiating fractures, sharp, well-defined fractures, and less longitudinal fractures except with axial loading, also
- 2) Low to high energy blunt impact results in fractures perpendicular to the bone surface, break away bone spurs, plastic deformation, flakes caused by compression fractures, and blocky, stepped or secondary fractures.

In summary, post-mortem carnivore trauma is characterised by the coalescence of fractures due to the chewing action, whereas peri-mortem blunt force trauma is characterised by the sharp appearance of fractures, radiating fractures as well as enhanced compression fractures (Symes, 2005a).

A fracture consists of an incomplete or complete break in the continuity of a bone. The most common types of fractures, such as transverse, spiral, oblique and crush fractures result from direct and indirect trauma. Fractures resulting from stress and those secondary to pathology are less common and have distinct etiologies (Lovell, 1997). In this study, fractures as well as the associated mechanisms of injury were analysed and recorded as either the result of direct or indirect trauma occurring ante-, peri- or post-mortem.

Fractures were examined and recorded according to the following mechanisms of injury and types of fractures outlined by Lovell (1997) and Djurić (2006), (Figure 4.13 and 14):

Direct trauma

1. Transverse fractures, results from force applied in, and appears as, a line perpendicular to the longitudinal axis of the bone;
2. Penetrating fractures, produced by projectiles of high or low velocity;
3. Comminuted fractures, when the bone is broken in more than two pieces; and
4. Crushed fractures, where the bone is either extensively comminuted or broken transversely; segmental fractures are also included here.

Indirect trauma

1. Oblique (angulation) fractures, where the line angles across the longitudinal axis, is indicative of a combined angulated/rotated force;
2. Spiral (rotational) fractures, where a twisting force is applied to a bone, producing a characteristic spiral fracture line;
3. Greenstick (torus) fractures, results from bending or buckling of bone when stress is applied;
4. Impaction (compression) fractures, where force is applied in an axial direction; this is rare in long bones, but when it happens, the shaft is driven (impacted) into the cancellous end;
5. Burst fractures, located in the spine, results from a vertical compression that ruptures the intervertebral disc through the vertebral end plate, forcing disc tissue into the vertebral body; and
6. Avulsion fractures, caused when a joint capsule, ligament or tendon is strained and pulls away from its attachment to the bone, tearing a piece of bone with it.

4.4 Skeletal Measurements

Standard skeletal measurements by Buikstra and Ubelaker (1994) were performed on all cranial and post-cranial bones present in the sample, where possible. Metric analysis

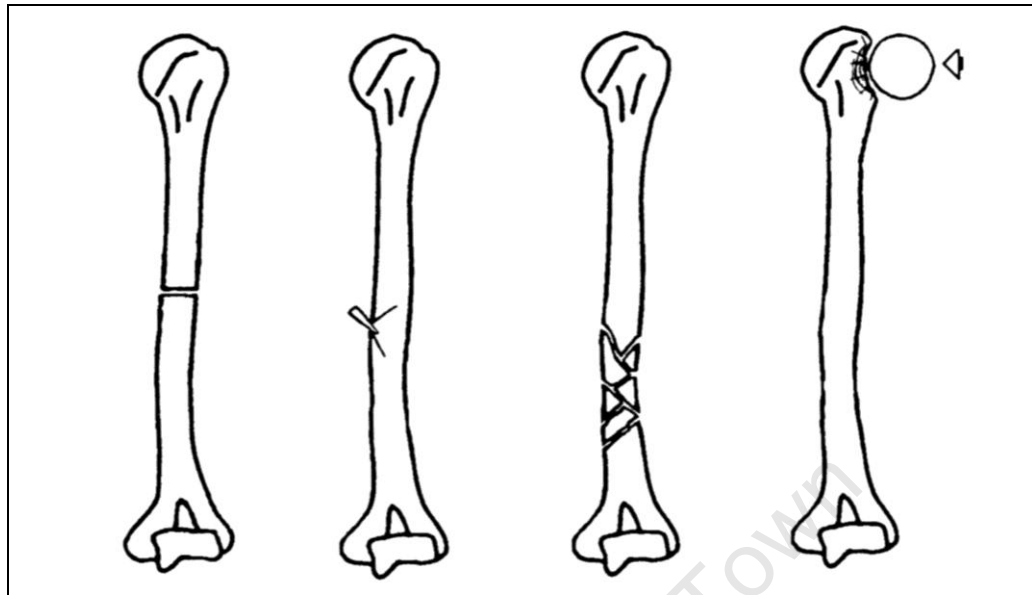


Figure 4.13 Fractures caused by direct trauma. From left to right: transverse, penetrating, comminuted, and crush (after Lovell, 1997).

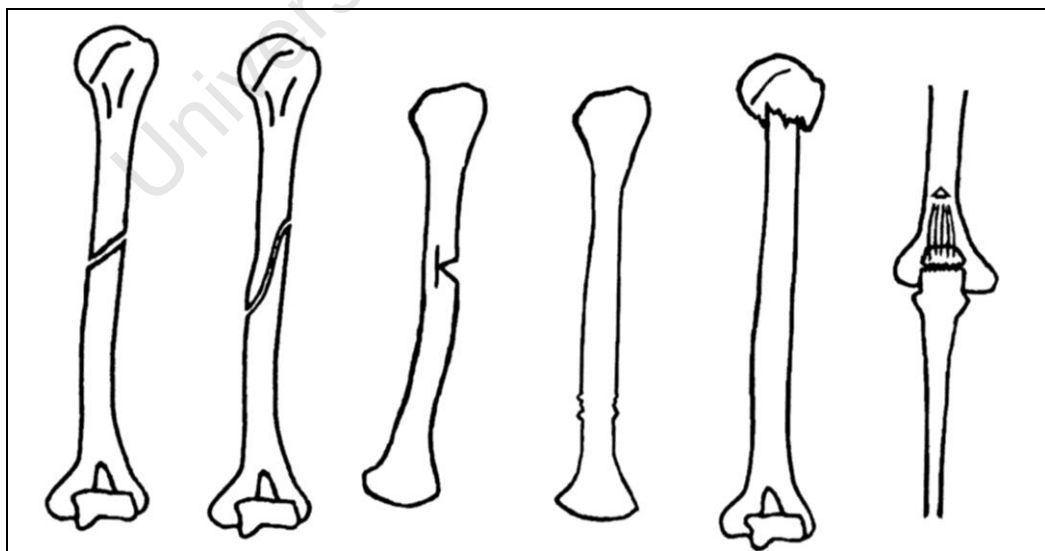


Figure 4.14 Fractures caused by indirect trauma. From left to right: oblique, spiral, greenstick "Butterfly" due to angular force, greenstick due to compression, impaction, and avulsion (after Lovell, 1997).

performed in this study involved recording the size of various attributes of the human skeleton, such as cranial morphology for principle component analysis, and size measurements for statute reconstruction. In addition, measurements were taken in order to produce a catalogue for record purposes.

4.4.1 Cranial and mandibular measurements

Both cranial and mandibular measurements were carried out using spreading or sliding callipers. See Appendix 2 for definitions of osteometric landmarks.

Cranial measurements (Figure 4.15, Figure 4.16 and Figure 4.17) (as described by Buikstra and Ubelaker, 1994)

1. **Maximum Cranial Length:** The distance between glabella (g) and opisthocranium (op) in the midsagittal plane, measured in a straight line.
2. **Maximum Cranial Breadth:** The maximum width of the cranium perpendicular to the midsagittal plane, from euryon (eu) to euryon (eu).
3. **Basibregmatic Height:** The direct distance from the lowest point on the anterior margin of the foramen magnum (ba) to bregma (b).
4. **Bi-stephanic Breadth:** The direct distance between the points where the inferior temporal line intersects the coronal suture.
5. **Bi-asterionic Breadth:** The direct distance between the points where the squamous and lambdoid sutures intersect.
6. **Frontal Sagittal Arc:** The distance between nasion (n) and bregma (b), measured with a string.
7. **Parietal Sagittal Arc:** The distance between bregma (b) and lambda (l), measured with a string.
8. **Occipital Sagittal Arc:** The distance between lambda (l) and opisthion (o), measured with a string.
9. **Transverse Arc:** The direct distance from porion to porion through bregma.
10. **Frontal Sagittal Chord:** The direct distance between nasion (n) and bregma (b).
11. **Parietal Sagittal Chord:** The direct distance between bregma (b) and lambda (l).

12. **Occipital Sagittal Chord:** The direct distance between lambda (l) and opisthion (o).
13. **Foramen Magnum Length:** The maximum distance between basion (ba) and opisthion (o).
14. **Foramen Magnum Breadth:** The greatest width of the foramen at right angles to the length.
15. **Mastoid Height:** The vertical projection of the mastoid process below and perpendicular to the eye-ear plane.
16. **Least Frontal Breadth:** The direct distance between the most medial points on the temporale lines of the frontal bone; from frontotemporale (ft) to frontotemporale (ft).
17. **Nasion-bregma Subtense:** The maximum subtense, at the highest point on the convexity of the frontal bone in the midplane, to the nasion-bregma chord.
18. **Nasion-subtense Fraction:** The distance along the nasion-bregma chord, recovered from nasion (n), at which the nasion-bregma subtense falls.
19. **Nasion-Basion Length:** The direct distance between nasion (n) and basion (ba).
20. **Prosthion-Basion Length:** The distance from basion (ba) to prosthion (pr).
21. **Bizygomatic Breadth:** The direct distance between the most lateral points on the zygomatic arches (zy).
22. **Upper facial Height:** The direct distance from nasion (n) to prosthion (pr).
23. **Outer Bi-orbital Breadth:** The direct distance from the most laterally projecting point on the fronto-zygomatic suture; from frontomalare temporale (fmt) to frontomalare temporale (fmt).
24. **Inner bi-orbital breadth:** the distance between the medial margins of the frontozygomatic sutures.
25. **Interorbital Breadth:** The direct distance from joint at which the sutures between the frontal, maxillary and lacrimal bones meet; from dacryon (d) to dacryon (d).
26. **Orbital Breadth:** The laterally sloping distance from dacryon (d) to ectochochion (ec).
27. **Orbital Height:** The maximum height of the orbit at right angles to the breadth.
28. **Nasal Aperture Height:** The direct distance from nasion (n) to the midpoint of a line connecting the lowest points of the inferior margin of the nasal notches (ns).

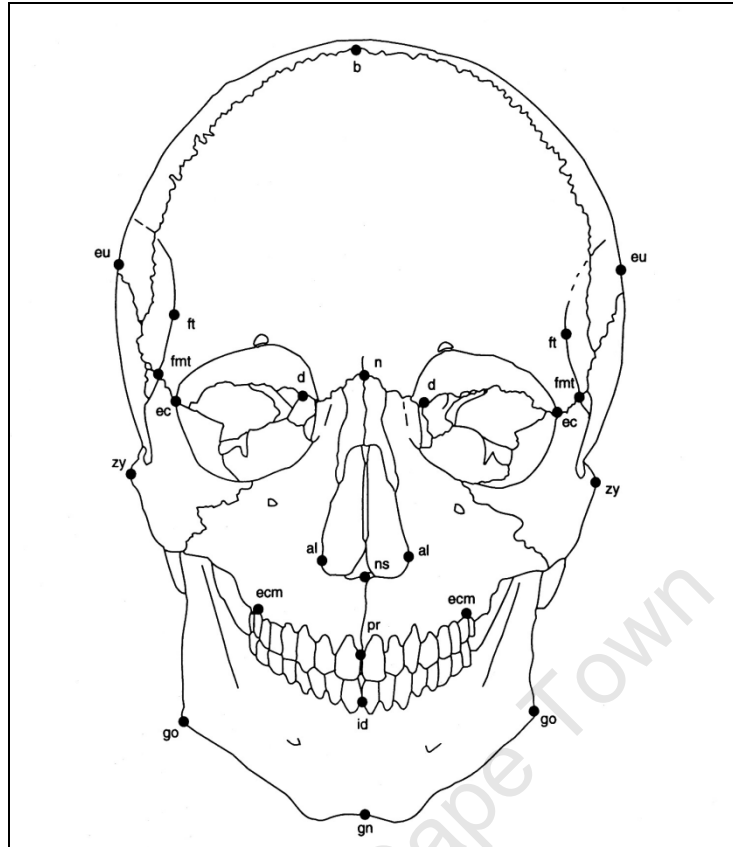


Figure 4.15 Anatomical landmarks of the cranium, anterior view used for biometric cranial measurements (after Buikstra and Ubelaker, 1994: 71).

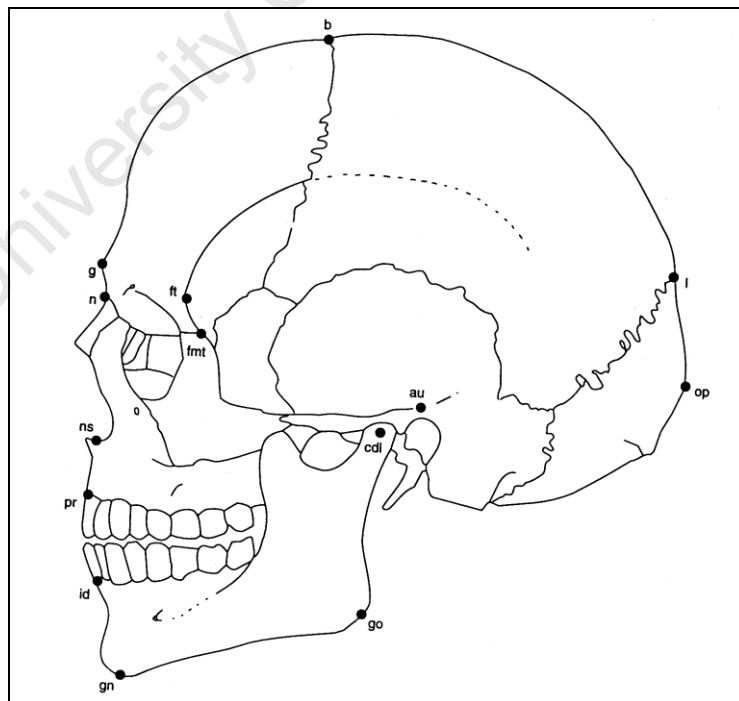


Figure 4.16 Anatomical landmarks on the lateral view of the cranium, used for biometric cranial measurements (after Buikstra and Ubelaker, 1994: 72).

29. **Nasal Aperture Breadth:** The maximum breadth of the nasal aperture (al) at right angles to the nasal height.
30. **Least Nasal Breadth:** The minimum breadth of the nasal apertures (al).
31. **Maxillo-alveolar Length:** The maximum length of the external palate from prosthion (pr) to alveolon (alv).
32. **Maxillo-alveolar Breadth:** The maximum breadth across the alveolar borders of the maxilla measured on the lateral surfaces at the location of the second maxillary molars (ecm).
33. **Palatal Length:** The direct distance from orale (ol) to staphylion (sta).
34. **Palatal Breadth:** The direct distance from endomalare (edm) to endomalare (edm).
35. **Bimaxillary Breadth:** The direct distance between the most inferior point of the suture between the zygomatic arch and the maxilla, zygomaxillare (zm).
36. **Bimaxillary Subtense:** The projection or subtense from subspinale (ss) to the bimaxillary breadth.
37. **Bifrontal Breadth:** The direct distance from frontomalare anterior (fma) to frontomalare anterior (fma).
38. **Naso-frontal Subtense:** The subtense from the bi-frontomalare anterior chord to nasion (n). Use the co-ordinate callipers.
39. **Bi-mastoid breadth:** The direct distance between the right and left mastoids.
40. **Bi-temporal breadth:** The maximum width between the temporal bones perpendicular to the midsagittal plane.

Mandibular measurements (Figure 4.18 and Figure 4.19) (as described by Buikstra and Ubelaker, 1994; Schwartz, 1995)

1. **Maximum breadth outside condyles:** The direct distance between the most lateral points on the two condyles (cdl).
2. **Bicoronoidal breadth:** the direct distance from the right coronion (cr) to the left coronion (cr).
3. **Bigonial breadth:** The direct distance between the right and left gonion (go).
4. **Bimental breadth:** the direct distance between the right and left mental foramen.
5. **Projective height of ramus:** The maximum height from the most superior part of the condyle to the standard horizontal plane.

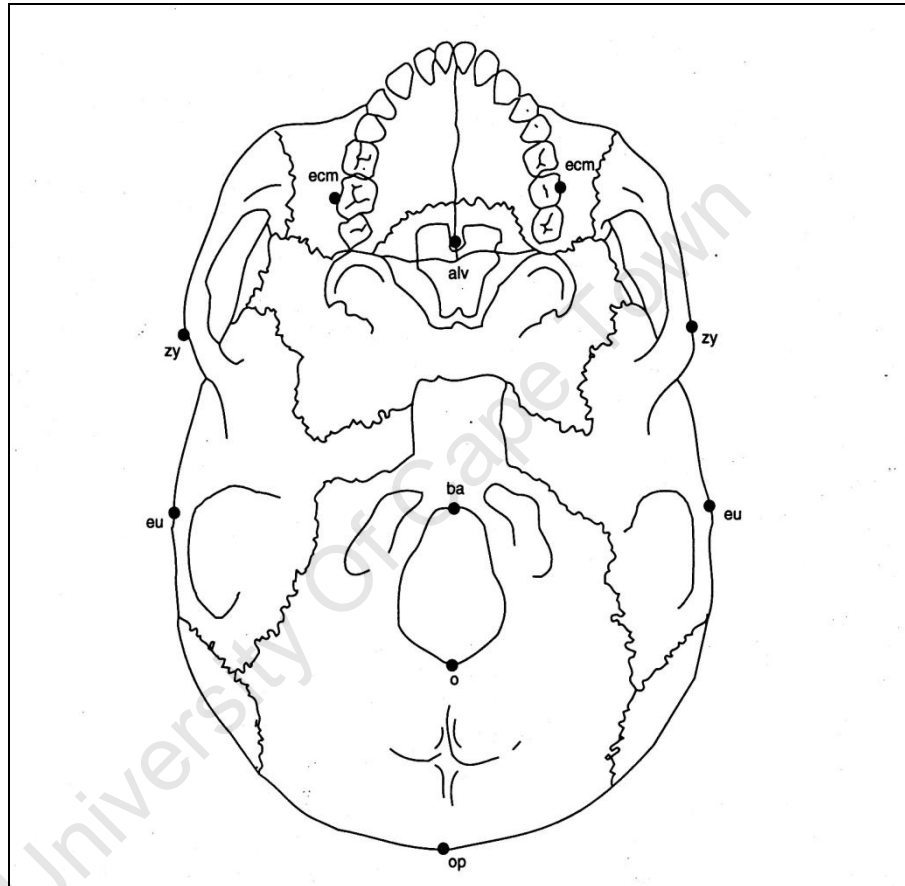


Figure 4.17 Anatomical landmarks on the base of the cranium used for biometric cranial measurements (after Buikstra and Ubelaker, 1994: 73).

6. **Projective height of coronoid:** The mandible is placed so that the left ramus is close to and parallel with the vertical rameal wing, on which the setsquare is moved until it is in contact with the coronoid process.
7. **Projective height of corpus:** measured at the midpoint of the outer alveolar margin of the second left molar tooth.
8. **Projective height of mandible:** The greatest distance from a line joining the most posterior points on the condyles to the most anterior point on the mental symphysis.
9. **Length of condyle:** The maximum length from the medial to the lateral condyle.
10. **Breadth of condyle:** The direct distance from the anterior to the posterior condyle on the articular surface.
11. **Mandibular notch Subtense:** The greatest depth or sigmoid notch from the chord formed by the highest point of the Coronoid process and the most superior point on the condyle.
12. **Minimum width of ramus:** The distance across the “waist” of the ramus, about the level of the molars. This measurement can be taken at any inclination.
13. **Molar-premolar chord:** the chord between the points on the left outer alveolar margins at the middle of the second molar tooth.
14. **Mental foramen breadth:** The direct distance between the right and left mental foramen.
15. **Symphyseal height:** The direct distance from infradentale (idi) to gnathion (gn).
16. **Corpus height at M2:** The direct distance from gnathion (gn) to gonion (go).
17. **Corpus width at M2:** The maximum thickness at the position of the second molar taken perpendicular to the long axis of the body.
18. **Mandibular angle:** The angle formed by the inferior border of the corpus and the posterior border of the ramus – measured with a mandibular board.

4.4.2 Post-cranial measurements

Each individual bone element was measured whenever possible in this study in order to establish sexual dimorphism and stature reconstruction. Long bones were measured using an osteometric board. Diameters were measured with sliding callipers and the

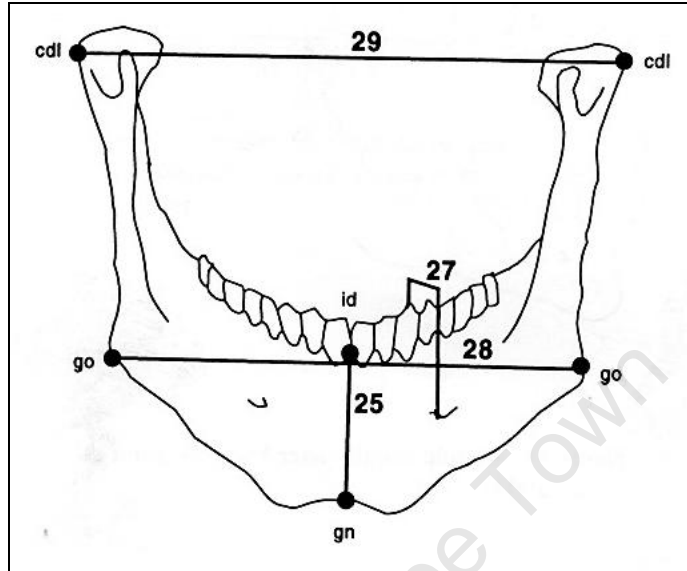


Figure 4.18 Anatomical landmarks on the anterior view of the mandible (after Buikstra and Ubelaker, 1994: 78).

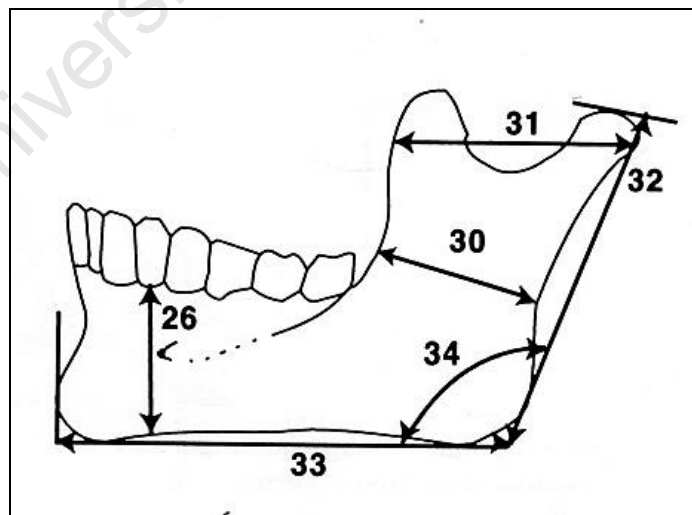


Figure 4.19 Anatomical landmarks on the lateral aspect of the mandible (after Buikstra and Ubelaker, 1994: 78).

circumferences with a measuring tape. Both the left and right bone sides were measured and recorded. All bone measurements were recorded to the nearest millimetre.

The following measurements with recorded as described by Buikstra and Ubelaker (1994):

Clavicle (Figure 4. 20)

1. **Maximum length:** The maximum distance between the most extreme ends of the clavicle.
2. **Antero-posterior diameter:** The distance from the anterior to the posterior surface at midshaft.
3. **Supero-inferior diameter:** The distance from the superior to the inferior surface at midshaft.

Scapula (Figure 4. 21)

1. **Anatomical breadth (height):** The direct distance from the most superior point of the cranial angle to the most inferior point on the caudal angle.
2. **Anatomical length (breadth):** The distance from the midpoint on the dorsal border of the glenoid fossa to midway between the two ridges of the scapular spine on the vertebral border.

Humerus (Figure 4. 22)

1. **Maximum length:** The direct distance from the most superior point on the head of the humerus to the most inferior point on the trochlear with the humeral shaft parallel to the long axis of the osteometric board.
2. **Epicondylar breadth:** The distance of the most laterally protruding point on the epicondyle from the corresponding point on the medial epicondyle.
3. **Vertical diameter of head:** The direct distance between the most superior and inferior points on the border of the articular surface.
4. **Maximum diameter midshaft:** The maximum diameter at midshaft.
5. **Minimum diameter midshaft:** The minimum diameter at midshaft.

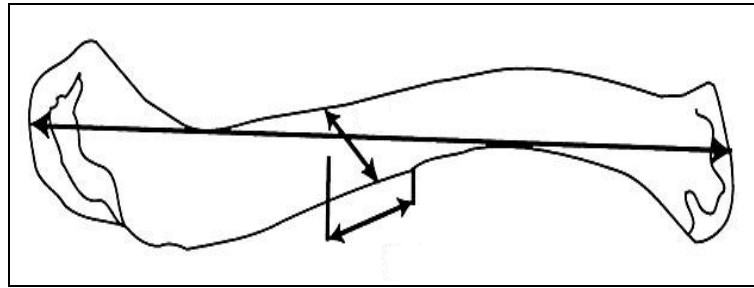


Figure 4.20 Clavicle measurements, superior view of left clavicle (after Buikstra and Ubelaker, 1994: 79).

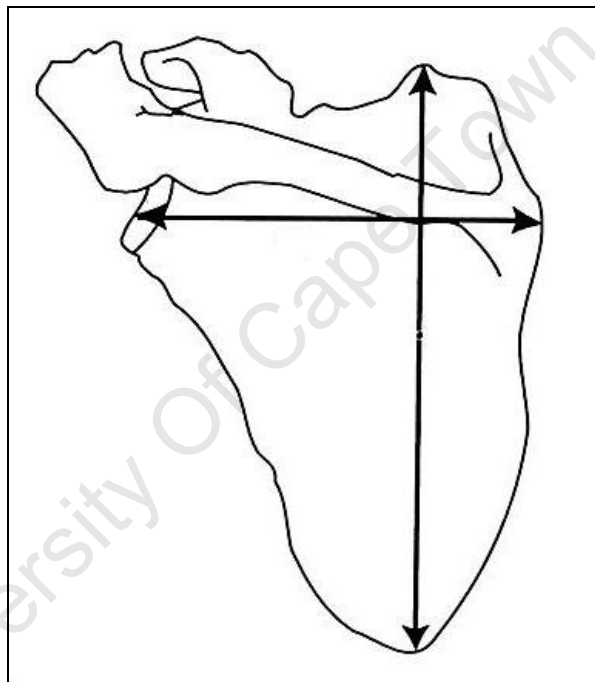


Figure 4.21 Scapular measurements, dorsal view of left scapular (after Buikstra and Ubelaker, 1994: 79).

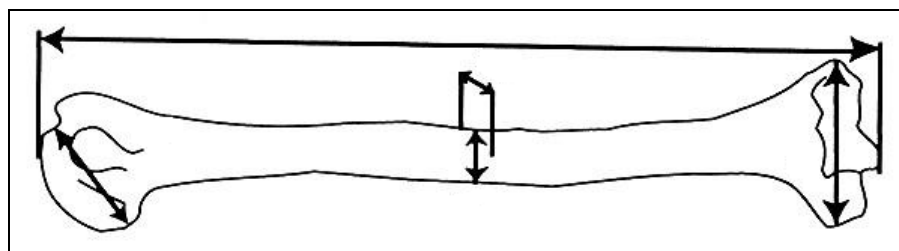


Figure 4.22 Measurements of the left humerus, anterior view (after Buikstra and Ubelaker, 1994: 80).

Radius (Figure 4. 23)

1. **Maximum length:** The distance from the most proximally positioned point on the radial head to the tip of the styloid process without regard for the long axis of the bone.
2. **Antero-posterior diameter:** The distance between the anterior and posterior surfaces at midshaft.
3. **Medio-lateral diameter:** The distance between the medial and lateral surfaces at midshaft.

Ulna (Figure 4. 24)

1. **Maximum length:** The distance from the most superior point on the Olecranon to the most inferior point on the styloid process.
2. **Antero-posterior diameter:** The maximum diameter of the diaphysis where the crest exhibits the greatest development in the antero-posterior plane.
3. **Medio-lateral diameter:** The distance between medial and lateral surface at the level of the greatest crest development.
4. **Physiological length:** The distance between the most distal point on the coronoid process and the most distal point on the inferior surface of the distal head of the ulna.
5. **Minimum circumference:** The least circumference near the distal end of the bone.

Sacrum (Figure 4.25)

1. **Anterior length:** The distance from a point on the promontory positioned in the midsagittal plane to a point on the anterior border of the tip of the sacrum.
2. **Anterior Superior breadth:** The maximum transverse breadth of the sacrum at the level of the anterior projection of the auricular surface.
3. **Maximum Transverse diameter of base:** The direct distance between the two most laterally projecting points on the sacral base measured perpendicular to the midsagittal plane.

Femur (Figure 4. 26)

1. **Maximum length:** The distance from the most superior point on the head of the femur to the most inferior point on the distal condyles.

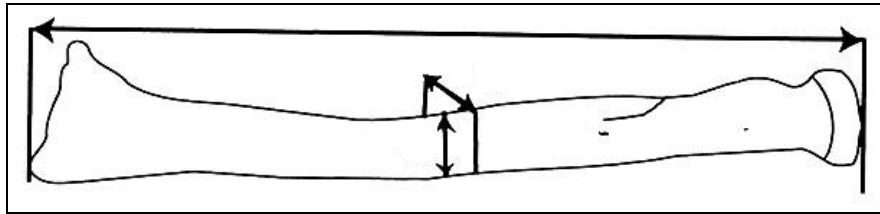


Figure 4.23 Measurements of the left radius, anterior view (after Buikstra and Ubelaker, 1994: 80).

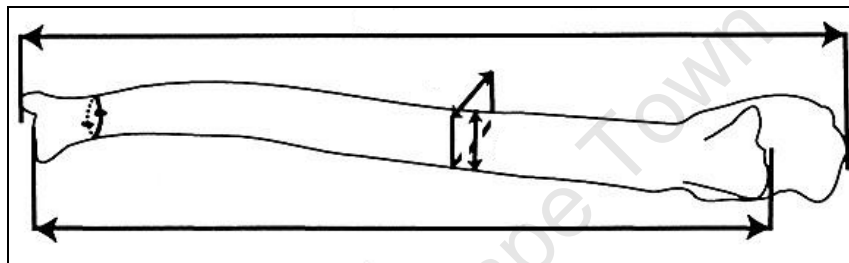


Figure 4.24 Measurements of the left ulna, anterior view (after Buikstra and Ubelaker, 1994: 81).

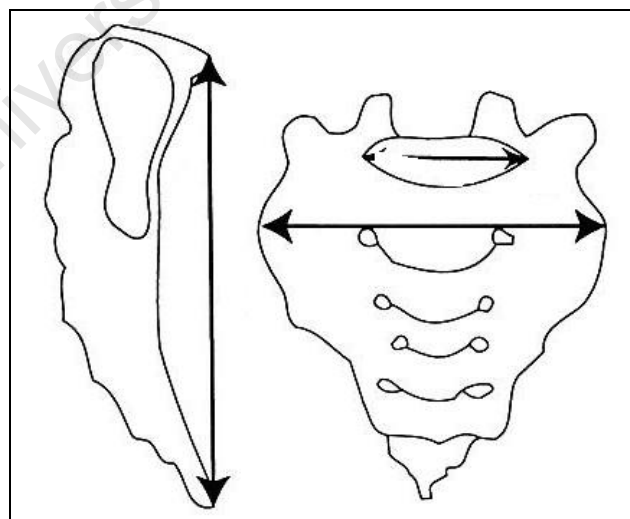


Figure 4.25 Measurements of the sacrum (after Buikstra and Ubelaker, 1994: 81).

2. **Bicondylar length:** The distance from the most superior point on the head to a plane drawn along the inferior surfaces of the distal condyles.
3. **Epicondylar length:** The distance between the two most laterally projecting points on the epicondyles.
4. **Maximum diameter of head:** The maximum diameter of the femur head.
5. **Supero-inferior diameter:** The distance across the narrowest part of the femoral neck (Seidemann, *et al.*, 1998), (Fig. 4.07).
6. **Antero-posterior subtrochanteric diameter:** The distance between the anterior and posterior surfaces at the proximal end of the diaphysis.
7. **Medio-lateral subtrochanteric diameter:** The distance between the medial and lateral surfaces of the proximal end of the diaphysis at the point of its greatest lateral expansion below the base of the lesser trochanter.
8. **Antero-posterior midshaft diameter:** The distance between the anterior and posterior surfaces measured at the midpoint of the diaphysis, at the highest elevation of the linear aspera.
9. **Medio-lateral midshaft diameter:** The distance between the medial and lateral surfaces at midshaft, measured perpendicular to the antero-posterior diameter.
10. **Midshaft circumference:** The circumference measured at the level of the midshaft diameter.

Tibia (Figure 4. 27)

1. **Length:** The distance from the superior articular surface of the lateral condyle to the tip of the medial malleolus.
2. **Maximum proximal epiphyseal breadth:** The maximum distance between the two most laterally projecting points on the medial and lateral condyles of the proximal articular epiphysis.
3. **Maximum distal epiphyseal breadth:** The maximum distance between the two most laterally projecting points on the medial malleolus and the lateral surface of the distal articular epiphysis.
4. **Medio-lateral diameter at nutrient foramen:** The straight-line distance of the medial margin from the interosseous crest at the level of the nutrient foramen.
5. **Antero-posterior diameter at nutrient foramen:** The straight-line distance of the anterior and posterior margins at the level of the nutrient foramen.

6. **Circumference at nutrient foramen:** The circumference measured at the level of the nutrient foramen.

Fibula (Figure 4. 28)

1. **Maximum length:** The maximum distance between the most superior point on the fibula head and the most inferior point on the lateral malleolus.
2. **Maximum diameter at midshaft:** The maximum diameter at midshaft.

Calcaneus (Figure 4. 29)

1. **Maximum length:** The distance between the most posteriorly projecting point on the tuberosity and the anterior point on the superior margin of the articular facet for the cuboid measured in the sagittal plane.
2. **Middle breadth:** The distance between the most laterally projecting point in the dorsal articular facet and the most medial point on the sustentaculum tali.

4.4.2.1 Stature estimation

Stature increases between birth and adolescence. During adulthood, it is relatively unchanging and it decreases towards senility (Brothwell, 1981). Estimation of stature from skeletal material is based on the relationship between lengths of bones, especially the limb bones and living stature (Sjovold, 2000).

The estimation of maximum living stature for the Khoraxa-ams individuals was based on the mathematical method which uses regression formulae (or ratios) proposed by Lundy (1983), and revised by Lundy and Feldesman (1987). These regression formulae are based on the correlation of individual skeletal elements to living stature (Raxter *et al.*, 2006). Long bone regressions produce the most accurate estimations, as long bones are the elements most highly correlated to total stature (Raxter *et al.*, 2006). Lengths of the long bones were used in combination or individually to estimate stature. The bones used to estimate stature included the upper and lower limb bones (humerus, ulna, radius, femur, tibia and fibula). They were measured using a standard osteometric board according to measurements described by Buikstra and Ubelaker (1994). The measurements were recorded in centimetres to one decimal point. Complete bones on the left side were used but substituted with their right counterparts if the former was missing or incomplete. Incomplete bones were excluded from stature estimation. Total

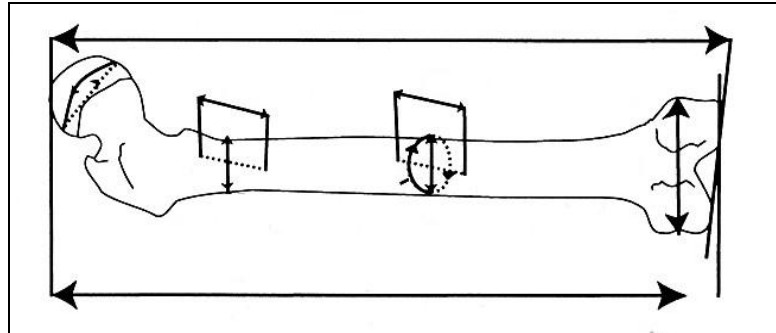


Figure 4.26 Measurements of the left femur, posterior view (after Buikstra and Ubelaker, 1994: 83).

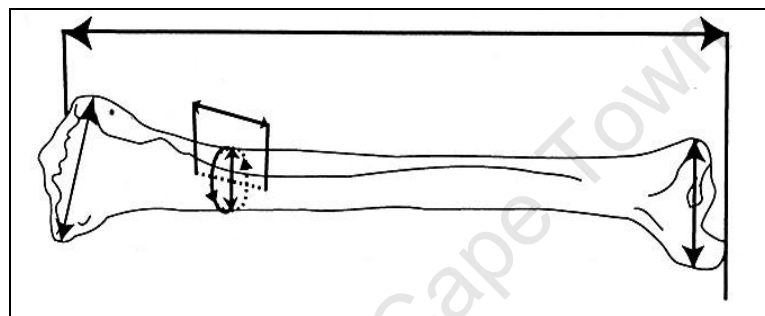


Figure 4.27 Measurements of the left tibia, anterior view (after Buikstra and Ubelaker, 1994: 83).

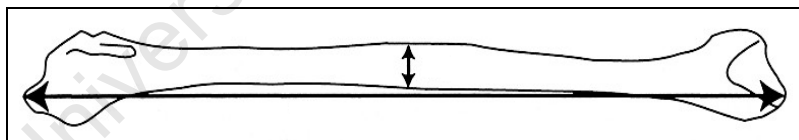


Figure 4.28 Measurements of the left fibula, lateral view (after Buikstra and Ubelaker, 1994: 84).

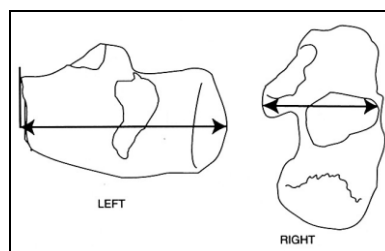


Figure 4.29 Measurements of both the left and right calcaneus (after Buikstra and Ubelaker, 1994: 84).

skeletal height (TSH) was determined using the revised regression formulae by Lundy and Feldesman (1987). Living stature was calculated using revised correction factors by Raxter *et al.*, (2006). Raxter and colleagues (2006) proposed modifications to Fully's technique that incorporated new "soft-tissue" correction factors. They determined that the original factors recommended by Fully, (1956) to convert summed skeletal height to living stature underestimated the necessary correction on average by 2.4 cm (Raxter *et al.*, 2006).

The regression equation for calculating total skeletal height (cm) is as follows (Lundy and Feldesman, 1987):

$$y = c + mx \pm \text{std err. est.}$$

Where *Total skeletal height = intercept + [Bone length (cm) X Slope] ± standard error of estimate* (Dayal *et al.*, 2008).

The equation for estimating „Living Stature’ from total skeletal height (both in cm) when age (years) is not known is as follows (Raxter *et al.*, 2006):

$$\text{Living stature} = 0.996 \times \text{Skeletal height} + 11.7$$

(r = 0.952, SEE = 2.31).

4.4.3 Standardization of measurements and observations

All measurements were recorded in millimetres and where unilateral measurements were required; they were performed on the left side. The right side was used only if the left was missing or distorted. It is assumed that asymmetry is not a major distinguishing factor in the shape of the cranium (Howells 1973).

Most of the measurements selected were direct linear distances as measured with sliding or spreading callipers. Arc curvatures on the vault were measured with a tape measure. A mandibular board was used in taking many of the mandibular dimensions and is specifically required for the mandibular angle. Co-ordinate callipers were used for contour readings when a recording of subtense or projections was required. A

special co-ordinate calliper, the palatometre, was used to determine the palatal height (Morris, 1984).

4.5 Activity Patterns

According to Larsen (1997), bones are living tissue that receive blood and adapt to mechanical and physiological stress. For example, habitual physical activity that requires exertion leads to a readily visible expansion of the related muscle attachments on the skeleton. If this action continues in a particular direction, the bones adapt to the load by thickening in the direction of the plane of motion. Similarly the habit of squatting repetitively has an effect on the axial skeleton, resulting in what is known as „squatting facets.’

4.5.1 Squatting facets

These facets are the result of hyperextension of the articular surface of the long bones or the development of new facets, mainly affecting the distal end of the tibia and fibula as well as the neck of the talus and femur (Brothwell, 1981). On the distal tibia, squatting facets present as extensions of the distal articular surface onto the anterior aspect of the metaphysis. In the talus, they present as extensions of the articular facets similar to those of the tibia, located on the superior surface anterior to the articular facet of the tibia (Buikstra and Ubelaker, 1994).

Squatting facets were observed and analysed on the proximal and distal ends of all tibias present in the sample, and scored according to the following method:

- 0 = none
- 1 = squatting facet at distal end of tibia
- 2 = squatting facet at proximal end of tibia
- 3 = squatting facets at both distal and proximal ends of tibia

4.6 Radiography

The LODOX (Low Dose X-ray) machine, used to X-ray long bones for the examination of Harris lines and estimation of age at death based on radiography (discussed under **Radiographic analysis of long bones**), uses technology that combines low dose radiation with computer generated X-rays. The X-rays are then stored in digital format (dicom) using digital databases. Harris lines measuring approximately one third of the diameter of the shaft were counted. The locations of the lines were measured from the diaphysis, in order to identify the time the insult occurred.

4.6.1 Harris lines

Harris lines (HL) are transverse lines of dense calcification most commonly observed at the epiphyseal ends of long bones and were first described by Harris in 1933 (Larsen 1997). It has been demonstrated that these lines are a result of slowing or total arrest of the growth of a long bone associated with metabolic insults, such as disease and psychological stress (Wells, 1964; Mays, 1995; Larsen, 1997; Piontek *et al.*, 2001; Alfonso *et al.*, 2005). The lines form during the recovery phase following growth arrest, in which mineralization of bone at the growth plate continues in the absence of epiphyseal cartilage deposition (Larsen, 1997).

In the event of repeated episodes of infection or starvation, a series of HL may be formed and their total number and spacing gives an appropriate indication of the age at which these checks of growth occurred (Suter *et al.*, 2008). HL can be produced only during the growing period and therefore give no information about illness in adult life. Their presence is thus a record only of growth arrest, not of a specific disease (Wells 1964).

HL were recorded using LODOX radiographs taken at Groote Schuur Hospital's Trauma Centre by a trained LODOX operator, Mr. Stefan Steiner with the Bio-medical Engineering unit from the Department of Human Biology, UCT. Both right and left distal and proximal ends of the femora and tibia were scanned for HL. Although the tibia is most commonly affected by HL (Larsen, 1997; Alfonso *et al.*, 2005), the femora were also analysed.

The frequency of Harris lines (HL) were classified into the following three groups:

- 0 = none observed
- 1 = one Harris line
- 2 = more than one Harris line

The location of HL, as well as the maximum length of the bone under examination, was measured in order to calculate the age of an individual at the time of the line formation. The method proposed by Byers (1991) was used to estimate the age at which radiopaque transverse line(s) were formed in each „individual’ represented by recovered long bones. This technique presents formulae for calculating the percent of mature bone length at the time of the radiopaque formation for the tibia and femur.

The two measurements required for the formulae proposed by Byers (1991) include:

- 1. The total length from the proximal to the distal end of the bone, parallel to the long axis of the bone and the,
- 2. The distance from the transverse line to the closest end also parallel to the long axis.

The distance between the lines were measured using LODOX computer software, and all measurements were recorded in millimetres. A percentage is obtained that corresponds to an estimated age of line development formulated by Byers (1991).

4.7 Dental Analysis

The analysis of dental morphology, dental wear, oral pathologies and enamel hypoplasia permits the reconstruction of the lifestyle of the individuals being studied (Friedling, 2007). Since enamel does not remodel after formation, a permanent record of dental defects, as a result of either poor nutrition or infectious disease are present (Buikstra and Ubelaker, 1994; Steckel, 2005). Dental caries and tooth wear (attrition and abrasion) were recorded following Buikstra and Ubelaker (1994), and Morris (1984).

4.7.1 Dental condition and inventory

A detailed inventory was recorded for the sample, since the analysis of dental data requires knowledge of the presence and condition of all teeth. Both the maxillary and mandibular teeth were examined and recorded where possible.

Condition of teeth was recorded as follows (modified from Buikstra and Ubelaker, 1994):

- 1 = absent (tooth missing, socket unbroken)
- 2 = present
- 3 = unerupted
- 4 = erupting
- 5 = socket resorbed (ante-mortem tooth loss)
- 6 = socket broken (tooth missing)

$$\text{Ante-mortem loss (\%)} = \frac{\text{Ante-mortem tooth loss} \times 100}{\text{Number of teeth erupted}}$$

$$\text{Post-mortem loss (\%)} = \frac{\text{Post-mortem tooth loss} \times 100}{\text{No. erupted} - \text{No. missing positions} - \text{Ante-mortem loss}}$$

Where *No. erupted* = the assessed number of erupted teeth on the basis of available space for socket positions in jaws. *No. missing position* = number of missing socket positions and related teeth (Maat *et al.*, 2002 courtesy of Friedling, 2007).

4.7.2 Dental wear

Dental wear, or attrition, is the erosion of the occlusal or incisal surface of teeth or the contact points between teeth, caused by mastication, and have proven useful in age at death estimation (Brothwell, 1963; Lovejoy, 1985; Buikstra and Ubelaker, 1994; Prince *et al.*, 2008). However, despite age groups, more extreme attrition is associated with the consumption of coarser foods and dental wear reduces the sites of caries formation (Buikstra and Ubelaker, 1994). Both maxillary and mandibular teeth were examined for dental wear and the findings were recorded.

Dental wear was recorded as follows (see Table 4.02):

- 0 = unworn
- 1 = minimal wear
- 2 – 2.5 = slight / moderate wear
- 3 = heavy wear
- 4 = extreme wear

The anterior, posterior and mean attrition scores were calculated. The anterior attrition score is the average rate of occlusion for the incisors and canines in the sample set, per age category and sex category. The posterior attrition score is the average rate of occlusion for the premolars and molars in the sample set, per age category and sex category. Finally, the mean attrition score is the average between the anterior and posterior attrition scores calculated for the sample set, per age category and sex category (Peckmann, 2002).

4.7.3 Dental disease processes

Non-metric observations for disease processes were analysed on the dentition, both maxillary and mandibular. These include:

1. **Linear enamel hypoplasia:** is characterized as deficiencies in the amount or thickness of the enamel and appear as „bands’ of depression or pitting on the tooth crown, parallel to the long axis of the mandible and/or maxillary body (Brothwell, 1981).
2. **Dental caries:** decay of the teeth that appear as dark eroded regions on the enamel (Buikstra and Ubelaker, 1994).
3. **Ante-mortem tooth loss:** resorption of alveolar bone that results from ante-mortem loss of a tooth (Hillson, 1996).
4. **Abscess:** a resorption of the maxillary or mandibular bone, signifying inflammation of the pulp chamber following excessive attrition or dental caries (Buikstra and Ubelaker, 1994).
5. **Periodontitis:** periodontal disease is defined as a chronic, slowly progressive and destructive inflammatory disease process that affects the periodontium (Larsen, 1997).

Table 4.02 Numerical classification and description of tooth wear categories (adapted from Morris, 1984: 185, Table 4.2)

Stages	Incisors and Canines	Premolars	Molars
0 unworn	No wear	No wear	No wear
1 minimal wear	Enamel only	Enamel only	Enamel only
2 slight wear	Dentine exposed as a thin line or in a mesio-distal ellipse	Cusps worn and one or two dentine patches are visible	All cusps have some exposure of dentine
2.5 moderate wear	Dentine patch is wide	Dentine exposure have coalesced	At least two dentine patches have coalesced but entire occlusal enamel is not yet removed
3 heavy wear	Large dentine exposure with only enamel rim remaining, surface may be flat, cupped or rounded	Enamel rim with one large dentine exposure	One large dentine exposure with enamel rim, but crown wear may be enough to remove rim from one side
4 extreme wear	Tooth crown lost, pulp cavity exposed and roots may be functioning in occlusal surface	Tooth crown lost, pulp cavity exposed and roots may be functioning in occlusal surface	Tooth crown lost, pulp cavity exposed and roots may be functioning in occlusal surface

4.7.3.1 Linear enamel hypoplasia

Dental enamel hypoplasias are deficiencies of enamel thickness that disrupt the normal contour of the crown surface of a tooth and are formed during the secretion of enamel matrix, i.e. amelogenesis (Goodman and Armelagos, 1985; Goodman and Rose, 1990; Schwartz, 1995; Hillson, 1996; Steckel *et al.*, 2002; Ritzman *et al.*, 2008). Linear enamel hypoplasias (LEH) are evident as bands, or sharply-defined horizontal grooves around the circumference of a tooth's crown, but can also be characterized as pits and grooves on the surface of the tooth crown; where the groove is basically an incomplete layer of matrix that did not mineralize properly (Goodman and Rose, 1990; Aufderheide and Rodriguez-Martin, 1998).

Formation of the linear groove of enamel hypoplasia is viewed as an arrest of amelogenic growth during a period of stress, halting the completion of that particular increment. Subsequent growth resumption following termination of the stressful episode will involve the formation of new increment, leaving the previous one as an incomplete layer, viewed from the surface as a zone of thinner enamel representing the 'hypoplastic groove' (Goodman and Rose, 1990; Aufderheide and Rodriguez-Martin, 1998).

These enamel defects may be the result of a wide range of environmental factors associated with the disruption of ameloblastic physiology which include, childhood disturbances, local trauma, hereditary conditions, pre-mature birth, weaning, malnutrition and even deficiencies in vitamins A, C and D (Goodman and Armelagos, 1985; Larsen, 1997; Aufderheide and Rodriguez-Martin, 1998; Steckel *et al.*, 2002). Whatever the cause, prolonged or chronic stress may not produce enamel hypoplasias as the lesions have been related to acute, episodic physiological disruption (Goodman and Rose, 1990; Aufderheide and Rodriguez-Martin, 1998).

Macroscopic observations were performed on all maxillary and mandibular permanent teeth available. Due to the fragmentary state of the crania and dentition present in the sample, it was decided that all anterior and posterior teeth would be examined for LEH generating a broader data set.

The severity of the lesions was recorded and measured using sliding callipers (Danforth *et al.*, 1994):

- 1 = Slight: visible only in low incidence lighting
- 2 = Moderate: visible in ordinary room lighting, ca. 0.5 to 1.2 mm in occluso-cervical width
- 3 = Severe: >1.5 mm in occluso-cervical width

4.7.3.2 Dental caries

Dental caries is a multifactorial, multibacterial disease of the calcified teeth tissues (Aufderheide and Rodriguez-Martin, 1998). They are among the most common observed dental pathologies. Caries appear as foci of eroded regions on the tooth enamel, usually dark-stained from the action of bacteria. Carious lesions are characterized by demineralization of the inorganic portion (enamel and dentine) and destruction of the organic component of the tooth (Buikstra and Ubelaker, 1994; Aufderheide and Rodriguez-Martin, 1998; White, 2000b). It is a progressive disease that is caused by the destruction of enamel, dentine and cement resulting from organic acid production by bacterial fermentation of dietary carbohydrates, especially sugars causing a build-up of dental plaque, and eventually leading to the formation of a cavity (Hillson, 1996; Steckel *et al.*, 2002). Aufderheide and Rodriguez-Martin (1998) state that the vulnerability of teeth to decay is related to tooth type. Cusped teeth (molars and premolars), with their grooves and pits provide a haven for bacterial flourish that could result in higher occurrences of carious lesions when compared to flatter teeth (incisors and canines).

All permanent teeth present were examined for the presence of caries. Carious lesions were scored present when an area of the enamel was compromised enough to be seen with the naked eye. Several carious lesions on one tooth tallied as one observation.

Carious lesions present in the dentition were recorded as follows (adapted from Buikstra and Ubelaker, 1994):

- 1 = none
- 2 = interproximal
- 3 = buccal
- 4 = lingual

- 5 = occlusal

$$\text{Caries frequency (\%)} = \frac{\text{No. carious teeth} \times 100}{\text{No. inspected}}$$

Where *No. carious teeth* = number of teeth with caries (NOT total number of caries). *No. inspected* = number of teeth inspected (Lukacs, 1995)

$$\text{Caries teeth per mouth (\%)} = \frac{\text{No. carious lesions} \times 100}{\text{Total no. of individuals affected by caries}}$$

$$\text{Caries intensity (\%)} = \frac{\text{No. of carious lesions} \times 100}{\text{No. of teeth in sample}}$$

$$\text{Disease Missing Index (DMI) (\%)} = \frac{\text{Total no. of carious teeth} + \text{No. resorbed sockets} \times 100}{\text{Total no. of teeth} + \text{Total no. of resorbed sockets}}$$

4.7.3.3 Ante-mortem tooth loss

The loss of teeth during life could be as a result of trauma and infectious diseases involving the dentition and soft tissue (i.e. gums) of the oral cavity. When a tooth is lost ante-mortem, the alveolar bone begins to resor, resulting in a decrease in the height of the affected maxilla and mandible, at the specific foci (Burns, 1999).

Ante-mortem tooth loss (AMTL) was assessed on all sockets present, both maxillary and mandibular, in the sample. A tooth was scored as lost ante-mortem if there was evidence of alveolar bone resorption. The percentage of ante-mortem tooth loss was determined following the equation proposed by Buikstra and Ubelaker (1994), as described above (see **4.7.1 Dental condition and inventory**).

4.7.3.4 Dental abscesses

Abscesses are caused by an inflammation of the pulp cavity following a spread of bacterial infection at the tooth root where the build up of pus occurs. The accumulation of pus in the pulp cavity creates pressure that eventually causes the destruction and resorption of the surrounding alveolar bone (Aufderheide and Rodriguez-Martin, 1998;

White, 2000b). Dental caries and excessive attrition have been suggested as causality for abscess formation (Aufderheide and Rodriguez-Martin, 1998).

Abscesses can be identified by the presence of a drainage channel leading from the apex of the tooth root through the alveolar bone (Buikstra and Ubelaker, 1994). The presence of abscesses, seen in alveolar bone destruction, was recorded for all maxillary and mandibular elements present.

Criteria proposed by Buikstra and Ubelaker (1994) were used to assess presence and location of the abscess as follows:

- 1 = indicating a buccal or labial alveolar channel
- 2 = denoting a lingual perforation.

The location of the abscess, when present, was also recorded visually in relation to the affected or associated tooth.

4.7.3.5 Periodontal disease

Periodontal disease may be classified according to the stage of the inflammation present, as acute or chronic. Periodontitis is thus recognized as a chronic slowly progressive and inflammatory process affecting one or more of the four components of the periodontium, as a result of infection of the alveolar bone and adjacent tissue (Aufderheide and Rodriguez-Martin, 1998). Anatomically, it appears as a horizontal reduction or recession of the alveolar bone or as a pocket of bone rarefaction (Larsen, 1997). This recession manifests as either horizontal lowering of the crest of the alveolar process or an irregular lowering of the process, with wells expanding into the cancellous bone of the maxilla and/or mandible (White, 2000b). The agents of infection are micro-organisms, and the disease is usually caused by combined effects of large, mixed communities of bacteria. In severe cases, resorption of the alveolar socket can lead to ante-mortem tooth loss of the teeth involved (Larsen, 1997). According to Aufderheide and Rodriguez-Martin (1998), periodontitis is responsible for more antemortem tooth loss than dental caries.

On observation, periodontitis was recorded in both maxillae and mandibulae present in the sample based on criteria classified by Lukacs (1989).

Periodontitis was recorded using scoring degrees of alveolar resorption as follows (Lukacs, 1989):

- 0 = absent – no resorption
- 1 = slight – less than one-half of the root exposed
- 2 = moderate – more than one-half of the root exposed
- 3 = severe – evulsion of the tooth, remnants of the alveolus discernible
- 4 = complete – tooth avulsed, alveoli completely obliterated

4.7.4 Dental modification

The occurrence of dental modification such as filing, chipping, inlays and other alterations, often referred to as dental mutilations, were observed in the mandible and maxilla present in the sample. The deliberate removal of teeth, usually the anterior teeth, termed ablation, was also examined and recorded for the mandible and maxilla. Central and Northern Namibia are known locations where these practices have been recorded historically (Van Reenen 1986). Any other dental modification observed in the sample was recorded.

4.8 Physio-chemical Analysis

It has been stated (İşcan, 2001; Archer *et al.*, 2005; Baraybar and Gasior, 2006; Cattaneo, 2007) that the best approach to a forensic investigation is a multidisciplinary one. Therefore, approaches beyond straight forensic anthropology were used to generate data that would also be useful in identifying the skeletal remains. These include radiocarbon ^{14}C dating to establish a time frame with regards to the period of interment, stable light isotopic analysis for diet reconstruction, and the application of geological sciences in determining the levels of trace elements in order to sort the remains.

4.8.1 Radiocarbon dating

The discovery that as time passes the ^{14}C in dead organic matter decays at a given and measurable rate by Libby *et al.*, (1949) has been an invaluable tool in the estimation of age of organic remains from archaeological sites (Libby *et al.*, 1949; Currie, 2004;

Gravina *et al.*, 2005). Thus, radiocarbon dating is the technique of choice for determining the era of death for human remains up to about 60,000 years (Plastino *et al.*, 2001). The technique measures the ratio of the unstable radioactive isotope ^{14}C , to the stable non-radioactive isotopes ^{12}C and ^{13}C (Currie, 2004). Radiocarbon dating is therefore based on the rate of decay of ^{14}C ; once a living organism dies, the metabolic function of carbon uptake ceases and there is decay rather than uptake of ^{14}C (Libby *et al.*, 1949).

Using the half-life of radiocarbon ^{14}C , 5730 ± 40 years, the specific activity to be expected after any given time interval elapsed since the removal of any carbonaceous material from equilibrium with the life cycle can be calculated (Libby *et al.*, 1949). For living material, this is assumed to coincide with the time of death. Thus, by measuring the ^{14}C concentration or residual radioactivity of a sample of unknown age, it is possible to obtain the count rate per gram of carbon. By comparison with modern concentrations (by convention, 1950 AD), it becomes possible to calculate an estimated date for the time of death of a living organism (Aitken, 1990).

For this study, two bone samples were sent for radiocarbon dating. One sample was analysed at the Quaternary Dating Research Unit (QUADRU) at the CSIR in Pretoria. The other sample was sent to the Groningen Laboratory in Germany for Accelerator Mass Spectrometry (AMS) dating. AMS dating is a more sensitive and efficient dating technique. It differs from other forms of mass spectrometry in that it accelerates ions to extraordinary high kinetic energies before mass analysis. The advantage of AMS is its power to separate a rare isotope from an abundant neighbouring mass (“abundance sensitivity”, e.g. ^{14}C from ^{12}C) (Budzikiewicz and Grigsby, 2006).

It is common practice that bone fragments are sent to the laboratory for dating, as this removes the necessity to sample skeletal material and therefore avoids unnecessary destruction. If however the remains are not fragmentary, then a rib is sent for ^{14}C dating, as this is less detrimental to the analysis of the skeleton and the radiocarbon test only requires ~ 100 g of bone product. However, due to the fact that this study involved co-mingled remains and that the state of preservation was very poor; it was not possible to send either bone fragments or individual ribs. Instead two clavicae from the right side of the skeleton were sent for radiocarbon dating:

- B4108 H4: 1 complete right clavicle
- B4108 H4: 6 right clavicle, missing both medial and lateral ends

This allowed us to assume that each clavicle represented a separate individual; therefore the radiocarbon dates would represent two individuals placed in the same cave.

4.8.2 Stable light isotopic analysis

Stable light carbon and nitrogen isotope measurements have long been used to estimate human dietary practice (DeNiro, 1985; Ambrose, 1991; Cox and Sealy, 1997; Cox *et al.*, 2001). This method of dietary analysis is based on two well-established observations as outlined by DeNiro (1985). The first observation is that bone collagen $^{13}\text{C}/^{12}\text{C}$ and $^{15}\text{N}/^{14}\text{N}$ ratios reflect the corresponding isotope ratio of a mammal's diet. The second is that groups of foods have characteristically different $^{13}\text{C}/^{12}\text{C}$ and/or $^{15}\text{N}/^{14}\text{N}$ ratios. Taken together, the two observations indicate that the isotope ratios of collagen in the bones of a living mammal reflect the amount of these groups of foods that the mammal ate (DeNiro, 1985).

In the case of carbon there are three distinct pathways (C_3 , C_4 , and CAM) through which plants synthesize carbon-containing compounds using carbon dioxide from the atmosphere (Cox and Sealy, 1997). Carbon forms part of the human diet in both plants and animal foods and is a major constituent of bone. The isotopic composition of bone depends upon the foods eaten so that analysis of calcified tissue reports whether the diet was based on C_3 or C_4 foods or a mixture of the two (Cox and Sealy, 1997; Cox *et al.*, 2001). For the purpose of this study C_3 and C_4 are the pathways of interest.

Nitrogen gas (N_2) however, is the most common constituent of the atmosphere and is incorporated into organic nitrogen in a variety of ways. Moreover, nitrogen isotope ratios are not influenced by the photosynthetic pathway (Cox *et al.*, 2001). The study of stable nitrogen isotope ratios ($^{15}\text{N}/^{14}\text{N}$) allows for the ability to distinguish nitrogen-fixing versus non-fixing plants and marine versus terrestrial organisms (Figure 4.28). Nitrogen in bone protein has $^{15}\text{N}/^{14}\text{N}$ derived from the ratios in the foods eaten. In most environments low $\delta^{15}\text{N}$ collagen values indicate a terrestrial diet, while higher values

reflect the consumption of seafood (Ambrose, 1991; Cox and Sealy, 1997; Cox *et al.*, 2001).

Both carbon and nitrogen were used to reflect the diet of the individuals present in the study sample and in turn, determine if a similar dietary pattern was observed among the remains (crania). In addition to determining the dietary pattern, carbon and nitrogen ratios were used to determine a ‚relationship’ between the remains. The assumption being that similar dietary signatures reflect similar foods eaten by a group of individuals with access to foods from a similar region. Therefore, the possibility exists that the individuals were ‚related’ or belong to a closely linked population.

4.8.2.1 Sampling

Isotopic analysis was performed on 14 Crania. Of the 14 crania, seven were male, four female and three indeterminate, ages varied from sub-adult to adult. Since this was an incomplete recovery of the skeletal remains, and the remains were not articulated, it was suggested that the crania (the most represented bone element) be analysed for isotopic measurements. The rationale for using crania was based on the assumption that the crania offer the most morphological variation and therefore is able to generate a substantial data record that can be used to compare and analyze the isotopic results.

Once the appropriate samples were prepared, they were sent to the Light Isotope Mass Spectrometry Laboratory (LIMS), which forms part of the Archaeometry Research Unit based at the Archaeology Department, UCT. The samples were prepared (extraction of bone collagen), according to standard laboratory protocol for the analysis of carbon and nitrogen isotope ratios and measured on a Finnigan MAT 252 light isotope mass spectrometer and a venerable (but venerated) VG602E. Internal laboratory standards were measured at intervals throughout the run to ensure consistency (Cox and Sealy, 1997).

4.8.3 Trace elemental analysis

The hydroxyapatite of which bone mineral is composed is far from chemically pure. There are a host of other elements present in small quantities and given that the concentration of many of these is low, they are termed ‚trace elements’ (Mays, 1998).

The concentration of bone trace elements is such that they are quantified not in terms of percentage of bone weight, but rather in parts per million (ppm) – i.e. micrograms per gram of bone (Mays, 1998).

Various elements found in both the organic (collagen) and the inorganic (mineral or apatite) components of bone tissue have dietary and nutritional significance (Larsen, 1997). Thus, dietary practices are reflected in the trace element concentrations of skeletal remains (İşcan *et al.*, 1989), and are used as a guide to the reconstruction of various aspects of palaeodiet (Klepinger *et al.*, 1986; Mays, 1998). In addition, trace metals function as catalysts for enzymatic activity in human bone and are therefore required to assist with various systems of the body (Rao, 2005).

The purpose for gathering trace elemental data from the Khoraxa-ams remains was to sort the co-mingled remains into separate individuals. The assumption being that trace element concentrations of each bone element would be similar in range between individuals. For example, if the trace element concentration of a single cranium, two humeri, a femur and two tibiae were comparable, it could be assumed that the remains belong to a single individual. It should be noted however, that there may be too much variation in trace element concentrations between bone elements of a single individual as well as diagenetic influences that may alter the elemental concentration post-mortem.

4.8.3.1 Sampling

14 cranial fragments, of which seven were male, four female and three unknown of varying ages were used to measure trace elements within the sample. The samples were prepared to a maximum size of a 2 cm square per bone element, in order for it to fit into the laser ablation sample chamber. When sampling skeletal material, preference is given to dense bone. Multiple fragments (2 or 3) per bone element, at the required size were prepared for the analysis. The prepared bone fragments were sent to the Inductively Coupled Plasma Mass Spectrometry (ICP-MS) facility at the Department of Geological Sciences, UCT where trace elemental analysis was conducted. The analysis was performed on a Perkin-Elmer Elan600 quadruple ICP-MS with a Cetax LSX-200 UV laser. The calcium concentration of 270 mg/g (Heaney, 2000) found in bone material was used as reference material to standardize the analysis.

In this study, 10 trace elements for which there is substantial evidence of importance in the human metabolic and physiological processes (Bogden, 2000) were analysed using the highly sensitive technique of inductively coupled plasma emission spectroscopy (ICP-ES). These include: Magnesium (Mg), Chromium (Cr), Manganese (Mn), Cobalt (Co), Nickel (Ni), Copper (Cu), Zinc (Zn), Selenium (Se), Strontium (Sr) and Molybdenum (Mo). Magnesium is an essential intracellular cation, a co-factor of many basic cellular processes, particularly those involving energy metabolism and is essential to sustain biological life (Heaney, 2000; Rao, 2005). The transition metals, zinc, manganese, copper, cobalt and molybdenum are required for growth, development and maintenance of healthy bones as well as reproduction (Beattie and Avenell, 1992; Rao, 2005).

The 'precision' with which bone trace elements are measured, percentage relative standard deviation (% rsd) is sometimes better for one line analyses than between repeat analysis. Therefore, 'precision' is inversely proportional to the coefficient of variation (relative standard deviation) as derived from multiple determinations on a given sample. A high degree of precision is therefore desirable (Mertz, 1975).

4.9 Statistical Methods

Multivariate analysis was performed using principle component analysis (PCA) to reduce the number of variables and to detect structure in the relationships between variables, so as to classify the variables (StatSoft, Inc 1984-2008). In this study, PCA was used to determine the divergence of male and female cranial variation compared with known data sets, in order to confirm sex. It was also used to distinguish if possible, ethnic affiliation of the study sample compared with known Negro and Khoesan data sets gathered by Morris (1984) as part of his PhD dissertation.

The analysis of principle components examines size and shape variation in three-dimensional space and morphometric distances between populations. This is achieved as PCA calculates the varying principal component of cranial shape (Roseman and Weaver, 2004). The stepwise procedure ranks the measurements in order of their

discriminatory and power of variation. The selected measurements are then used to compute eigenvalues. These eigenvalues are displayed to show the success of the separation produced by the principal components (Powell and Neves, 1999). The relative size of the eigenvalue for each component gives an estimation of the importance of the component in terms of accounting for variation (Morris, 1984).

PCA reduces a large number of intercorrelated measurements to a smaller number of new, uncorrelated variables, allowing a different apportionment of variation for each statistically independent component. Analysing size and statistically independent shape components separately has the potential to be more useful than a simple pooling of the variance, because a range of estimates are produced that can be individually and collectively compared with estimates from other sources (Roseman and Weaver, 2004).

Furthermore, PCA is a descriptive measure that employs the pooled variance-covariance structure of the total data set despite the geographic origin of the samples. The variance structure of the total sample is then converted to a series of orthogonal vectors (the principle components) that summarise variation in craniofacial shape (Manly, 1994 courtesy of Powell and Neves, 1999). According to Powell and Neves (1999), individual observations can be plotted by their resulting principal component scores as a means of describing their multivariate morphological relationship to all other observations (measurements). The resultant scatter plots are the graphical representation of the cranial variables for each group mean and case (Morris, 1984).

Samples or individuals that occupy similar spaces in the PCA plots are morphologically similar and are considered to be, to some degree; genetically similar under the assumption that genotypic covariance is related to phenotypic covariance in the relationship $G = h^2P$ (Cheverud, 1988; Powell and Neves, 1999). The assumption being that the additive genetic variance-covariance matrix (G) among traits is proportional to the phenotypic variance-covariance (P), where h^2 is some constant proportionality (Konigsberg and Ousley, 1995).

PCA statistical analysis was performed using SPSS15.0 for Windows and carried out by Anneli Hardy with the Statistical Consultancy unit, Department of Statistical Science, UCT, Cape Town. The purpose for using PCA over other multivariate

methods such as cranial discrimination analysis is that PCA does not exaggerate between-group variation (Powell and Neves, 1999). This being a very small sample size, a degree of caution was practiced during the examination of the data, as well as their significance. See Appendix 3A for list of cranial measurements used in this study for PCA.

University Of Cape Town

RESULTS

5.1 Total Number of Individuals

A total of 254 bone elements and fragments were recovered from the sinkhole in Khoraxa-ams, north-western Namibia (Table 5.01). Although the remains were co-mingled, it was possible to identify separate bone elements (e.g., femora, humeri, cervical vertebrae, carpals) and associate mandibles with crania, pair upper and lower limbs, and a few axial skeletal bones in this study. Within the sample a total of 22 miscellaneous bones, that could not be identified, were present. These included bones that were fragmented or so poorly preserved that the specific anatomical element could not be identified.

5.1.1 Sorting into individuals

Table 5.02 illustrates the sorting of crania and cranial fragments into individuals. Crania were matched with cranial fragments based on the re-union of broken edges, morphological size as well as preservation. In addition, mandibles were “fitted” to crania based on re-articulation of the temporomandibular joint as well as the degree of occlusion of the dentition.

A total of 16 individual crania were sorted from the co-mingled sample, with 11 crania being “complete” of which eight had paired mandibles. Completeness refers to the ability to measure the cranium using at least 50% of the standard cranial measurements by Buikstra and Ubelaker (1994). In addition, eight crania were observed as adults, four as sub-adults and two crania could not be determined for estimated age at death. Two additional individuals (UCT1O and UCT1P) were represented by cranial fragments of the cranial vault and therefore could not be aged and were not linked to any of the other 14 crania (see MNI count below).

Table 5.01 Summary of the total number of skeletal elements recovered from a cave site in Khoraxa-ams (B4108), north-western Namibia

Bone element	No. of Partial		No. of Complete		Total
<u>CRANIAL</u>					
Cranium	5		11		16
Mandible	2		6		8
	Left side	Right side	Midline	Un-sided	Total
<u>POST-CRANIAL</u>					
Cervical vertebra			16		16
Thoracic vertebra			29		29
Lumbar vertebra			9		9
Ribs	21	21		3	45
Sacrum			2		2
Ilium	1	1		1	3
Ischium		1		2	3
Clavicle	4	4			8
Scapula	4	4			8
Humerus	5	4			9
Ulna	3	2			5
Radius	3	4			7
Carpal		1			1
Metacarpal	6	10			16
Phalanx	3	7		5	15
Femur	5	5			10
Patella	1	2			3
Tibia	4	4			8
Fibula	2	3			5
Tarsal		1		1	1
Phalanx		1			1
Sternum			3		3
Manubrium			1		1
Unidentified					22
TOTAL No. OF SKELETAL ELEMENTS					254

Table 5.02 Fitting individuals based on cranial and mandibular skeletal elements, matching achieved by re-union of broken edges, size and preservation

Crania and Mandibles	B4108* numbered fragments	Comments	Sub-adult or Adult
UCT1A [^]	H1: 4, 43, 61, 55	Complete cranium and mandible	Adult
UCT1B	H1: 7, 37	Complete cranium and mandible	Sub-adult
UCT1C	H1: 10, 20	Complete cranium and mandible	Adult
UCT1D	H1: 5, 30	Complete cranium and mandible, missing right zygoma and maxilla	Adult
UCT1E	H1: 9, 54	Complete cranium and mandible	Sub-adult
UCT1F	H1: 8, 15, 31	Complete cranium missing right half of facial cranium and partial mandible	Adult
UCT1G	H1: 28, 16, 11, 12	Complete cranium missing occipital bone and mandible	Sub-adult
UCT1H	H1: 2, 41, 40, 56	Complete cranium missing lower half of facial cranium and partial mandible	Adult
UCT1I	H1: 1, 60	Complete cranium missing left zygoma, maxilla and mandible	Adult
UCT1J	H1: 44, 63	Base of cranium – occipital, temporal and maxilla	Sub-adult
UCT1K	H1: 6, 14, 29	Complete cranium and mandible	Adult
UCT1L	H1: 3	Complete cranium missing mandible	Adult
UCT1M	H1: 24,25,22,26,34, 35,36	Cranial vault – parietal bones	Unknown
UCT1N	H1: 23, 39, 49, 50, 51	Cranial vault – parietal and occipital bones	Unknown
UCT1O	H1: 19,17,21,33	Cranial vault – right parietal bone	Unknown
UCT1P	H1: 13,18	Cranial vault – right parietal bone	Unknown

*B4108 “H-” numbered fragments refers to the site name and National Museum of Namibia (NMN) accession numbers assigned to each bone element or fragment.

[^]UCT individual sample name assigned to “fitted” bone elements.

A University of Cape Town (UCT) sample number (e.g. UCT1A) was assigned to each of the re-articulated remains, for the purpose of identifying paired or otherwise associated sorted bone elements. UCT1 was used for crania and mandibulae, and sequential numbers (UCT2 to UCT7) were used for post-cranial remains. Separate individuals within each body segment were identified with the letters A to P. This sample number, representing a single individual, was used throughout the study.

Table 5.03 details the sorting of individuals based on the post-cranial skeletal elements present in the sample. Due to the extent of co-mingling, the re-articulation of skeletal elements was performed in terms of separate bones, i.e., the upper and lower limbs were “fitted” independently by the re-articulation of broken edges, size dimorphism and state of preservation. It should be noted that each post-cranial region was labelled separately and that UCT2A is not necessarily the same individual as UCT3A, UCT4A and UCT7A, but rather that UCT2E, UCT4C and UCT7A is likely to be the same person.

Seven “individuals” were sorted according to the vertebral bones as well as the ribs. It was not possible to re-articulate complete vertebral columns due to the low frequency of vertebrae available in the sample. Thus, vertebrae that appeared similar in their state of preservation and that re-articulated with each other were sorted into possible individuals. Emphasis was placed on the re-articulation of vertebrae according to the various vertebral types, e.g., cervical, thoracic and lumbar. The upper limbs were sorted into four individuals, represented by a pair of clavulae, scapulae, humeri, ulnae and radii where possible. The lower limbs were sorted into five individuals based on paired femora, tibiae and fibulae combined.

Of the four individuals sorted by the upper limb bones, three were observed as adult and one as a sub-adult. With regards to the lower limbs, of the five individuals four were observed as adult and one as a sub-adult. One sub-adult and six adults were observed in the sorting of the vertebral remains. However, it was not possible to determine the age distribution of the rib fragments as they were extremely fragmented and most of the sternal ends were either missing or so poorly preserved that re-articulation or sorting was not possible.

According to Tables 5.02 and 5.03, the total number of individuals present in the sample is 16 based on the crania, however based on the upper and lower limbs; four and five individuals are present in the sample respectively. Although the vertebrae and ribs represent a total of seven individuals respectively, it cannot be assumed that this is the total number of individuals present in the sample due to the possibility that these vertebrae or ribs belong to a single individual rather than separate individuals.

5.1.2 Minimum number of individuals

The minimum number of individuals (MNI) analysed in this study is presented in Tables 5.04 and 5.05 in the form of frequency tables. Table 5.04 shows that the MNI represented by the cranial bones is 16 based on the highest minimum number count of the parietal and occipital bones respectively. The side to which each bone belonged was determined for all cranial bones in the sample.

The MNI represented by the post-cranial bone elements (Table 5.05) was five based on the highest minimum number count for femora and humeri present in the sample. It should be noted that this is an estimate of the MNI based on the post-crania recovered. Not all the post-cranial bones were sided or positively identified due to the remains being poorly preserved. This is particularly true for the rib bones as well as the vertebrae, as they were extremely fragmented. In addition, not all post-cranial skeletal elements were recovered. Both the coccyx and pubic bones, with exception of two sacra, were not represented within the sample. The bones of the hands and feet were not included in the MNI count as they are very few and offer little assistance in the determination of MNI. For the purpose of this study, the cranial MNI of 16 will be used as the total number of individuals represented in the sample set.

Table 5.03 Fitting individuals based on post-cranial skeletal elements, matching achieved by re-union of broken edges, size and preservation

Post-cranial	B4108* numbered fragments	Comments	Sub-adult or Adult
<u>Vertebrae</u>			
UCT2A^	H2: 8, 14, 20	Atlas and axis vertebrae (C1 and C2)	Adult
UCT2B	H2: 5, 34, 36	T7 – T9	Adult
UCT2C	H2: 3, 29, 35, 37 H2: 18	Vertebral body of L1 C4	Adult
UCT2D	H2: 19, 22, 25, 26, 39	Vertebral body of T1 and T5	
UCT2E	H2: 6, 7, 13, 18, 31	T2 and C3, C4, C5, C6	Adult
UCT2F	H2: 11, 23	T3 and T4	Sub-adult
UCT2G	H2: 17, 30, 32, 40 H2: 27, 41	T4 – T7 T9 and T10	Adult Adult
<u>Rib fragments</u>			
UCT3A	H3: 32, 22, 27, 34, 40, 35, 33, 28, 23, 14	Right and left rib fragments with left rib 1	Unknown
UCT3B	H3: 16, 41, 5, 46, 20, 47, 18, 38	Right and left rib fragments	Unknown
UCT3C	H3: 49, 44, 9	Right rib fragments	Unknown
UCT3D	H3: 1, 10, 6, 45, 17, 19, 39, 7	Sternum; Right and left rib fragments with left rib 1 and right rib 2	Unknown
UCT3E	H3: 31, 24	Right rib 2 and left rib fragment	Unknown
UCT3F	H3: 42, 48, 26, 13, 43, 15, 8, 11, 36	Right rib fragments	Unknown
UCT3G	H3: 30, 29, 12, 21	Right and left rib fragments	Unknown
<u>Upper Limbs</u>			
UCT4A	H4: 1, 4, 9, 10 and H5: 17, 16, 9, 14, 3, 4 and H7: 17	Paired clavicae, scapulae, humeri, ulnae and radii	Adult
UCT4B	H4: 5, 2, 14, 12 and H5: 20, 15, 6, 7, 13	Paired clavicae, scapulae, humeri, radii. Left ulna	Adult
UCT4C	H4: 3, 8, 13, 11 and H5: 19, 23, 1, 8, 2	Paired clavicae, scapulae, humeri. Left radius	Sub-adult
UCT4D	H4: 6, 7, 16, 15 and H5: 18, 22, 5, 10, 11, 12	Paired clavicae, scapulae, humeri, ulnae and radii	Adult
UCT 4E	H5: 21	Unpaired left humerus	Adult
<u>Lower Limbs</u>			
UCT7A	H7: 4, 7, 13, 18, 21	Paired femora and tibiae	Sub-adult
UCT7B	H7: 9, 8, 16, 23, 28, 25	Paired femora, tibiae and fibulae	Adult
UCT7C	H7: 3, 2, 6, 20, 14, 22, 24, 27	Paired femora, tibiae and fibulae	Adult
UCT7D	H7: 1, 10, 12, 15, 26	Paired femora, tibiae and right fibula	Adult
UCT7E	H7: 5, 19	Unpaired right femur	Adult
UCT7F	H7: 11	Unpaired left femur	Adult

*B4108 “H-” numbered fragments refers to the site name and National Museum of Namibia (NMN) accession numbers assigned to each bone element or fragment.

^UCT individual sample name assigned to “fitted” bone elements. Each post-cranial region is labelled separately, therefore all the bones labelled “A” are not from the same individual.

Table 5.04 The minimum number of individuals represented by crania from the B4108 site

Bone element	Left side	Right side	Midline structure	Minimum number (MNI)
Frontal			14	14
Parietal	15	16		16
Occipital			16	16
Temporal	15	12		15
Greater wing of Sphenoid	12	10		12
Zygomatic	9	9		9
Maxilla	9	11		11
Nasal	10	10		10
Lacrimal	4	8		8
Ethmoid	8	9		9
Mandible			8	8
Highest minimum number count				16

Table 5.05 The minimum number of individuals represented by post-cranial bones from the B4108 site

Bone element	Left side	Right side	Midline structure	Unidentified fragments	Total Bones
<u>Cervical vertebrae</u>				5	5
C1			1		1
C2			3		3
C3			1		1
C4			3		3
C5			1		1
C6			1		1
C7			1		1
TOTAL BONES					16
<u>Thoracic vertebrae</u>				13	13
T1			3		3
T2			1		1
T3			1		1
T4			2		2
T5			2		2
T6			1		1
T7			2		2
T8			1		1
T9			2		2
T10			1		1
T11			-		-
T12			-		-
TOTAL BONES					29
<u>Lumbar vertebrae</u>				8	8
L1			1		1
L2			-		-
L3			-		-
L4			-		-
L5			-		-
TOTAL BONES					9
Sacrum			2		2
Coccyx			-		-
Rib fragments	21	21		3	45
Sternum			2		2
Manubrium			1		1
Ilium	1	2		1	4
Ischium		1		2	3
Pubis	-	-			-
Clavicle	4	4			8
Scapula	4	4			8
Humerus	5	4			9
Ulna	3	2			5
Radius	3	4			7
Femur	5	5			10
Patella	1	2			3
Tibia	4	4			8
Fibula	2	3			5
Highest minimum number count				5*	

* From humerus and femur.

5.2 Sex Distribution

The estimation of sex using sexually dimorphic cranial features (Table 5.06) resulted in the identification of seven males, five females and four unknown individuals in the sample. The four unknown individuals, (UCT1M, UCT1N, UCT1O and UCT1P) were not included in further analyses of the crania in this study because they were severely fragmented and offered little information pertaining to identification and morphological dimorphism.

5.2.1 Sex distribution – Distal humerus method

All humeri with intact distal ends in the sample set were analysed using four traits of the distal humerus method. “Estimated sex” was obtained based on a combination of all four visual traits (Rogers, 1999; Vance, 2007). In the Khoraxa-ams sample nine intact humeri were found, five of which presented as males, three as females, and one was not sexed because it presented both male and female characteristics (Table 5.07). The latter humerus was an individual under 18 years of age, and thus fell into the sub-adult category.

The standard visual method based on size dimorphism at the site of muscle attachments (Table 5.08) sexed three humeri as females (as did Rogers’, 1999 method, see Table 5.07), thus showing a high degree of confidence in sexing the female humeri in the sample. The standard visual method could not however identify the sex of two humeri. Both these humeri presented as an individual less than 18 years of age. Of the two unsexed sub-adults, one was positively identified as male using the distal humeri method (Table 5.07). These results show an 88.9% confirmation of existing adult sex estimation and an 11.1% difference from existing sex estimation.

5.2.2 Sex distribution – Femoral neck method

Using the femoral neck method, two of the 10 intact femora presented as male, five as female, and three could not be sexed as both femora were missing the femoral head and neck region (Table 5.09). Of the three unsexed femora, two (H7: 1 and H7: 5, 19) were positively identified as male using the standard morphological method based on size

Table 5.06 Sex distribution for Khoraxa-ams site based on cranial regions following guidelines by Buikstra and Ubelaker, 1994 using The Five Point Scale* scoring system

UCT Sample No.	B4108 no. For Crania	Nuchal crest	Occipital protuberance	Mastoid process	Supra-orbital margin	Glabella	Orbital socket	Mental eminence	Mandible (chin)	Gonial flare	Mean score	Estimated SEX
UCT1A	H1: 4,43,61	4	4	4	4	4	4	5	4	4	4.1	MALE
UCT1B	H1: 7	-	1	2	3	1	1	1	1	-	1.4	FEMALE
UCT1C	H1: 10	5	-	4	4	4	4	5	3	4	4.1	MALE
UCT1D	H1: 5	4	4	5	4	5	5	5	3	5	4.4	MALE
UCT1E	H1: 9	2	2	1	2	1	2	3	1	1	1.7	FEMALE
UCT1F	H1: 8,15	4	5	5	4	-	3	5	-	4	4.3	MALE
UCT1G	H1: 28,26,11,12	-	-	3	2	2	2	-	-	-	2.3	FEMALE
UCT1H	H1: 2,41	5	5	4	-	4	-	5	3	4	4.3	MALE
UCT1I	H1: 1,60	-	2	1	2	2	2	-	-	-	2.3	FEMALE
UCT1J	H1: 44,63	5	4	5	-	-	5	-	-	-	4.3	MALE
UCT1K	H1: 6	-	2	2	1	1	2	-	-	-	1.6	FEMALE
UCT1L	H1: 3	5	4	5	4	4	4	-	-	-	4.3	MALE
UCT1M	H1: 24,25,22, 26,34,35,36	-	-	-	-	-	-	-	-	-	-	UNKNOWN
UCT1N	H1: 23,39,49, 50, 51	-	-	-	-	-	-	-	-	-	-	UNKNOWN
UCT1O	H1: 19,21,33,17	-	-	-	-	-	-	-	-	-	-	UNKNOWN
UCT1P	H1: 18,13	-	-	-	-	-	-	-	-	-	-	UNKNOWN

* - = undetermined sex, Insufficient data available for sex determination, therefore not included in score; 1= female, There is little doubt that the structures are more likely female than male; 2 = probable female, The structures are more likely female then male; 3 = ambiguous sex, Sexually diagnostic features are ambiguous; 4 = probable male, The structures are most likely male than female; 5 = male, there is little doubt that the structures represent a male.

Table 5.07 Sex estimation using the distal humeri method

Bony Features Used in Distal Humeri Method*						Mean Score	Estimated SEX
UCT Sample No. [§]	B4108 No. For Humeri	Trochlear constriction	Trochlear symmetry	Olecranon fossa shape	Angle of medial epicondyle		
UCT4A	H5: 18 L	1	1	2	2	1.5	Male
	H5: 22 R	1	1	2	2	1.5	Male
UCT4B	H5: 15 L [^]	3*	4	4	4	3.75	Female
	H5: 20 R	3	4	4	4	3.75	Female
UCT4C	H5: 16 L	-	1	1	3	1.7	Male
	H5: 17 R	2	1	1	2	1.5	Male
UCT4D	H5: 19 R	-	-	-	-	-	Unknown
	H5: 23 L	3	4	4	4	3.75	Female
UCT4E	H5: 21 L	2	2	2	2	2	Male

*Adapted from Rogers, 1999. [§]UCT sample number assigned to „fitted” individuals.

[^]Refers to either the Left or Right bone element.

[¥]Scoring: - =unobservable; 1 = male; 2 = probable male; 3 = probable female; 4 = female. SA = sub-adult.

Table 5.08 Sex distribution using the distal humeri method in comparison with standard visual methods (adapted from Friedling, 2007)

Sex	Standard Visual Method	Distal Humeri Method
Male	4	5
Female	3	3
Unknown	2	1
Total	9	9

Table 5.09 Estimation of sex based on femora present in study sample, comparing standard morphological traits (France, 1998) to the femoral neck method (after Seidemann, *et al.*, 1998)

UCT Sample No.	B4108 No. For Femora		Standard Morphological Traits				Femoral Neck Method		
			Linea aspera	Muscle attachments	Mean Score	Est. SEX	SID [‡]	Sex = 0.510 X SID – 15.356	Estimated SEX
UCT7A	H7: 7	L*	-	-	-	Unknown	30.1	0.00	Unknown
	H7: 4	R	-	-	-	Unknown	21.58	-4.35	Female
UCT7B	H7: 8	R	1 [^]	1	1	Male	32.76	1.35	Male
	H7: 9	L	1	1	1	Male	31	0.45	Male
UCT7C	H7: 3	R	3	3	3	Female	29.2	-0.46	Female
	H7: 2,6	L	4	4	4	Female	25.7	-2.25	Female
UCT7D	H7: 1	R	2	1	1.5	Male	-	-	Unknown
	H7: 10	L	3	2	2.5	Unknown	25.7	-2.25	Female
UCT7E	H7: 5,19	R	2	3	2.5	Male	-	-	Unknown
UCT7F	H7: 11	L	4	-	4	Female	25.26	-2.47	Female

[‡]SID = Supero-inferior diameter.

*Refers to either the Left or Right bone element.

[^]Scoring: - = unobservable; 1 = male; 2 = probable male; 3 = probable female; 4 = female.

Table 5.10 Summary of sex distribution using femoral neck method (SID)

Sex	Standard Visual Method	Femoral Neck Method
Male	4	2
Female	3	5
Unknown	3	3
Total	10	10

Table 5.11 Summary of sex identification of skeletal remains based on various methods

Sex identification methods	No. Males	No. Females	Unknown	Ratio of Male:Female
Cranioscopic	7	5	4	1.4:1
Distal humerus	5	3	1	1.6:1
Femoral neck	2	5	3	1:2.5

dimorphism at the site of muscle attachments (France, 1998), while the other unsexed femur (H7: 7) could not be sexed using the standard morphological method either (Table 5.10). Two femora visually sexed by the standard method as unknown, presented as female using the femoral neck method.

5.2.3 Sex distribution – Summary of various methods

Table 5.11 summaries the sexual distribution of skeletal elements within the sample, where features of sexual dimorphism are observable, based on various sexing methods. Based on the cranial features, there were approximately as many males as there were females recovered from the cave. The male to female ratio is 1.4:1. The estimation of sex was indeterminate for four crania, UCT1M, UCT1N, UCT1O and UCT1P due to the absence of sexual dimorphic features. According to the distal humerus method, there are five males and three females represented in the sample, with a ratio of 1.6:1 respectively. Sex could not be determined for one individual as the features necessary to determine sexual dimorphism were unobservable. Finally, the femoral neck method identified two males and six females in the sample (1:3). Sex could not be determined for two femora due to the absence of their femoral heads. Due to the disarticulation of the remains, the final count of male and female individuals within the sample was therefore based on the crania. Not only were the crania the most frequent bone element represented in the sample, the crania were also used to determine the minimum number of individuals recovered from the cave.

5.3 Distribution of Age at Death

The estimation of age at death was achieved based on the closure of cranial sutures in adult individuals (Table 5.12) as well as the state of dental eruption observed in juvenile and sub-adult individuals (Table 5.13). The examination of relative tooth wear was used as a means to separate the adult individuals within the sample based on the degree of visible occlusal wear (Table 5.14).

According to cranial suture closure (Table 5.12), six crania were identified as being over the age of 40 years and five as under the age of 40. Age at death could not be identified for

three individuals; UCT1J, UCT1M and UCT1N because of post-mortem damage obscuring most of the cranial sutures and reducing observability. It should be noted that given the MNI of 16, based on cranial bones within the sample, only 11 crania could be analysed for cranial suture closure. Cranial sutures were present on three individuals, however they were too poorly preserved to be aged, while two more individuals did not have preserved sutures and therefore could not be analysed. Single or multiple cranial bones that were fractured along their sutures therefore represent the remaining five crania that could not be analysed.

Table 5.13 details the estimation of age at death based on the eruption of the third molar (M3), to determine the presence of adult and sub-adults crania in the sample. Based on the eruption of M3, 11 crania presented as adults and one as sub-adult. The percentage of adult individuals as determined by the eruption of M3 is 91.7% of the total number of crania with M3 sockets or teeth available for analysis, only one individual was aged as a sub-adult.

Table 5.14 indicates the degree of occlusal tooth wear visible on the maxillary and mandibular molars, where available. The patterns of tooth wear visible on the three (M1, M2 and M3) molars were used to separate the adult individuals into more defined adult age range. However, it should be noted that age-attribution scores are a relative age at death estimation and should be used in conjunction with more specific age estimates. According to Table 5.14, three individuals were aged over 45 years; one individual UCT1B was aged between 17 – 25 years, which is consistent with the unerupted state of the M3 on the same specimen. Of the remaining eight individuals, four were estimated to have an age between 33 – 45 years, and four presented between the ages of 25 – 35.

A summary of the estimation of age at death based on cranial suture fusion, dental eruption of the third molar and occlusal tooth wear is presented in Table 5.15. The estimation of age as determined by the closure of cranial sutures correlates with occlusal tooth wear in that six individuals were estimated to be over the age of 40 according to cranial suture closure, while seven individuals were estimated to be

Table 5.12 Age at death estimation for crania recovered from Khoraxa-ams using cranial suture fusion* (Buikstra and Ubelaker, 1994)

UCT Sample No. And B4108 No. For crania														
	UCT1A	UCT1B	UCT1C	UCT1D	UCT1E	UCT1F	UCT1G	UCT1H	UCT1I	UCT1J	UCT1K	UCT1L	UCT1M	UCT1N
	H1: 4, 43,61	H1: 7	H1: 10	H1: 5	H1: 9	H1: 8, 15	H1: 28, 16, 11, 12	H1: 2, 41	H1: 1, 60	H1: 44, 63	H1: 6	H1: 3	H1: 24, 25, 22, 26, 34, 35, 36	H1: 23, 39, 49, 50, 51
<u>Cranial Suture Closure</u>														
Midlambdoid	1	1	1	2	1	2	1	1	1	1	2	3	0	0
Lambda	3	1	2	3	2	2	3	3	3	1	2	2	0	-
Obelion	3	2	3	2	1	2	2	3	2	-	2	3	-	1
Anterior sagittal	1	0	3	3	2	1	2	3	2	-	3	3	-	0
Bregma	1	0	3	3	0	1	1	3	1	-	3	3	-	-
Midcoronal	2	0	2	3	2	2	2	3	2	-	2	3	-	-
Pterion	2	1	2	3	2	2	2	2	2	-	2	2	-	-
Sphenofrontal	2	1	1	3	2	1	2	-	2	-	2	2	0	-
Inferior sphenotemporal	3	1	2	3	2	2	2	2	2	1	2	-	1	0
Superior sphenotemporal	3	1	2	2	1	3	3	2	3	1	2	2	0	-
Mean Score	2.1	0.8	2.1	2.7	1.5	1.8	2	2.2	2	1.0	2.2	2.6	0.2	0.25
Adult Age Categories[‡]	> 40	< 40	> 40	> 40	< 40	< 40	< 40	> 40	< 40	Unknown	> 40	> 40	Unknown	Unknown

*Score: Blank = unobservable; 0 = open; 1 = minimal closure; 2 = significant closure; 3 = complete obliteration. Adapted from Buikstra and Ubelaker, 1994.

^Cranial suture closures unobservable due to post-mortem damage, as a result there was insufficient bone available to perform complete analysis.

‡Adult age categories: 1 or 2 = < 40 years of age; 2 or 3 = > 40 years of age.

Table 5.13 Age at death estimation for crania recovered from Khoraxa-ams using dental eruption (Buikstra and Ubelaker, 1994)

UCT Sample No.	B4108 No. for Crania	Dental eruption of M3	Estimated AGE
UCT1A	H1: 4, 43, 61, 55	Yes	Adult
UCT1B	H1: 7, 37	No	Sub-adult
UCT1C	H1: 10, 20	Yes	Adult
UCT1D	H1: 5, 30	Yes	Adult
UCT1E	H1: 9, 54	Yes	Adult
UCT1F	H1: 8, 15, 31	Yes	Adult
UCT1G	H1: 28, 16, 11, 12	Yes*	Adult
UCT1H	H1: 2, 40, 41	Yes*	Adult
UCT1I	H1: 1, 60	Yes	Adult
UCT1J	H1: 44, 63	Yes*	Adult
UCT1K	H1: 6, 14, 29	Yes	Adult
UCT1L	H1: 3	Yes	Adult

*Third molar erupted but missing post-mortem.

Table 5.14 Estimation of age at death using relative tooth wear (attrition) as a means to separate adult individuals within the sample (Brothwell, 1981)

UCT Sample No.	B4108 No. for Crania	Occlusal tooth wear*			Estimated AGE [^]
		M1	M2	M3	
UCT1A	H1: 4, 43, 61, 55	5+	4+	3	About 45 +
UCT1B	H1: 7, 37	1	-	-	17 – 25
UCT1C	H1: 10, 20	5++	5	3+	About 45 +
UCT1D [‡]	H1: 5, 30	3+	3	2+	33 – 45
UCT1E	H1: 9, 54	3-	2	2	25 – 35
UCT1F	H1: 8, 15, 31	3-	2	-	25 – 35
UCT1G	H1: 28, 16, 11, 12	3	2	-	25 – 35
UCT1H [‡]	H1: 2, 40, 41	4+	4	-	33 – 45
UCT1I	H1: 1, 60	4	2+	2	25 – 35
UCT1J	H1: 44, 63	5+	-	-	About 45 +
UCT1K	H1: 6, 14, 29	4+	3-	2+	33 – 45
UCT1L	H1: 3	-	3+	-	33 – 45

*Scoring based on molar wear as proposed by Brothwell, 1981.

[^]Age categories (years) as signed by Brothwell, 1981.

[‡]Only the mandible was analysed, due to absence of the maxilla.

(Note: Some patterns are more common than others, and there are minor differences between upper and lower dentitions.)

Table 5.15 Summary of estimating age at death based on cranial suture closure, dental eruption of M3 and occlusal tooth wear

UCT Sample No.	B4108 No. for Crania	Estimation of Age at Death		
		Cranial suture closure*	Dental eruption of M3 [^]	Occlusal tooth wear*
UCT1A	H1: 4, 43, 61, 55	> 40	Adult	45 +
UCT1B	H1: 7, 37	< 40	Sub-adult	17 – 25
UCT1C	H1: 10, 20	> 40	Adult	45 +
UCT1D	H1: 5, 30	> 40	Adult	33 – 45
UCT1E	H1: 9, 54	< 40	Adult	25 – 35
UCT1F	H1: 8, 15, 31	< 40	Adult	25 – 35
UCT1G	H1: 28, 16, 11, 12	< 40	Adult	25 – 35
UCT1H	H1: 2, 40, 41	> 40	Adult	33 – 45
UCT1I	H1: 1, 60	< 40	Adult	25 – 35
UCT1J	H1: 44, 63	Unknown	Adult	45 +
UCT1K	H1: 6, 14, 29	> 40	Adult	33 – 45
UCT1L	H1: 3	> 40	Adult	33 – 45
UCT1M	H1: 24,25,22,26, 34 ,35,36	Unknown	Unknown	Unknown
UCT1N	H1: 23,39,49,50, 51	Unknown	Unknown	Unknown

*Adult age categories: 2 or less = < 40 years of age; greater than 2 = > 40 years of age.

[^]If M3 is erupted = Adult; if M3 is not erupted = Sub-adult.

*17-25 = minimal wear; 25-35 = moderate wear; 33-45 = heavy wear; About 45+ = extreme wear.

between the ages of 33 and 45+ according to dental attrition. Of the seven older-adult individuals examined for attrition, four were between the ages of 33 – 45 and three were over the age of 45, these age ranges fit the > 40 years of age category. One individual, UCT1B was estimated as being 17 – 25 years of age at the time of death, while the same individual was estimated as a sub-adult based on the non-eruption of M3.

5.3.1 Age distribution – Radiographic method

The estimated age at death based on radiographs of the proximal femora present in the sample are listed in Table 5.16. Individual UCT7D and one un-paired femora (H7: 5, 19) were not aged due to the absence of a femoral head. Standard visual age estimation was determined using Buikstra and Ubelaker's (1994) epiphyseal fusion method for the stage of fusion of the proximal and distal femur. The two age estimates were compared, and where the radiographic method was unable to age UCT7D and H7: 5, 19; both femora were aged as adult by epiphyseal closure.

5.3.2 Age distribution – Epiphyseal closure

The union of epiphyseal ends in the post-cranial bones were analysed to estimate the age at death of sub-adult individuals present in the sample and are listed in Table 5.17. According to this method, it was observed that most of the epiphyseal ends of the long bones were fused. However, a few of the long bones presented with prominent fusion lines, indicating a 'recent' fusion of epiphyses (50%). This was evident in individuals UCT4C, UCT4B, UCT7A, UCT7C and a sacrum (H2: 4) that could not be associated to an individual based on poor preservation. In one individual, UCT4B, the medial epiphyses of the clavicae were not fused at all (0%).

Table 5.18 is a summary of the individuals that presented with prominent fusion lines and unfused epiphyseal ends, as well as the crania of the sub-adult individual as determined by the non-eruption of the third molar (Table 5.13). Age at death was estimated on the time of cranial suture closure and epiphyseal union. The age of one individual (UCT1B, UCT4C and UCT7C) was determined based on the partial fusion of the distal and proximal humerus (13 – 16 years), as well as the union of the head of the femur, femoral trochanters and the distal tibia and fibula (16 – 20 years). Three individuals presented as young adults UCT7A, UCT4D and H2: 4. Individual UCT7A was aged based on the non-fusion of the

Table 5.16 Estimation of age at death using the femoral radiographic method compared to epiphyseal union

UCT Sample No.	B4108 No. For Femora	Morphological Phase	Radiographic AGE [‡]	State of epiphyseal Union
UCT7A	H7: 7 R*	4	35-39	Adult
	H7: 4 L	5	40-44	Adult
UCT7B	H7: 8 R	6	45-49	Adult
	H7: 9 L	6	45-49	Adult
UCT7C	H7: 3 R	1	15-20	Sub-adult
	H7: 2,6 L	2	25-29	Adult
UCT7D	H7: 1 R	- [^]	-	Adult
	H7: 10 L	-	-	Unknown
UCT7E	H7: 5,19 R	-	-	Adult
UCT7F	H7: 11 L	5	40-44	Adult

*Refers to either the Left or Right bone element.

[^]Femoral heads missing post-mortem therefore histological age could not be assigned.

[‡]Radiographic age based on categories proposed by Walker and Lovejoy, 1985.

Table 5.17 Estimation of age based on the fusion of epiphyses of the post-cranial skeleton in sub-adult individuals

UCT Sample No.	B4108 no. for post-crania	Stage of fusion*	Age at death	
<u>Distal humerus</u>				
(Age of fusion 13-19) [^]	UCT4A	H5: 17, 16	100%	Adult
	UCT4B	H5: 20, 15	100%	Adult
	UCT4C	H5: 19, 23	50%	Sub-adult
	UCT4D	H5: 18, 22	100%	Adult
	UCT4E	H5: 21	100%	Adult
<u>Proximal radius – ulna</u>				
(Age of fusion 13-19)	UCT4A	H5: 3, 4, 9, 14 + H7: 17	100%	Adult
	UCT4B	H5: 6, 7, 13	100%	Adult
	UCT4C	H5: 1,2,8	100%	Adult
	UCT4D	H5: 5, 10, 11, 12	50%	Sub-adult
<u>Head femur - trochanter</u>				
(Age of fusion 15-20)	UCT7A	H7: 4, 7	50%	Sub-adult
	UCT7B	H7: 9, 8	100%	Adult
	UCT7C	H7: 3, 2, 6	100%	Adult
	UCT7D	H7: 1, 10	-	Unknown*
	UCT7E	H7: 19, 5	-	Unknown
	UCT7F	H7: 11	100%	Adult
<u>Distal tibia – fibula</u>				
(Age of fusion 16-20)	UCT7A	H7: 21, 18, 13	100%	Adult
	UCT7B	H7: 16, 23, 25, 28	100%	Adult
	UCT7C	H7: 20, 22, 14, 24, 27	50%	Sub-adult
	UCT7D	H7: 15, 12, 26	100%	Adult
<u>Distal femur – proximal tibia – fibula</u>				
(Age of fusion 16-23)	UCT7A	H7: 4, 7, 21, 18, 13	-	Unknown
	UCT7B	H7: 9, 8, 16, 23, 25, 28	100%	Adult
	UCT7C	H7: 3, 2, 6, 20, 22, 14, 24, 27	50%	Sub-adult
	UCT7D	H7: 1, 10, 15, 12, 26	100%	Adult

Table 5.17 Estimation of age based on the fusion of epiphyses of the post-cranial skeleton in sub-adult individuals

	UCT7E	H7: 19, 5	100%	Adult
	UCT7F	H7: 11	100%	Adult
<u>Distal radius – ulna</u>				
(Age of fusion 15-23)	UCT4A	H5: 3, 4, 9, 14 + H7: 17	100%	Adult
	UCT4B	H5: 6, 7, 13	100%	Adult
	UCT4C	H5: 1,2,8	-	Unknown
	UCT4D	H5: 5, 10, 11, 12	100%	Adult
<u>Proximal humerus</u>				
(Age of fusion 16-25)	UCT4A	H5: 17, 16	100%	Adult
	UCT4B	H5: 20, 15	100%	Adult
	UCT4C	H5: 19, 23	50%	Sub-adult
	UCT4D	H5: 18, 22	100%	Adult
	UCT4E	H5: 21	-	Unknown
<u>Iliac crest</u>				
(Age of fusion 16-23)		H6: 4	100%	Adult
<u>Acetabulum</u>				
(Age of fusion 13-16)		H6: 6	-	Unknown
<u>Sacrum (S1 and S2)</u>				
(Age of fusion 18->32)		H2: 4	50%	Young adult
		H2: 9, 12, 38	100%	Adult
<u>Medial clavicle</u>				
(Age of fusion 18-30)	UCT4A	H4: 1, 4	100%	Adult
	UCT4B	H4: 2, 5	-	Unknown
	UCT4C	H4: 3, 8	100%	Adult
	UCT4D	H4: 6, 7	0%	Young adult

*Stage of fusion as presented by a percentage of completeness, 100% = completely fused; 50% = fused with visible fusion line; 0% = un-fused.

^Age of fusion as proposed by Buikstra and Ubelaker (1994)

Table 5.18 Summary of estimated age at death of sub-adult and young adult cranial and post-cranial bones using the union of epiphyseal ends method

UCT Sample No.	Partial fusion	Time of fusion (years)	Estimated AGE	Possible linkage of individuals
UCT1B	Crania and mandible	-	17 – 25	1 sub-adult
UCT4C	Distal humerus	13 – 19		
	Proximal humerus	16 – 25	19 – 25	
UCT7C	Distal tibia and fibula	15 – 20		
	Distal femur, proximal tibia and fibula	15 – 20	15 – 20	
UCT7A	Head of femur and trochanter	16 – 23	16 – 23	1 young adult
UCT4D	Proximal ulna and radius	13 – 19	13 – 19	1 young adult
	Medial clavicle (unfused)	18 – 30		
(H2: 4)	Sacrum	18 – 32	18 – 32	1 young adult

head of the femur and trochanters (16 – 23 years). Individual UCT4D was observed as having the proximal ulna and radius unfused (13 – 19 years) as well as an unfused medial clavicle (18 – 30 years). The sacrum H2: 4 was unfused at S1 and S2 and could not be re-assigned to either of the other two young adult individuals. Therefore, based on the epiphyseal union of the post-cranial remains, only one sub-adult individual was identified and three young adults were represented in the sample.

5.3.3 Age distribution – Summary of various methods

Tables 5.19 and 5.20 illustrate the estimation of age at death determined by various methods for adult, young adult and sub-adult individuals in the study sample. According to the analysis of the dental state, which includes both age ranges estimated by dental eruption and occlusal tooth wear, the adult crania presented with five ‚individuals’ being less than 40 years of age, while six were older than 40 years, one individual was aged as a sub-adult, and two could not be analysed for the state of dental eruption due to the loss of dentition post-mortem. The state of dentition in both sub-adult and adult crania was examined for the eruption of the third molar as well as the state of dental attrition⁴ observed on the occlusal surface of the teeth.

The radiographic method for the estimation of age at death of five individuals, based on the trabecular bone of the femoral head and neck, identified one individual less than 40 years of age, two individuals greater than 40 years of age, as well as one individual presenting as a sub-adult. One individual could not be assessed for radiographic age estimation due to the absence of the proximal head of the femur, post-mortem (Table 5.19).

In addition, the closure of cranial sutures was used to determine the distribution of age based on the available crania in the sample (Table 5.19). Of the 12 complete crania present in the sample, five presented as being less than 40 years of age, while it was observed that six crania presented as being greater than 40 years of age. Three ‚individuals’ could not be assigned to a specific adult age at death category because of unobservable cranial sutures due to post-mortem damage. No sub-adults were identified using the cranial suture closure method.

¹ Dental attrition will be discussed in more detail in section **5.5.1 Dental features**.

The estimation of age at death among the young adult and sub-adult remains within the sample was based on the eruption of the third molar as well as the degree of epiphyseal closure observed at the joints of the skeleton (Table 5.20). Due to co-mingling, the skeletal remains were examined independently for the degree of epiphyseal closure (Table 5.18). According to the state of dentition in sub-adults, one cranium presented as an individual between the ages of 11 - 18 years and 11 presented as individuals over the age of 18 years. Based on the degree of epiphyseal closure observed in the sample, the upper and lower limbs of one individual presented as being between the ages of 11 – 18 years, while approximately three individuals were observed as being just over the age of 18 years, young adults.

Table 5.21 summarises the estimated age at death of skeletal elements where developmental features are observable and sorts them into five age categories as presented by Peckmann (2002). Included in the summary is a comparison of male and female individuals identified in the sample, sorted into the various age categories, as well as bone elements that could not be sexed. The males are represented by one younger adult (20.1 – 40 years) and six older adults (40.1 + years). The females present in the study sample are represented by two younger adult individuals (20.1 – 40 years), and two old adult (40.1 + years) individuals. One sub-adult (15.1 – 20 years) that could not be sexed was also present in the sample. In addition, four individuals could neither be sexed nor aged according to standard demographic methods due to them being represented by single fragmented cranial bones. A total of 16 individuals were identified in the sample based on crania and post-cranial bones. This is in agreement with the MNI of 16 individuals recovered from the cave, as determined by the crania. Based on the estimation of age and sex on the cranial features of developmental stages and sexual dimorphism, four out of 16 crania in the sample could not be aged or sexed due to the poor preservation and fragmentation of the cranial bones.

A summary of the identified individuals based on re-articulation of skeletal elements where possible is listed in Table 5.22, and was assigned a UCT individual number (e.g. UCT1A) to identify each individual present in the sample. According to the „fitting’ of skeletal remains, a maximum of 16 individuals were present in the sample. An attempt was made at re-articulating the crania and post-cranial remains in the sample.

Table 5.19 Age at death estimation of adult skeletal remains based on various methods

Age identification methods	n*	Sub-adult	< 40 years	> 40 years	Unaged Adult
Suture closure	12	-	5	6	3
Dental state [^]	12	1	5	6	2
Femoral Radiographic	5 [‡]	1	1	2	1

*n = The total number of individuals analysed per method.

[^]Dental state = pooled age estimation of the eruption of M3 and occlusal tooth wear.

[‡]Paired femora, with a MNI of 5.

Table 5.20 Age at death estimation of juvenile/sub-adult skeletal remains based on various methods

Age identification methods	n	< 5 years	6 – 10 years	11 – 18 years	> 18 years	Unknown
Dental state	12*	0	0	1	11	0
Epiphyseal closure	- [^]	0	0	1	3	0

*The total number of crania available for analysis.

[^]The total number of individuals for which epiphyseal closure was observed cannot be identified due to the remains being co-mingled.

Table 5.21 Summary of age at death estimation and distribution of sex among skeletal remains from the sample based on five age categories presented by Peckmann (2002)

	Infant*	Juvenile	Sub-adult	Younger adult	Older adult	Unknown	Total Min no. [^]
Males	-	-	-	1	6	0	7
Females	-	-	-	2	2	0	4
Unsexed	0	0	1	0	0	4	4
Minimum no. [‡]	0	0	1	3	8	4	16

*Infant = birth to 5 years; Juvenile = 5.1 – 15 years; Sub-adult = 15.1 – 20 years; Young adult = 20.1 – 40 years; Old adult = 40.1 + years.

[^]Minimum number of males and females.

[‡]Total number of individuals in each age category.

In the sample six older adult males were identified along with two older adult females. Among the young adult category, two females and one male were identified in the sample. One sub-adult individual was present in the sample; however the individual could not be sexed due to the ambiguity in sexing sub-adult individuals.

Re-articulation was performed using both sex and age at death estimation when available. However, due to some of the remains being fragmented, four crania were present in the sample that could not be assigned sex or age at death. If post-cranial remains could not be matched to crania, they were re-articulated to other post-crania where possible. The remains that could not be re-assigned according to the above method were not included in the total number of possible individuals.

It should be noted that UCT2B could possibly be the thoracic vertebrae of one of the six older adult males or one of the two older adult females. The same principle applies to UCT2C, UCT2D, UCT2F and UCT2G, as they could possibly be re-signed to the one young adult male or the two young adult females. It is also likely however that UCT2E could re-articulate with either the one sub-adult female or male.

Table 5.22 Possible linkages of cranial and post-cranial elements

UCT Individual No.*	Representation	Sex	Age	Individuals present in sample	
UCT1A UCT4B UCT7B	Cranium and mandible Upper limbs Lower limbs	Male Male Male	40+ 40+ 45+	6 older adult males	
UCT1J UCT7E	Cranial fragments Lower limbs	Male Male	45+ 40+		
UCT1C	Cranium and mandible	Male	40+		
UCT1D	Cranium and mandible	Male	40+		
UCT1H	Cranium and mandible	Male	40+		
UCT1L	Cranium and mandible	Male	40+		
UCT1I UCT7D	Cranium Lower limbs	Female Female	40+ 40+		2 older adult females
UCT1K UCT7F	Cranium and mandible Lower limbs	Female Female	40+ 40+		
UCT1F UCT4D	Cranium and mandible Upper limbs	Male Male	20.1 – 40 20.1 – 40	1 younger adult male	
UCT2A	C1 and C2 (vertebrae)	-	20.1 – 40		
UCT1E UCT4A UCT7A H2: 4	Cranium and mandible Upper limbs Lower limbs Sacrum	Female Female Female Female	20.1 – 40 20.1 – 40 20.1 – 40 20.1 – 40		2 younger adult females
UCT1G UCT4E	Cranium Upper limbs	Female -	20.1 – 40 20.1 – 40		
UCT1B UCT4C UCT7C	Cranium and mandible Upper limbs Lower limbs	Unknown Unknown Unknown	15.1 – 20 15.1 – 20 15.1 – 20	1 sub-adult individual	
Total number of individuals					
UCT1M	Cranial fragments	Unknown	-		1 unknown individual
UCT1N	Cranial fragments	Unknown	-	1 unknown individual	
UCT1O	Cranial fragments	Unknown	-	1 unknown individual	
UCT1P	Cranial fragments	Unknown	-	1 unknown individual	
UCT2B	Thoracic vertebrae (T7-T9)	-	40+	-	
UCT2C	C4, T1 – T5 and L1	-	20.1 – 40	-	
UCT2D	C3 – C6 and T2	-	20.1 – 40	-	
UCT2F	Thoracic vertebrae (T4 – T7)	-	20.1 – 40	-	
UCT2G	Thoracic vertebrae (T9, T10)	-	20.1 – 40	-	
UCT2E	Thoracic vertebrae (T3, T4)	-	15.1 – 20	-	
UCT3A	Ribs (x10) including first rib	-	-	-	
UCT3B	Ribs (x8)	-	-	-	
UCT3C	Ribs (x3)	-	-	-	
UCT3D	Ribs (x7) including first and second rib	-	-	-	
UCT3E	Ribs (2) including second rib	-	-	-	
UCT3F	Ribs (x9)	-	-	-	
UCT3G	Ribs (x4)	-	-	-	
Total number of possible individuals				16	

*UCT individual number given to remains identified as separate individuals.

5.4 Morphological Features

5.4.1 Body size and stature

In this study, skeletal height was estimated using the revised equations for estimating living stature from the long bones of South African Negroes by Lundy and Feldesman (1987). Because the upper and lower limbs could not be confidently associated, skeletal height was estimated for the long bones of the upper and lower limbs separately (Table 5.23 and 5.24). Table 5.23 presents the estimated skeletal height for the long bones of the upper limb of male and female individuals associated in the sample. Based on the revised equation by Lundy and Feldesman (1987), a male individual UCT4A was estimated to have a skeletal height of 168.6 cm, two female individuals UCT4B and UCT4C were estimated to have heights of 155.9 cm and 153.4 cm respectively, and a male individual UCT4D was estimated to have a skeletal height of 170.1 cm. The mean estimated skeletal height of associated individuals based on the upper limbs is 162.0 cm.

Table 5.24 shows the estimated skeletal height calculated from the long bones of the lower limbs of individuals that could be associated. One female individual UCT7A was estimated to have a skeletal height of 155.7 cm, though it should be noted that the tibia was the only long bone available for measurement. Two male individuals, UCT7B and UCT7C were estimated at having a skeletal height of 177.0 cm and 159.1 cm respectively. UCT7F could not be associated with any other lower limb bones and was therefore measured and recorded as a separate bone element belonging to a separate female individual. It was estimated to have a skeletal height of 157.3 cm.

Table 5.25 compares the estimated skeletal height of male and female adult individuals based on two methods that use the maximum femur length (Lundy and Feldesman, 1989; Feldesman and Fountain, 1996), the revised equation (uncorrected) for the lower limbs by Lundy and Feldesman (1987), as well as the modified correction factor for estimating living stature by Raxter *et al.*, (2006). In the sample, it is evident that a similarity exists between the estimated heights of individuals as calculated from the two methods that only use the femur length (Lundy and Feldesman, 1989; Feldesman and Fountain, 1996). When comparing the uncorrected skeletal height as calculated using

Lundy and Fieldsman's (1987) method, to the two femur length methods, there appeared to be a similarity between two individuals (UCT7A and UCT7F). However, when comparing uncorrected skeletal height to the two femur length methods, the estimated stature for UCT7B and UCT7C was somewhat dissimilar. The estimated stature of UCT7D could not be calculated using the femur length methods, as both the right and left femora were incomplete. However, when the revised correction factors for calculating living stature was added to the averaged skeletal heights for UCT7B (176.5 cm) and UCT7C (160.2 cm), the estimated statures as calculated by all three methods for these individuals were more consistent.

5.4.2 Squatting facets

In the study sample squatting facets were observed in both the proximal and distal ends of the tibia (Table 5.26). A higher degree of incidence of squatting facets occurred at the distal end of the tibia more frequently among the male individuals (four incidents) than the females (one incident). Among the male individuals (UCT7C, UCT7A and UCT7B) that presented with squatting facets, the extension of the notch at the anterior medial malleolus on the right tibia was the most frequent location for the occurrence of squatting facets. Squatting facets in two males and one female individual, UCT7C, UCT7D and UCT7A respectively, were observed at both the proximal and distal end of the tibia, i.e., these individuals displayed signs of habitual squatting, or a similar posture, during their lifetime.

Table 5.27 shows the occurrence of squatting facets between the female and male individuals within the study sample. The total number of tibiae observed in the sample was eight belonging to four individuals, three males and one female. A total of five squatting facets were observed on the tibia of four individuals; one on a female tibia and four on male tibiae. Despite the female individual demonstrating a frequency of 100.0% for the presence of squatting facets, it should be noted that the paired tibiae of only one female individual was available for analysis. Of the paired tibiae belonging to the three male individuals analysed, two had squatting facets on one of their tibiae and one individual had visible squatting facets on both tibiae.

Table 5.23 Estimated skeletal height calculated from the long bones of the upper limbs using Lundy and Feldesman (1987)

Individual Sample No.	Sex	Bone	Ratio	Skeletal Height (cm)	± Standard error of estimate
UCT4A	Male	Ulna		157.7*	3.727
		Radius		160.0	3.643
		Humerus		156.7	3.834
		Uncorrected Height			158.1
		Average Height[^]			168.6
UCT4B	Female	Ulna		146.3	3.629
		Radius		145.7	3.387
		Humerus		145.9	3.715
		Uncorrected Height			145.9
		Average Height[^]			155.9
UCT4C	Female	Ulna		-	3.629
		Radius		142.1*	3.387
		Humerus		144.6	3.715
		Uncorrected Height			143.4
		Average Height[^]			153.4
UCT4D	Male	Ulna		157.4	3.727
		Radius		156.1	3.643
		Humerus		165.4	3.834
		Uncorrected Height			159.6
		Average Height[^]			170.1

*Measurements taken from the right bone.

[^]Average Height was calculated using the correction formulae proposed by Lundy and Feldesman, 1987.

Table 5.24 Estimated skeletal height calculated from the long bones of the lower limbs using Lundy and Feldesman (1987)

Individual Sample No.	Sex	Bone(s)	Ratio	Skeletal Height (cm)	± Standard error of estimate
UCT7A	Female	Femur (physiol)		-	2.789
		Tibia (physiol)		145.7*	3.056
		Fibula		-	3.168
		Uncorrected Height			145.7
		Average Height[^]			155.7
UCT7B	Male	Femur (physiol)		172.5	2.777
		Tibia (physiol)		166.8	2.78
		Fibula		157.3	2.98
		Uncorrected Height			165.5
		Average Height[^]			177.0
UCT7C	Male	Femur (physiol)		152.7	2.777
		Tibia (physiol)		148.6	2.78
		Fibula		146.1*	2.98
		Uncorrected Height			149.1
		Average Height[^]			159.1
UCT7D	Female	Femur (physiol)		-	2.777
		Tibia (physiol)		154.5	2.78
		Fibula		148.0*	2.98
		Uncorrected Height			151.3
		Average Height[^]			161.3
UCT7F	Female	Femur (physiol)		147.3	2.789
		Tibia (physiol)		-	3.056
		Fibula		-	3.168
		Uncorrected Height			147.3
		Average Height[^]			157.3

*Measurements taken from the right bone.

[^]Average Height was calculated using the correction formulae proposed by Lundy and Feldesman, 1987.

Table 5.25 Estimated living stature using maximum femur length and the sum of the lower limb bones, comparing three methods developed for the estimation of living stature

Bone	Individual Sample No.	Sex	Calculated Height "Femur length X 3.745" (Lundy and Feldesman, 1989)	Generic Equation "Height = 31.263362 + 3.019390 X femur length" (Feldesman and Fountain, 1996)	Uncorrected Skeletal Height (Lundy and Feldesman, 1987)	Estimated Living Stature [^] (Raxter <i>et al.</i> , 2006)
Femur		Female	140.4	144.2	145.7	156.8
	UCT7A					
	UCT7B	Male	194.4	187.9	165.5	176.5
	UCT7C	Male	167.4	166.2	149.1	160.2
	UCT7D	Female	-	-	151.3	162.4
	UCT7E					
	UCT7F	Female	153.5*	155.1*	147.3	158.4

[^]To estimate living stature the following correction equation was used: Living stature = 0.996 X Skeletal height + 11.7.

*Measurements taken from the right bone.

Table 5.26 Squatting facets observed on the tibia of samples from Khoraxa-ams by individual

UCT Sample No.	B4108 No. for tibia	Sex	Age	Location of Squatting facet
<u>PROXIMAL TIBIA</u>				
UCT7C	H7: 20	M	15.1-20	Right tibia with extension (rounded) of anterior margin
UCT7A	H7: 13,18	F	20.1-40	Right tibia with extension of anterior margin
UCT7D	H7: 15	M	40+	Left tibia with slight extension of anterior margin
<u>DISTAL TIBIA</u>				
UCT7C	H7: 20	M	15.1-20	Right tibia – extension of notch at anterior medial malleolous
UCT7A	H7: 13,18	F	20.1-40	Right tibia – extension of notch at anterior medial malleolous
UCT7B	H7: 16	M	45+	Right tibia – extension of notch at anterior medial malleolous
UCT7D	H7: 12	M	40+	Right tibia –rounded fibular articular surface
	H7: 15			Left tibia – rounded fibular articular surface

M = Males; F = Females

Table 5.27 Occurrence of squatting facets in the study sample

	Females	Males	Unknown	Total
n*	1	3	0	4
No. of tibia with squatting facets^	1	4	0	5
No. of individuals with squatting facets	1	3	0	4
% of individuals with squatting facets	100.0	75.0	0.0	80.0

*n = No. of individuals according to paired tibia.

^No. of unpaired tibia with visible squatting facets.

5.5 Ante-mortem Features

5.5.1 Dental features

5.5.1.1 Dental health

The dental health of the Khoraxa-ams sample was examined for signs of occlusal attrition, enamel hypoplasias, carious lesions, abscesses, periodontitis as well as ante-mortem tooth loss and dental modification respectively, according to Buikstra and Ubelaker (1994).

A. Occlusal Attrition

The incidence and severity of occlusal attrition was examined in all the adult crania and compared with the known age and sex of the individual. These variables are important since patterns of wear in males and females can provide information about differences in diet and behaviour between the sexes. For these reasons the unsexed individual crania were not included in the analysis. The number of individuals (n) is calculated based on the proportion of maxilla and mandibles present. Individuals represented by one half of a maxilla or mandible, were counted as one quarter of an individual (0.25).

The state of occlusal attrition in the adult dentition is presented in Table 5.28. The attrition scores for male individuals present in the sample were higher for the posterior teeth (1.7) than the female individuals (1.3), i.e., there was a higher degree of wear on the posterior dentition among male individuals present in the sample (Figure 5.01). With regards to anterior attrition, the female individuals had no data recorded due to absence or damage to the anterior teeth.

The pooled posterior attrition score for both the males and females is 1.5; however the score for pooled anterior attrition could not be calculated, as there is no data for the females. The mean attrition score (pooled anterior and posterior scores) for the male individuals is 1.9. The mean attrition score for the females could not be calculated; neither could the total mean attrition score for both the males and females (Table 5.28).



Figure 5.01 UCT1C – Mandible showing heavy occlusal wear

Table 5.28 Average stage of occlusal attrition on adult dentition

n*	Female 115		Male 148		Total 263	
	No.^	Attrition scores	No.^	Attrition scores	No.^	Attrition scores
Tooth Type						
I1	12	- [‡]	15	1.8	27	1.8
I2	14	-	20	2.3	34	2.3
C	14	-	20	2.3	34	12.3
PM1	15	2.0	20	1.8	35	1.9
PM2	15	1.4	19	1.6	34	1.5
M1	15	1.2	18	2.4	33	1.8
M2	15	1.1	18	1.7	33	1.4
M3	15	0.8	18	1.2	33	1.0
Anterior Attrition Score		-		2.1		-
Posterior Attrition Score		1.3		1.7		1.5
Mean Attrition Score		-		1.9		-

*n = Total number of tooth places observed.

^No. = Total number of tooth places per tooth type observed.

‡Tooth absent or damaged therefore wear cannot be determined.

It should be noted that due to the absence of the anterior teeth from the female individuals as a result of post-mortem damage, it is not accurate to assume that the females did not experience significant occlusal attrition on these teeth.

B. Dental Caries

Of a total of 126 teeth with intact crowns, no carious lesions were observed in the sample, resulting in a caries frequency of ,,0' (Table 5.29).

C. Enamel Hypoplasias

A total of 126 teeth with intact crowns in male, female and unsexed individuals were examined for the presence of Linear Enamel Hypoplasia (LEH). Only one male individual presented with a single enamel hypoplasia on the left mandibular canine, while no enamel hypoplasias were observed on the female dentition (Table 5.30). Among the teeth that could not be sexed, two central incisors and two canines presented with enamel hypoplasias. Therefore, of a total of 126 teeth with intact crowns, only three teeth presented with linear enamel hypoplasias.

D. Dental Abscesses

The number of individuals in the sample presenting with dental abscesses are shown in Table 5.31, with respect to the location of dental abscess(s). Of the individuals present, two males (UCT1A and UCT1D) and one female (UCT1K) individual presented with dental abscesses on the both maxilla and the mandible respectively (Figure 5.02). The mandibular abscess observed in UCT1D shows signs of active infection surrounding the abscess where the alveolar bone appears porous. It is possible that the abscess was active at the time of death. The dental abscess observed in UCT1K resulted in an infection of the left maxillary canine (Figure 5.03).

Table 5.32 details the occurrence of dental abscesses between the males and females. Within the sample, one abscess with observed in a female individual, while four abscesses with present in two male individuals. The number of individuals (n) is calculated based on the proportion of maxilla and mandibles present. Individuals represented by one half of a maxilla or mandible are counted as one quarter of an individual (0.25). Of the 8.75 individuals in the sample, dental abscesses affected three

Table 5.29 Tooth types affected by carious lesions in adult individuals

n*	Males		Females		Unsexed		Total
	47		43		36		126
Tooth Type	No.^	No. with caries	No.^	No. with caries	No.^	No. with caries	Total No. of caries
I1	2	0	0	0	2	0	0
I2	2	0	2	0	4	0	0
C	3	0	1	0	4	0	0
PM1	5	0	3	0	6	0	0
PM2	5	0	5	0	5	0	0
M1	13	0	13	0	7	0	0
M2	12	0	13	0	5	0	0
M3	5	0	6	0	3	0	0
Total	47	0	43	0	36	0	0

*n. = Total number of teeth with intact crowns observed.

^No. = Total number of tooth types with intact crowns.

Table 5.30 Incidence of Linear Enamel Hypoplasia in the sample per tooth type

n*	Males		Females		Unsexed	
	47		43		36	
Tooth Type	No.^	No. with LEH [‡]	No.^	No. with LEH	No.^	No. with LEH
I1	2	-	0	0	2	2
I2	2	0	2	0	4	0
C	3	-	1	1	4	2
PM1	5	0	3	0	6	0
PM2	5	0	5	0	5	0
M1	13	0	13	0	7	0
M2	12	0	13	0	5	0
M3	5	0	6	0	3	0
Total	47	0	43	1	36	2

*n. = Total number of teeth with intact crowns observed.

^No. = Total number of tooth types with intact crowns.

[‡]LEH = Linear Enamel Hypoplasia.



Figure 5.02 UCT1D – Abscesses at maxillary incisor and premolar positions showing infection surrounding the abscess

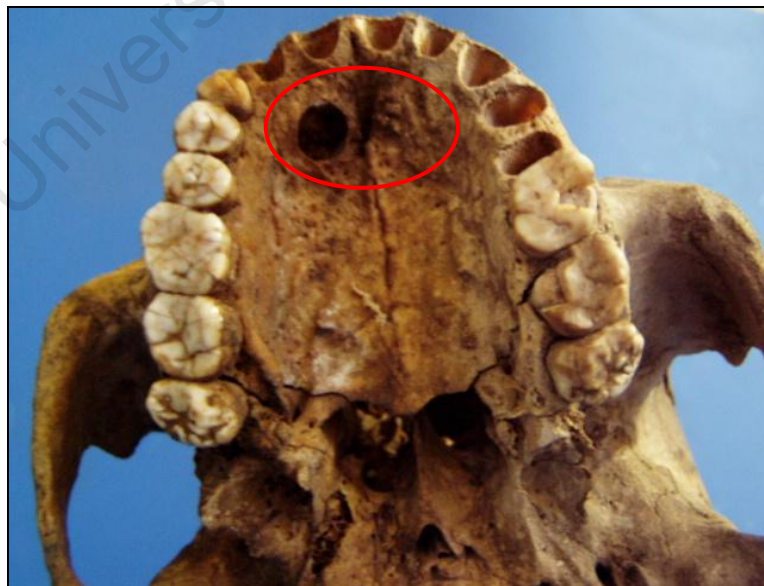


Figure 5.03 UCT1K – Abscess on maxillary palate at position of right central incisors

individuals (34.3%). However, the frequency of abscesses is low with only five abscesses recorded from 280 sockets (1.79%).

E. Periodontal Disease

Periodontal disease was examined and the severity recorded for adult individuals present in the study sample. Only the adult individuals of known sex were used. The number of individuals (n) was calculated based on the proportion of maxilla and mandibles present. Individuals represented by one half of a maxilla or mandible, were counted as one quarter of an individual (0.25).

The incidences of periodontal disease in the sample are presented in Table 5.33. All observed periodontitis within the sample were recorded in mature adults, i.e., > 40 years of age. This correlates with the theory that periodontitis progresses with increasing age. Individual UCT1D shows the most severe form of periodontitis affecting all the tooth sockets, resulting in ante-mortem tooth loss of most of the maxillary dentition (Figure 5.04). Periodontitis observed in UCT1C has affected both the maxillary and mandibular dentition in this individual (Figure 5.05).

Table 5.34 lists the incidence of periodontitis observed in the tooth sockets of both the male and female dentition present in the sample. A total of five tooth sockets presented with moderate periodontitis in the female dentition, with more than half of the tooth root exposed. In the male dentition, a total of 21 tooth sockets were observed to have moderate to severe periodontitis with the remnants of avulsion visible. Of a total number of 263 available tooth sockets, 26 tooth sockets were observed to have moderate to severe periodontitis within the sample.

The overall frequency of individuals with periodontitis is considerably higher in the adult male (88.9%) individuals than in the adult females (23.5%) within the sample. The overall frequency for sexes pooled is 57.1% (Table 5.35).

5.5.1.2 Ante-mortem tooth loss

The incidence of ante-mortem tooth loss (AMTL) was analysed using adult individuals where sex had been determined. The number of individuals (n) was calculated based on

Table 5.31 Dental abscesses observed in individuals from Khoraxa-ams sample

UCT Sample No.	B4108 No. For Crania	Sex	Age	Position of Abscess
UCT1A	H1: 4,43,61,55	M	40+	Left mandibular M3 buccal surface
UCT1D	H1: 5,30	M	40+	Left maxillary PM1 + PM2 buccal surface Right maxillary I1 labial surface Right mandibular I2 labial surface
UCT1K	H1: 6	F	40+	Right maxillary I1 + I2 palatal

M = Males; F = Females

Table 5.32 Occurrence of dental abscesses in adult individuals

n*	Female	Male	Total
	4.25	4.5	8.75
No. of abscesses	1	4	5
No. of individuals with abscesses	1	2	3
Ave. no. of abscesses per mouth	0.2	0.9	0.6
% Abscesses per individual	23.5	44.5	34.3
% Frequency of abscess per total sockets	0.07	2.78	1.79

*n = individuals represented by only one half of a maxilla or mandible are counted as one quarter of one individual.

Table 5.33 Location of periodontal disease observed in the sample

UCT Sample No.	B4108 No. for Crania	Sex	Age	Location of Periodontal Disease
UCT1A	H1: 4,43,61,55	M	40+	Maxillary and mandibular periodontal disease
UCT1C	H1: 10,20	M	40+	Maxillary and mandibular periodontal disease
UCT1D	H1: 5,30	M	40+	Maxilla edentulous periodontal disease
UCT1K	H1: 6,14,29	F	40+	Right maxillary and mandible periodontal disease
UCT1L	H1: 3	M	40+	Maxillary periodontal disease

M = Males; F = Females

Table 5.34 Periodontal disease observed per socket in adult individuals

n*	Females		Males		Total	
	115		148		263	
Tooth Types	No.^	Periodontitis	No.^	Periodontitis	No.^	Periodontitis
I1	12	0	15	2	27	2
I2	14	0	20	3	34	3
C	14	0	20	3	34	3
PM1	15	1	20	4	35	5
PM2	15	1	19	2	34	3
M1	15	1	18	3	33	4
M2	15	1	18	3	33	4
M3	15	1	18	1	33	2
Total No. of Periodontitis	115	5	148	21	263	26

*Total No. = Total number of available tooth sockets observed.

^No. = Total number of tooth sockets per tooth type observed.

Table 5.35 Occurrence of periodontitis in adult individuals

n*	Females	Males	Total
	4.25	4.5	8.75
No. of individuals with periodontitis	1	4	5
% of individuals with periodontitis	23.5	88.9	57.1

*n = individuals represented by only one half of a maxilla or mandible are counted as one quarter of one individual.



Figure 5.04 UCT1D – Severe maxillary periodontal disease affecting all the sockets and resulting in a partially edentulous maxilla

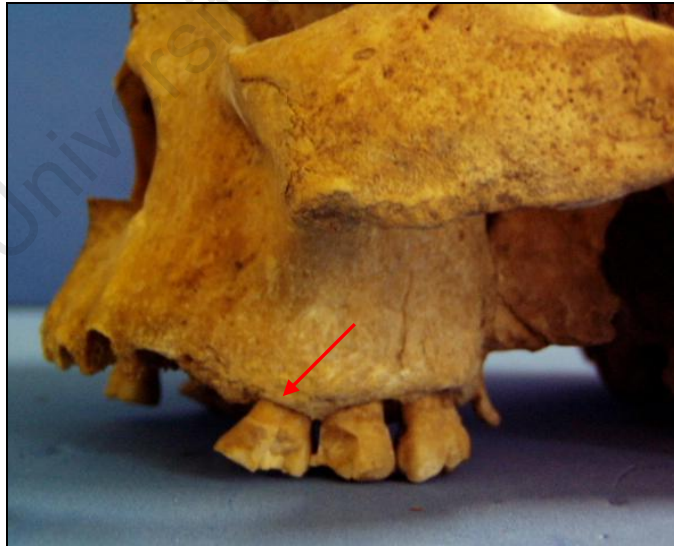


Figure 5.05 UCT1C – Periodontal disease affecting the maxillary dentition, shows resorption of the sockets.

the proportion of maxilla and mandibles present. Individuals represented by one half of a maxilla or mandible, were counted as one quarter of an individual (0.25).

The adult male individuals had a high number of teeth lost ante-mortem, with AMTL affecting 12.5% of the male dentition. Thus, approximately half of the male population in the sample presented with some form of AMTL (Table 5.36). The adult females in the sample had no incidence of visible AMTL. Therefore, a total of 18 teeth were lost ante-mortem (6.43%) based on the male individuals within the sample, affecting 40.0% of the total sample set.

Table 5.37 gives a summary of the percentage of AMTL per tooth type within the study sample. The most commonly lost teeth among the males were the central incisors, with a total of five central incisors lost within the male population of the sample. It is possible though; that the AMTL observed in the male central incisors is as a result of dental modification. The remaining AMTL observed refers to one male individual and is the result of severe periodontitis, as described above, causing an edentulous maxilla. No AMTL was observed in the adult female individuals within the study sample.

5.5.1.3 Dental anomalies and modification

The presence of dental and palatal anomalies in the study sample were examined and recorded for all dentition where available. Table 5.38 shows the occurrence of dental anomalies observed in three adult individuals, UCT1A, UCT1F and UCT1I, two males and one female individual respectively. UCT1A presented with a unilateral torus maxillaris on the lingual aspect of the alveolar bone at the position of the left molars (Figure 5.06). Torus maxillaris and other oral exostosis (torus palatinus and torus mandibularis) are nodular protuberances composed of mature dense cancellous bone with a rim of cortical bone of variable thickness (Jainkittivong and Langlais, 2000; Belsky *et al.*, 2003). Intraoral exostoses are not a disease or a sign of disease; however several researchers (Haugen, 1992; Seah, 1995 and Gorsky *et al.*, 1996) have postulated that the etiology of tori consists of an interaction of multifactorial genetic and environmental factors (Jainkittivong and Langlais, 2000).

Individual UCT1F was observed to have a malformed root and crown of the right maxillary central incisor (Figure 5.07). The malformation of I1 resulted in it being

Table 5.36 Occurrence of ante-mortem tooth loss in adult individuals

n*	Female		Male		Total	
	4.25		4.5		8.75	
	No.	%	No.	%	No.	%
No. of teeth lost ante-mortem	0	0	18	12.5	18	6.43
No. of individuals with AMTL [^]	0	0	3.5	77.8	3.5	40.0
Ave. no. of teeth lost ante-mortem / mouth	-	-	4.0	-	2.1	-
Total no. of tooth places observed in preserved sockets	136	-	144	-	280	-

*n = individuals represented by only one half of a maxilla or mandible are counted as one quarter of one individual.

[^]AMTL = ante-mortem tooth loss.

Table 5.37 Summary of ante-mortem tooth loss percentage per tooth type in the sample

n*	Female		Male		Sexes Pooled
	No. [^]	AMTL	No. [^]	AMTL	263
Tooth Types					
I1	12	0	15	5	5
I2	14	0	20	2	2
C	14	0	20	2	2
PM1	15	0	20	2	2
PM2	15	0	19	2	2
M1	15	0	18	2	2
M2	15	0	18	2	2
M3	15	0	18	3	3
Total no. AMTL	115	0	148	20	20

*n. = Total number of teeth lost ante-mortem compared to the.

[^]No. = Total number of tooth places observed.

positioned anterior-superiorly with the lingual surface of the incisor positioned labially, at right angles to the upper lip. The malformation may have adversely affected mastication. Individual UCT1I has a supernumerary cusp on the buccal side of the right maxillary second molar, known as a Paramolar (Figure 5.08). Paramolar is a small cusp located on the mesial portion of the buccal surface of the maxillary molar (Steele and Bramblett, 1988). These should not be confused with Carabelli Cusp that is often present on the lingual surface of the tooth (especially molars), and metastylid and protostylid cusps that are commonly located on the mandibular molars (Buikstra and Ubelaker, 1994; Schwartz, 1995).

Signs of dental modification of any kind were examined on all anterior and posterior permanent teeth including anterior-tooth positions present. Since ante-mortem tooth loss can result from severe periodontal disease, abscesses and various other dental disease processes, it is best to exclude individuals with heavily diseased mouths from the analysis of intentional tooth extraction, known as ablation.

Table 5.39 presents a short list of all individuals exhibiting signs of dental modification. Two forms of modification observed within the study sample are the result of interproximal grooving on the left maxillary third molar (M3) of UCT1C, and ablation or deliberate removal of the anterior teeth (Buikstra and Ubelaker, 1994) in two individuals (UCT1E and UCT1H), ante-mortem. In the sample ablation occurred repeatedly on the mandible with the extraction of the central incisors in each case (Figure 5.09). Of the two individuals presenting with ablation, one was a mature adult male (40+ years of age), and one a young adult female (20.1-40 years of age).



Figure 5.06 UCT1A – Unilateral torus maxillaris on the lingual surface below the left molars



Figure 5.07 UCT1F – Malformation of maxillary anterior tooth

Table 5.38 Individuals presenting with dental anomalies in the sample

UCT Sample No.	B4108 No. For Crania	Sex	Age	Dental Anomaly
UCT1A	H1: 4,43, 61,55	M	40+	Unilateral torus maxillaris on the lingual surface below the left maxillary molars.
UCT1F	H1: 8,15,31	M	20.1-40	Right maxillary I1 malformed root and crown at right angles to the lip
UCT1I	H1: 1,60	F	40+	Well-defined extra cusp on buccal side of right maxillary M2

M = Males; F = Females

Table 5.39 Individuals presenting with dental modification in the sample

UCT Sample No.	B4108 No. For Crania	Sex	Age	Type of Dental Modification
UCT1C	H1: 10,20	M	40+	Interproximal grooving on left maxillary M3.
UCT1H	H1: 2,41,40	M	40+	Mandibular ablation* of both central incisors
UCT1E	H1: 9,54	F	20.1-40	Mandibular ablation* of both central incisors

M = Males; F = Females

*Ablation is the deliberate removal of the anterior teeth from the mandible or maxillae (Buikstra and Ubelaker, 1994).

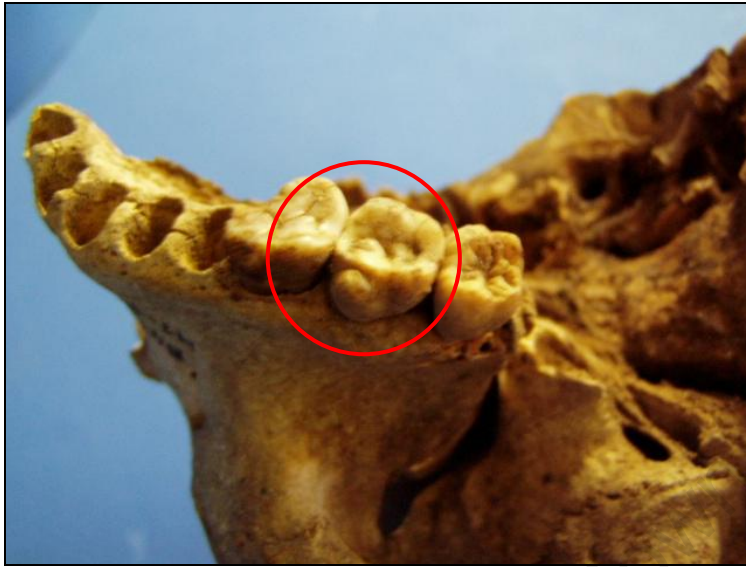


Figure 5.08 UCT1I – Extra cusp on buccal side of right maxillary M2



Figure 5.09 UCT1E – Mandibular ablation of both central incisors

5.5.2 Physio-chemical analysis

5.5.2.1 Stable light isotope analysis

A total of 14 Crania were sent to the Light Isotope Mass Spectrometry Laboratory (LIMS) at the Department of Archaeology, UCT for stable light isotope analysis. Table 5.40 details the carbon and nitrogen concentrations measured from bone collagen extracted from the cranial samples. The results of the C/N analysis indicate that all samples were of well-preserved collagen, with C/N ratios ranging from 2.74 to 4.32. The range of $\delta^{13}\text{C}/^{12}\text{C}$ values is -10.76‰ to -16.13‰ with a mean of -13.4‰ and a standard deviation of 1.61. Results of stable nitrogen isotopes show a range of 11.00‰ to 17.11‰ with a mean of 13.9‰ and a standard deviation of 1.86.

Within the male individuals, the C/N ratio ranged from 2.83 to 4.17 with a mean of 3.36, while the females had a C/N ratio ranging from 2.74 to 4.32 with a mean of 3.13. In comparison, the range of $\delta^{13}\text{C}/^{12}\text{C}$ values for males and females were very similar with mean values of -13.36 and -13.44 respectively. However, the standard deviation for $\delta^{13}\text{C}/^{12}\text{C}$ values for the males and females were 1.30 and 1.96 respectively. The $\delta^{15}\text{N}/^{14}\text{N}$ values were slightly higher in the females with a mean of 14.32 and a standard deviation of 1.62, than the males with a mean of 13.56 and a standard deviation of 1.16.

5.5.2.2 Trace elemental analysis

Trace element analysis (TEA) is the study of element concentrations within the human body and is used as a tool to determine mobility (Tafari *et al.*, 2003), as well as a guide to the reconstruction of various aspects of palaeodiet (Klepinger *et al.*, 1986). The use of elemental analysis of excavated bone in this study was as a potential means of sorting co-mingled remains into separate individuals. In this study a total of 10 elements were analysed, with human tissue samples taken from the crania of 14 individuals, seven males, four females and three unknown individuals. The concentration of bone trace elements is such that they are quantified not in terms of percentage of bone weight, but rather in parts per million (ppm) – i.e. micrograms per gram of bone (Mays, 1998).

The highest concentration of trace elements found within the sample was that of magnesium followed by zinc and strontium with mean concentrations of 11601.83,

175.3 and 173 ppm respectively (Table 5.41). It is evident from the increased levels of magnesium, that this is the trace element most concentrated within the bone collagen. However, the concentration of zinc and strontium are fairly equal within the bone collagen extracted from the crania.

Table 5.42 presents the interpretation of relative standard deviation (% RSD) calculated by repeated elemental analysis in order to determine the reliability of trace element concentrations in biological material. In this study, reliability of the mean % RSD was assumed below 20.0%, as the higher the % RSD the more unreliable the analyses. Of the ten elements analysed in this study, four elements were determined to be the most reliable (Mo, Mg, Zn and Sr), with all four elements having a mean % RSD below 20.0%. Ni and Co obtained the highest mean % RSD of 63.1 and 49.2 % respectively, indicating that they are not reliable trace element concentrations, appearing heterogeneous in repeated sample analyses.

The four trace elements that were determined to have reliable concentrations are presented in Table 5.43. According to the mean values (trace element concentration taken in parts per million) for each element, Mg had the highest recording of 6975.0 and 8426.0 ppm for male and female means respectively. Mo had the lowest element concentrations in both the males and females, with a mean of 0.6457 and 0.4300 ppm respectively. Thus, according to trace elemental concentration, Mg is the only element that showed variation in concentration among individual crania, and could therefore possibly be used to sort individuals.

It should be noted that although the purpose of performing trace element analysis in this study was to possibly establish a means of sorting the remains into separate individuals, the crania were the only bones tested. It was decided that the crania be analysed first in order to determine the competence and effectiveness of the technique. Thereafter the remaining co-mingled post-cranial bones were to be analysed for the purpose of identifying and sorting remains based on homogeneous trace element concentrations for each individual. However, due to faulty laboratory equipment experienced at the Inductively Coupled Plasma Mass Spectrometry (ICP- MS) facility at the Department of Geology, UCT this was not the case.

Table 5.40 $\delta^{13}\text{C}/^{12}\text{C}$ and $\delta^{15}\text{N}/^{14}\text{N}$ results from bone collagen of cranial samples sent for stable light isotope analysis

UCT Sample No.	B4108 No. For Crania	Sex	Age	C/N ratio (by wt)	$\delta^{13}\text{C}/^{12}\text{C}$ [per mil]* vs VPDB [^]	$\delta^{15}\text{N}/^{14}\text{N}$ [per mil]* vs AIR [¥] N ₂
UCT1A	H1: 4,43	Male	Adult	2.83	-13.04	14.38
UCT1C	H1: 10	Male	Adult	2.97	-13.34	13.52
UCT1D	H1: 5	Male	Adult	3.63	-13.68	14.36
UCT1H	H1: 2	Male	Adult	3.11	-12.42	13.67
UCT1J	H1: 44,63	Male	Adult	3.36	-15.57	13.03
UCT1L	H1: 3	Male	Adult	2.96	-11.44	13.95
UCT1F	H1: 8,15	Male	Young adult	3.87	-12.70	14.60
UCT1E	H1: 9	Female	Young adult	4.17	-14.68	11.00
UCT1G	H1: 28,12,11, 16	Female	Young adult	2.78	-13.60	14.32
UCT1K	H1: 6	Female	Adult	2.97	-10.76	14.29
UCT1I	H1: 1,60	Female	Adult	2.82	-13.35	13.18
UCT1B		Unknow		2.74	-11.84	14.70
	H1: 7	n	Sub-adult			
UCT1M		Unknow		3.15	-14.93	12.34
	H1:24,25,22	n	Unknown			
UCT1N		Unknow		4.32	-16.13	17.11
	H1: 23,39	n	Unknown			

*per mil = ‰ (parts per thousand).

[^]VPDB = volume of The Peedee Formation *Belemnitella americana* marine fossil limestone from South Carolina used as standard reference material for C₂ and O₂ isotope ratios.

[¥]AIR = atmospheric N₂ used as the standard for nitrogen.

Table 5.41 Mean trace element concentration (in ppm) and precision of methodology (% RSD) for cranial samples

Sample	Sex	Mg		Cr		Mn		Co		Ni		Cu		Zn		Se		Sr		Mo	
		X*	RSD^	X	RSD	X	RSD	X	RSD	X	RSD	X	RSD	X	RSD	X	RSD	X	RSD	X	RSD
UCT1A	M	3887	1.96	1.42	5.12	83.2	8.14	0.2	6.67	0.28	18.3	6.08	17.15	279	7.57	8.09	19.97	217	1.79	0.79	6.48
UCT1C	M	17330	44.5	5.8	7.31	8.2	74.5	0.01	317	0.20	61.4	2.1	36.1	218	14.2	5.1	6.80	200	30.1	0.21	63.3
UCT1D	M	6962	50.4	7.2	40.2	5.2	123	0.12	143	0.31	146	2.6	13.0	173	24.0	4.7	29.0	199	2.35	0.35	19.4
UCT1F	M	6802	7.06	1.08	16.18	35	13.55	0.25	28.82	1.78	42.04	8.25	40.69	234	11.75	13.2	23.35	197	13.06	1.69	22.35
UCT1H	M	4357	1.82	1.15	6.93	66.8	7.46	0.27	5.1	0.34	17.49	4.07	2.12	378	5.69	10.2	28.97	166	1.84	0.61	5.65
UCT1J	M	4789	1.6	1.77	30.95	101	6.63	0.38	19.48	0.75	52.11	8.93	20.0	321	3.19	6.46	46.19	219	2.46	0.84	4.4
UCT1L	M	4698	2.11	0.66	7.28	0.21	38.09	0.03	31.81	0.07	31.89	0.31	21.2	187	6.1	7.11	36.12	146	6.53	0.03	46.25
UCT1E	F	6084	24.4	5.5	51.8	3.5	98.9	0.19	28.1	0.64	113	6.6	30.9	197	4.06	6.7	16.7	208	0.65	0.90	7.54
UCT1G	F	5568	1.27	-	32.94	409	16.33	0.31	7.76	0.45	19.58	21.4	6.33	595	2.28	14.4	22.66	156	3.36	0.21	10.0
UCT1I	F	3904	2.41	0.33	7.13	0.25	64.52	0.04	14.01	0.84	44.93	1.94	48.05	160.2	5.31	4.72	44.08	114.6	2.51	0.04	17.28
UCT1K	F	6105	35.3	9.9	71.7	71	3.16	0.44	44.2	0.15	125	18.0	35.5	267	1.08	5.6	7.08	175	10.9	0.24	29.6
UCT1B	U	20468	3.60	5.3	11.8	8.7	17.2	0.07	8.78	0.27	86.1	3.2	16.1	158	0.50	6.2	8.67	135	1.00	0.85	2.92
UCT1M	U	7364	5.69	0.97	10.9	1426	2.48	0.63	5.75	0.48	19.01	14.0	5.29	325	5.69	13.5	21.3	227	1.19	1.48	6.32
UCT1N	U	12662	21.6	3.9	8.39	76	11.8	0.14	28.5	1.3	107	4.2	21.7	235	7.40	6.9	12.2	121	3.59	0.79	8.13

M = Males; F = Females; U = Unknown sex

*X = in parts per million, the actual trace element concentration value.

^RSD = relative standard deviation, the reliability of the variant.

Table 5.42 Interpreting relative standard deviation (% RSD) to determine reliable trace elemental concentrations in biological material

Element	n	% RSD*
Ni	14	63.1
Co	14	49.2
Mn	14	34.7
Se	14	23.0
Cu	14	22.5
Cr	14	22.1
Mo[^]	14	17.8
Mg[^]	14	14.5
Zn[^]	14	7.1
Sr[^]	14	5.8

*% RSD = the mean relative standard deviation calculated for each element measured on cranial samples.

[^]Reliability = mean % RSD as calculated from repeated analyses of trace element from bone (< 20%).

Table 5.43 Elements with reliable mean % RSD

Element	Males		Females	
	n	Range* (ppm)	n	Range* (ppm)
Mo	7	0.6457	5	0.43
Mg	7	6975.0	5	8426.0
Zn	7	255.82	5	275.0
Sr	7	192.01	5	158.0

*Range = trace element concentration taken in parts per million (ppm) for cranial bones.

5.5.3 Stress indicators

5.5.3.1 Harris lines

The incidence of transverse lines of radio-density at the distal ends of long bones known as Harris lines (HL) were recorded and analysed in all femora and tibia present in the sample. However, no HL were observed in the femora, so only the HL observed in the tibia are listed below (Table 5.44). Of the HL observed in the sample, the lines nearest the midline of the bone shaft precede those nearer the ankle joint. The distance of any one of these scars from the end of the bone indicates the length of the shaft at the time it was produced, and from this the age at which it occurred can be inferred (Suter *et al.*, 2008).

In the sample, two males expressed HL and one female was found to express HL (Table 5.44). For the one female individual UCT7A, a total of four HL were observed. Two male individuals with HL were UCT7B and UCT7C. A summary of HL expressed in the sample is given in Table 5.45. Of the two males, UCT7B had three lines and UCT7C had 2 lines observed on their tibiae. It should be noted that only three individuals had confirmed HL and therefore caution should be taken when interpreting the data.

5.5.4 Skeletal pathology

The presence of pathologies on the skeletal material from Khoraxa-ams were observed and recorded for each bone element. Observations were recorded where bones were remodelled due to a disease process. The following aspects of disease processes visible in osteological material were investigated: cribra orbitalia and porotic hyperostosis, degenerative joint disease, periostitis as well as trauma in the form of Schmorl's nodes.

5.5.4.1 Non-specific pathologies

A. Cribra orbitalia

Cribra orbitalia (CO) is a lesion located on the orbital roof and is characterised by the pitting of the compact bone on the orbital roof. In the sample, two adult male individuals, UCT1C and UCT1F showed signs of healed CO on their left orbit (Table 5.46).

Table 5.44 Individual long bones specifically the tibia, exhibiting Harris lines in the sample

UCT Sample No.	B4108 No. for Tibia	Sex	Age at death	Number of lines per bone side	Number of lines on paired bones	Age of line formation (years)
UCT7A	H7: 21* L	F	20.1-40	2	4	-
	H7: 18,13 R			3		< 1 10-11 11-12
UCT7B	H7: 16 R	M	45+	3	3	< 1 12-13 14-15
	H7: 23* L			2		-
UCT7C	H7: 20 R	M	15.1-20	2	2	12-13 13-14
	H7: 22,14* L			1		-

M = Males; F =Females

*Tibia exhibit Harris lines, but total length could not be measured, thus age of line formation cannot be calculated.

Table 5.45 Summary of Harris line formation in the study sample

	Females*	Males*	Unknown	Total
No. of Individuals	3	3	0	6
No. with Harris lines	1	2	0	3
No. of Harris lines	4	5	0	9
% Harris lines	33.3	66.7	0	50
No. Harris lines per individual	4.0	2.5	0.0	3.0

*Refers to the number of individuals that are male or female with Harris lines.

B. Porotic hyperostosis

Porotic hyperostosis (PH) is characterized by pitting on the outer compact bone of the cranium, generally located on the parietal and frontal bones and less frequently of the occipital bone (Friedling, 2007) (Figure 5.10). In the sample, only two individuals, presented with PH, one adult male and one young adult female (Table 5.46). The adult male individual, UCT1F, also presented with CO. In both individuals, PH appeared inactive or remodelled, i.e., the lesions appear healed at the time of death with the bone being smooth to the touch but with pitting still visible.

Individual UCT1C that presented with CO did not present with PH and the reverse was true for individual UCT1G that presented with PH.

5.5.4.2 Joint disease

A. Osteoarthritis of synovial joints

Osteoarthritis is the most frequently diagnosed degenerative condition affecting both synovial and non-synovial joints, although there are also non-degenerative forms of the disorder. Generalised arthritis is more likely to be age-related, while osteoarthritis caused by disease is usually localised (Burns, 1999). The joints of all available skeletal elements were examined for the presence and severity of osteoarthritis in the study sample among male and female individuals. In the upper body, the temporomandibular, shoulder, elbow, radio-carpal, intervertebral synovial articular joints (zygopophyses), and sacro-iliac joints were examined and analysed (Table 5.47). In the lower body, the hip, knee and tibia-calcaneal joints were examined and analysed below.

For the Khoraxa-ams remains, the female individuals showed a slightly higher degree of osteoarthritis (3.75%) compared to the males (3.57%) within the study sample (Table 5.47). The total number of joints affected with osteoarthritis was however greater in the males (47.4%) than in the females (29.4%). It should be noted however, that the total number of joints presenting with osteoarthritis is not a true reflection of the number of individuals affected, but rather the total number of joints with observed synovial joint arthritis. The total number of individuals presenting with osteoarthritis could not be determined due to the difficulty in sorting the remains.

Table 5.46 Occurrence and state of Cribrum Orbitale and Porotic Hyperostosis

UCT Sample No.	B4108 No.	Sex	Age	Pathology
UCT1C	H1: 10	M	40+	Cribrum orbitale left orbit - inactive
UCT1F	H1: 8,15	M	20.1-40	Cribrum orbitale left orbit - inactive
UCT1F	H1: 8,15	M	20.1-40	Porotic hyperostosis right parietal only - inactive
UCT1G	H1: 28,12, 11, 16	F	20.1-40	Porotic hyperostosis left parietal only - inactive

M = Males; F = Females

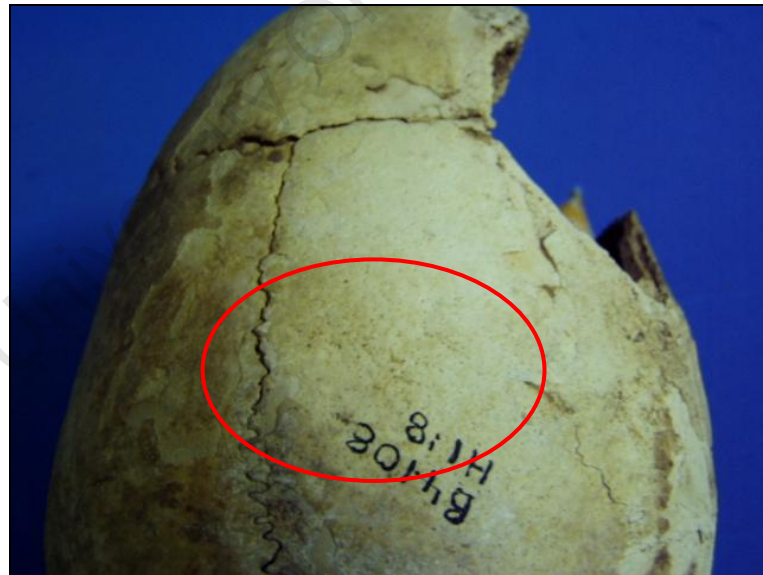


Figure 5.10 UCT1F – Porotic Hyperostosis – inactive

Of the male individuals that presented with osteoarthritis, the synovial joints that were most affected were the shoulder, elbow and radio-carpal joints in the upper limb, and the hip, knee and tibial-calcaneal joints in the lower limb (Table 5.47). Among the females the synovial joints most often affected by osteoarthritis were the joints of the upper limb and the hip and knee joints. One unknown individual presented with osteoarthritis of the joints of the lower limb. Caution should be taken when analysing synovial and non-synovial degenerative joint disease in the study sample due to the small sample size.

Another form of joint disease, temporomandibular joint disease (TMJ), was observed in three male individuals from the study sample (Table 5.47). No females presented with TMJ and the three male individuals that did present with TMJ fell within the category of mature adult. The zygopophyses were also examined for degenerative joint disease; however they could not be classified in terms of male and female individuals. Of the 35 unsexed pooled vertebrae that presented with intact superior and inferior articular facets, 16 presented with osteoarthritis of either the superior or inferior or both articular facets.

It should be noted that the hands and feet were not included in the analysis because there were too few bones present in the sample. However, no osteoarthritis was observed on the bones of the hands and feet that are present. In addition, due to the small sample size, the incidence of joint disease in the Khoraxa-ams sample should be observed with caution.

B. Osteoarthritis of non-synovial joints

Osteophytosis, bone-remodelling producing focal nodules of new bone formation at the bone margin, is a result of degeneration of the intervertebral disc. The bodies of available vertebrae were examined for visible changes of the disk joints as well as for non-synovial joint changes (Table 5.48). Where vertebrae could not be correctly identified, they were grouped into the three major categories of the vertebral column and analysed as such.

Table 5.48 summaries the incidence of osteoarthritis observed on the intervertebral disc and articular joints of the available vertebrae present in the sample. Of a total of 16

Table 5.47 Anatomical location of synovial joint arthritis in the Khoraxa-ams sample per individual

	Females			Males			Unsexed		
	n*	No. of specimens with arthritis	%	n*	No. of specimens with arthritis	%	n*	No. of specimens with arthritis	%
<u>UPPER BODY</u>									
Temporo-mandibular	5	0	0	7	3	42.9	4	0	0
Shoulder	1	1	100.0	2	1	50.0	2	-	-
Elbow	1	1	100.0	2	1	50.0	2	0	0
Radio-carpal	1	0	0	2	1	50.0	2	1	50.0
Sacro-iliac [^]	0	0	0	0	0	0	2	-	-
Zygopophyses [‡]	-	-	-	-	-	-	3 5	16	45.7
<u>LOWER BODY</u>									
Hip	3	1	33.3	2	1	50.0	1	1	100.0
Knee	3	2	66.7	2	1	50.0	1	1	100.0
Tibia-calcaneal	3	-	-	2	1	50.0	1	1	100.0
TOTAL**	1 7	5	29.4	1 9	9	47.4	5 0	20	40.0
TOTAL***	5	3	3.75	7	4	3.57	6	1	1.04

*n = Total number of individuals.

**Total number of joints observed for the presence of osteoarthritis.

***Total number of individuals presenting with osteoarthritis as per the minimum number of individuals in the sample (MIN = 16).

[^]Anterior sacro-iliac joint is synovial.

[‡]Zygopophyses of the cervical, thoracic and lumbar vertebrae were pooled.

cervical vertebrae, 10 showed signs for disc joint arthritis while six showed signs of articular joint changes. Only seven thoracic vertebrae had observable disc joint changes and eight with articular joint arthritis from a total of 29 thoracic vertebrae. The lumbar vertebrae showed the least sign of both intervertebral disc changes as well as articular joint changes within the sample. It should be noted that the lumbar vertebrae were the least represented vertebral bones in the study sample (n = 9).

In addition, other non-synovial degenerative joint disease was examined in the sample. Schmorl's nodes were observed in one adult individual, UCT2C of unknown sex (Table 5.49), on the anterior surface of two lumbar vertebral bodies, H2: 29 and H2: 37 respectively. Schmorl's nodes are formed by vertical vertebral disk herniation, and the depression it leaves can look like an erosive (lytic) lesion (Figure 5.11).

Severe osteophytosis was observed on the sternal body of individual UCT3D at the position of the attachments of the costal cartilage (Table 5.49). Another possibility is that UCT3D could simply present with ossified rib cartilage due to progressive age, however the ossification proceeded beyond the cartilage boarded. This is more indicative of osteophytosis, rather than ossified rib cartilage. In addition, a large osteophyte was observed at the sternal end of the first right rib (H3: 10) of the same individual UCT3D. The osteophyte appeared as a swelling of the sternal end of the rib and showed signs of severe "lipping".

5.5.4.3 Other skeletal pathological processes

Two individuals (UCT1C and UCT1F) within the study sample, both males presented with periostitis on their crania (Table 5.50). In UCT1C (Figure 5.12), the periostitis has affected the outer table into the diploë of the ecto-cranium along the site of muscle attachments at the nuchal crest. It also spread to infect the mastoid processes bilaterally. It appears as if the periosteal infection observed on UCT1C could be the result of inflamed muscles of the neck at the site of attachment along the occipital bone. It could also be stress-related or hypertrophic. However, due to the disordered nature of the ecto-cranial periosteum along the nuchal margin, it is more likely to be infectious. The infection was healing but was still active at time of death. The periosteal infection observed in UCT1F has infected the right mastoid process and appeared unhealed (unremodelled).

Table 5.48 Incidence of observed osteoarthritis of the intervertebral disc and articular (synovial and non-synovial) joints

	n	Non-synovial disc joint changes	Synovial articular joint changes	Total
C1	1	1	1	2
C2	3	1	0	1
C3	1	1	1	2
C4	3	2	1	3
C5	1	1	1	2
C6	1	1	1	2
C7	1	1	1	2
Unknown Cervical*	5	2	0	2
TOTAL	16	10	6	16
T1	3	-	0	0
T2	1	0	0	0
T3	1	1	0	1
T4	2	0	2	3
T5	2	-	1	1
T6	1	1	1	2
T7	2	0	0	0
T8	1	0	0	0
T9	2	0	0	0
T10	1	1	1	2
T11	-	-	-	-
T12	-	-	-	-
Unknown Thoracic*	13	4	3	7
TOTAL	29	7	8	9
L1	1	1	0	1
L2	1	0	0	0
L3	1	0	1	1
L4	1	0	1	1
L5	1	1	-	1
Unknown Lumbar*	4	2	-	2
TOTAL	9	4	2	6

*Unknown = cervical, thoracic and lumbar vertebrae that could not be identified.

In the study sample, bowed tibiae were observed in individual UCT7B, affecting both the right and left tibial shafts with slight visible curvature (H7: 16 and H7: 23 respectively) (Table 5.50). Pronounced “bowing” is most often observed in the lower limb long bones of skeletal remains and can be caused by either dietary deficiencies or post-mortem deformation.

5.5.4.4 Skeletal anomalies

Skeletal anomalies were observed in the skeletal remains of the Khoraxa-ams sample and are listed in Table 5.51. Individual UCT2A (Figure 5.13), identified by re-articulation of the first two cervical vertebrae, i.e. atlas and axis, the incomplete fusion of the posterior vertebral arch of the atlas (H2: 8) was observed, known as cleft vertebrae (spina bifida). Spina bifida is a congenital malformation involving the non-union or imperfect fusion of the vertebral arches (Sadler, 2006). In some cases, the bony defect is covered by skin, and no neurological deficits occur (spina bifida occulta). As a direct result of the cleft vertebra affecting the atlas vertebrae, the axis (H2: 20) presented with a malformed bifid spinous process that is diverted on the right spinous process.

Among the anomalies observed in skeletal remains, flared metaphyses of the distal humerus and septal apertures were the most frequent anomalies observed in the sample. Flared metaphyses is characterized as the unusual widening of the distal portion of the humerus (Friedling, 2007). A septal aperture is a perforation or pinhole between the olecranon fossa and coronoid fossa of the distal humerus (Lundy, 1986; Buikstra and Ubelaker, 1994), (Figure 5.14).

Four individuals from the Khoraxa-ams sample presented with flared metaphysis, based on available humeri in the study sample (Table 5.51). Of the four individuals, all four were adults, two were male and two were unable to be sexed. Two individuals from the study sample presented with both flared metaphyses and septal (trochlear) apertures, one male (UCT4D) and one unknown individual (UCT4E).

A total of nine humeri, representing five individuals were analysed for the presence of flared metaphyses and septal apertures. Of the five individuals one was female, two male and two could not be sexed (Table 5.52). The one female individual was not



Figure 5.11 UCT2C – Schmorl's node on body of lumbar vertebrae



Figure 5.12 UCT1C – Periostitis observed on the base of the occipital bone, unhealed

Table 5.49 Incidence of other non-synovial degenerative joint disease observed on the post-crania

UCT Sample No.	B4108 No.	Sex	Age	Other pathological processes
UCT2C	H2: 29	U	Adult	Lumbar vertebrae - Schmorl's node on superior surface of vertebral body
	H2: 37			Lumbar vertebrae – Schmorl's node on superior surface of vertebral body
UCT3D	H3: 1	U	Adult	Sternal body with severe osteophytosis– advanced “lipping”
	H3: 10			First right rib with large osteophyte at sternal end

U = Unknown sex of individual

Table 5.50 Incidence of other skeletal pathologies observed on the crania and post-crania

UCT Sample No.	B4108 No. for crania	Sex	Age	Other pathological processes
UCT1C	H1: 10,20	M	40+	Periostitis – infection on base of occipital bone; bilateral infection at mastoid process, unhealed
UCT1F	H1: 8,15,31	M	20.1-40	Periostitis – infection on the right mastoid process, unhealed
UCT7B	H7: 23	M	45+	Left Tibia with bowed shaft
	H7: 16			Right Tibia with bowed shaft

M = Males

observed as having either flared metaphysic or septal apertures. Of the two males, both individuals presented with flared metaphyses on both the right and left humeri, and only a septal aperture on the left humerus of one of the individuals. The same pattern was observed on the two unknown individuals, with both having flared metaphyses on the right and left humeri, but only a septal aperture on the left humerus of one of the humeral pairs.

5.5.4.5 Summary of skeletal pathologies

Despite the Khoraxa-ams sample being small in number, various disease processes, skeletal anomalies and stress indicators were observed on a few of the individuals. Of a minimum number of 16 individuals recovered from the cave, a total of nine individuals presented with one or more skeletal pathology. Thus a total of four males, four females and one unknown individual were affected.

A similar number of Harris lines were observed on three individuals, of which two were male and one female, with the timing of appearance being similar for all three individuals (approximately between 12 - 14 years).

Among the non-specific pathologies, both cribra orbitalia and porotic hyperostosis were visible in two individuals respectively. The two individuals that presented with cribra orbitalia were both adult males, and in both cases the left orbit was affected. Of the two individuals that presented with porotic hyperostosis, one was female and the other male.

Osteoarthritis was fairly widespread in the sample, with a total of eight individuals presenting with some form of joint disease. It was not only confined to the older adult individuals, with the younger adults also exhibiting signs of osteoarthritis, typically affecting the joints of the upper limb and the temporomandibular joint, while the joints of the lower limb was most affected in the older adult individuals.

Osteoarthritis of the intervertebral disc and articular (synovial and non-synovial) joints were observed on all 16 cervical vertebrae, nine thoracic vertebrae from a total of 29, and six lumbar vertebrae from a total of nine identified vertebrae in the sample. However, due to the difficulty in sorting the vertebrae into separate individuals, the total number of individuals affected by osteoarthritis of the spine could not be established.



Figure 5.13 UCT2A – atlas and axis vertebrae showing cleft vertebrae (Spina bifida) and malformed bifid spinous process



Figure 5.14 UCT4D – Flared distal metaphysis (yellow arrow) with septal aperture (red arrow) on left humerus

Table 5.51 Observed skeletal anomalies in the post-crania of the Khoraxa-ams sample

UCT Sample No.	B4108 No.	Sex	Age	Skeletal anomalies	
UCT2A	H2: 8	M	20.1-40	Atlas vertebrae – incomplete fusion of the vertebral arch resulting in a cleft vertebra (spina bifida)	
	H2: 20	M	20.1-40	Axis vertebrae – malformed bifid spinous process	
UCT4B	H5: 15	L*	M	40+	Flared distal metaphysis of left humerus
	H5: 20	R			Flared distal metaphysis of right humerus
UCT4D	H5: 18	L	M	20.1-40	Flared distal metaphysis of left humerus
	H5: 22	R			Flared distal metaphysis of right humerus
UCT4C	H5: 17	R	U	15.1-20	Flared distal metaphysis of right humerus
	H5: 16	L			Unflared distal metaphysis of left humerus
UCT4E^	H5: 21	L	U	20.1-40	Flared distal metaphysis of left humerus
UCT4D	H5: 18	L	M	20.1-40	Trochlear aperture in left humerus
	H5: 22	R			No trochlear aperture in right humerus
UCT4E^	H5: 21	L	U	20.1-40	Trochlear aperture in left humerus

M = Males; F = Females; U = Unknown sex

*Refers to either the Left or Right bone element.

^Unpaired left humerus.

Table 5.52 Occurrence of flared metaphysis and septal apertures in study sample

	Females			Males			Unknown		
	n*	No. of specimens with anomaly	%	n*	No. of specimens with anomaly	%	n*	No. of specimens with anomaly	%
Flared metaphysis	1	0	0	2	2	100.0	2	2	100.0
Septal (trochlear) aperture	1	0	0	2	1	50.0	2	1	50.0
TOTAL	1^	0	0	2^	3	60.0	2^	3	60.0

*n = Total number of individuals based on distal humeri method for sex estimation.

^Total number of individuals represented by the humeri = five; with one identified as female, two male and two unknown.

Several skeletal anomalies as well as other pathologies were also found within the study sample. Two older male individuals were observed to have unhealed Periostitis on their crania. Schmorl's nodes were visible on two lumbar vertebrae of an adult of unknown sex. The skeletal anomalies present in the sample include unfused vertebral arch of first and second cervical vertebrae, as well as flared metaphyses and septal apertures affecting a total of four individuals.

5.5.5 Cranial morphology

Cranial measurements, using standard linear skeletal anthropometric landmarks on all available crania in the sample were performed. Linear morphometric cranial analysis was used to establish the degree of cranial morphological variation within the sample compared to known reference groups. The purpose being to statistically identify, using multivariate principal component analysis (PCA), which reference group the Khoraxams sample closely resemble.

PCA has the ability to reduce the number of variables and detects structure in relationships between variables (StatSoft, Inc. 1984-2008). It examines the shape and size variation in three-dimensional space and morphometric distances between populations. The stepwise procedure ranks the measurements in order of their discriminatory function as well as power of variation. The selected measurements are then used to compute eigenvalues. These eigenvalues are displayed to show the success of the separation produced by the principal components (PC) (Morris, 1984; Powell and Neves, 1999).

When using multivariate techniques, it is preferable to use a complete list of cranial and mandibular measurements. This is prevented however, by the need for complete specimens in the PCA. The analysis of the cranium in terms of three separate structural categories, the vault, face and mandible reduces this problem. Also, if the sample size is drastically decreased due to specific missing measurements, these measurements must be removed from the analyses (Morris, 1984). The measurements that were removed are the nasion-bregma subtense, nasion-subtense fraction, bimaxillary subtense, naso-

frontal subtense, palatal height, mandibular notch subtense, molar-premolar subtense, sigmoid notch, projected length of corpus, and condylar-coronoidal angle.

The reason for removing these specific measurements is due to the poor preservation and destruction of these bony landmarks. The Khoraxa-ams samples, specifically the crania were poorly preserved⁵ and very fragile when handled. Thus, the ability to measure certain landmarks was not possible and limited the number of measurements obtained. The final list of measurements used for PCA consisted of 16 vault, 18 facial and 14 mandibular measurements (Appendix 3A). For cranial measurement values see Appendix 3B.

In this study, the mean PCA scores for the vault, face and mandible were computed separately for each of the three populations, two being the reference data and plotted in three dimensions using ordination. This technique provides a visual assessment of the overall morphological relationships within and between groups (Powell and Neves, 1999).

The PCA analysis was separated into three „Activities’ for the vault, face and mandible respectively. The results are presented below according to the three cranial regions for both males and females. Included in the results is the total variance explained by computed eigenvalues, the selected measurements in rank order of the computed components showing the greatest variation, and a scatter plot illustrating the dispersion of variation in three dimensions for each computed PC.

Activity 1: Vault

Table 5.53 presents the total variance explained for the measurements of the vault, based on computed eigenvalues for each principal component (PC). The percentage of variation explained is defined by eigenvalue per component compared to the total eigenvalues of all components. The relatively large scale of the first eigenvalue suggests that size is very important in these analyses as the first component is primarily

⁵ The state of preservation of the Khoraxa-ams remains will be discussed in detail in section **5.62 Preservation States**.

influenced by width dimensions and overall cranial length (Morris, 1984; González-José *et al.*, 2005).

Components 1 – 5 collectively account for 74.2% and 77.7% of the variation of males and females respectively. While the percentage of the total variance explained by the first three PCs for the vault measurements (Table 5.53) account for 57.6% and 60.1% of the variation for the males and females, respectively. Despite the size factor being slightly more evident in the variation of the vault of males (32.7%) than of females (31.7%), the females displayed more variation within the first three components.

The variables used in the computation of these PCs are listed in Table 5.54 for measurements of the vault of both male and females. They are ranked in order of their relative power of loading, strongest to the weakest, in this case Component 1 being the strongest and Component 3 being the weakest. These components have been rotated so that their maximum power is in line with the x or y-axis.

In Table 5.54, the first PC for the males seems to express mainly the transversal profile and cranial height. The second PC is primarily influenced by the length and curvature of the parietals. The third PC is influenced by occipital length and curvature as well as the length of the vault. However, the first PC computed for the female vaults (Table 5.55) expresses the length and curvature of the parietals, the length of the occipital and the height of the cranium. The second PC is influenced by the length and curvature of the frontal bone. The third PC is influenced by occipital length and curvature and the transversal profile of the vault.

Information regarding the distribution of variation between and within individuals based on PCs computed for each group is presented in scatter plots for the PC scores of males and females (Figure 5.15a and b). PC1 and PC3 collectively account for 42.8% of the variation of the males. While PC1 and PC2 account for 47.2% of the variation of the females. The circles represent the mean score of each sample based on PC1 and PC2 for analysis 1. Analysis 1 refers to the computed PCA for the vault measurements. Based on the visible pattern of dispersion of coloured circles in Figure 5.16a and b, the Khoraxa-ams sample (Blue circles) tends to cluster with the Negro reference sample (Orange circles) and is the case with each repeated analysis. The dispersion of the

circles point towards the measurements being highly variable and that each reference sample looks different to each other.

Another pattern that appears on the scatter plot (Figure 5.15a and b) is the distribution (spread of circles) of the Negro samples clustering at the top right of the graph, with the Khoesan samples (Green circles) tending to cluster at the bottom left. This illustrates the difference in cranial morphology and variation in the appearance of the reference samples. Throughout the PCA and its visual display using scatter plots, the Khoraxams sample repeatedly clustered with the Negro reference samples.

University Of Cape Town

Table 5.53 Total variance explained for vault measurements for males and females

Component*	Male		Female	
	Eigenvalue	% of Total	Eigenvalue	% of Total
1	5.228	32.7	5.073	31.7
2	2.395	14.9	2.476	15.5
3	1.623	10.1	2.072	12.9
4	1.533	9.6	1.450	9.1
5	1.111	6.9	1.353	8.5
6-16	4.110	25.7	3.576	22.3
TOTAL	16.00	100.0	16.00	100.0

*Component = REGR factor score 1 –16, where REGR is the name assigned to the factor analysis by SPSS version 15.

Table 5.54 Selected vault measurements in rank order of computed components for males and females using Principal Component Analysis* (PCA)

Component ^	Measurements	
	Males	Females
1	Frontal Arc Frontal Chord Transverse Arc Basibregmatic Height	Parietal Chord Parietal Arc Mastoid Height Basibregmatic Height Occipital Chord
2	Parietal Arc Parietal Chord	Frontal Arc Frontal Chord Maximum Cranial Length
3	Occipital Arc Occipital Chord Maximum Cranial Length Mastoid Height	Occipital Arc Transverse Arc Bi-Asterionic Breadth

*Extraction Method: Principal Component Analysis, 3 components extracted.

^Rotation Method: Varimax with Kaiser Normalization. Rotation converged in 6 iterations.

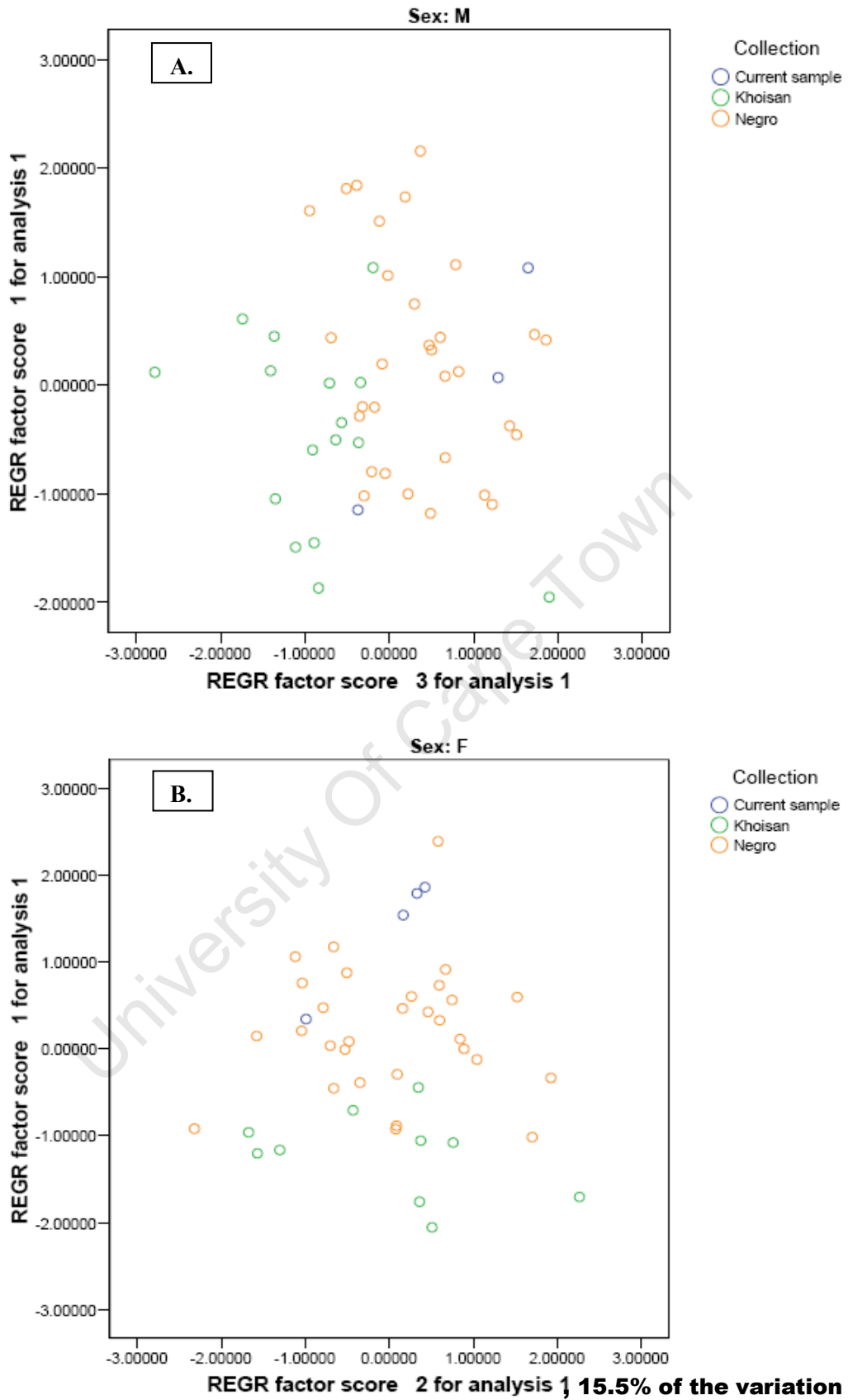


Figure 5.15 Scatter plots based on factor scores for vault measurements for males plot of PC3 (10.1%) and PC1 (32.7%) (**A.**) and females, plot of PC2 (15.5%) and PC1 (31.7%) (**B.**). PC1 and PC3 account for 42.8% of variation of the males, and PC1 and PC2 for 47.2% of variation of the females.

Activity 2: Face

Table 5.55 presents the total variance explained for the measurements of the face, based on computed eigenvalues for each PC. Collectively, components 1 – 5 account for 80.6% and 81.3% of the variation of males and females, respectively. The percentage of the first three PCs account for 67.8% and 68.6% of the variation of the males and females, respectively. Once again the females displayed more variation within the first three components, despite the PC1 score for the males (48.5%) being greater than the females (43.0%).

Table 5.56 ranks the variables used to compute the PC for measurements of the facial region, from strongest to weakest. The first PC for the males is primarily influenced by the size and shape of the face, orbital region, maxilla and palate. PC2 mainly expresses the size and shape of the facial region as well as the height of the orbits and the size and shape of the nose. PC3 is influenced by the size and shape of the maxilla and palatal region as well as the height of the upper-mid facial region. In the females, PC1 seems to mainly express the size and shape of the orbital and facial region. PC2 is primarily influenced by the height of the upper-mid facial region, the size and shape of the maxilla and palate as well as facial projection. Finally, PC3 is influenced by the size and shape of the nasal, maxilla and palatal regions.

Scatter plots illustrating the distribution of variation of plotted PC scores based on the PCs computed for the study sample and the reference groups of males and females are presented in Figure 5.16a and b, respectively. PC1 and PC2 collectively account for 59.2% of the variation within and between the male samples, while PC1 and PC2 account for 51.4% of the variation within the between the females. The circles represent the mean score of each sample based on PC1 and PC2 for analysis 2. Analysis 2 refers to computed PCA for the face measurements.

The distribution of the mean PCA scores for the facial measurements of each group is presented in Figure 5.16. In Figure 5.16a both reference groups could not be separated into neat clusters within the scatter plot, owing to a lack of discriminate power of variation between the Negro and Khoesan reference samples. As the result, the

Khoraxa-ams samples are not clearly distributed within the plot and no assumption as to the resemblance in cranial morphology based on the face can be made for the male individuals. A similar pattern can be seen in Figure 5.16b, however the Negro reference group is slightly clustered to the right and bottom portion, while the Khoesan reference samples are clustered in the middle and left portion of the graph. The female Khoraxa-ams samples tend to cluster on the bottom of the graph, among the Negro samples, with one Khoraxa-ams sample on the periphery of the graph. The single Khoraxa-ams individual on the periphery of the graph is therefore considered an outlier.

University Of Cape Town

Table 5.55 Total variance explained for face measurements for males and females

Component*	Male		Female	
	Eigenvalue	% of Total	Eigenvalue	% of Total
1	8.725	48.5	7.742	43.0
2	1.920	10.7	3.091	17.2
3	1.549	8.6	1.504	8.4
4	1.268	7.0	1.276	7.1
5	1.046	5.8	1.015	5.6
6-16	3.491	19.4	3.370	18.7
TOTAL	18.00	100.0	17.623	100.0

*Component = REGR factor score 1 –16, where REGR is the name assigned to the factor analysis by SPSS version 15.

Table 5.56 Selected face measurements in rank order of computed components for males and females using Principal Component Analysis* (PCA)

Component^	Measurements	
	Males	Females
1	Bizygomatic Breadth Bifrontal Breadth Outer Bi-orbital Breadth Maximum Alveolar Breadth Inner Bi-orbital Breadth Palatal Breadth	Outer Bi-orbital Breadth Inner Bi-orbital Breadth Orbital Breadth Bifrontal Breadth Bizygomatic Breadth
2	Orbital Height Nasal Height Upper Facial Height Bi-maxillary Breadth	Prosthion-Basion Length Maximum Alveolar Length Nasion-Basion Length Palatal Length
3	Maximum Alveolar Length Palatal Length Prosthion-Basion Length	Maximum Alveolar Breadth Palatal Breadth Nasal Breadth

*Extraction Method: Principal Component Analysis, 3 components extracted.

^Rotation Method: Varimax with Kaiser Normalization. Rotation converged in 7 iterations.

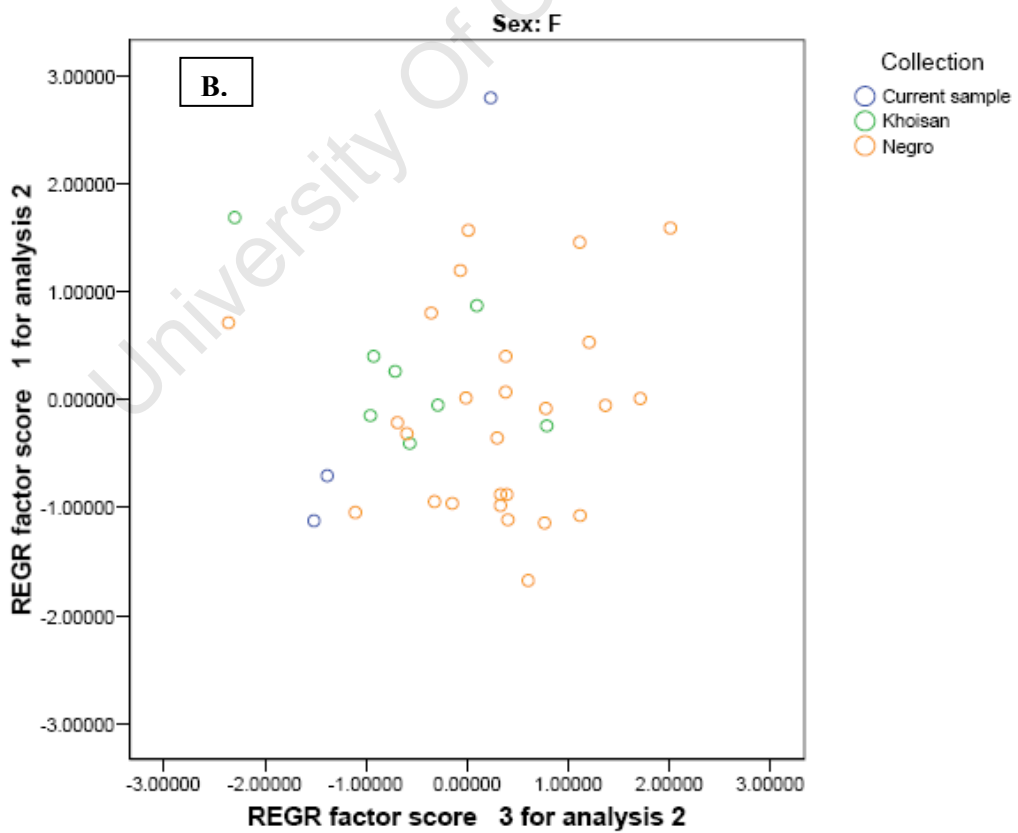
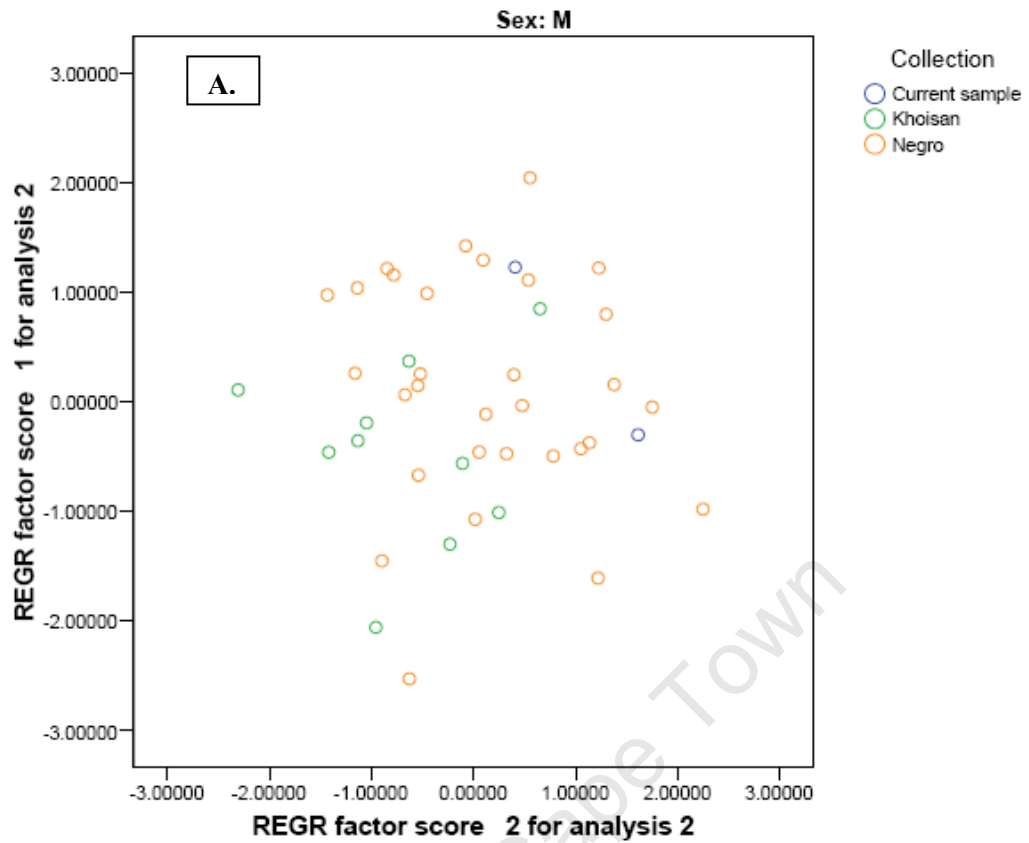


Figure 5.16 Scatter plots based on factor score for facial measurements for males, plot of PC2 (10.7%) and PC1 (48.5%) (**A.**) and females, plot of PC3 (8.4%) and PC1 (43.0%) (**B.**). PC1 and PC2 account for 59.2% of variation of the males and PC1 and PC3 account for 51.4% of the variation of females.

Activity 3: Mandible

The total variance explained for the PC scores of the mandibular measurements are presented in Table 5.57 for males and females. Components 1 – 5 collectively account for 78.1% of the variation of the males and 74.5% for the females. The percentage of the first three PC scores account for 64.1% and 57.6% of the variation of the males and females, respectively. In this case, the males display more variation within the first three components as well as in the first PC.

Table 5.58 ranks the selected variable used to compute the PC scores for mandibular measurements from strongest to weakest. The first PC for the males mainly expresses the size and shape of the ramus and the mandible as a whole. PC2 is influenced by the width of the ramus, as well as the length and breadth of the condyles. PC3 for the males is primarily influenced by the size and shape of the mandible as a whole. Among the females, PC1 is primarily influenced by the size and shape of the corpus mandibulae as well as the overall size and shape of the mandible. PC2 mainly expresses the size and shape of the ramus, while PC3 is influenced by the length and breadth of the condyles.

Figure 5.17a and b illustrates the spread of variation based on plotted PC scores for the study sample and the reference groups for male and female mandibular measurements. PC1 and PC2 collectively account for 53.3% of the variation of the males, and PC1 and PC2 account for 47.3% of the variation of the females. The circles depicted on the scatter plot represent the mean score of each sample across PC1 and PC2 for analysis 3. Analysis 3 refers to computed PCA for mandibular measurements.

The pattern of distribution for the reference samples and the Khoraxa-ams samples are visible in Figure 5.17. In Figure 5.17a the Negro reference group clusters on the top portion, with the Khoesan reference groups clustering on the bottom portion of the graph. The three Khoraxa-ams samples are dispersed on the top portion of the graph, with two samples on the periphery of the main Negro cluster. In Figure 5.17b the Negro and Khoesan reference samples are distributed in a similar pattern as in Figure 5.17a. Once again, the Khoraxa-ams samples tend to cluster at the bottom of the graph, though at the periphery of the main Khoesan cluster. Therefore it can be said, once again, that

the male individuals tend to cluster with the Negro reference group, while the females tend to cluster with the Khoesan reference group.

Of the three PC analyses that were conducted on the study sample, it is evident that the least effective discriminate measurements were that of the face (Figure 5.16). Both the reference groups as well as the Khoraxa-ams sample could not be differentiated from each other and therefore the dispersion of the samples could not cluster into separate morphological groups. The power of variation with regards to the facial measurements was therefore very low. Despite the lack of dispersion among the facial measurements, cranial morphological variation between and within each group was achieved. In summary, it is evident that the Khoraxa-ams samples tend to cluster more closely with the Negro reference sample group and therefore morphologically resemble the Negro reference group based on cranial measurements.

Table 5.57 Total variance explained for mandible measurements for males and females

Component*	Male		Female	
	Eigenvalue	% of Total	Eigenvalue	% of Total
1	4.902	35.0	3.923	28.0
2	2.560	18.3	2.697	19.3
3	1.510	10.8	1.442	10.3
4	1.075	7.7	1.395	10.0
5	0.890	6.3	0.973	6.9
6-16	3.063	21.9	3.569	25.5
TOTAL	14.00	100.0	14.00	100.0

*Component = REGR factor score 1 –16, where REGR is the name assigned to the factor analysis by SPSS version 15.

Table 5.58 Selected mandible measurements in rank order of computed components for males and females using Principal Component Analysis* (PCA)

Component^	Measurements	
	Males	Females
1	Projected Height of Ramus Corpus Height at M2 Projected Height of Coronoid Mandibular Angle	Maximum Length of Mandible Symphyseal Height Maximum Breadth outside Condyles Bicoronoidal Breadth Bimental Breadth Bigonial Breadth
2	Minimum Width of Ramus Breadth of Condyle Length of Condyle	Projected Height of Ramus Mandibular Angle Projected Height of Coronoid Minimum Width of Ramus Corpus Height at M2
3	Bicoronoidal Breadth Bigonial Breadth Maximum Breadth outside Condyles	Length of Condyle Breadth of Condyle

*Extraction Method: Principal Component Analysis, 3 components extracted.

^Rotation Method: Varimax with Kaiser Normalization. Rotation converged in 8 iterations.

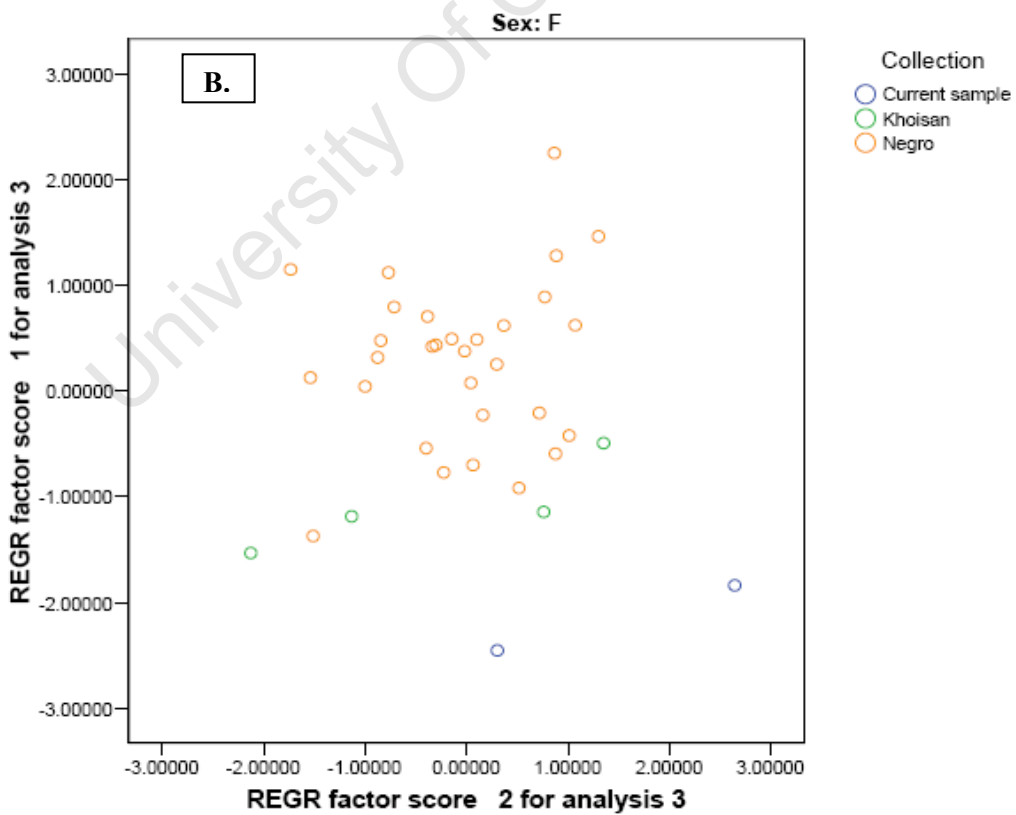
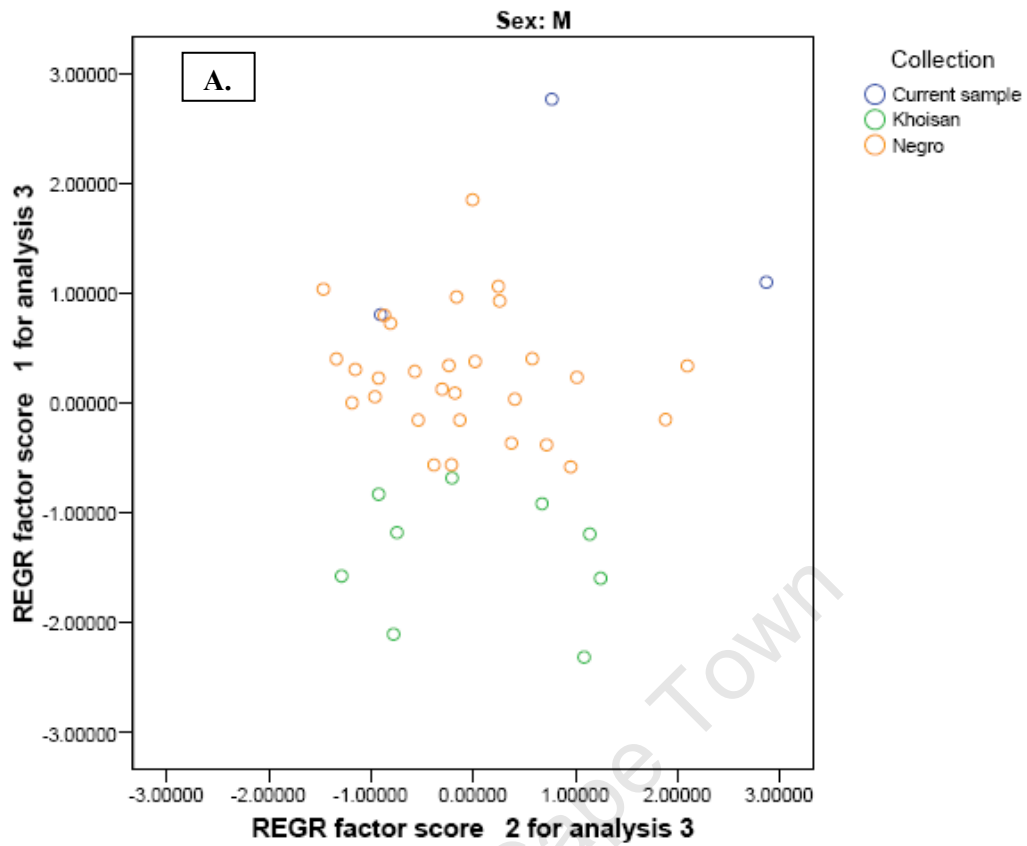


Figure 5.17 Scatter plots based on factor scores for mandibular measurements for males, plot of PC2 (18.3%) and PC1 (35.0%) (**A.**) and females, plot of PC2 (19.3%) and PC1 (28.0%) (**B.**). PC1 and PC2 account for 53.3% of the variation of the males, and PC1 and PC2 for 47.3% of variation of the females.

5.6 Peri- and Post-mortem Features

5.6.1 Breakage patterns

The occurrence of skeletal trauma and breakage patterns observed on the crania from Khoraxa-ams is presented in Table 5.59. Of the 16 crania in the sample, 11 individuals (68.75%) presented with some form of trauma or cranial fractures. Of the 11 individuals, five were female and six male, ranging in age from 15.1-20 to 45+. Fractures observed on the post-cranial remains are listed in Table 5.60 and were more prevalent on the long bones. The long bones of the upper and lower limbs were examined and the fracture patterns recorded with reference to the type of injury and the location on the bone. Fractures were more prevalent on the lower limbs and were equally present on both male and female individuals.

Of the cranial bones (Table 5.59), individual UCT1K presented with an impact above the left orbit, causing bone loss of the superior-medial orbital shelf. The impact caused radiating fractures, both superior and inferiorly and is known as Le Fort's fracture. Le Fort fractures are defined as fracture patterns of the facial skeleton based on areas of failure that are directed by areas of reinforcement, caused by blunt force trauma to the face (Berryman and Symes, 1998). The inferior radial fracture transected the nasal bone as well as the right and left zygomas', terminating on the right and left maxilla. Superiorly, the radial fracture terminated on the frontal bone above the left orbit (Figure 5.18). Individual UCT1B, an unknown sub-adult, had a depression fracture at Bregma with concentric and radial fractures radiating from the primary impact (Figure 5.19). It was also noted that UCT1B had an unhealed nasal bone causing a change in bone contour. UCT1E, a female individual aged 20.1-40, presented with bone loss and delamination to the right parietal bone above the external auditory meatus (Figure 5.20). A similar fracture was observed on the left parietal of UCT1E, possibly causing the complete separation of the frontal bone to the left and right parietals along the coronal suture (Figure 5.21). This separation of the coronal suture resulted in plastic deformation of the cranial vault.

Skeletal trauma was observed on a few individuals where extensive bone loss had occurred (Table 5.59). Individual UCT1J was represented only by the basal cranium

Table 5.59 Incidence of skeletal trauma and fracture patterns as visible on the crania

UCT Sample No.	B4108 No.	Sex	Age	Location of Trauma
UCT1K	H1: 6	F	40+	Impact above left orbit causing bone loss at superior-medial orbital shelf with superior and inferior radial fractures through nasal bone, right and left zygoma's, terminating on right and left maxilla inferiorly. Le Fort's fracture.
UCT1I	H1: 1, 60	F	40+	Transverse fracture at right infra-orbital margin, terminating on right zygoma with most of left half of face missing.
UCT1E	H1: 9, 54	F	20.1-40	Trauma to right parietal bone causing delamination and bone loss. Left parietal bone fractured at base of coronal suture, possibly causing separation of the frontal bone to parietals along coronal suture as well as plastic deformation. Fracture at greater sphenoid transecting left mastoid and terminating at left temporal squamous suture.
UCT1G	H1: 28, 12, 11, 16	F	20.1-40	Unhealed linear fracture above left orbit with complete fracture along the coronal and sagittal sutures separating left and right parietal bones.
UCT1B	H1: 7, 37	U	15.1-20	Depression fracture with concentric and radial fracture patterns at Bregma. Unhealed linear fracture on nasal bone causing change in bone contour.
UCT1J	H1: 44, 63	M	45+	Cranium very fragmentary with only basal cranium and maxilla remaining.
UCT1H	H1: 2, 40, 41, 56	M	40+	Complete fracture along mid-facial region causing bone loss from inferior orbital sockets to maxilla. Complete fracture on right and left mandibular ramus.
UCT1A	H1: 4, 43, 61, 55	M	40+	Compression fracture at right coronal suture, transecting Bregma down third of sagittal suture, terminating laterally at mid-point of left parietal. Fracture at left temporal and zygomatic arch intersecting left mastoid. Fracture at right condylar process of mandible.
UCT1D	H1: 5, 30	M	40+	Complete fracture at left zygomatic arch. Bone loss of right inferior orbital socket, zygomatic bone and posterior aspect of right maxilla.
UCT1L	H1: 3	M	40+	Bone loss of foramen magnum and both wings of the sphenoid on the base of the cranium with resulting fracture transecting base of occipital bone and right lower parietal bone, terminating at mid-point of occipital. Complete fracture circling left mastoid, running along squamous suture and terminating at mid-point of left zygomatic arch. Fracture from left maxilla, running superior through sphenoid bone along superior margin of left orbital socket. Then transecting nasal bone (left) and running inferior to terminate at maxilla, causing bone loss of anterior alveolar bone.
UCT1F	H1: 8, 15, 31	M	20.1-40	Fracture transecting midline of face, beginning at maxillary mid-point, transecting frontal bone, crossing coronal suture and terminating on right root of zygoma, resulting in loss of left orbit, maxilla and zygomatic arch.

F = Females; M = Males; U = Unknown

and maxilla (Figure 5.22). The cranial vault, upper-facial region as well as most of the mid-facial region was missing. The remaining cranial bones were very fragmentary. UCT11 presented with trauma to the left facial region, resulting in bone loss to most of the left facial bones, i.e. the zygoma and maxilla, including the inferior orbital socket and zygomatic arch (Figure 5.23).

A total of eight individuals presented with fractures on the post-cranial bone elements (Table 5.60). Of the eight, three were female, three male and two could not be sexed. Three individuals (UCT4A-UCT7A; UCT4B-UCT7B; UCT4C-UCT7C) presented with fractures to both their upper and lower limb long bones, while two individuals were observed to have fractures only on their upper limbs and three only on their lower limb bones.

Individual UCT4A-UCT7A, a female between the ages of 20.1-40, was observed as having a crush fracture on the epiphysis of the left humerus, a transverse fracture on the shaft of the left radius, as well as a longitudinal fracture on the shaft of the left ulna (Table 5.60). On the lower limbs individual UCT4A-UCT7A presented with an unhealed oblique fracture on the distal left tibia with radiating fractures, an oblique fracture on the distal left femur, as well as a transverse fracture on the distal right femur.

A male individual over the age of 45, UCT4B-UCT7B presented with a transverse fracture on the mid-shaft of the right radius, as well as transverse fractures on the distal left fibula and on the proximal and distal epiphyses of the right fibula (Table 5.60). Individual UCT4C-UCT7C, a sub-adult had a transverse fracture on the distal right humerus, a longitudinal fracture along the vertical shaft of the right radius as well as a transverse fracture at the radial neck. On the lower limbs, individual UCT4C-UCT7C had an unhealed spiral fracture on the proximal left tibia, a longitudinal fracture along the shaft of the left femur, as well as an oblique fracture on the proximal left fibula.

Of the 11 individuals that presented with skeletal trauma discussed above, most were observed as having post-mortem injuries with a few presenting with peri-mortem injuries, occurring at or around the time of death. No ante-mortem injuries were observed among the individuals of Khoraxa-ams. Of particular interest in interpreting

the traumatic injuries experienced at Khoraxa-ams are peri-mortem fractures observed among five individuals, listed in Table 5.61. They include UCT1K and UCT1I, older adult females, UCT1G and UCT1E younger adult females and UCT1B, a sub-adult with indeterminate sex. The extent of the injuries observed on the aforementioned individuals was discussed in Table 5.59 and Table 5.60 for cranial and post-cranial remains, respectively.

University Of Cape Town

Table 5.60 Incidence of skeletal trauma and fracture patterns present on the post-cranial remains

UCT Sample No.	B4108 No.	Sex	Age	Location of Trauma
<u>UPPER LIMBS</u>				
UCT4A	H5: 16 H7: 17 H5: 3, 4	F	20.1-40	Crush fracture on posterior aspect of distal epiphysis of left humerus. Transverse fracture at proximal third of shaft of left radius. Longitudinal fracture at proximal two-thirds of shaft of left ulna.
UCT4B	H5: 6	M	45+	Transverse fracture at mid-shaft of right radius.
UCT4D	H5: 5 H5: 10 H5: 12	M	20.1-40	Transverse fracture at proximal epiphysis of right radial neck. Transverse fracture at proximal third of shaft of left radius. Oblique fracture at distal third of shaft of left ulna.
UCT4C	H5: 19 H5: 1, 2, 8	U	15.1-20	Transverse fracture at distal third of shaft of right humerus. Longitudinal fracture along vertical shaft of right radius and transverse fracture at radial neck.
UCT4E	H5: 21	U	20.1-40	Spiral fracture at mid-shaft of left humerus.
<u>LOWER LIMBS</u>				
UCT7A	H7: 4 H7: 7 H7: 21	F	20.1-40	Transverse fracture at distal two-thirds of right femur. Oblique fracture at distal one-third of left femur. Unhealed oblique fracture of left tibia on distal two thirds of shaft with radiating fractures on medial aspect of shaft.
UCT7D	H7: 1 H7: 10 H7: 12 H7: 26	F	40+	Sub-intertrochanteric fracture to neck of right femur. Transverse fracture at neck of left femur Unhealed spiral fracture on distal third of left femur, resulting in parallel radiating fractures on anterior and posterior surface of shaft. Oblique fracture at proximal third of right tibia. Unhealed transverse fracture of right fibula transecting two thirds of shaft at proximal end.
UCT7F	H7: 11	F	40+	Oblique fracture at base of greater trochanter of left femur.
UCT7B	H7: 25 H7: 28	M	45+	Transverse fracture at distal third of left fibula. Transverse fractures at both proximal and distal epiphyses of right fibula.
UCT7E	H7: 5, 19	M	40+	Longitudinal fracture as well as oblique fracture at base of lesser trochanter of right femur.
UCT7C	H7:2, 6 H7: 27 H7: 22, 14	U	15.1-20	Longitudinal fracture along three quarters of left femur. Oblique fracture at proximal third of left fibula. Unhealed spiral fracture of proximal left tibia on medial side of tibial tuberosity running obliquely, terminating on one third of shaft anterior-posterior.

F = Females; M = Males; U = Unknown sex

Table 5.61 Individuals from Khoraxa-ams with observed peri-mortem injuries

UCT Sample No.	Sex	Age	Bone(s) affected	Type of peri-mortem injury
UCT1K	F	40+	Cranium	LeFort 2 fracture
UCT1I (UCT7D)*	F	40+	Femur, left Femur, right	Unhealed spiral fracture on distal third Sub-intertrochanteric fracture to neck of femur
UCT1G	F	20.1-40	Cranium	Unhealed linear fracture above left orbit
UCT1E (UCT4A)*	F	20.1-40	Cranium Humerus, left	Delamination and bone loss to right parietal Coronal suture separation with plastic deformation
(UCT7A)*			Radius, left Ulna, left Tibia, left	Crush fracture at distal epiphysis, posteriorly Transverse fracture at proximal third Longitudinal fracture at proximal two-thirds Unhealed oblique fracture at distal two-thirds with radiating fractures on medial shaft
UCT1B (UCT7C)*	U	15.1-20	Cranium Femur, left Tibia, left Fibula, left	Depression fracture with concentric and radial fractures at Bregma Unhealed linear fracture on nasal bone Longitudinal fracture along three-quarters of shaft Unhealed spiral fracture at proximal third Oblique fracture at proximal third

*Corresponding paired upper limb and lower limb UCT sample no.

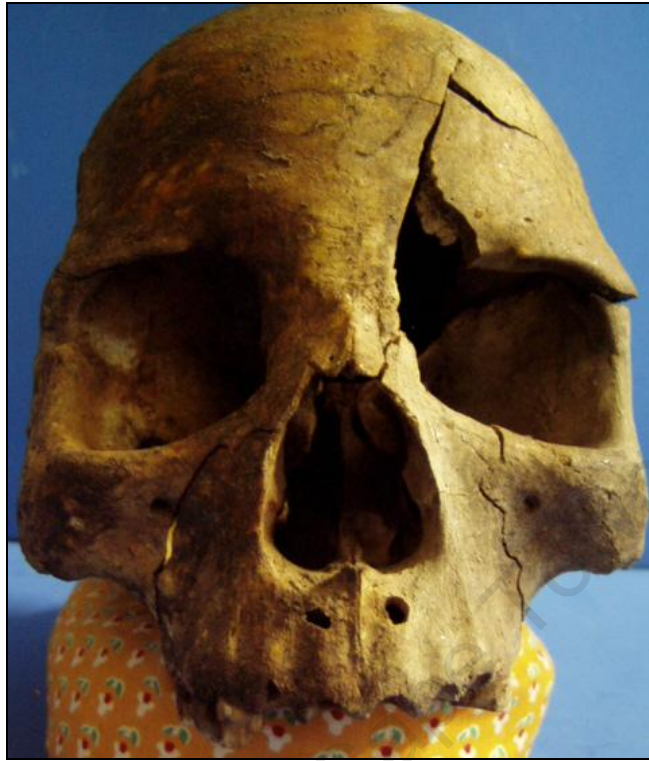


Figure 5.18 UCT1K – Le Fort's fracture with resultant radial fractures due to blunt force trauma to the face.

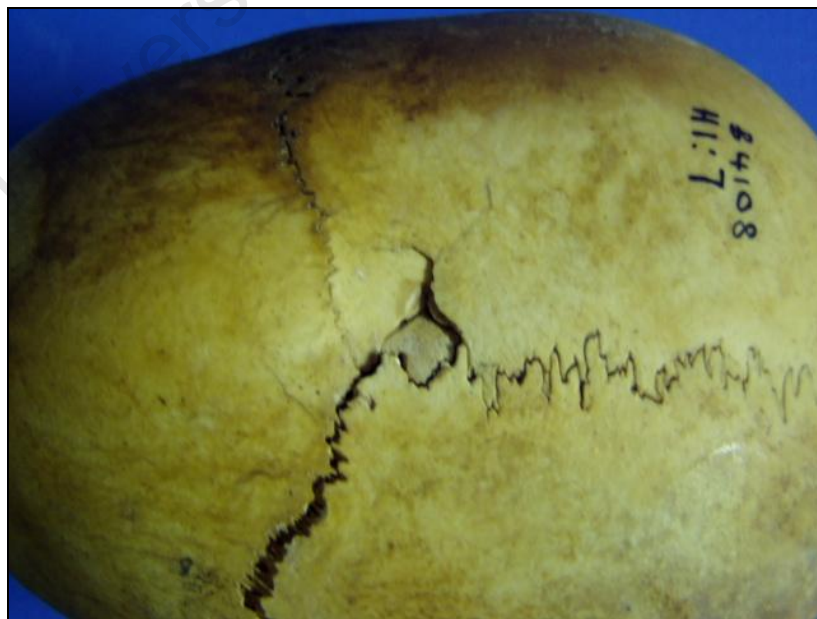


Figure 5.19 UCT1B – Depression fracture at Bregma with concentric and radial fractures

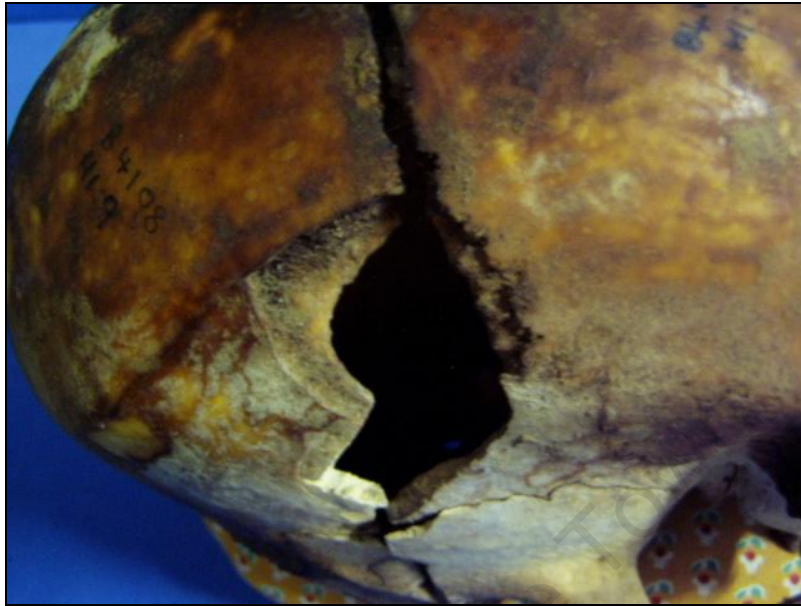


Figure 5.20 UCT1E – Trauma on right parietal bone resulting in delamination and bone loss



Figure 5.21 UCT1E – Complete separation of the frontal bone to the parietals along the coronal suture, resulting in plastic deformation of the cranial vault



Figure 5.22 UCT1J – Fractures to cranium causing extensive bone loss



Figure 5.23 UCT1I – Trauma to the left facial region resulting in bone loss to most of the left facial bones

5.6.2 Preservation states

5.6.2.1 Completeness

The Bone Representation Index (BRI*)

Table 5.62 shows the Bone Representation Index (BRI*) for each bone element in the study sample. This measure of preservation was based on the frequencies of each bone expressed as a percentage of the entire study sample (total number of skeletal remains that should be present, $n = 16$)⁶. The hands and feet represented in the study sample were included in the analysis as single entities. The vertebral column was divided into cervical, thoracic and lumbar vertebrae, however the sacrum was analysed as a single element. The coccyx was not included in the analysis, as it was not represented in the study sample.

According to the BRI* determined for all the bone elements in the sample, the cranial bones (67.5%) appear to be more represented than the post-cranial (18.8%). With the highest BRI* calculated for the occipital and right parietal bones (100%) (Table.5.62). The most highly represented post-cranial bones as determined from the BRI* were the right and left femoral bones as well as the left humeri (31.3%). The lowest represented bone elements present in the sample were the left and right hand bones (2.1 and 4.2%). Within the cranial bones, the lowest represented bone element as determined by the BRI* was the left lacrimal bone (25%). With regards to the bone representation of paired bone elements, the BRI* is evenly distributed between the right (41.7%) and left (40.1%) paired skeletal elements.

Frequency of skeletal elements recovered

The frequency of bone was calculated in order to determine the representation of individual bones within the sample. Given that an MNI of 16 was determined for the sample, it was therefore possible to calculate the relative frequency of bones in the sample based on the maximum number of bones possible (e.g. parietal bone paired in cranium, therefore 2×16

⁶ The BRI* was determined using 16 as the total number of individuals recovered from the cave. This is based on 16 being the highest minimum number count for occipital and parietal bones present in the sample (MNI).

= 32, possible parietal bones in sample). Adiaagnostic fragments were not calculated in this process.

Table 5.63 illustrates the number of skeletal elements, both cranial and post-cranial recovered from the site. For the purpose of determining the frequency of skeletal elements, the cranium was separated into individual cranial bones and counted as such. However, the bones of the vertebral column were pooled for each vertebral category, e.g. cervical, thoracic and lumbar. The phalanx of the hands and feet were also pooled (n = 56) for determining their frequency within the sample.

The most frequent skeletal elements represented in the sample were ranked for the cranial and post-cranial bones, Tables 5.64 and 5.65 respectively. The occipital bone was the bone used to calculate MNI, therefore 100% frequent by definition. In addition, the parietal bone (96.9%) and the frontal bone (87.5%) were well represented within the sample.

Table 5.65 ranks the most frequent post-cranial bones recovered from the site. The femora (31.3%) and humeri (28.1%) were the most represented post-cranial elements in the sample. While the phalanx (1.8%), tarsals (0.5%) and the carpals (0.4%) were the least frequent bone elements present in the sample.

5.6.2.2 Fragmentation

The Anatomical Preservation Index (API*)

The API* is a method proposed by Bello *et al.*, (2006) that assesses preservation based on the amount of bone material present. For the bone elements present in the sample, a mean score for the API* was 3.02 (Class 3), where more than half of the shaft with or without the epiphysis is present (75%), (Table 5.66). Thus, the skeletal elements within the sample were fairly well preserved with 75% of the amount of bone material present for each bone element.

The highest API* score was observed in the humeri, ulnae and patellae with a mean API* score of 4.67 (Class 5), 100% complete bone (Table 5.66). The mandibles, clavicularae,

Table 5.62 The Bone Representation Index (BRI*) scores for all bone elements represented in the study sample (adapted from Henderson, 1987 and Bello *et al.*, 2006)

Bone Element	Frequency	BRI*	Bone Element	Frequency	BRI*
<u>Cranial bones</u>					
Frontal	14	87.5			
Occipital	16	100.0			
Mandible	8	50.0			
Left parietal	15	93.8	Right parietal	16	100.0
Left temporal	15	93.8	Right temporal	12	75.0
Left sphenoid	12	75.0	Right sphenoid	10	62.5
Left ethmoid	8	50.0	Right ethmoid	9	56.3
Left maxilla	9	56.3	Right maxilla	11	68.8
Left nasal	10	62.5	Right nasal	10	62.5
Left zygoma	9	56.3	Right zygoma	9	56.3
Left lacrimal	4	25.0	Right lacrimal	8	50.0
<u>Post-cranial bones</u>					
Sterna [^]	3	18.8			
Cervical vertebrae	16	14.3			
Thoracic vertebrae	29	15.1			
Lumbar vertebrae	9	11.3			
Sacra	2	12.5			
Left clavicae	4	25.0	Right clavicae	4	25.0
Left scapulae	4	25.0	Right scapulae	4	25.0
Left rib fragments	21	10.9	Right rib fragments	21	10.9
Left humeri	5	31.3	Right humeri	4	25.0
Left ulnae	3	18.8	Right ulnae	2	12.5
Left radii	3	18.8	Right radii	4	25.0
Left pelvis fragments [¥]	1	6.3	Right pelvis fragments [¥]	3	18.8
Left hand	9	2.1	Right hand	18	4.2
Left femora	5	31.3	Right femora	5	31.3
Left patellae	1	6.3	Right patellae	2	12.5
Left tibiae	4	25.0	Right tibiae	4	25.0
Left fibulae	2	12.5	Right fibulae	3	18.8
Left foot	0	-	Right foot	2	0.5

[^]Sterna = sternum and manubrium.

[¥]Pelvic bone fragments = ilium, ischium and pubis.

Table 5.63 The relative frequency of individual skeletal elements recovered from the sinkhole in Khoraxa-ams within the total sample

Bone element	No. Recovered	Maximum possible No.*	% Recovered
<u>CRANIAL</u>			
Frontal	14	16	87.5
Parietal	31	32	96.9
Occipital	16	16	100.0
Temporal	27	32	84.4
Greater wing of Sphenoid	22	32	68.8
Zygomatic	18	32	56.3
Maxilla	20	32	62.5
Nasal pair	10	16	62.5
Lacrima	12	32	37.5
Ethmoid	17	32	53.1
Mandible	8	16	50.0
<u>POST-CRANIAL</u>			
Cervical vertebra	16	112	14.3
Thoracic vertebra	29	192	15.1
Lumbar vertebra	9	80	11.3
Sternum	2	16	12.5
Manubrium	1	16	6.3
Ribs	45	384	11.7
Sacrum	2	16	12.5
Ilium	3	32	9.4
Ischium	3	32	9.4
Clavicle	8	32	25.0
Scapula	8	32	25.0
Humerus	9	32	28.1
Ulna	5	32	15.6
Radius	7	32	21.9
Carpal	1	256	0.4
Metacarpal	16	160	10.0
Phalanx^	16	896	1.8
Femur	10	32	31.3
Patella	3	32	9.4
Tibia	8	32	25.0
Fibula	5	32	15.6
Tarsal	1	224	0.5
Metatarsal	-	160	-

*Maximum number of possible bones based on minimum number of individuals (n = 16).

^Phalanx of the hands and feet were pooled.

Table 5.64 Summary of cranial bone frequency ranked from the most frequent to the least frequent cranial bone elements recovered

Bone Element	% Recovered
Occipital	100.0
Parietal	96.9
Frontal	87.5
Temporal	84.4
Sphenoid	68.8
Maxilla	62.5
Nasal	62.5
Zygomatic	56.3
Ethmoid	53.1
Mandible	50.0
Lacrimal	37.5

Table 5.65 Summary of post-cranial bone frequency ranked from the most frequent to the least frequent post-cranial bone elements recovered

Bone Element	% Recovered
Femur	31.3
Humerus	28.1
Clavicle	25.0
Scapula	25.0
Tibia	25.0
Radius	21.9
Ulna	15.6
Fibula	15.6
Thoracic vertebra	15.1
Cervical vertebra	14.3
Sternum	12.5
Sacrum	12.5
Rib fragments	11.7
Lumbar vertebra	11.3
Metacarpal	10.0
Ilium	9.4
Ischium	9.4
Patella	9.4
Manubrium	6.3
Phalanx	1.8
Tarsal	0.5
Carpal	0.4

radii, sacra and the bones of the lower limb scored a mean API* of 3.96 (Class 4), with 75-99% of the bone material present or the complete shaft with single full epiphysis and part of the other epiphysis present. The zygomatic bones and the pelvic bone fragments scored the lowest API* with a mean of 1.13 (Class 1); that is 1-24% of the bones present with a single epiphysis or part thereof, part of the shaft or fragmentary remains.

5.6.2.3 Bone quality

The Qualitative Bone Index (QBI*)

The Qualitative Bone Index (QBI*), proposed by Bello *et al.*, (2006) assesses preservation based on the condition of the bone cortical surface. For the bone elements present in the sample, the mean QBI* scored for the state of the cortical surface per bone element, was 1.66 (Class 2) (Table 5.67). Class 2 is defined as the observation of 1-24% of sound cortical surface; with the bone surface relatively rough (Bello *et al.*, 2006). Therefore, it is evident that the cortical surfaces of the cranial and post-cranial bone elements present in the sample were not qualitatively well preserved.

The sterna, including the manubrium and sternal body, scored a mean QBI* of 3.00 (Class 3), this being the highest QBI* score for individual bone elements in the sample (Table 5.67). It should be noted however, that the sterna were under represented in the sample, with a total of three sterna present. The three sterna scored a mean anatomical preservation index (API*) of 2.67 (Class 3), with 75% preservation or more than half of the shaft with or without an epiphysis present. Despite the humeri and ulnae scoring a mean API* of 4.67 and 4.6 respectively (Class 5 = 100% complete bone), both upper limb bones scored a low QBI* of 1.45 and 2.40 respectively, indicating minimal cortical surface and roughened bone surface with spongy bone exposed.

In the analysis of the API* and QBI* preservation scores, the hands and feet were not included. However, when the hand and foot bones were included in the analysis it was determined that they were better preserved than the cranial and post-cranial bones. Despite the hands and feet being vastly under represented within the total sample (3.2%), they were less fragmented and qualitatively better preserved, scoring a mean QBI* of 3.67 (Class 4).

Table 5.66 The Anatomical Preservation Index (API*) ranked per bone element for the Khoraxa-ams remains (adapted from Bello *et al.*, 2006)

Bone Element	Frequency	API*	Bone Element	Frequency	API*
Humeri	9	4.67	Parietal bones	31	2.69
Patellae	3	4.67	Sterna [^]	3	2.67
Ulnae	5	4.60	Occipital bones	16	2.56
Mandibles	8	4.22	Scapulae	8	2.50
Femora	10	4.11	Thoracic vertebrae	29	2.43
Tibiae	8	4.00	Maxillae	20	2.31
Sacra	2	4.00	Nasal bones	20	2.06
Claviculae	8	3.88	Greater wing of Sphenoid	22	2.00
Fibulae	5	3.80	Ethmoid bones	17	1.94
Radii	7	3.71	Temporal bones	27	1.50
Lumbar vertebrae	9	3.10	Zygomatic bones	18	1.25
Cervical vertebrae	16	3.00	Pelvic bone fragment [¥]	6	1.00
Frontal bones	14	2.88	Coccyx	0	-

[^]Sterna = sternum and manubrium.

[¥]Pelvic bone fragments = ilium, ischium and pubis.

Table 5.67 The Qualitative Bone Index (QBI*) ranked per bone element for the Khoraxa-ams remains (adapted from Bello *et al.*, 2006)

Bone Element	Frequency	QBI*	Bone Element	Frequency	QBI*
Sterna [^]	3	3.00	Tibiae	8	1.50
Cervical vertebrae	16	2.44	Humeri	9	1.45
Ulnae	5	2.40	Sacra	2	1.40
Fibulae	5	2.40	Thoracic vertebrae	29	1.35
Patellae	3	2.33	Temporal bones	27	1.31
Radii	7	2.14	Greater wing of Sphenoid	22	1.27
Mandibles	8	2.13	Maxillae	20	1.27
Claviculae	8	1.75	Occipital bones	16	1.23
Frontal bones	14	1.67	Ethmoid bones	17	1.18
Zygomatic bones	18	1.64	Lumbar vertebrae	9	1.13
Scapulae	8	1.63	Nasal bones	20	1.10
Parietal bones	31	1.53	Pelvic bone fragments [¥]	6	0.67
Femora	10	1.50	Coccyx	0	-

[^]Sterna = sternum and manubrium.

^yPelvic bone fragments = ilium, ischium and pubis.

5.7 ¹⁴C Radiocarbon Dating

Two clavicolae were sent to the Quaternary Dating Research Unit (QUADRU) housed at the CSIR in Pretoria for ¹⁴C radiocarbon dating. The initial radiocarbon date received from the QUADRU laboratory for one right clavicle Pta 9767 H4: 1 was vastly over estimated at approximately 13 000 years BP (Table 5.68). This date was in contrast with the presumed time frame of approximately 1000 years BP, as obtained from the associated archaeological artefacts.

A possible reason for the vast disparity of the initial ¹⁴C radiocarbon date from the QUADRU laboratory could be that the sample had insufficient collagen yield when it was prepared for radiocarbon dating. The laboratory added extra laboratory grade carbon to the sample because of its low carbon value on the assumption that block carbon does not affect the C¹²/C¹⁴ ratios and therefore would not affect the date (S. Woodborne, pers. comm., 24 June 2008)

Given the disparity between the cultural association date and the radiocarbon date, the QUADRU laboratory recommended that sample H4: 6, a right clavicle, should be sent to the Groningen Laboratory in Germany for Accelerator Mass Spectrometry (AMS) dating. It was presumed that the AMS dating would offer a more plausible date for the time period in which the skeletal remains belonged. The revised AMS date tested on bone collagen from the right clavicle H4: 6, at the Groningen Laboratory in Germany achieved a date of 900 years BP ± 25 years (Table 5.69).

Considering the two vastly divergent radiocarbon dates obtained from the Khoraxa-ams samples, it is more plausible that the AMS date of 900 years BP is the more reliable date. This implies that the Khoraxa-ams site dates from the beginning of the last millennium.

Table 5.68 Initial ^{14}C radiocarbon date for sample B4108 H4: 1 as prepared by the QUADRU laboratory, South Africa. The results are reported using the convention of Stuiver, M. and Polach, H, A. (1977)

Analysis No.	Sample Name	δ^{13} (‰PDB)	Percent Modern Carbon (PMC)*	Radiocarbon ages, yrs BP**	Calibrated date***
Pta 9767	Right Clavicle no. H4: 1	-14.9	17.8 ± 2.8	13900 ± 1200	16050 (14670) 13189 BC

*Percent modern carbon is the radiocarbon content of the sample relative to the NBS standard. Values >100% post-date AD 1950. **Given in years Before Present (BP), i.e. before AD 1950; dates are reported in conventional radiocarbon years, i.e. using a half-life of 5568 years for C. Ages are corrected for isotope fractionation.

***Age is calibrated after Talma, A, S. and Vogel, J, C. (1993).

Table 5.69 Amended AMS date for sample B4108 H4: 6 as prepared by the Groningen laboratory, Germany. The results are reported using the convention of Stuiver, M. and Polach, H, A. (1977)

Analysis No.	Sample Name	δ^{13} (‰PDB)	Percent Modern Carbon (PMC)*	Radiocarbon ages, yrs BP**	Calibrated date***
GrA 39806	Right Clavicle no. H4: 6	NA	88.6 ± 0.0	970 ± 25	AD 1035 (1047, 1097, 1136) 1159

*Percent modern carbon is the radiocarbon content of the sample relative to the NBS standard. Values >100% post-date AD 1950. **Given in years Before Present (BP), i.e. before AD 1950; dates are reported in conventional radiocarbon years, i.e. using a half-life of 5568 years for C. Ages are corrected for isotope fractionation.

***Age is calibrated after Talma, A, S. and Vogel, J, C. (1993).

DISCUSSION

With no documented history with regards to the site and its occupants, the aim of this project involved a forensic anthropological approach to determine the identity and circumstances that lead to the deposition of human remains in the cave. In order to achieve this, various objectives were formed which included determining the total number of individuals present in the sample (MNI) and their demographics, the ante-mortem characteristics of the individuals, their biological and ethnic affinity as well as the events that occurred at death that lead to their deposition in the cave, and the degree of post-mortem preservation. The outcomes of these investigations have been outlined in the Results chapter. It is important now to marshal these results in order to meet the objectives of the study. The most prominent objective being, “Who are the people of Khoraxa-ams?”

6.1 How Many People are Present in the Khoraxa-ams Sample?

In order to fully analyze the human skeletal remains recovered from the cave and determine the circumstances surrounding their deposition on the cave floor, it is essential to establish numerical and demographic totals of people in the sample.

The Khoraxa-ams sample consists of a total of 254 co-mingled bones and bone fragments. Of the bone fragments, 22 could not be assigned to an element due to the absence of identifiable anatomical (morphological) features (Table 5.01). Twenty-four out of the total sample were identified as cranial bones of which eight were mandibles. A total of 208 post-cranial remains were identified in the sample including hand and foot bones. Demographically the Khoraxa-ams sample is comprised of six older adult males, two older adult females, one younger adult male and two younger adult females (Table 6.01). Included in the sample is one sub-adult individual for who sex could not be determined.

From possible linkages of cranial and post-cranial elements, a total of 16 individuals were identified in the sample. Of the 16 individuals, seven were male and four female, of whom eight were estimated as being older adults and three as younger adults (Table 6.01). Four of the 16 individuals could not be sexed nor aged as they were represented by cranial fragments alone. The remaining skeletal elements, mostly vertebrae and ribs could not be re-articulated to the aforementioned individuals based on the absence of the first two cervical vertebrae, Atlas and Axis.

Table 6.01 Summary of sex and age at death estimates for individuals from Khoraxa-ams

AGE	SEX			TOTAL
	Males	Females	Unknown	
Older Adults	6	2	-	8
Younger Adults	1	2	-	3
Sub-adults	-	-	1	1
Unknown	-	-	4	4
TOTAL	7	4	5	16

6.1.1 Mortality profile

Mortality curves only illustrate those individuals who have died in a population, though they are still useful for interpreting what life was like while those individuals were alive. Similarly Wood *et al.*, (1992) states that skeletal samples are only representative of those who die at that age. Thus, the question can be asked; do the remains of Khoraxa-ams represent the „normal mortality’ of a population? If so, then one would expect the demographic profile to represent an equal number of males and females (50:50), with an age profile showing young and elderly adults with relatively few teenagers and young adults. According to Weiss (1973), the general pattern for mortality as seen in historical human populations from death records and excavated cemeteries should include high infant and juvenile mortality (~20%), lower sub-adult mortality (~14%) as well as higher younger adult (~16%) and older adult mortality (~45%). This is not the case for the Khoraxa-ams

sample, where no infants or juveniles are present; rather an overwhelming number of adults (50.0%) and younger adults (18.75%) are represented in the sample (Table 6.02). Thus, the remains of Khoraxa-ams do not represent a „normal’ mortality for a historic population.

Table 6.02 shows a comparison between the present study sample and mortality profiles of various „normal’ cemeteries. The sex ratio of Khoraxa-ams shows a similar pattern to that displayed by the Cobern Street samples (Friedling, 2007) with the male to female ratio being more or less equal. However, the mortality profile of Cobern Street is in stark contrast with that of Khoraxa-ams. Friedling (2007) noted that the Cobern Street site represented a „normal’ mortality profile for historic populations, as there were relatively large numbers of infants and juveniles, fewer sub-adults and more adults. The mortality profile of the Marina Residence site (Friedling, 2007) is more comparable with that of Khoraxa-ams, as it does not represent the „normal’ mortality profile for historic populations. However, the sex ratio for Marina Residence shows unequal male to female number discrepancies. The site at Polyoak (Morris, 2000) is representative of a „normal’ mortality profile with comparatively equal numbers of males and females, as well as high infant and juvenile mortality, moderately high young adult mortality and lower older adult mortality.

Table 6.02 Comparison of sex and age at death ratios for „normal’ cemetery burials

	Cobern Street*	Marina Residence*	Polyoak**	Khoraxa-ams[^]
Male/Female ratio	1.4 : 1	2.6 : 1	1 : 1.3	1.4 : 1
% <20 years	30.25	7.69	55.88	6.25
% 20-40 years	26.89	34.61	23.53	18.75
% 40+ years	19.32	48.72	17.65	50.0

*Data from Friedling (2007)

**Data from Morris (2000)

[^]This study

It is apparent that the demography of death for the Khoraxa-ams sample is not indicative of the 'normal' mortality profile as there are an overwhelming number of adults and younger adults present in the sample and no infants and juveniles. However, the death demographics in an archaeological site does not automatically characterise the greater population living at the time (Grauer and McNamara, 1995). The only characteristics shared by all the subjects are their burial or deposition at the same cemetery or site respectively.

6.1.2 Does the MNI reflect the real number of people present at the site?

A MNI of 16 was determined for the Khoraxa-ams sample. This was based on the highest minimum count for the parietal and occipital bones present in the sample. However, this number bears no necessary relation to the total number of bones present in a given sample (Horton, 1984).

Table 6.03 Comparison of relative frequency of MNI per bone element

% of MNI	Cobern burials*	Cobern scatter*	Matjes River**	Mancos^	Khoraxa-ams‡
Crania	91.7	100.0	100.0	55.2	100.0
Mandibles	91.7	66.7	91.1	100.0	50.0
Upper limb long bones	95.8	81.5	69.6	58.6	21.9
Thorax	85.4	29.6	39.2	34.5	12.5
Shoulder Girdle	89.6	59.3	38.0	62.1	25.0
Pelvis	93.8	48.2	34.2	37.9	9.4
Lower limb long bones	100.0	100.0	55.7	69.0	24.0

*Data from Dembetembe (2007)

**Data from L'Abbé *et al.*, (2008)

^Data from White (1992)

‡This study

Table 6.03 represents a comparison of relative bone frequencies based on the MNI for the present study and various other studies. These studies include Cobern Street burial and

scatter remains (Dembetembe, 2007), co-mingled bones from Matjes River (L'Abbé *et al.*, 2008) and the cannibalised remains from Mancos (White, 1992). The remains from Cobern Street represent primary burials as well as disturbed remains, the Matjes River remains are reshuffled remains and the Mancos is a special case where the presence of bone was determined by at-mortem modification.

The figures in Table 6.03 are relative to the maximum MNI count for each site. Therefore, the Khoraxa-ams MNI of 16 based on the cranial bones represents 100% bone frequency for cranial bones in the sample. The frequency of skeletal elements present at the other sites is especially high, with the Cobern Street burials displaying complete skeletons and good preservation of remains with a mean frequency of 92.6%. The scatter remains from Cobern Street displays a slightly lower frequency (69.3%) of recovered bone elements. Scatter of the remains at Cobern Street was caused by the differential collection of bones by grave diggers who disturbed earlier burials. However, they still represent a higher degree of frequency compared to the present study (34.7%). The Matjes River burials (61.1%) and the cannibalised remains from Mancos (59.6%) also display a higher degree of bone frequency compared to that of Khoraxa-ams. In the case of Mancos where cannibalism was a factor, the slightly lower frequency of bone elements present in the sample was due to the bones being the result of „food processing”.

Based on the frequency of represented bone elements at sites of similar circumstance/nature discussed above, it is evident that something is amiss with the frequency of skeletal elements in the Khoraxa-ams sample. Why are the skulls more common and the other bones missing from the sample? The loss of post-cranial bones could be the result of at-mortem issues suggesting that only some body parts were thrown into the cave. However, this seems unlikely as there are no signs of dismemberment visible on the remains. Another possibility is that the loss in bone elements could have been caused by scavenging of the bones while in the cave, as a nearly complete leopard skeleton was recovered along with the human remains at Khoraxa-ams (J. Kinahan, *pers. comm.*, 19 March 2007). This also seems unlikely, as there are no signs of animal chewing visible on the bones.

The cause of bone loss could be a result of the storage process. However, the Matjes River assemblage was mis-handled during storage, and although there are bones missing, it is not as significant as seen at Khoraxa-ams. In the Matjes River assemblage bones were mis-sorted but not „lost”. Thus, it is unlikely that storage alone caused the loss of bone. The only other cause of the missing bones in the present study is the result of the actual recovery and the process of bone collection.

6.1.3 Challenges with excavation

6.1.3.1 Problems with recovery of remains

The excavation of the site at Khoraxa-ams was not conducted under the strictest conditions, but rather as an emergency excavation with no detailed archaeological recovery. No formal archaeological excavation was carried out at the site due to the topography of the cave and the difficulty experienced in recovering the remains. As a consequence no site report or field notes were gathered, as well as any cave sketches, site-map and site photographs taken to document the excavation (J. Kinahan, *pers. comm.*, 19 March 2007). Therefore, no physical evidence exists to assist with establishing the context of the site and the circumstances surrounding the deposition of human remains within the cave.

Not only was the excavation not conducted correctly, but the geographical location of the site added to the physical difficulty in accessing the site. According to Dr Kinahan (*per. comm.*, 01 March 2007), Khoraxa-ams is situated approximately 700 km north of Windhoek and is a rather difficult site to enter. The cave is a classic karst “bell chamber” with a small entrance via the top of a large cavern. Due to the cave having a 30 metre direct drop from its opening, the excavation team (Dr. John Kinahan and Dr. Eugene Marais) had to abseil into the depth of the cave (and climb out again) in order to reach the base of the cave. Once they were on the cave floor, the remains were collected off the surface of the floor around a talus cone, in very poor light and under extremely humid and claustrophobic conditions. The remains were then hoisted to the surface using buckets and a „pulley” (J. Kinahan, *pers. comm.*, 19 March 2007).

Considering the practical difficulty experienced in removing the skeletons from the cave, the enormous size and depth of the cave, and the geographical location of the site, there was strong reluctance to return to the site to complete the excavation. Consequently, with the unwillingness to return to the site, this became a once off excavation with an incomplete recovery of skeletonised remains located within the cave.

6.1.3.2 Impact of storage on the remains

According to Dr Kinahan (*pers. comm.*, 19 March 2007), the remains were stored at the museum in Windhoek for approximately 10 years. The impact of the museum storage on the remains was minimal with only a few bone losses. However, as evident from the condition of the remains, the post-discovery handling caused damage to the bones that were already brittle and fragmentary. Further destruction of the bone elements affected the ability to link clusters of bones into single individuals. From a forensic perspective the study was only partially successful in sorting individuals from the Khoraxa-ams sample.

6.1.4 Problems confronted in sorting individuals

6.1.4.1 Incomplete recovery of the remains

As mentioned previously, the skeletal material collected from the cave at Khoraxa-ams was not recovered completely, and a bias towards the crania and long bones prevailed during the excavation. Also, smaller bone elements, such as hand and foot bones were not fully recovered as they were rare in the surface collection (J. Kinahan, *pers. comm.*, 19 March 2007). For these reasons, it was not possible to estimate the total number of individuals deposited on the cave floor. Coupled with extreme fragmentation of some of the remains and poor preservation as a result of taphonomic loss, it was fairly challenging to identify all the bone elements. This in turn caused great difficulty in sorting the remains into separate individuals.

6.1.4.2 Trace elemental analysis

The results of trace element analysis (TEA) in this study demonstrated that of the ten elements that were analysed, magnesium showed the highest concentration within the

cranial bones. Thus, it was evident from the increased levels of magnesium, that it is the trace element most concentrated within the bone collagen of the remains. With regards to the relative standard deviation (% RSD) it was determined that four (Mo, Mg, Zn and Sr) of the ten elements illustrated reliability by obtaining % RSD below 20.0%, as the higher the % RSD the more unreliable the analyses. In a study by Lambert *et al.*, (1982) similar trends in Sr, Zn and Mg were reported between ribs and femurs from the same site, but their data base is not comparable to that of this study.

According to the mean values for each of the four reliable elements, Mg recorded the highest values for both males and females. Thus, magnesium (Mg) is the only element that showed sufficient variations in concentrations between individual crania, and hence could possibly be used to identify separate individuals. Whether the variation of Mg reflects physiological differences, diagenetic change or as a result of the small amount of material analysed is unknown. Numerous studies have encountered similar problems when analysing elemental concentration in archaeological bone (Lambert *et al.*, 1982, 1985; Klepinger *et al.*, 1986) and have concluded that if the evidence for intra-individual variation is more than an artefact of the sampling procedure, then the traditional method of sampling individual skeletons or bone elements may not give an accurate approximation of relative body burden of several elements. In addition, a major drawback of bone is its susceptibility to post-mortem chemical alteration that can quickly obliterate the biological elemental concentrations (Lee-Thorp and Sponheimer, 2006).

It was evident from the results that too much variation in trace element concentrations existed between separate bone elements. And it is unknown if either physiological or diagenetic influences that alter elemental concentrations of post-mortem bone elements was the cause of this variation. It is for this reason that TEA could not be used as a tool to sort the remains into separate individuals. Thus, further research into the differentiation of trace element variation in bone collagen, as the result of *in vivo* differences or diagenetic changes should be attempted in the future.

6.1.5 Summary

The individuals who were recovered from the site in Khoraxa-ams do not represent an entire population such as the mortuary population of Polyoak (Morris, 2000) and cemeteries of the historic poor in the Cape (Friedling, 2007). They are not characteristic of a normal mortality profile or demographic die-off either, as seen in normal mortality profiles for historic populations. Thus, it can be assumed that they were ‚selected’ to be deposited (dumped) in the cave. Secondly, the incompleteness of the sample is the result of excavation sampling, and not an issue of preservation.

It is evident from various studies of archaeological sites (White, 1992; L’Abbé *et al.*, 2008), and the analyses of disarticulated human remains that each site has its own challenges and contextual circumstances. What is most important when analyzing these sites is the proper documentation and complete recovery of all skeletal material, not excluding archaeological artefacts. Despite the difficulty in sorting human remains into separate individuals, when excavations are accurate and complete, it is possible to determine the number of individuals removed from the site. This was the case with the Matjes River Rock Shelter assemblage (L’Abbé *et al.*, 2008). It is also possible to establish a culturally defined cohort with significant genetic overlap such as in the case of the Iroquoian ossuaries (Pfeiffer *et al.*, 1985).

6.2 Identifying Ethnicity

In any forensic investigation of unknown human remains, the establishment of identity is of the utmost importance. In this case, we can never determine an individual identification because there are no records of missing persons, but instead we can attempt to link the bodies to a known ‚ethnic identity’ present in Namibia in pre-historic or early historic times. In southern Africa, the key to ethnicity is often language, but unfortunately it is not possible to find out languages that people spoke from the remains of these bones. But, different ethnicities can be separated by signs of different belief systems, diets and activity

patterns, and sometimes by biological differences where people of different ethnic identities also have different biological origins.

6.2.1 Who could the people of Khoraxa-ams be historically?

In this study radiocarbon dating was performed in order to establish a date to determine the age of the site. According to accelerator mass spectrometry (AMS), the site was dated at 970 years BP \pm 25 years, achieving a date of approximately ca 1035 AD. A survey of the various Namibian population groups present in the region surrounding the site was performed to determine if the remains recovered from Khoraxa-ams could be assigned to one of the various population groups who may have been present in the region a millennium ago.

The San

The San are accepted as being the earliest aboriginal group in southern Africa and were scattered over a vast area of the region (Smith *et al.*, 2000). They were primarily hunter-gatherers and occupied areas in the east of Namibia and the Kalahari Desert in Botswana (Gordon, 1992). Schapera (1930) identified several San groups in the general area of north-western Namibia. Therefore, based on geography alone the San cannot be excluded as possible ethnic identity as the distribution of peoples 1000 years ago is unknown.

Nama-speaking groups

There are two Nama-speaking groups present in the region, the Nama and Dama. The origins of the Dama are unknown, though speculation exists that they migrated from West Africa possibly before the arrival of Bantu-speakers in the region. The Dama are said to be of Negroid origin but speak Khoekhoegowab, a dialect of the Nama language, though they are physically distinct from other Nama-speaking tribes (Hahn *et al.*, 1928; Nurse *et al.*, 1985). They were the most southerly „Negroid’ tribe in historic Namibia, and cultivated maize and vegetables as well as kept livestock (Van Reenen, 1986). The Nama are recognised as a Khoesan group whose livelihood was specifically through herding. Much has been written about their origins (Hahn *et al.*, 1928; Fauvelle-Aymar and Sadr, 2008; Smith, 2008) and they are ethnically very similar to the Dama as both groups are Nama-

speaking and pastoralist in occupation. The most important difference between them is therefore biological rather than cultural. Early historic Nama-speakers were widely distributed across Namibia, especially in the central regions (Haacke, 2008) and therefore their presence at Khoraxa-ams is certainly possible.

The Bantu-speakers

The Bantu-speakers are mainly a cultural and linguistic delimitation of people who share many common features within their cultural traditions and chosen language (Malan, 1980). It is proposed that Bantu-speaking people had their origins in central Africa and migrated into southern Africa, including Namibia, during the first millennium AD (Hammond-Tooke, 1974). Their arrival in the region co-incident with the earliest evidence of cattle pastoralism and iron work in Namibia (Tobias, 1974; Nurse, 1983; Denbow, 1986). Of the modern Bantu-speaking populations of Namibia, the most numerous are the Ovambo and Herero-Himba.

Ovambo versus Herero-Himba

The Ovambo people constitute the majority of the Namibian population and comprise roughly fourteen autonomous tribes living in Angola and Namibia (Serfontein, 1976). Of these, seven live in Ovamboland, six tribes live in Angola and two live on the northern boundary of Namibia and Angola (Van Reenen, 1986). The Ovambo are generally agriculturalists and are known to produce millet and for cattle farming (Vedder, 1938; Malan, 1980). Geographically, the Khoraxa-ams site may be too far south for historic Ovambo settlement, but it is certainly well within the range of historic Herero-speaking peoples.

There are approximately nine groups of Herero-speaking people. Their language, although Bantu in origin, differs considerably from that of other ethnic groups in Namibia (Serfontein, 1976; Van Reenen, 1986). Of the nine sub-groups, the Himba are of particular interest as they occupy the north-western parts of Namibia where they migrated with their cattle. The Himba therefore share the same origin, culture and language with the Herero but they are semi-nomadic pastoralists who spread wherever conditions were suitable for

their herds (Jacobsohn, 1990; Kinahan, 2001; 2004) whereas the other Herero-speaking groups are pastoralists who settled in the central and eastern parts of Namibia with their cattle (Kinahan, 2001).

Given the geographical location of the site at Khoraxa-ams and the estimated period to which the remains date, the individuals recovered from the sinkhole cave in north-western Namibia could be any of the above groups. It is therefore imperative to ascertain the biological origin of the people (Khoesan versus Negroid) and anything that might shed light on their subsistence economy (foragers, pastoralists, or agriculturalists).

6.2.1.1 Differences based on biological markers

Differences in biological origin are based on morphological cranial variation between the Negroid and Khoesan populations, as well as the divergence in living stature between the two populations with respect to the Khoraxa-ams sample. The estimation of living stature for the individuals from Khoraxa-ams can also be used to differentiate between the biological markers of the groups from Namibia, since stature is influenced by the dynamic interplay of genetics as well as environmental agents.

Cranial Morphology

The morphological analysis of the Khoraxa-ams skeletons has shown that the osteological structure of the crania is similar to that of the Negroid reference group in pattern. This was well demonstrated by principle component analysis (PCA) in which all cranial characters for males and females of the Khoraxa-ams sample were statistically inseparable from those of the Negroid reference group. According to Powell and Neves (1999), samples or individuals that occupy similar space in the PCA plots are morphologically similar and are considered to some degree to be genetically similar as well. The only exception was the facial characters, for which both reference groups as well as the present sample could not be differentiated from one another morphologically. The few anatomical features, mostly facial, of the Khoraxa-ams skulls that differ from those of the Negroid group suggest a distinctive characteristic for the population, rather than a genotypic relationship with a different population. The variability of the Khoraxa-ams samples indicates that the

skeletons are likely to represent a single, relatively homogeneous population or a small number of very closely related populations. Thus it is likely, given that morphologically the Khoraxa-ams crania resembles the Negroid reference group, that their origin is either Dama or Herero.

Despite numerous studies (Powell and Neves, 1999; Roseman and Weaver, 2004; Franklin *et al.*, 2005; González-José *et al.*, 2005; Pucciarelli *et al.*, 2008) showing great success with craniometrics and PCA used to compare linear dimensions made by traditional anthropometric techniques, criticisms still exist. Stojanowski and Duncan (2009:286) stated that comparative craniometry is “too nihilistic in eschewing the allocation success rates for each specific comparative craniometric analysis”. If the variables successfully discriminate between groups, and the groups selected are the most appropriate for the specific hypothesis being tested, then craniometric analysis in a forensic setting can provide useful information for concerned and descendant communities. Unfortunately, the success of the specific population approach depends on having comparative samples available and this emphasizes the need to document craniometric data fully and in all forensic and archaeological contexts (Stojanowski and Duncan, 2009).

Adult Stature

While in all human societies males are on average taller than females, societies vary in the degree to which mean male height is greater than mean female height. The living stature of individuals from Khoraxa-ams is no different. Males are consistently taller than females with a mean height of 168.4 cm and 159.2 cm respectively. The only exception, UCT7D, an older adult female presented with a living stature of 162.4 cm. The exact reason for this tall female is not known, though genetics and nutritional factors could have played a role in ultimately determining her living stature.

Comparison of the statures of the present study with that of other studies (Table 6.04) shows that the Khoraxa-ams males are comparable to the mean stature of males from the Dama (Eveleth and Tanner, 1976) and the Ovambo (Tobias, 1974) of Namibia, the South African (SA) references groups, especially the Venda (Tobias, 1974) and within the range

of the modern „Negro’ (Wilson and Lundy, 1994) and the South African Negro medium height (Tobias, 1972) group. The Khoraxa-ams females are comparable (Table 6.05) to the mean stature of the Ovambo (Ambo) group (Tobias, 1974), the Zulu SA reference group (Tobias, 1974), and the modern „Negro’ group (Wilson and Lundy, 1994) as well as the upper ends of the San group (Wilson and Lundy, 1994).

Both the males and females from Khoraxa-ams are comparable with the modern „Negro’ group from Wilson and Lundy’s (1994) study. The Khoraxa-ams males are also overwhelmingly similar to the mean stature for Dama males (Eveleth and Tanner 1976). Thus, it is likely that the individuals from Khoraxa-ams share similar genetic traits and to a lesser extent were exposed to similar environmental conditions and nutritional factors while living, as the „Negro’ group or possibly the Dama, who are Negroid in origin. Similarly, the mean stature for males and females in this study were both comparable with the mean stature of the Ovambo group from Tobias’ (1974) study. The Khoraxa-ams statures consistently fall at the extreme top end of the range for Khoesan groups sampled in the literature. Thus, confirming the likelihood that the individuals from Khoraxa-ams are of Negroid ancestry and likely to be Ovambo/Herero or Dama.

6.2.1.2 Differences based on lifestyle habits

Since it is known that the San are foragers, the Nama and Dama are pastoralists, the Ovambo agriculturalists and the Herero-Himba semi-nomadic pastoralists; it may be possible to differentiate between these historical groups using lifestyle habits and biological profiles to determine the ethnic identity of the people of Khoraxa-ams. These include dietary patterns, dental health, arthritis and disease patterns, lifestyle stresses and activity patterns as well as dental modification practiced by a few historic groups in Namibia.

Dietary Habits of the People of Khoraxa-ams

Chemical analysis of human remains such as isotopic analysis provides important dietary information, based on behaviour and nutritional ecology. The results of stable isotope analysis for the Khoraxa-ams sample showed mostly positive (enriched) $\delta^{15}\text{N}$ and negative

Table 6.04 A comparison of adult stature with other samples for males

Population Group	Stature Range (cm)	Source
Khoraxa-ams	168.35*	This study
Herero (Angola)	171.0*	Tobias (1974)
Ambo (Ovambo)	170.0*	Tobias (1974)
Zulu**	166.5*	Tobias (1974)
Venda**	167.9*	Tobias (1974)
Dama	167.5	Eveleth and Tanner (1976)
San	144.1 - 164.8 (146.1*)	Wilson and Lundy (1994)
South African ‚Negro‘	149.4 - 176.5 (162.9*)	Wilson and Lundy (1994)
Khoekhoe	150.5 – 176.1 (162.4*)	Wilson and Lundy (1994)
Magon and Motokwe Bushmen	146.5 - 148.2	Tobias (1962)
Nama ‚Hottentots‘	161.9 - 163.3	Tobias (1972)
South African Negro (short)	150.0 - 160.0	Tobias (1972)
South African Negro (medium)	160.0 - 170.0	Tobias (1972)
South African Negro (tall)	170.0 - 180.0	Tobias (1972)

*Mean stature value

**South African reference groups used by Tobias (1974) in this study

Table 6.05 A comparison of adult stature with other samples for females

Population Group	Stature Range (cm)	Source
Khoraxa-ams	159.2*	This study
Herero (Angola)	162.0*	Tobias (1974)
Ambo (Ovambo)	160.5	Tobias (1974)
Zulu**	156.5	Tobias (1974)
Venda**	154.0	Tobias (1974)
San	135.6 - 159.4 (146.1)	Wilson and Lundy (1994)
South African ‚Negro‘	141.3 - 166.9 (154.1)	Wilson and Lundy (1994)
Magon and Motokwe Bushmen	157.4 - 158.6	Tobias (1962)

*Mean stature value

**South African reference groups used by Tobias (1974) in this study

(depleted) $\delta^{13}\text{C}$ values. An enriched nitrogen value in the sample is due to arid environments and reflects high trophic level consumption with an emphasis on animal foods lower on the trophic scale. These results are in agreement with the arid conditions found in Namibia, and are similar to the results from the Kakamas group also known to come from an arid environment in the northern Cape (Morris, 1984). According to Lee-Thorp and colleagues (1993), $\delta^{13}\text{C}$ and $\delta^{15}\text{N}$ values are negatively correlated in dry regions.

Overall, samples with more depleted (negative) $\delta^{13}\text{C}$ values had enriched (positive) $\delta^{15}\text{N}$ values, while those with less depleted $\delta^{13}\text{C}$ values had lower $\delta^{15}\text{N}$ values. A similar inverse relationship between $\delta^{13}\text{C}$ and $\delta^{15}\text{N}$ values has been observed for animals in southern Africa (Lee-Thorp *et al.*, 1993). This pattern may be related to the geography and climate of southern Africa, since the C_4 grassland areas of the summer-rainfall regions are in general moister than the more arid western parts where more scrub vegetation exists (Lee-Thorp *et al.*, 1993).

The semi-desert and dry savanna regions of Namibia (IDAF, 1989) are likely to be a mixed region with browsers, both wild and domestic such as bushbuck, kudu and goats following the C_3 photosynthetic pathway, and grazers such as zebra, cattle and sheep following the C_4 pathway (Lee-Thorp *et al.*, 1993). According to Smith and Epstein (1972), in African savanna environments most grasses eaten by grazers follow the C_4 photosynthetic pathway, which discriminates less against ^{13}C than the C_3 pathway used by trees and shrubs, eaten by most browsers. With the samples from the present study depicting relatively depleted carbon values, this indicates a mixed diet of C_3 and C_4 foods and reveals that the people from Khoraxa-ams were not primarily agriculturalists (C_4). It also suggests a heavier reliance on gathered wild-plant foods (C_3).

According to a study by Lee-Thorp and colleagues (1993) on the isotopic evidence for diets of prehistoric farmers in South Africa, populations from different regional locations show predictable changes according to the biome and rainfall. Though they are quick to point out that more often variability within each region obscures regional differences. The results from the study show an overall pattern related to the distribution of rainfall and

vegetation in South Africa. Proportions of C₃ and C₄ plants were shown by stable carbon isotopes to be influenced by biome type, and nitrogen isotope values reflect both aridity and trophic level.

How can stable-isotope variations in bone provide insight into seasonality in diet and climate? The answer lies in the different ¹³C/¹²C ratios of different types of plants. Tropical grasses (and a few herbaceous broadleaf plants) as well as millet and sorghum fix atmospheric CO₂ using the C₄ photosynthetic pathway, therefore these plants have high ¹³C/¹²C ratios. Conversely, most broadleaf plants, including trees, bushes, shrubs and herbs as well as cultivated foods use the C₃ pathway and are strongly depleted in ¹³C relative to CO₂ (Cox and Sealy, 1997; Ambrose, 2006; Sponheimer *et al.*, 2006). Therefore C₃ plants have a lower δ¹³C value compared to C₄ plants. The carbon-isotope ratios of mixed feeders reflect the proportions of C₃ and C₄ plants in their diets (Ambrose, 2006), as with the individuals from Khoraxa-ams.

The isotopic analysis of carbon and nitrogen values clearly indicates that the people of Khoraxa-ams had a mixed diet dependent on both C₃ and C₄ foods and thus were not only reliant on agriculture produce as their only means of acquiring food, but relied heavily on other sources including gathered foods. Therefore, it is likely that the people of Khoraxa-ams could be related to the agriculturalist Ovambo or the agropastoralists Herero and supplemented their diets by consuming gathered wild foods as noted by Vedder (1938). These included wild fruits, berries and tubers, making up for the lack of fresh vegetables. It is also likely, given the heavy reliance on gathered plant foods, that the people of Khoraxa-ams could be Dama, though their subsistence economy was more focused on pastoralist activities as well as hunter-gathering (Hahn *et al.*, 1928).

Dental Patterns as a Sign of Economic Activity

In determining the ethnic identity of the people of Khoraxa-ams, the presence and patterns of dental pathologies may be useful to infer dietary patterns and social status among prehistoric peoples, as well as establish their lifestyle habits and economic activities.

Based on the various subsistence strategies of historic Namibian populations, it is possible to predict how dental patterns would present in living agriculturalists, pastoralists and foragers in this region. Given the dietary patterns of foragers (Larsen, 1997), one would expect high levels of attrition, low frequencies in caries and ante-mortem tooth loss, as well as dental abscesses (Morris, 1992; Peckmann, 2002). This is due to the „fibrous’ foods eaten by foragers, with large amounts of abrasive material present in the food or incorporated during its preparation (Buikstra and Ubelaker, 1994). Pastoralists would present with similar dental patterns as the foragers, as they are hunter-gatherers who also herd cattle (Denbow and Wilmsen, 1986). According to Kinahan (1991), archaeological records confirm the historical evidence that hunter-gatherers in some instances acquired the dietary habits of pastoralism, while pastoralists were occasionally reduced to living as hunter-gatherers. With regards to the agriculturalists lifestyle, one would expect low attrition rates, with increased caries and ante-mortem tooth loss frequencies mainly as a result of their subsistence strategy and lifestyle (Morris, 1992; Steyn, 1994; Dlamini, 2006).

Dental Attrition

Differences in economic mode and lifestyle are revealed through analyses of dental attrition. Occlusal wear patterns reflect different masticatory and dietary behaviours. Studies have revealed that generally, foragers have more severe wear than agriculturalists, while agriculturalists show higher angles of occlusal wear than hunter-gatherers and wear is usually cupped in agricultural populations and flat in hunter-gatherer communities (Larsen, 1997). Added to this, hunter-gatherers would present with heavy wear on all dentition, while agriculturalists would have more wear on the molars due to their early eruption. Within the study sample, occlusal wear among male individuals was observed on all the teeth and the wear pattern was either flat or at an angle.

Comparative dental occlusal wear is presented in Table 6.06, and is used to determine lifestyle patterning within and between communities so as to assist with the identification of the individuals from Khoraxa-ams. Since sex and age are important variables within the interpretation of attrition, those individuals of indeterminate age and sex are not included

in this discussion. The degree of occlusal wear for Khoraxa-ams is compared to prehistoric agriculturalists from central and southern Africa, the Dry savanna, Wet savanna and Forest sites (Dlamini, 2006), the Griqua pastoralists who also grow agricultural produce as well as the Colesberg and Wolmaransstad agriculturalists (Peckmann, 2002), and K2 and Mapungubwe as early African agriculturalist (Steyn, 1994) samples. In addition, data on occlusal wear patterns among the San was published by Van Reenen (1964). Observations were made on two San groups, the „wild bushmen’ and the „farm bushmen’. Both groups were mainly hunter-gatherers, with the „farm’ group also reliant on pastoral/agricultural dietary additions (Morris, 1992). Despite the usefulness of documented wear patterns among the San, the data base is not comparable with this study, as no raw data list was published.

Table 6.06 Comparison of occlusal attrition scores in adult dentition

Site	Male	Female	Anterior Attrition Score			Posterior Attrition Score			Mean Attrition Score		
	n*	n*	Male	Female	Total	Male	Female	Total	Male	Female	Total
Khoraxa-ams**	4.5	4.25	2.1	-	-	1.7	1.3	1.5	1.9	-	-
Griqua***	25.5	18	3.1	3.5	3.4	2.6	3.0	2.9	2.9	3.3	3.1
Dry savanna^	16.9	11.3	1.9	2.1	2.1	1.6	1.9	1.8	1.8	2.0	1.9
Wet savanna^	10.3	4.8	1.9	1.3	1.7	1.5	1.0	1.3	1.7	1.1	1.5
Forest^	9.1	8	1.7	1.9	1.8	1.6	1.4	1.5	1.5	1.6	1.6
K2 and Mapungubwe [¥]	8	5	2.0	2.1	2.0	2.1	1.9	1.9	2.0	2.0	2.0
Colesberg***	21.8	18.8	3.3	2.9	3.2	3.0	2.5	2.8	3.1	2.5	2.9
Wolmaransstad***	11.0	1	3.4	2.9	3.3	2.7	2.5	2.7	3.0	2.6	3.0

*n = number of individuals calculated differently between this study and comparative samples

**data from this study

***data from Peckmann, 2002

^data from Dlamini, 2006

¥data from Steyn, 1994

According to Table 6.06, mean occlusal wear for the male individuals in the present study is most comparable with the Dry and Wet savanna groups (Dlamini, 2006), and the K2 and Mapungubwe site (Steyn, 1994). The total mean attrition for the present sample could not be calculated as the anterior teeth of the female individuals were absent post-mortem. It has

been documented that the individuals from K2 and Mapungubwe sites as well as the Dry savanna, Wet savanna and Forest regions are representative of prehistoric African agriculturalists (Peckmann, 2002; Friedling, 2007). Based on the occlusal wear pattern of the Khoraxa-ams individuals, it is evident that they ate a fairly mixed diet with a heavy reliance on abrasive foods or foods that introduced abrasive elements during processing, such as grinding, causing considerable wear on all the dentition.

Dental Health

Based on the assessment of dental pathologies, such as ante-mortem tooth loss (AMTL), caries, periodontal disease and abscesses, a pattern of overall dental health may be obtained. This may also aid in identifying the ethnicity of the Khoraxa-ams sample. Among hunter-gatherers, dental disease is fairly low while dental attrition is heavy across all the teeth due to high levels of abrasive foods consumed. Based on the diet of agriculturalists, high in plant carbohydrates (sugars and starch), high dental disease levels are expected such as caries, with dental wear more concentrated on the molars. Numerous studies have suggested similar patterns in dental disease and attrition among hunter-gatherers and agriculturalists (Morris, 1984; Smith, 1984; Walker and Hewlett, 1990).

The adult male individuals showed a higher incidence of AMTL than the females. It is possible that the high frequency of AMTL observed in the male central incisors is the result of dental modification. However, differential access to food and other food resources are more likely to have caused the slight difference seen between AMTL among males and females. Generally most teeth affected by carious lesions are the posterior teeth, probably because of their morphology and the fact that M1 is the first to erupt and therefore has a longer exposure time (Friedling, 2007). Thus, one would expect to see a higher prevalence of AMTL in the first and second molars as well as increased caries in these same teeth. With the first central incisor being the most commonly affected tooth for AMTL in the present study, it is highly unlikely that these teeth were affected by increased caries rates. However, the effects of dental attrition causing the AMTL of the central incisors among the male individuals cannot be entirely ruled out.

Of a total of 126 teeth with intact crowns in the sample, no carious lesions were observed. This could indicate that the people of Khoraxa-ams were eating a cariostatic diet that was high in abrasives and therefore the frequent mechanical cleaning protected the posterior teeth.

According to Cohen and Armelagos (1984), agricultural foods have a high starch or sugar content that often sticks in stagnant areas of the tooth, and dental caries are encouraged through consumption of such foods. Also, the practice of agriculture is directly related to a high prevalence of dental disease such as AMTL caused by high levels of carious lesions. The lack of caries in the present sample could therefore be due to differential access to food and other resources. Morris (1984) noted in a study on skeletons from Kakamas, that the attrition rates observed in the sample were consistent with an interpretation that the Kakamas individuals were living primarily on gathered “veldkos” (field foods). These foods produce marked occlusal wear throughout the tooth row, which in turn inhibits caries development.

Another possibility for the lack of caries in the sample is based on processing methods, like grinding that introduces abrasive elements into the diet and encourages mechanical cleaning, thus reducing the occurrence of carious lesions. According to Morris (1992), the interpretation of a lack of caries may not be due to diet alone, but to the chemical content of the drinking water. Ockerse (1943:445) stated during a study he performed on the incidence of dental caries in a South African population, “It appears that an optimum amount of fluorine in the drinking water assists the proper calcification of the teeth making them more resistant to caries.” Thus, the individuals from Khoraxa-ams could have had access to drinking water enriched with fluorine, therefore inhibiting the formation of caries. No evidence is available to support these claims since no comparative data are available.

Periodontal disease was observed in five individuals of mature age (Table 5.33), correlating with the theory that periodontitis progresses with increasing age. Of the five individuals, four were male and one female. The difference in prevalence among the males

and females could be as a result of differential food sources or the introduction of mixed bacteria into the mouths of the male individuals as a result of increased carbohydrates. According to Lukacs (1995), periodontal disease, caries and AMTL is markedly increased in populations that have high consumption rates of plant carbohydrates.

Individuals presented with a slightly high prevalence of dental abscesses. However, abscesses and ante-mortem tooth loss were more common among older adult individuals, reflecting an increase in these types of dental pathology with age. It can therefore be concluded that the diet of the people of Khoraxa-ams must have been high in foods causing relatively poor oral health. It is also suggested by Hillson (1996) that the incidence of dental caries and occlusal wear can predispose an individual to the development of dental abscesses through exposure of the pulp cavity and infiltration by bacteria. With the lack of caries observed in the sample, it is more likely that the incidence of dental abscesses could be due to occlusal wear.

The people of Khoraxa-ams presented with medium/slightly heavy dental wear, no caries, few cases of dental abscesses and periodontitis, evident of a population reliant on a mixed diet with high levels of abrasive foods commonly consumed among hunter-gatherers and frequently seen in pastoralist populations where gathered foods are introduced in the diet as an alternative food source.

Dental Modification

Despite biological markers lending evidence towards ethnic identity and economic mode for the people of Khoraxa-ams, cultural behaviour and traditions, as in the case of dental modification, may also assist in the identification of the remains.

The various reasons for dental modification have long been studied and these often include tribal identification (Van Reenen, 1986), social stratification (Gould *et al.*, 1984), beautification (Jones, 2001), initiation at puberty and punishment (Hillson, 1996), therefore purely cultural. According to Van Reenen (1986), the practice of tooth modification was fairly common in South West Africa (Namibia), specifically among the Bantu-speaking

groups and well documented in the literature. Each tribe adopted an individual style of tooth modification which was shown to be linked with the geographical distribution of the various tribes. Van Reenen (1986) goes on to explain that a small number of Ovambo practiced tooth modification involving the removal of both mandibular first incisors, and in some cases all four. Tooth extraction and tooth modification practices were widespread amongst the Herero-speaking peoples. The typical style of the Herero involved the removal of the four mandibular incisors and filing of a V-shaped notch between the maxillary first incisors. Van Reenen (1986) upon investigation discovered that the Dama did not practice any form of tooth extraction or tooth modification. However, the San (Bushmen) were observed to practice tooth modification in the form of the removal of the mesial tips of the maxillary first incisors, producing an inverted V-shaped notch between the teeth. No data for the practice of dental modification among the Nama was recorded in Van Reenen's (1986) study.

Dental modification in the form of avulsion or deliberate removal of the central incisors was observed in two individuals, a sub-adult of indeterminate sex and an older adult male. The deliberate removal of the anterior teeth from these individuals was characterised by healed/resorbed central incisor sockets, evidence of possible intentional extraction ante-mortem on the mandible in both cases. A similar pattern of tooth extraction has been documented amongst the Herero-speaking people of Namibia. However, tooth modification or filing was not observed in the present study on the maxillary central incisors, owing to the fact that most of the anterior maxillary teeth were absent post-mortem or badly damaged. Thus, based on the observed style of dental modifications, it is likely that the Khoraxa-ams sample shares similar traditions with the Herero-speaking tribes of Namibia at least in comparison to the historic distribution of this dental modification pattern.

Activity Patterns, Health Status and Disease Patterns

A biological profile was established to assist in determining the health status as well as activity patterns of the people of Khoraxa-ams at the time of their death. These include non-specific diseases such as cribra orbitalia (CO) and porotic hyperostosis (PH),

osteoarthritis, Harris lines and squatting facets observed in a small number of individuals from Khoraxa-ams.

Distinctions between agriculturalists, pastoralists and foragers in historic Namibia produce variations in health and disease prevalence, similar to that seen in the dentition. Research on southern and central Africa has shown a tendency towards lower parasite burdens on pastoral people, with an increased risk of exposure to zoonotic diseases (Morris, 1984; 1992; Peckmann, 2002). According to Cohen and Armelagos (1984), in terms of improvements in the quality and reliability of food supplies, the agricultural economy was less than advantageous when compared to hunting and gathering. Thus, agriculturalists tend to have higher parasite loads and infectious diseases (Steyn, 1994). Also, studies have argued that there is a reduction in the prevalence of osteoarthritis from foraging to agricultural communities caused by a decline in mechanical loading with the adoption of agriculture (Larsen, 1997). Thus, foragers tend to have increased degenerative joint disease in the form of osteoarthritis due to mechanical loading caused by hunting and gathering for food.

The relatively low incidence of CO and PH observed in the study sample (18.75%) indicates that the individuals from Khoraxa-ams were not strongly affected by nutritional deficiencies, particularly diets poor in protein that cause iron-deficiency anaemia. Though, the same individuals ($n = 2$) with CO and PH also presented with an infectious disease, periostitis of the cranial bones. Despite CO, PH and periostitis observed in a few of individuals, the general health of the individuals from Khoraxa-ams was relatively good. Thus, no lifestyle stresses or infectious diseases affected most of the individuals while they were alive. The overall good health of the people of Khoraxa-ams lends no evidence towards their subsistence economy.

Osteoarthritis indicates the degree of regular strenuous activity and quality of life (Goodman and Martin, 2002). However, it should be noted that osteoarthritis is a multifactorial disease resulting from a combination of factors such as age, sex, hormones, mechanical stress or genetic predisposition. It can also be initiated as a result of direct

trauma or via bacterial invasion of the joints (White, 2000b). Among observed degenerative joint disease (DJD) in the sample, the males showed a greater number of total joints affected with osteoarthritis than age-matched females. The females however, demonstrated a slightly higher degree of osteoarthritis frequency. Signs of osteoarthritis as observed on both male and female joints could be evidence of labour-related changes as a result of physical activity performed by both sexes, or as a result of a combination of the aforementioned factors affecting males and females separately.

If the Khoraxa-ams cave was simply a burial place for those who were ill and dying, then we could speculate that we would expect to find a greater disease load present on the skeletal remains. However, this was not the case for the Khoraxa-ams sample. Despite a few individuals presenting with patterns of disease, the overall health of the people of Khoraxa-ams seems reasonably good, indicating that the remains were possibly not removed from the 'group' due to sickness and were 'otherwise healthy'. However, given the lack of sufficient evidence, the possibility that the individuals from Khoraxa-ams contracted acute fatal disease, in all likelihood owing to their death and subsequent deposition cannot be completely ruled out.

The results of Harris lines (HL) in the sample, though small, indicate that some form of metabolic insult affected a small proportion of the population during their developmental stage. Of the six individuals whose tibiae were radiographed, three were observed with HL. Multiple lines occurred in all three individuals. From the calculation of age at which the illness occurred up to the cessation of bone growth it was evident that HL peaked at between 10 and 15 years. Although the adolescent period is generally associated with good health and low mortality, the high rate of growth arrest lines could be correlated to the adolescent growth spurt (Aufderheide and Rodriguez-Martin, 1998). According to Steinbock (1976) and Grolleau-Raoux *et al.*, (1997), only about a quarter of HL that present in sub-adults persists into adulthood. According to Peckmann (2002), the relative scarcity of published data for HL among hunter-gatherer populations suggests a lack of stress episodes inflicted on hunter-gatherers.

With regards to the activity patterns observed among the people of Khoraxa-ams, the appearance of squatting facets lent evidence towards the possible occurrence of daily activities involving squatting among a few individuals. A squatting posture is defined as the persistent flexion of the knees and ankles. Its frequent and prolonged use produces specific bone markers due to the strong pressure and traction forces on the knee and ankle joints when the lower limbs are in hyperflexion (Mays, 1998).

Table 6.07 Frequency of squatting in Khoraxa-ams compared to Later Stone Age foragers from South Africa

Site	Squatters		Non-squatters		Total n
	n	%	n	%	
Khoraxa-ams* (20 th century AD)	4	25	12	75	16
LSA foragers [^] (1 st millennium BC)	28	50	28	50	56
JA' farmers [^] (5 th -19 th century AD)	13	76.5	4	23.5	17
Cobern Street [^] (18 th century AD)	1	4.8	20	95.2	21
Modern cadavers [^] (20 th century AD)	0	0	29	100	29

*Khoraxa-ams = this study.

[^]adapted from Dlamini (2006).

According to a study by Dlamini and Morris (2005), on the frequency of squatting facets in Later Stone Age (LSA) foragers from South Africa, over half (76.5%) of the early farmers and 50% of the LSA foragers were habitual squatters (Table 6.07). In the present study however, only 25% of the sample were habitual squatters. It was therefore suggested that both the farmers and the LSA foragers must have used the squatting posture in repose and when engaged in their daily vocations. In a squatting position, the body weight is supported with minimal muscular activity (Mays, 1998). It must be noted, that given the reduced sample size of the present study, any comparison with previous studies looking at squatting among ancient populations (Dlamini and Morris, 2005) and modern samples (Boulle, 2001) should be taken with caution.

6.2.2 Summary of lifestyle observations and possible ethnic identity

With regards to the general physical character of the Khoraxa-ams sample, based on cranial morphological variation and living stature, it is evident that the individuals are likely of Negroid origin. Regarding their subsistence economy, it is likely that they were reliant on a mixed diet which involved agricultural produce as well as gathered foods as an alternative food source. Their dental health suggests that they accessed a mixed diet, more likely true for a pastoralist group. Their overall health status is suggestive of people who practiced activities that did not require great strenuous exercise, such as low-impact labour common among agriculturalists and pastoralists. They were generally in good health with no signs of severe malnutrition or infectious diseases observed on the remains. They were also involved in activities prone towards assuming the squatting posture, common among both foraging and farming populations. Dental modification observed among the individuals from Khoraxa-ams was similar in the style of tooth extraction as documented for the Herero-speaking peoples of Namibia.

As has been discussed above, variations in biological profile, subsistence economy, lifestyle habits and cultural-ecological environments exist between the numerous ethnic groups in Namibia. Table 6.08 summarises the features that differentiate these historic groups while comparing the biological and cultural-economic patterns of the Khoraxa-ams sample in order to identify ethnicity. Since the Khoraxa-ams sample was identified as having similar cranio-morphological traits as the Negroid reference group it is possible that they could belong to the Dama, Ovambo or Herero-speaking groups, as they all share Negroid origins. According to mean adult stature for males, the present sample is most comparable with the Dama as well as the Herero. The Khoraxa-ams individuals had a mixed economic mode probably encompassing elements of foraging and small-scale horticulture. This is similar to most of the ethnic groups, especially the Herero and Dama who are mainly pastoralists who hunted, fished and foraged as alternative food sources as well as the Ovambo who were chiefly agriculturalists. The dental health of the Khoraxa-ams people suggests a mixed diet, most similar to pastoralist populations such as the Dama and Herero. Based on cultural practices, the Khoraxa-ams sample shared a similar style of

dental modification as the Ovambo and Herero, though the Ovambo often only removed the mandibular first incisors.

Table 6.08 Differences in biological and cultural-economic patterns among historic ethnic Namibian groups compared to Khoraxa-ams

	San	Nama	Dama	Ovambo [†] /Herero [‡]	Khoraxa-ams [§]
Cranial shape*	Khoesan	Khoesan	Negroid	Negroid	Negroid
Stature**	144.1 – 164.8	161.1 – 163.3	167.5	160.5***/171.0 [^]	168.05
Economic mode	Foragers - "veldkos"	Pastoral nomads who also foraged	Pastoralists, agriculturalists and foragers	Agriculturalists[†], Pastoralists[‡] , hunted, fished and foraged	Assessed as mixed diet including foraged foods
Dental Modification	Mesial tips of maxillary first incisors removed, producing inverted V-shaped notch between teeth.	-	-	Removal of all four [¥] mandibular incisors, filing a V-shaped notch between maxillary central incisors	Removal of mandibular first incisors

*Cranio-morphological features based on ancestral origins for comparative groups (Hahn *et al.*, 1928).

**Stature based on mean adult stature for males in centimetres (Tobias, 1972; 1974; Eveleth and Tanner, 1976; Wilson and Lundy, 1994)

***Mean adult stature for Ovambo (Tobias, 1974)

[^]Mean adult stature for Herero (Tobias, 1974).

[¥]The Ovambo generally removed only the mandibular first incisors (Van Reenen, 1986).

[†]The Ovambo are agriculturalists (Malan, 1980)

[‡]The Herero are pastoralists (Kinahan, 2001)

[§]Data from this study

Given the differentiation of biological and lifestyle features between the historical groups of Namibia and the comparison of demographic data obtained for the Khoraxa-ams sample, it is clear that the people of Khoraxa-ams are not San or Nama. The answer to the question, "Who could the people of Khoraxa-ams be historically?" is therefore likely to be Dama, Herero or Ovambo. Given that their dental health suggests that they consumed a mixed diet, more true for pastoralist groups, it is unlikely that the people of Khoraxa-ams are

Ovambo as they are chiefly agriculturalists. Based on the cultural practice of dental modification, it is unlikely that they are Dama, as no evidence of dental modification among the Dama exists. Thus, the people of Khoraxa-ams are more likely Herero, though the possibility exists that they could be a Bantu-speaking group ancestral to the Herero

6.3 How Did They Die and How Did They Get into the Cave?

The exact events that culminated in the deposition of the remains in a cave in Khoraxa-ams may never be determined. No oral history has come to light that speaks of the events and therefore all information that we can make use of is circumstantial. Added to this, the logistics of the cave and the surrounding topography of the site lent little evidence as to the placement of the remains in the cave. In brief, the cave at a depth of 30 metres is not humanly accessible without abseiling equipment and the remains were scattered along the height of a talus cone with the bulk of the remains at the base of the cone.

An important issue in investigating the deposition of the remains in the cave is whether or not the bones were moved after death. From a forensic perspective, if the bones remained where they were ‚placed,‘ then a single (complete) skeleton within its initial context would be found. But if the remains have moved after decomposition, then the original information about the placement of the body would be lost and the location of the bones at discovery would reflect the secondary placement of the bones. In the case of the Khoraxa-ams sample, the remains were deposited on the surface of the cave floor and not buried in the cave. According to Kinahan (*pers. comm.*, 19 March 2007), the skeletal material recovered from the cave was found scattered along the length of the talus cone with the larger, heavier bones found around its base. This suggests that heavier bones, such as skulls and long bones rolled off the cone during decomposition and came to rest along its perimeter. All of this is consistent with the bones moving down the talus slope after decomposition of the bodies on site. There are no signs that the bodies decomposed elsewhere and that only the bones were dropped into the cave.

6.3.1 How did they end up in the cave?

Establishing the events at death not only assists in determining the possible cause(s) of death, but also in the identification of the individuals from Khoraxa-ams. In order to establish the possible events at death, it is essential to firstly determine if the individuals were alive when they entered the cave.

6.3.1.1 Were they alive when they entered the cave?

If the traumatic injuries observed on the remains were all a result of falling into the cave, were the people dead before or after they were dropped into the cave? A strong possibility exists that the individuals were deposited in the cave after death. No complete skeleton was located at the bottom of the talus cone or elsewhere at the base of the cave despite the presence of a complete leopard skeleton. It is unlikely that anyone would survive a 30 metre fall, but not everyone who fell or was thrown in would be killed outright. Had they been alive when they were dropped in, then at least one or two would survive long enough to crawl into a location where complete skeletons would be found. Also, if the individuals were alive when dropped in, they would likely present with wounds consist with bracing against the impact. Colles' fractures occur when an individual attempts to break a fall by thrusting their arms forward (Larsen, 1997). No colles' fractures were observed on the remains. Therefore, the most obvious conclusion is that the people were already dead when they were dropped into the cave.

However, if the individuals were deposited after death, one would expect to find their remains ‚scattered’ on the base of the cave due to differential decomposition and bone preservation (Stiner *et al.*, 2001). As a consequence of the talus cone situated directly beneath the opening of the cave, a similar pattern of differential bone preservation resulted entitled ‚talus-cone taphonomy,’ a term used by Stiner and colleagues (2001). How this works is that the remains landed on the floor of the cave, around the base of the cone and begun to decompose. Heavier bones such as the skull and long bones then rolled off the cone and came to rest along the perimeter of the cave. This resulted in the scattered distribution of disarticulated remains. Such as is the case with the remains from Khoraxa-

ams. Given that the remains were deposited in the cave after death, could this have been a burial ritual?

6.3.1.2 Burial style

The burial practice of the Himba as described in the Background chapter is in stark contrast with the deposition of remains in a sinkhole. And no ethnographic evidence of such a burial practice involving the deposition of human remains in historic or prehistoric Namibia has been recorded in literature to date. Unless this wasn't a formal burial but rather 'dumping' of the remains after death, be it of natural or un-natural causes. The presence of individuals both male and females, and ranging in age from 15.1 to 40+ years makes this deposition all the more suspicious. This leads to the likelihood that an entire village, with the exception of the children, was placed in the cave as a means of disposal supporting a speculative notion of ethnic cleansing. What happens to the children during ethnic cleansing? According to a report on slavery in South Africa by Eldredge (1994), during the 19th century the tradition of slave raiding practiced by the Boers in the eastern Cape saw mainly Khoesan men and women being killed as well as Bantu-speaking people further in the interior, and their children taken as labourers by pastoral farmers. The purpose of slave raids was the procurement of children rather than adults, because they could be easily controlled from the point of capture and were easier to retain and exchange (Eldredge, 1994).

If the site at Khoraxa-ams was indeed a burial deposition site, then one would expect to see infants and juveniles represented in the sample. Only one sub-adult individual was identified among the remains. The excavation techniques used at this site did not aid in the complete recovery of all remains present in the cave and a bias existed towards larger or more visible bones of the skeleton and crania. Therefore, the possibility exists that infant and juvenile skeletons were present in the cave but not recovered. It can be argued however, that if infant and juvenile skeletons were among the remains deposited in the cave, then some form of evidence of their presence should have been observable in the sample. This was not the case with the Khoraxa-ams remains. Therefore, the demography

of cultural burial in historic and prehistoric Namibia is incorrect, increasing the possibility of the site being an execution location.

6.3.2 How were they killed?

Since it has been determined that the individuals were probably already dead once they were dropped into the cave, it is important that the cause of their death be established. Skeletal injuries present on the remains give speculative clues as to how they died or were killed.

Despite the high frequency of skeletal trauma (68.75%) observed in the Khoraxa-ams sample, most of the fractures were identified as being peri- or post-mortem. No ante-mortem injuries were observed in the sample. An important issue concerning the etiology of peri-mortem fractures in the sample is the fact that the actual cause of the breaks is ambiguous. Thus, the peri-mortem fractures need to be divided into those that were inflicted by blunt force and possibly caused by events at death prior to be dropped into the cave and fractures that were caused by the 30 metre drop into the cave.

6.3.2.1 Absence of ante-mortem fractures

From the analysis of skeletal trauma observed on the Khoraxa-ams sample, it was determined that no ante-mortem injuries occurred. This was evident as there were no signs of healing associated with any of the visible fractures. According to Lovell (1997), fractures begin to heal immediately after the bone is broken when the bone is still living. Thus, no traumatic event or change brought about by pathology resulting in fractured bones occurred during their lifetime as was visible on their remains.

6.3.2.2 Peri-mortem fractures caused by blunt force trauma

Four individuals presented with injuries that were possibly caused by blunt force trauma at or around the time of their death. Though, it is unlikely that any of these fractures were the cause of death.

UCT1K, an older adult female had an impact above the left orbit causing radial fractures across the nasal bone and both zygomas. This type of injury is typical of LeFort II fractures (Figure 6.01). Rogers (1982) noted that a LeFort II pattern sometimes known as a pyramidal fracture separates the mid-portion of the face from the cranium and is produced by a centrally or slightly downwardly directed blow to the mid-face (courtesy of Berryman and Symes, 1998). It is believed that LeFort's are fracturing patterns of the facial skeleton based on areas of failure that are directed by areas of buttressing (reinforcement), caused by blunt force trauma to the face (Berryman and Symes, 1998).

A younger adult female, UCT1G presented with an unhealed linear fracture above the left orbit, horizontally splitting the left orbital shelf directly in half. Low velocity, blunt force trauma to the head may result in simple linear fractures of the skull. The kinetics involved in this type of injury may relate to acceleration injuries, in which the head is struck by an object and set in motion. Or deceleration injuries, in which the moving head suddenly comes to a halt by hitting a surface or being dropped from a significant height (Lovell, 1997). Given that the damage to the skull is more localised, this suggests that the trauma was caused by some sort of object and not the result of a deceleration injury, as this would result in widespread damage in the form of radiating and concentric fractures, to the cranial vault.

A blow to the right side of the head of UCT1E, a younger adult female, resulted in an injury on the right parietal, causing extensive bone loss and delamination of the surrounding 'hole.' A similar blow to the left parietal caused a similar pattern of bone loss and delamination to the left side as well. It is suggested that as a consequence of the two injuries on either side of the head, the cranium split in half along the coronal suture. This resulted in plastic deformation of the cranial vault. Plastic deformation usually occurs when slow loading (force) allows the bone to pass through its elastic and plastic phase before fracturing (Berryman and Symes, 1998). What is important to note is that delamination of the diploë occurs when tissue still adheres to bone and can present with multiple blows.

Individual UCT1B, a sub-adult of indeterminate sex presented with a depression fracture at Bregma and an unhealed nasal fracture. Depression fractures are defined as an inward displacement of a portion of the cranium. These fractures occur primarily on the skull and result from direct blunt force trauma that causes “caving-in.” In the case of UCT1B, concentric and radiating fractures were coupled with the depression fracture. Thus, the blow to the apex of the cranium had enough velocity to not only depress the bones, but cause resulting fractures, as well as slightly penetrate the outer table. Although the area of impact on the cranium is small, this could be as a result of high velocity impact on a small area of the skull. This is probably the result of blunt force trauma during an at-mortem attack. It is likely that the broken nose occurred at-mortem as no sign of healing was observed. This type of injury also results from blunt force trauma, and is usually caused by a direct blow to the mid-facial region.

6.3.2.3 Peri-mortem fractures caused by 30 metre drop

It would be expected that a number, if not all, individuals recovered from Khoraxa-ams presented with fractures as a result of being dropped into the 30 metre cave. Many of the individuals with observed blunt force trauma presented with peri-mortem injuries caused by a fall from a great height as well.

Individual UCT11, an older adult female was seen with an unhealed spiral fracture of the left femur and a sub-intertrochanteric fracture on the right femoral neck. Spiral fractures are caused by a rotational force (torsile loading) on the bone and tend to be the result of low velocity forces such as falling from a significant height. According to Lovell (1997), these fractures wind down around a long bone shaft due to rotational and downward loading stress on the longitudinal axis. A sub-intertrochanteric fracture is caused by an explosive force, classified as both blunt and ballistic trauma, termed axial loading (Symes, 2005a). Axial loading is when the forces of impact are directed

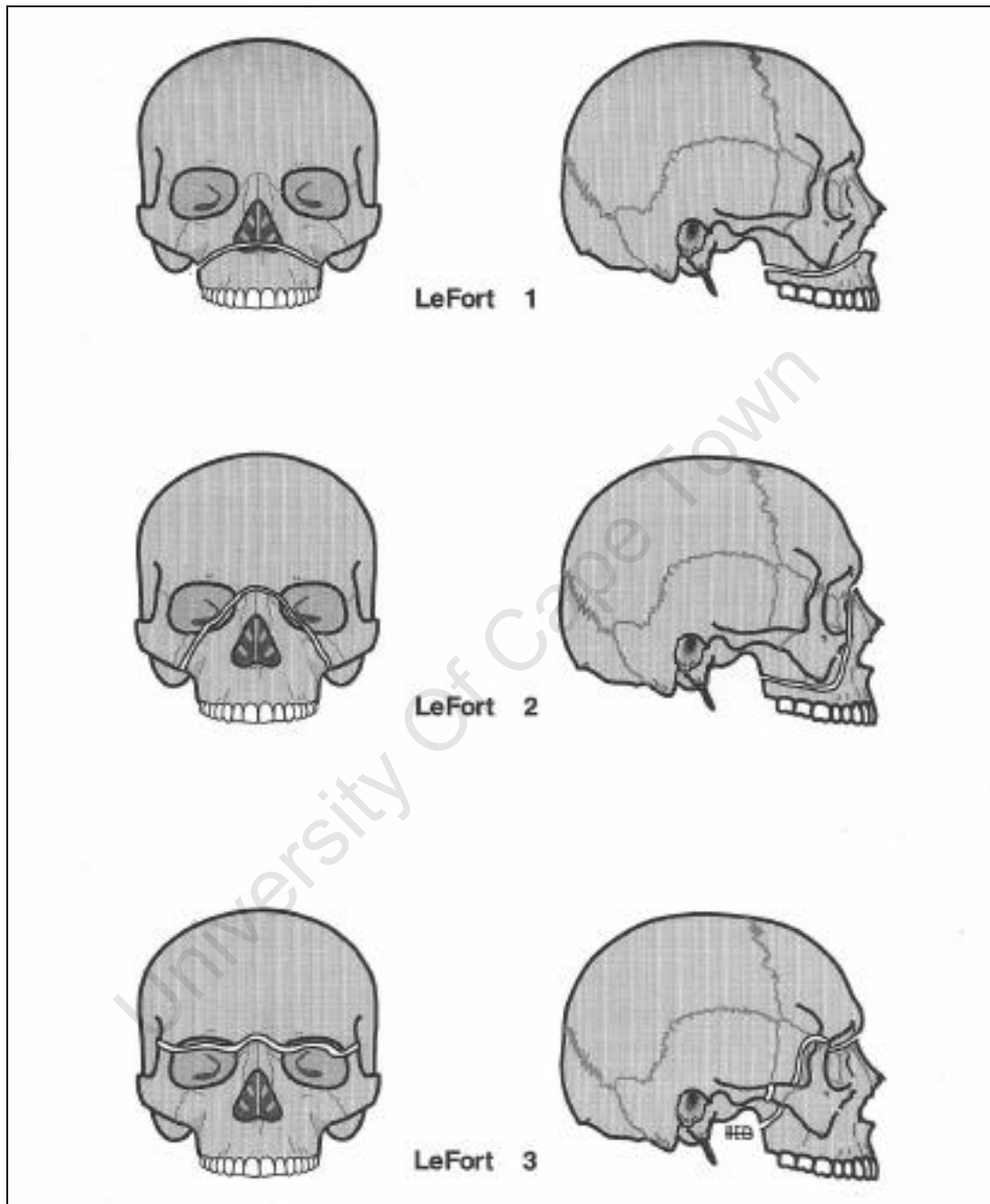


Figure 6.01 LeFort I, II, and III fractures are directed by areas of buttressing. Complicated patterns involving a combination of more than one Lefort type may occur (Berryman and Symes, 1998).

through the long axis of the bone. This type of loading is most commonly seen in the leg bones following vertical falls if someone lands on their feet. However, if an individual lands at an oblique angle or falls flat against the ground, the stressors are perpendicular to the long bone, producing compression and tension fractures instead (Smith *et al.*, 2003). Thus, it is possible that the injuries observed on the femora of UCT1I were caused by a vertical fall from a significant height.

UCT1E also experienced trauma to the left upper limb. Injuries include a crush fracture on the posterior distal humerus, transverse fracture on the proximal radius and a longitudinal fracture on the proximal ulna. Given the anatomical location of these injuries with regards to their proximity, it is possible that they were caused by the same traumatic force during a single event. Crush fractures occur when a force is applied over a large area of the body and results in the bone collapsing on itself. The degree of damage varies from transverse to severely comminuted fractures, as seen on the humerus of UCT1E. The radial transverse fracture is typical of direct trauma. Complete and displaced transverse fractures are caused by mechanisms of high energy such as injuries involving encounters with cars or falls from significant heights (Pierce *et al.*, 2004). The longitudinal fracture on the ulna can be caused by compression. According to Symes (2005b), post-mortem carnivore trauma results in low energy vice-like crushing and can cause among others, increased longitudinal fractures. However, this is not the case with UCT1E as no gnawing marks were seen on the bones. Also, in peri-mortem blunt trauma, longitudinal fractures are less common. Thus, it is likely that the injuries seen on UCT1E were caused by falling from a great height and landing on the left upper limb close to the elbow.

In UCT1B, fractures of the lower left limb include a longitudinal fracture along the shaft of the femur, an unhealed spiral fracture at the proximal tibia and an oblique fracture at the proximal fibula. These injuries could possibly be related as they all occur on the left lower limb in the proximity of the knee and all three bones were involved. This pattern of fracturing is seen in falls from a great height and could involve landing on the knee. Another possibility is that the knee was knocked or hit something while it was falling, but this would not achieve the explosive force needed to cause such severe damage to the

bones surrounding the knee. Thus, it is suggested that UCT1B fall from a significant height and landed on its left knee.

6.3.2.4 Summary

It is not known what the exact nature of the cause of death for the individuals from Khoraxa-ams was, though there is some evidence to suggest that they were dead before their bodies were deposited in the cave. No cut marks or signs of weapon wounds were observed on the remains, indicating that no violence by sharp force trauma was afflicted upon the individuals. However, signs of blunt force trauma mainly to the crania, as experienced by a number of individuals peri-mortem could possibly serve as a likely cause of death. Though, this cannot be confirmed due to insufficient evidence and serves only as speculation.

The blunt force trauma experienced by UCT1K could possibly be the result of an impact caused by falling from a significant height and landing on the mid-facial region. The fracture caused by axial loading on the femora of UCT1I was possibly the result of falling and either landing on their feet or hitting the ‚ground’ at an angle which caused a spiral fracture. It is more likely that the unhealed linear fracture on the cranium of UCT1G was caused by an acceleration injury in which the head was struck by an object. The possibility exists that the complete fracture along the coronal suture of UCT1E could have resulted when the individual was dropped into the cave, along with the crush fracture to the left elbow. The depression fracture seen on the skull of UCT1B could possibly have resulted from a blow to the apex of the skull with a blunt object causing radiating and concentric fractures. The possibility also exists that the skull landed on the tip of a rock or stone causing the small depression fracture at Bregma, though the resultant damage to the top of the skull would have been widespread.

Most of the individuals recovered from Khoraxa-ams presented with post-mortem injuries, while few were identified as having peri-mortem injuries as well. Given the extent of injuries observed on the skeletal remains from Khoraxa-ams, it is evident that the individuals received peri-mortem blunt force trauma at or near the time of death and post-

mortem trauma just after death by being dropped into the 30 metre cave. It is also evident, based on the fractures inflicted by the drop that the individuals were dead before they entered the cave.

With regards to the demographic profile of the individuals that presented with peri-mortem injuries, women and children presented with more severe blunt force trauma than male individuals. Though the actual reason for this phenomenon will never be known, it is possible that the site at Khoraxa-ams represents an execution location. Therefore, a similar speculation exists that the individuals were ‚killed’ (or died) prior to being dropped („dumped’) into the cave and were already dead when they reached the cave floor, as the injuries appear to have been caused by initial blunt force trauma and from a subsequent fall from a great height. It should be noted once again that due to a lack of supporting evidence, all plausible theories as to how they died and how they got into the cave are based on mere speculation.

6.3.3 What could the events at death have been?

One of the most important aspects of a forensic investigation is the determination of events at death. This includes the identification of violent as well as accidental trauma and rules out the possibility of a crime being committed. Coupled with determining events at death is the identification of the manner of death, which is far more challenging and less accurate. In the case of the individuals from Khoraxa-ams, the question of exact manner of death might never be resolved.

From the skeletal injuries observed on the remains it is likely that the individuals of Khoraxa-ams were initially killed and then dropped into the cave as means of disposal. Therefore, they were dead before they hit the base of the cave. This begs the question, why were they killed? The answer will never be determined due to the lack of evidence, though what is suspicious is the sex ratio of individuals presenting with traumatic injuries. Only women and children in the sample demonstrate severe blunt force trauma. Could this be as a result of ethnic cleansing?

Ethnic cleansing is generally understood as the expulsion of an “undesirable” population from a given territory due to religious or ethnic discrimination, political, strategic or ideological considerations, or a combination of these (Bell-Fialkoff, 1993). Varying methods of violent expulsion were used in cases of ethnic cleansing, such as executions; people rounded up and burned in churches, being killed along ditches and then buried or dumped into rivers, or thrown alive into holes in frozen lakes as well as being buried alive. Ethnic cleansing can take the form of a small scale event performed by neighbouring communities/tribes similar to the raids of livestock in Namibia carried out by bands of Nama stock thieves on the Himba, killing anyone who stood in their way and in turn wiping out entire villages (Jacobsohn, 1990). It can also be on a large scale as seen in Rwanda in 1994, in which Hutu militias supporting the government spearheaded a systematic slaughter of the approximately 800,000 Tutsis (Staub, 2000). Thus, ethnic cleansing in Rwanda was classified as genocide. The United Nations defines genocide as those “acts committed with intent to destroy, in whole or in part, a national, ethnical, racial or religious group” (Destexhe, 1994).

However, in the case of the Khoraxa-ams site, men were also present in the cave, but did not show extreme signs of violence. In addition, no cut marks or weapon wounds were seen on the remains, indicating that trauma, if inflicted by humans, was not the result of violence by sharp force. All traumatic injuries were the result of fractures, thus lending towards the possibility that the individuals were treated with enough blunt force to cause bone breakage. Most of the fractures were unhealed, indicating that they occurred just prior to death or shortly after. A plausible theory, though based on speculation, is that the breaks may have occurred during the post-mortem interval shortly after death, while the remains were still fresh.

Various scenarios and hypotheses exist that could explain the events at death, though many are not plausible. Initially it was thought that the individuals were killed and dumped in the cave as means of disposal of the bodies. However, this is highly unlikely due to the absence of defence wounds. If the forearm is employed to protect the head from an attack then the occurrence of forearm diaphyseal fractures and cranial injuries should coincide

(Larsen, 1997) and defence wounds should be present on the forearms. However, no 'parry' fractures were observed on the forearms of the present study. Parry fractures usually result from an individual's attempt to ward off a blow directed at their head or upper body (Larsen, 1997).

It could also be proposed that the bodies, having died of natural cause, were allowed to decompose naturally by means of exposure or via burial. Once the decomposition was complete, the separate bones were then collected and re-interred in the cave. However, no evidence exists to support the theory of a secondary burial. No signs of weathering and sun-bleaching due to exposure, or soil staining and other signs of deterioration caused by initial burial or natural decomposition were visible on the remains. The remains also showed no evidence of flesh-removal or dismemberment, commonly seen among bones from Iroquoian ossuaries where the remains are defleshed and disarticulated and reburied in a single communal pit (Weslager, 1942; Bathurst and Barta, 2004). No sign of cracks or fractures commonly observed on dried bone were present on the remains. Rather, overwhelming evidence exists that indicate that the pattern of injuries observed on the remains is consistent with fractures that occur on intact, fleshed bodies. Therefore, the site at Khoraxa-ams was not a secondary burial, but rather a primary burial where the remains were displaced due to decomposition movement after being deposited in the cave.

In addition, it is possible that the events, natural or otherwise, that lead to the death of these individuals took place in close proximity to the cave. This theory is based on the issue of transportation of a minimum of 16 individuals, and it is therefore more probable that the individuals or their remains were not carried from a far distance. It can be argued however, that the remains were not all deposited at the same time, refuting this theory. Determining whether or not Khoraxa-ams presents a single event or multiple events over a long time is fairly challenging due to the lack of contextual evidence. However, evidence for distinguishing between single and multiple events is highlighted in a case of co-mingled remains in South Africa by L'Abbé (2005). Various taphonomic processes were observed on the remains (e.g., the colour of the bones, desiccated tissue and mold), suggesting that the individuals had not died at the same time or had decomposed under different

conditions, evidence of a multiple event. The state of preservation and the degree of taphonomic processes observed on the Khoraxa-ams remains is fairly uniform and therefore disagrees with the likelihood of this being a multiple event over a long time. Therefore, based on speculation it is likely that Khoraxa-ams presents a single event. However, no solid evidence exists to support this argument. Given the thousand year time depth, it is possible that the state of preservation of the remains would appear similar, even if several decades lapsed between events.

Why were the remains deposited in a sinkhole in north-western Namibia and what happened to them prior to being deposited? The answers to these questions remain unknown. Though deductions can be made given the evidence gathered as to the most likely cause. The extent of the skeletal trauma observed on the remains is consistent with initial blunt force trauma before death and with post-mortem falling from a significant height and landing on an uneven surface after death. Thus, it is presumed that the individuals from Khoraxa-ams were dropped into the cave shortly after their death. The cause of death however, cannot be determined due to a lack of evidence. Though, the possibility exists, based on speculation, that the site at Khoraxa-ams was an execution location.

CONCLUSION

Human skeletal remains from a 1000 year old cave site in Khoraxa-ams, situated in the north-west region of Namibia were examined and their identification and possible circumstances surrounding their placement in the cave established.

Sorting and „siding’ of bone elements from the cave identified a minimum total of 16 individuals based on the representation of cranial bones in the sample. The remains consisted of adult individuals with the exception of one sub-adult. No children were present in the sample. The male to female ratio within the sample was roughly 1:1. The demography of death for the Khoraxa-ams sample therefore, does not represent a „normal’ mortality profile common among historic populations.

Ethnic identity of the people of Khoraxa-ams was determined by a combination of craniological and lifestyle observations. The craniological analysis of the Khoraxa-ams crania show that they consistently fall in the „Negroid’ rather than the „Khoesan’ range of variation. This strongly suggests that they are likely to have been related to the living Negroid populations of Namibia – the Herero, Ovambo and the Dama. The dental health and isotopic data suggests that the people of Khoraxa-ams consumed a mixed diet, most likely true among pastoralist groups. They were in fairly good health with no signs of malnutrition or infectious diseases observed on any of the post-cranial or cranial bones. The low incidence of arthritis and the generally gracile nature of the skeletal elements suggest that they did not take part in activities that required strenuous exercise; rather they were involved in low-impact labour and activities prone to assuming a squatting posture. These lifestyle markers observed in the Khoraxa-ams sample are therefore most similar to the pastoralist Herero and Dama. The cultural practice of dental modification was observed as being similar in style as documented for the Herero, while the practice has not been recorded historically among the Dama. If we assume that these dental practices have a time

depth which would encompass Khoraxa-ams, then the most likely identity of these people would be an ancestral Herero-like group, based on craniology, diet, activity patterns and dental mutilation patterns.

The exact nature of the cause of death for the individuals from Khoraxa-ams is not known, though evidence from the dispersion of the bones suggests that they were dead before their bodies were deposited in the cave. No signs of violence by sharp force trauma affected these individuals, as no cut marks or weapon wounds were evident. Instead, signs of blunt force trauma mainly concentrated on the crania as well as injuries caused by the drop into the cave observed on crania and post-crania were visible on the remains. It cannot be assumed however, that blunt force trauma to the cranium was the cause of death due to insufficient evidence. Though, based on the extent of injuries observed on the remains, it is evident that the individuals received peri-mortem blunt force trauma at or near the time of death as well as post-mortem trauma just after death by being dropped into the 30 metre cave.

Given that the individuals were dead before being dropped into the cave, and that the actual events at death that lead to them being deposited in the cave remains unknown, it begs the question, "Why?" Various possibilities concerning the events at death are therefore proposed in comparison to archaeological contexts elsewhere in the world, though it should be stressed that these theories are based strictly on speculation, as no secure evidence exists to support them. Ethnic cleansing as the result of inter-tribal conflict is one such possibility, though no evidence of violence due to sharp force trauma was observed on the remains. It is possible that the individuals were killed and their bodies dumped in the cave as means of disposal, but no defence wounds were visible on the upper limb bones, typically involved in shielding the face from harmful blows. Another possibility exists that the individuals died of natural causes and allowed to decompose naturally either via burial or exposure, similar to a secondary burial. However, no signs of deterioration commonly caused by initial burial or natural decomposition such as weathering, sun bleaching or soil staining were observed on the remains. In addition, no signs of flesh-removal or dismemberment were visible either.

It could not be determined whether the events at Khoraxa-ams that lead to the deposition of human remains in the cave occurred as a single episode or over multiple events, due to the thousand year time depth. Though, it was speculated based on the uniform state of preservation of the remains, that Khoraxa-ams represents a „single event.’ With the demographic profile of women and children presenting with more severe blunt force trauma to the crania, the lack of defence wounds, and the fact that the individuals were dead before they were dropped in the cave, the possibility exists that the site at Khoraxa-ams represents an execution location perhaps linked to ethnic cleansing. As no secure evidence exists to support this theory, it too remains mere speculation.

The information we learn from the past is important for interpreting the present human condition (Larsen, 2000). Thus, the evidence from Khoraxa-ams sheds light on the lives of a prehistoric people living in north-western Namibia, not only with regards to biographical information, but on the events that culminated in their deposition in a 30 metre deep cave. History is written from documents, but archaeology and biological anthropology can help to understand events that happened without documented record.

References

- Adams BJ and Byrd JE (2006) Resolution of small-scale commingling: A case report from the Vietnam War. Forensic Science International 156:63-69.
- Adams BJ and Konigsberg LW (2004) Estimation of the most likely number of individuals from commingled human skeletal remains. American Journal of Physical Anthropology 125:138-151.
- Aitken MJ (1990) Science-based dating in archaeology. England: Longman Publishers.
- Alfonso MP, Thompson JL and Standen VG (2005) Re-evaluating Harris lines – a comparison between Harris lines and enamel hypoplasia. Collegium Antropologicum 29(2):393-408.
- Ambrose SH (1991) Effects of diet, climate and physiology on nitrogen isotope abundances on terrestrial foodwebs. Journal of Archaeological Science 18(3):293-317.
- Ambrose SH (2006) A tool for all seasons. Science 314:930-931.
- Andelinović S, Sutlović D, Ivkošić IE, Škaro V, Ivkošić A, Paić F, Režić B, Definis-Gojanović M and Primorac D (2005) Twelve-year experience in identification of skeletal remains from mass graves. Croatian Medical Journal 46(4):530-539.
- Archer MS, Bassed RB, Briggs CA and Lynch MJ (2005) Social isolation and delayed discovery of bodies in houses: The value of forensic pathology, anthropology, odontology, and entomology in the medico-legal investigation. Forensic Science International 151(2-3):259-265.
- Aufderheide AC and Rodriguez-Martin C (1998) The Cambridge Encyclopaedia of Human Palaeopathology. Cambridge: Cambridge University Press.
- Bahn P (2003) Vilnius and the ghosts of the Grande Armée. In: Written in bones: how human remains unlock the secrets of the dead. Ontario, Canada: Firefly Books. Pp. 72-77.
- Baraybar JP and Gasior M (2006) Forensic anthropology and the most probable cause of death in cases of violations against international humanitarian law: an example from Bosnia and Herzegovina. Journal of Forensic Science 51(1):103-108.
- Barnard A (1983) Contemporary hunter-gatherers: current theoretical issues in ecology and social organization. Annual Review of Anthropology 12:193-214.
- Barnard A (2008) Ethnographic analogy and the reconstruction of early Khoekhoe society. South African Humanities 20(1):61-75.
- Bathurst RR and Barta JL (2004) Molecular evidence of tuberculosis induced hypertrophic osteopathy in a 16th-century Iroquoian dog. Journal of Archaeological Science 31:917-925.
- Beattie JH and Avenell A (1992) Trace element nutrition and bone metabolism. Nutrition Research Reviews 5:167-188

- Bell-Fialkoff A (1993) A brief history of ethnic cleansing. Foreign Affairs 72(3):110-121.
- Bello SM, Thomman A, Signoli M, Dutour O and Andrews P (2006) Age and sex bias in the reconstruction of past population structures. American Journal of Physical Anthropology 129(1):24-38.
- Belsky JL, Hamer JS, Hubert JE, Insogna K and Johns W (2003) Torus palatinus: a new anatomical correlation with bone density in postmenopausal women. Journal of Clinical Endocrinology and Metabolism 88(5):2081-2086.
- Berryman HE and Symes SA (1998) Recognising gunshot and blunt cranial trauma through fracture interpretation. In Reichs KJ (editor). *Forensic osteology: advances in the identification of human remains*. Springfield, IL: Charles C. Thomas. Pp. 333-352.
- Bierman PR and Caffee M (2001) Slow rates of rock surface erosion and sediment production across the Namib desert and escarpment, southern Africa. American Journal of Science 301:326-358.
- Bogden JD (2000) The essential trace elements and minerals: basic concepts. In: Bogden JD and Klevay LM (editors). *Clinical nutrition of the essential trace elements and minerals: the guide for health professionals*. Totowa, New Jersey: Humana Press. Pp.3-9.
- Boulle E (2001) Evolution of two human skeletal markers of the squatting position: a diachronic study from Antiquity to the Modern age. American Journal of Physical Anthropology 115(1):50-56.
- Brain CK (1981) *The hunters or the hunted? An introduction to African cave taphonomy*. Chicago, IL: University of Chicago Press.
- Brkic H, Strinovic D, Slaus M, Skavic J, Zecevic D and Milicevic M (1997) Dental identification of war victims from Petrinja in Croatia. International Journal of Legal Medicine 110:47-51.
- Brooks ST (1955) Skeletal age at death: the reliability of cranial and pubic age indicators. American Journal of Physical Anthropology 13:567-589.
- Brooks S and Suchey JM (1990) Skeletal age determination based on the os pubis: a comparison of the Acsádi-Nemeskéri and Suchey-Brooks methods. Human Evolution 5:227-238.
- Brothwell D (1963) The macroscopic dental pathology of some earlier human populations. In: Brothwell D (editor). *Dental Anthropology*. London: Pergamon Press. Pp. 271-288.
- Brothwell DR (1981) *Digging Up Bones*. 3rd ed. London: Oxford University Press.
- Brown KP, Pollintine P and Adams MA (2008) Biomechanical implications of degenerative joint disease in the apophyseal joints of human thoracic and lumbar vertebrae. American Journal of Physical Anthropology 136:318-326.
- Budimlija ZM, Prinz MK, Zelson-Mundorff A, Wiersema J, Bartelink E, MacKinnon G, Nazzaruolo BL, Estacio SM, Hennessey MJ and Shaler RC (2003) World Trade Center human identification project: experiences with individual body identification cases. Croatian Medical Journal 44(3):259-263.

- Budzikiewicz H, Grigsby RD (2006) Mass spectrometry and isotopes: a century of research and discussion. Mass Spectrometry Reviews 25(1):146-157.
- Buikstra J and Ubelaker DH (1994) Standards for data collection from human skeletal remains. Fayetteville: Arkansas Archaeological Survey research series; no. 44.
- Burns KR (1999) Forensic anthropology training manual. New Jersey: Prentice Hall.
- Byers S (1991) Technical note: Calculation of age at formation of radiopaque transverse lines. American Journal of Physical Anthropology 85:339-343.
- Byrd JE and Adams BJ (2003) Osteometric sorting of commingled human remains. Journal of Forensic Science 48:717-723.
- Cardoso HFV (2007) Accuracy of developing tooth length as an estimate of age in human skeletal remains: The deciduous dentition. Forensic Science International 172:17-22.
- Cardoso HFV (2008) Age estimation of adolescent and young adult male and female skeletons II, epiphyseal union at the upper limb and scapular girdle in a modern Portuguese skeletal sample. American Journal of Physical Anthropology 137(1):97-105.
- Cattaneo C (2007) Forensic anthropology: developments of a classical discipline in the new millennium. Forensic Science International 165:185-193.
- Cheverud JM (1988) A comparison of genetic and phenotypic correlations. Evolution 42(5):958-968.
- Churcher CS and Kenyon W (1960) The Tabor Hill ossuaries: A study in Iroquois demography. Human Biology 32:247-273.
- Cohen MN and Armelagos GJ (1984) Palaeopathology at the origins of agriculture. Orlando, Florida: Academic Press.
- Cox G and Sealy J (1997) Investigating Identity and Life Histories: isotopic analysis and historical documentation of slave skeletons found on the Cape Town foreshore, South Africa. International Journal of Historic Archaeology 3(1):207-224.
- Cox G, Sealy J, Schrire C and Morris A (2001) Stable carbon and nitrogen isotopic analyses of the underclass at the colonial Cape of Good Hope in the eighteenth and nineteenth centuries. World Archaeology 31(1):73-97. *The Archaeology of Slavery*
- Currie LA (2004) The remarkable metrological history of radiocarbon dating [II]. Journal of Research of the National Institute of Standards and Technology 109(2):185-217.
- Danforth ME, Cook DC and Knick SG (1994) The human remains from Carter Ranch Pueblo, Arizona: health in isolation. American Antiquity 59(1):88-101.
- Dayal MR, Steyn M and Kuykendall KL (2008) Stature estimation from bone of South African whites. South African Journal of Science 104:124-128.

- Dembetembe KA (2007) Bone preservation and burial pattern: an analysis of the 18th and 19th century burial remains from Cobern Street. Unpublished Honours thesis, Department of Human Biology, University of Cape Town.
- Denbow JR (1986) A new look at the later prehistory of the Kalahari. Journal of African History 27:3-28.
- Denbow JR and Wilmsen EN (1986) Advent and course of pastoralism in the Kalahari. Science 23:1509-1515.
- DeNiro MJ (1985) Postmortem preservation and alteration of *in vivo* bone collagen isotope ratios in relation to palaeodietary reconstruction. Nature 317:806-809.
- Destexhe A (1994) The third genocide. Foreign Policy 97:3-17.
- Dirkmaat DC, Cabo LL, Ousley SD and Symes SA (2008) New perspectives in forensic anthropology. Yearbook of Physical Anthropology 51(1):33-52.
- Djurić MP (2004) Anthropological data in individualization of skeletal remains from a forensic context on Kosovo – A Case History. Journal of Forensic Science 49(3):464-468.
- Djurić MP (2006) Fractures in late medieval skeletal populations from Serbia. American Journal of Physical Anthropology 130:167-178.
- Djurić MP, Dunjic D, Djonic D and Skinner M (2007) Identification of victims from two mass-graves in Serbia: A critical evaluation of classical markers of identity. Forensic Science International 171(2/3):125-129.
- Dlamini N and Morris AG (2005) An investigation of the frequency of squatting facets in Later Stone Age foragers from South Africa. International Journal of Osteoarchaeology 15:371-376.
- Dlamini N (2006) An assessment of the health status by non-specific stress indicators in early farming populations from central and southern Africa. Unpublished MSc thesis. Department of Human Biology, University of Cape Town.
- Dorandeu A, Coulibaly B, Piercecchi-Marti M, Bartoli C, Gaudart J, Baccino E and Leonetti G (2008) Age-at-death estimation based on the study of frontosphenoidal sutures. Forensic Science International 177(1):47-51.
- Ehret C (2008) The early livestock-raisers of southern Africa. South African Humanities 20(1):7-35.
- Eldredge EA (1994) Slave raiding across the Cape Frontier. In: Eldredge EA and Morton F (editors). *Slavery in South Africa: captive labor on the Dutch Frontier*. Pietermaritzburg: The University of Natal Press. Pp. 93-126.
- Eveleth PB and Tanner JM (1976) *Worldwide variation in human growth*. Cambridge: Cambridge University Press.
- Fauvelle-Aymar F-X and Sadr K (2008) Trends and traps in the reconstruction of early herding societies in southern Africa. South African Humanities 20(1):1-6.

Feldesman MR and Fountain RL (1996) "Race" specificity and femur/stature ratio. American Journal of Physical Anthropology 100:207-224.

Fourie DJ (1997) Educational language policy and the indigenous languages of Namibia. International Journal of the Sociology of Language 125(1):29-42.

France DL (1998) Lab Manual and Workbook for Physical Anthropology. 3rd ed. Belmont, California: West Wadsworth Publishing Company.

Franklin D, Freedman L and Milne N (2005) Three-dimensional technology for linear morphological studies: a re-examination of cranial variation in four southern African indigenous populations. Journal of Comparative Human Biology 56:17-34.

Friedling LJ (2007) Grave tales: an osteological assessment of health and lifestyle from 18th and 19th century burial sites around Cape Town. Unpublished PhD thesis, Department of Human Biology, University of Cape Town.

Gillett RM (1991) Determination of age at death in human skeletal remains: a comparison of two techniques. International Journal of Anthropology 6(2):179-189.

González-José R, Neves WA, Lahr MM, González S, Pucciarelli H, Martínez MH and Correal G (2005) Late Pleistocene/Holocene craniofacial morphology in Mesoamerican Paleoindians: Implications for the Peopling of the New World. American Journal of Physical Anthropology 128:772-780.

Goodman AH and Armelagos GJ (1985) Factors affecting the distribution of enamel hypoplasia within the human permanent dentition. American Journal of Physical Anthropology 68(4):479-493.

Goodman AH and Martin DL (2002) Reconstructing health profiles from skeletal remains. In: Steckel RH and Rose JC (editors). The backbone of history: health and nutrition in the Western hemisphere. New York, NY: Cambridge University Press. Pp. 11-60.

Goodman AH and Rose J (1990) Assessment of systemic physiological perturbations from dental enamel hypoplasia and associated histological structures. American Journal of Physical Anthropology 33(1):59-110.

Gordon RJ (1992) The Bushmen myth: the making of a Namibian underclass. In Whiteford S and Derman W (editors). Conflict and Social Change Series. Colorado, USA: Westview Press.

Gorsky M, Raviv M, Kfir E and Moskona D (1996) Prevalence of torus palatinus in a population of young and adult Israelis. Archives of Oral Biology 41:623-625.

Gould AR, Farman AG and Corbitt D (1984) Modifications of the dentition in Africa. Quintessence International 1:89-94.

Grabiner MD (1989) The elbow and radioulnar joints. In: Rasch PJ (editor). Kinesiology and applied anatomy. London: Lea and Febiger. Pp. 136-150.

Grauer AL and McNamara EM (1995) A piece of Chicago's past: exploring childhood mortality in the Dunning poorhouse cemetery. In: Grauer AL (editor). Bodies of Evidence. New York: Wiley-Liss. Pp. 91-104.

- Gravina B, Mellars P and Ramsey CB (2005) Radiocarbon dating of interstratified Neanderthal and early modern human occupations at the Chatelperrinian type-site. Nature 438(3):51-56.
- Grolleau-Raoux J-L, Crubezy E, Rouge D, Brugne J-F and Saunders SR (1997) Harris lines: a study of age-associated bias in counting and interpretation. American Journal of Physical Anthropology 103:209-217.
- Gruspier KL (1999) Pathological changes on human skeletal remains: before, during or after? In: Fairgrieve SI (editor). *Forensic osteological analysis: a book of case studies*. Illinois, USA: Charles C Thomas Publishers. Pp. 199-225.
- Gunby P (1994) Medical team seeks to identify human remains from mass graves of war in former Yugoslavia. Journal of the American Medical Association 272:1804-1806.
- Haacke WHG (2008) Linguistic hypotheses on the origin of Namibian Khoekhoe speakers. South African Humanities 20(1):163-177.
- Hahn CHL, Vedder H and Fourie L (1928) *The Native Tribes of South West Africa*. Cape Town: Cape Times Limited.
- Hammond-Tooke WD (1974) *The Bantu-speaking peoples of Southern Africa*. 2nd ed. London, UK: Routledge & Kegan Paul.
- Haugen LK (1992) Palatine and mandibular tori. A morphological study in the current Norwegian population. Acta Odontologica Scandinavica 50:65-77.
- Heaney RP (2000) Trace element and mineral nutrition in skeletal health and disease. In: Bogden JD and Klevay LM (editors). *Clinical nutrition of the essential trace elements and minerals. The guide of health professionals*. Totowa, New Jersey: Humana Press. Pp. 239-249.
- Henderson J (1987) Factors determining the state of preservation of human remains. In: Boddington A, Garland AN and Janaway RC (editors). *Death, decay and reconstruction*. Manchester, UK: Manchester University Press. Pp. 43-54.
- Hickerson H (1960) The Feast of the Dead among the seventeenth century Algonkians of the Upper Great Lakes. American Anthropology 62(1):81-107.
- Hillson S (1996) *Dental anthropology*. Cambridge, UK: University Press, Cambridge.
- Hirschfelder CA (1891) Burial Customs of the Hurons. Science 18(453):197-198
- Hoopa RD and Gruspier KL (1996) Estimating diaphyseal length from fragmentary subadult skeletal remains: implications for palaeodemographic reconstructions of a southern Ontario Ossuary. American Journal of Physical Anthropology 100:341-354.
- Horton DR (1984) Minimum numbers: a consideration. Journal of Archaeological Science 11:255-271.
- Howells WW (1973) *Cranial Variation in Man: a study by multivariate analysis of patterns of difference among recent human populations*. Papers of the Peabody Museum of Archaeology and Ethnology. Cambridge: Harvard University Press.

Inskeep R (1986) A preliminary survey of burial practices in the Later Stone Age, from the Orange River to the Cape coast. In: Singer R and Lundy JK (editors). Variation, culture and evolution in African populations: papers in honour of Dr. Hertha de Villiers. Johannesburg: Witwatersrand University Press. Pp. 221-239.

International Defence and Aid Fund for Southern Africa – IDAF Research, Information and Publications Department (1989) Namibia The Facts. London: IDAF Publications.

Irish J (1991) Conservation aspects of karst waters in Namibia. MADOQUA 17(2):141-146.

İşcan MY (1988) Rise of forensic anthropology. Yearbook of Physical Anthropology 31:203-230.

İşcan MY (2001) Global forensic anthropology in the 21st century: Editorial. Forensic Science International 117:1-6.

İşcan MY (2005) Forensic anthropology of sex and body size. Forensic Science International 147:107-112.

İşcan MY and Miller-Shaivitz (1984) Determination of sex from the tibia. American Journal of Physical Anthropology 64(1):53-57.

İşcan MY, Kessel MH and Marits S (1989) Spectrographic analysis of trace elements in archaeological skeletal material from Florida: a preliminary report. American Journal of Physical Anthropology 79(4):483-488.

İşcan MY, Loth SR and Scheurman EH (1992) Age assessment for the costal end of rib and pubic symphysis: a systematic comparison. Anthropologie 30:41-44.

Jackes MK (1996) Complexity in seventeenth century southern Ontario burial practices. In: Debating Complexity, Proceedings of the 26th Annual Chacmol Conference, University of Calgary.

Jacobsohn M (1990) Himba: Nomads of Namibia. Cape Town, South Africa: Struik Publishers.

Jainkittivong A and Langlais RP (2000) Buccal and palatal exostoses: prevalence and occurrence with tori. Oral Surgery Oral Medicine Oral Pathology Oral Radiology and Endodontics 90(1):48-53.

Jones A (2001) Dental disfigurements in Borneo. British Dental Journal 191:98-102.

Katzenberg MA and Saunders (2000) Biological anthropology of the human skeleton. New York, NY: Wiley-Liss.

Katzenberg MA and White R (1979) A paleodemographic analysis of the os coxae from Ossossané Ossuary. Canadian Review of Physical Anthropology 1(1):10-28.

Kidd KE (1953) The excavation and historical identification of a Huron ossuary. American Antiquity 18(4):359-379.

Kimmerle EH and Pablo BJ (2008) Differential diagnosis of skeletal injuries. In Skeletal trauma: identification of injuries resulting from human rights abuse and armed conflict. Abingdon, Oxford, UK: CRC Press-Taylor and Francis Group.

- Kinahan J (1991) Pastoral nomads of the Central Namib Desert: the people history forgot. Windhoek, Namibia: Hirt & Carter.
- Kinahan J (2001) The presence of the past: archaeology, environment and land rights on the lower Cunene River. Cimbebasia 17:23-39.
- Kinahan JHA (2004) Where the ancestors speak: a Himba experience. Windhoek, Namibia: Namibia Archaeological Trust.
- Klepinger LL, Kuhn JK and Williams WS (1986) An elemental analysis of archaeological bone from Sicily as a test of predictability of diagenetic change. American Journal of Physical Anthropology 70(3):325-331.
- Komar D (2008) Patterns of mortuary practice associated with genocide. Current Anthropology 49(1):123-133.
- Konigsberg LW and Ousley SD (1995) Multivariate quantitative genetics of anthropometric traits from the Boas data. Human Biology 67(3):481-498.
- L'Abbé EN (2005) A case of commingled remains from rural South Africa. Forensic Science International 151:201-206.
- L'Abbé EN, Loots M and Keough N (2008) The Matjes River Rock Shelter: a description of the skeletal assemblage. South African Archaeological Bulletin 63(187):61-68.
- Lambert JB, Vlasak SM, Thometz AC and Buikstra JE (1982) A comparative study of the chemical analysis of ribs and femurs in Woodland populations. American Journal of Physical Anthropology 59:289-294.
- Lambert JB, Simpson SV, Szpunar CB and Buikstra JE (1985) Bone diagenesis and dietary analysis. Journal of Human Evolution 14:477-482.
- Larsen CS (1997) Bioarchaeology: Interpreting behaviour from human skeleton. Cambridge: Cambridge University Press.
- Larsen CS (2000) Skeletons in our closet: revealing our past through bioarchaeology. Princeton, NJ: Princeton University Press.
- Lau B (1987) Namibia in Jonker Afrikaner's time. Windhoek Archives Publication No. 8. Windhoek, Namibia: National Archives, Department of Nat. Education.
- Lee RB and DeVore I (1976) Kalahari hunter-gatherers: studies of the !Kung San and their neighbours. Cambridge, Massachusetts: Harvard University Press.
- Lee-Thorp JA, Sealy JC and Morris, AG (1993) Isotopic evidence for diets of prehistoric farmers in South Africa. In Lambert JB and Grupe G (editors). Prehistoric human bone: archaeology at the molecular level. New York: Springer-Verlag. Pp. 99-120.
- Lee-Thorp JA and Sponheimer M (2006) Contributions of biogeochemistry to understanding hominin dietary ecology. Yearbook of Physical Anthropology 49:131-148.

- Libby WF, Anderson EC and Arnold JR (1949) Age determination by radiocarbon content: world-wide assay of natural radiocarbon. Science 109(2827):227-228.
- Loth SR (1995) Age assessment of the Spitalfields cemetery population by rib phase analysis. American Journal of Human Biology 7(4):465-471.
- Lovejoy CO (1985) Dental wear in the Libben population: Its functional pattern and role in the determination of adult skeletal age at death. American Journal of Physical Anthropology 68:47-56.
- Lovell NC (1997) Trauma analysis in paleopathology. Yearbook of Physical Anthropology 40:139-170.
- Lukacs JR (1989) Dental paleopathology: Methods for reconstructing dietary patterns. In: Işcan MY and Kennedy KAR (editors). Reconstruction of life from the skeleton. New York: Alan R. Liss. Pp. 261-286.
- Lukacs JR (1995) The „Caries correction factor’: a new method of calibrating dental caries rates to compensate for antemortem tooth loss. International Journal of Osteoarchaeology 5:151-156.
- Lundy JK (1983) Regression equations for estimating living stature from long limb bones in the South African Negro. South African Journal of Science 79:337-338.
- Lundy JK (1986) Intertribal metrical and morphological variation on the postcranial skeleton of the South African Negro. In: Singer R and Lundy JK (editors). Variation, culture and evolution in African populations. Johannesburg: Witwatersrand University Press. Pp. 85-95.
- Lundy JK and Feldesman MR (1987) Revised equations for estimating living stature from the long bones of the South African Negro. South African Journal of Science 83:54-55.
- Lundy JK and Feldesman MR (1989) The femur/stature ration: a method to estimate living height from the femur. Unpublished paper presented at the 41th Annual Meeting of the American Academy of Forensic Sciences, Las Vegas, Nevada, 13-18 February 1989.
- Malan JS (1980) Peoples of South West Africa/Namibia. 1st ed. Pretoria: HAUM Publishers.
- Martin H (1965) The Precambrian geology of South West Africa and Namaqualand. Precambrian Research Unit, University of Cape Town. Pp. 159.
- Mays S (1995) The relationship between Harris lines and other aspects of skeletal development in adults and juveniles. Journal of Archaeological Science 22:511-520.
- Mays S (1998) The Archaeology of human bones. London: Routledge Taylor and Francis Group.
- Meindl RS and Lovejoy CO (1985) Ectocranial suture closure: a revised method for the determination of skeletal age at death based on the lateral-anterior sutures. American Journal of Physical Anthropology 68:57-66.
- Meindl RS, Lovejoy CO, Mensforth RP and Walker A (1985) A revised method of age determination using the os pubis with a review and tests of accuracy of other current methods of pubic symphyseal aging. American Journal of Physical Anthropology 68(1):29-45.

Mendelsohn J, Jarvis A, Roberts C and Robertson T (2002) Atlas of Namibia: a portrait of the land and its people. Cape Town, South Africa: David Philips.

Mensforth RP, Lovejoy CO, Lallo JW and Armelagos GJ (1978) The role of constitutional factors, diet and infectious disease in the etiology of porotic hyperostosis and periosteal reactions in prehistoric infants and children. Medical Anthropology 2:1-59.

Mertz W (1975) Trace-element nutrition in health and disease: contributions and problems of analysis. Clinical Chemistry 21(4):468-475.

Miescher G and Henrichsen D (2000) New notes on Kaoko: the northern Kunene Region (Namibia) in texts and photographs. Switzerland: Basler Afrika Bibliographien.

Morris AG (1984) An osteological analysis of the protohistoric populations of the northern Cape and western Orange Free State, South Africa. PhD thesis, Department of Anatomy, University of the Witwatersrand, Johannesburg.

Morris AG (1992) The skeletons of contact: a study of prehistoric burials from the lower Orange River valley, South Africa. Johannesburg, South Africa: Witwatersrand University Press.

Morris AG (2000) Unpublished progress report of the 2000 excavation at the Polyoaks site, South Africa.

Myers FR (1988) Critical trends in the study of hunter-gatherers. Annual Review of Anthropology 17:261-282.

Newlands G and de Meillon E (1987) Venomous Creatures. Cape Town: C. Struik Publishers. Pp. 14-15.

Nienaber GS and Raper PE (1983) Hottentot (Khoekhoen) place names, southern African place names: 1. Pretoria: Butterworth Publishers.

Nurse GT (1983) Population movement around the northern Kalahari. African Studies 42(2):153-163.

Nurse GT, Weiner J and Jenkins T (1985) The peoples of southern Africa and their affinities. Oxford: University Press.

Ockerse T (1943) The chemical composition of enamel and dentin in high and low caries areas in South Africa. Journal of Dental Research 22(6):441-446.

Ortner DJ (2003) Identification of pathological conditions in human skeletal remains. San Diego, CA: Academic Press.

Paterson RS (1929) Radiological investigation of epiphyses of long bones. Journal of Anatomy 64:28-46.

Peckmann TR (2002) Dialogues with the dead: an osteological analysis of the palaeodemography and life history of the 18th and 19th century Northern Frontier in South Africa. Unpublished PhD thesis, Department of Human Biology, University of Cape Town.

Peleg Y (2002) Gender and Ossuaries: ideology and meaning. *Bulletin of the American Schools of Oriental Research*, No 325. Pp. 65-73.

Pfeiffer S and Fairgrieve SI (1994) Evidence from Ossuaries: The effect of contact on the health of Iroquoians. In: Larsen CS, Milner GR (editors). *In the wake of contact: biological responses to conquest*. New York, NY: Wiley-Liss. Pp. 47-61.

Pfeiffer S, Katzenberg MA and Kelley MA (1985) Congenital abnormalities in a prehistoric Iroquoian village: The Uxbridge ossuary. *Canadian Review of Physical Anthropology* 4:83-92.

Pierce MC, Bertocci GE, Vogeley E and Moreland MS (2004) Evaluating long bone fractures in children: a biomechanical approach with illustrative cases. *Child Abuse & Neglect* 28:505-524.

Piontek J, Jerszynska B and Nowak O (2001) Harris lines in subadult and adult skeletons from the mediaeval cemetery in Cedynia, Poland. *Variability and Evolution* 9:33-43.

Plastino W, Kaihola L, Bartolomei P and Bella F (2001) Cosmic background reduction in the radiocarbon measurement by scintillation spectrometry at the underground laboratory of Gran Sasso. *Radiocarbon* 43(2A):157-161.

Powell JF and Neves WA (1999) Craniofacial morphology of the First Americans: pattern and process in the peopling of the New World. *American Journal of Physical Anthropology* 42:153-188.

Primorac D, Andelinovic S, Definis-Gojanovic M, Drmic I, Rezic B, Baden MM, Kennedy MA, Schanfield MS, Skakel SB and Less HC (1996) Identification of war victims from mass graves in Croatia, Bosnia, and Herzegovina by the use of standard forensic methods and DNA typing. *Journal of Forensic Science* 41(5):891-894.

Prince DA, Kimmerle EH and Konigsberg LW (2008) A Bayesian approach to estimate skeletal age-at-death utilizing dental wear. *Journal of Forensic Science* 53(3):588-593.

Pucciarelli HM, González-José R, Neves WA, Sardi ML and Rozzi FR (2008) East-West cranial differentiation in pre-Columbian populations from Central and North America. *Journal of Human Evolution* 54:296-308.

Rainio J, Hedman M, Karkola K, Lalu K, Peltola P, Ranta H, Sajantila A, Söderholm N and Penttilä A (2001) Forensic osteological investigation in Kosovo. *Forensic Science International* 121:166-173.

Rao AN (2005) Trace element estimation – methods and clinical context. *Online Journal of Health Allied Sciences* 4(1):1-9.

Raper PE (2004) *New dictionary of South African place names*. Johannesburg: Jonathan Bell Publishers. Pp. 12-18.

Raxter MH, Auerbach BM and Ruff CB (2006) Revision of the fully technique for estimating stature. *American Journal of Physical Anthropology* 130:374-384.

- Richardson-Boedler C (1999) *Sicarius* (Six-Eyed Crab Spider): a homeopathic treatment for Ebola haemorrhagic fever and disseminated intravascular coagulation. British Homeopathic Journal 88:24-28.
- Ritzman TB, Baker BJ and Schwartz GT (2008) A fine line: a comparison of methods for estimating ages of linear enamel hypoplasia formation. American Journal of Physical Anthropology 135(3):348-361.
- Rogers TL (1999) A visual method of determining the sex of skeletal remains using the distal humerus. Journal of Forensic Science 44(1):57-60.
- Rojas-Sepúlveda C, Ardagna Y and Dutour O (2008) Paleoepidemiology of vertebral degenerative disease in a Pre-Columbian Muisca series from Colombia. American Journal of Physical Anthropology 135(4):416-430.
- Room A (2006) Placenames of the world: origins and meanings of the names for 6,600 countries, cities, territories, natural features and historic sites. 2nd ed. North Carolina, USA: McFarland & Company. Pp. 260-261.
- Roseman CC and Weaver TD (2004) Multivariate apportionment of global human craniometric diversity. American Journal of Physical Anthropology 125:257-263.
- Rösing FW, Graw M, Marré B, Ritz-Timme S, Rothschild MA, Röttscher K, Schmeling A, Schröder I and Geserick G (2007) Recommendations for the forensic diagnosis of sex and age from skeletons. Journal of Comparative Human Biology 58:75-89.
- Sadler TW (2006) Langman's Medical Embryology. 10th ed. USA: Lippincott Williams & Wilkins.
- Sadr K (2008) Invisible herders? The archaeology of Khoekhoe pastoralists. South African Humanities 20(1):179-203.
- Saunders C (1983) Perspectives on Namibia: past and present. Occasional Papers No. 4. Centre for African Studies, University of Cape Town.
- Schaefer MC and Black SM (2007) Epiphyseal union sequencing: aiding in the recognition and sorting of commingled remains. Journal of Forensic Science 52(2):277-285.
- Schapera I (1930) The Khoisan peoples of South Africa. London: Routledge.
- Schwartz JH (1995) Skeleton keys: An introduction to human skeletal morphology, development, and analysis. New York, NY: Oxford University Press.
- Seah YH (1995) Torus palatinus and torus mandibularis: a review of the literature. Australian Dental Journal 40:318-321.
- Seidemann RM, Stojanowski CM and Doran GH (1998) The use of the supero-inferior femoral neck diameter as a sex assessor. American Journal of Physical Anthropology 107:305-313.
- Serfontein JHP (1976) Namibia? Johannesburg, South Africa: Fokus Suid Publishers. Pp. 5-9.

Shahack-Gross R, Berna F, Karkanas P and Weiner S (2004) Bat guano and preservation of archaeological remains in cave sites. Journal of Archaeological Science 31:1259-1272.

Signoli M, Ardagna Y, Adalian P, Devriendt W, Lalys L, Rigeard C, Vette T, Kuncevicus A, Poskiene J, Barkus A, Palubeckaitė Z, Garmus A, Pugaciauskas V, Jankauskas R and Dutour O (2004) Discovery of a mass grave of Napoleonic period in Lithuania (1812, Vilnius). Human Palaeontology and Prehistory (Palaeopathology) 3:219-227.

Simmons T (2002) Taphonomy of a karstic cave execution site at Hrgar, Bosnia-Herzegovina. In Haglund WD and Sorg MH (editors). *Advances in forensic taphonomy: methods, theory, and archaeological perspectives*. Danvers, MA: CRC Press. Pp. 263-275.

Singer R (1953) Estimation of age from cranial suture closure. Journal of Forensic Medicine 1:52-59.

Sjovold T (2000) Stature estimation from the skeleton. *Encyclopaedia of Forensic Sciences*. London: Academic Press. Pp. 276-283.

Šlaus M, Strinović D, Pećina-Šlaus N, Brkić H, Baličević D, Petrovečki V and Pećina TC (2006) Identification and analysis of human remains recovered from wells from the 1991 War in Croatia. Forensic Science International 171(1):37-43.

Smith AB (2008) Pastoral origins at the Cape, South Africa: influences and arguments. South African Humanities 20(1):49-60.

Smith A, Malherbe C, Guenther M and Beren P (2000) *The Bushman of southern Africa: a foraging society in transition*. Cape Town, SA: David Philip Publishers.

Smith BH (1984) Patterns of molar wear in hunter-gatherers and agriculturalists. American Journal of Physical Anthropology 63(1):39-56.

Smith BN and Epstein S (1972) Two categories of $^{13}\text{C}/^{12}\text{C}$ ratios for higher plants. Plant Physiology 47:380-384.

Smith OC, Pope EJ and Symes SA (2003) Look until you see: identification of trauma in skeletal material. In Steadman DW (editor). *Hard evidence: case studies in forensic anthropology*. New Jersey, NY: Pearson Education. Pp. 138-154.

Snow CE (1948) The identification of the unknown was dead. American Journal of Physical Anthropology 6:323-328.

Sponheimer M, Passey BH, de Ruiter DJ, Guatelli-Steinberg D, Cerling TE and Lee-Thorp JA (2006) Isotopic evidence for dietary variability in the early hominid *Paranthropus robustus*. Science 314:980-982.

Staub E (2000) Genocide and mass killings: origins, prevention, healing and reconciliation. Political Psychology 21(2):367-382.

Steckel RH (2005) Young adult mortality following severe physiological stress in childhood: skeletal evidence. Economics and Human Biology 3:314-328.

- Steckel RH, Sciulli PW and Rose JC (2002) A health index from skeletal remains. In: Steckel RH and Rose JC (editors). *The backbone of history: health and nutrition in the western hemisphere*. New York, NY: Cambridge University Press.
- Steele DG and Bramblett CA (1988) *The anatomy and biology of the human skeleton*. College Station, Texas: A&M University Press.
- Steinbock RT (1976) *Paleopathological diagnosis and interpretation: bone diseases in ancient human populations*. USA: CC Thomas.
- Steyn M (1994) *An assessment of the health status and physical characteristics of the prehistoric population from Mapungubwe*. Unpublished PhD thesis, University of the Witwatersrand.
- Stiner MC, Kuhn SL, Surovell TA, Goldberg P, Meignen L, Weiner S and Bar-Yosef O (2001) Bone preservation in Hayonim cave (Israel): a macroscopic and mineralogical study. *Journal of Archaeological Science* 28:643-659.
- Stojanowski CM and Duncan WN (2009) Historiography and forensic analysis of the Fort King George "skull": craniometric assessment using the specific population approach. *American Journal of Physical Anthropology* 140:275-289.
- Stover E, Haglund WD and Samuels MS (2003) Exhumation of mass graves in Iraq: considerations for forensic investigations, humanitarian needs, and the demands of justice. *Journal of the American Medical Association* 290(5):663-666.
- Stuart-Macadam P (1985) Porotic hyperostosis: representative of a childhood condition. *American Journal of Physical Anthropology* 66:391-398.
- Stuart-Macadam P (1992) Porotic hyperostosis: a new perspective. *American Journal of Physical Anthropology* 87(1):39-47.
- Stuiver M and Polach HA (1977) Discussion: Reporting of ¹⁴C data. *Radiocarbon* 19(3):355-363.
- Sullivan A (2005) Prevalence and etiology of acquired anaemia in medieval York, England. *American Journal of Physical Anthropology* 128:252-272.
- Suter S, Hardens M, Papageorgopoulou C, Kuhn G, Székely G and Rühli FJ (2008) Technical note: standardized and semiautomated harris lines detection. *American Journal of Physical Anthropology* 137:362-366.
- Symes SA (2005a) Handout. What is the future of forensic anthropology?...assuming there is one? Mercyhurst Archaeological Institute, Department of Applied Forensic Sciences, Mercyhurst College, Erie, PA.
- Symes SA (2005b) Handout. Bone trauma biomechanics table. Mercyhurst Archaeological Institute, Department of Applied Forensic Science, Mercyhurst College, Erie, PA.
- Tafuri M, Robb J, Mastroberto M, Salvadei L and Manzi G (2003) Diet, mobility and residence patterns in bronze age Southern Italy. *Accordia Research Papers* 9:45-56.

- Talma AS and Vogel JC (1993) "A simplified approach to calibrating ^{14}C dates." Radiocarbon 35(2):317-322.
- Thevissen PW, Pittayapat P, Fieuws S and Willems G (2009) Estimating age of majority on third molars developmental stages in young adults from Thailand using a modified scoring technique. Journal of Forensic Science 54(2):1-5.
- Thomas G (2007) Napoleon and typhus: a tale of two generals. Microbiology Today 8-11.
- Tobias PV (1962) On the increasing stature of the Bushmen. Anthropos. 57:801-810.
- Tobias PV (1972) Growth and stature in southern African populations. In: Vorster DJM (editor). The human biology of environmental change. Proceedings of I.B.P. conference held in Blantyre, Malawi, April 5-15, 1971.
- Tobias PV (1974) The biology of the Southern African Negro. In: Hammond-Tooke WD (editor). The Bantu-speaking peoples of southern Africa. London, UK: Routledge & Kegan Paul. Pp. 3-30.
- Ubelaker DH (1978) Estimating sex, stature and age. In: Human skeletal remains: excavation, analysis, and interpretation. 1st ed. Chicago: Aldine Publishing Company. Pp. 41-55.
- Ubelaker DH (1989) Human skeletal remains: excavation, analysis, and interpretation. 2nd ed. Washington, DC: Taxaxacum. Pp. 19-26.
- Ubelaker DH (2008) Review of: The scientific investigation of mass graves: towards protocols and standard operating procedures. Journal of Forensic Science 53(4):1014.
- van Aswegen G, van Rooyen JM, van der Nest DG, Veldman FJ, De Villers TH and Oberholzer G (1997) Venom of a six-eyed crab spider, *Sicarius testaceus* (Purcell, 1908), causes necrotic and haemorrhagic lesions in the rabbit. Toxicon 35(7):1149-1152.
- Vance VL (2007) Age related changes in the human skeleton and its implication for the determination of sex. Unpublished PhD thesis, Department of Anatomy, University of Pretoria.
- Van Reenen JF (1964) Dentition, jaws and palate of the Kalahari Bushmen. Journal of the Dental Association of South Africa 19(1,2,3):1-65.
- Van Reenen JF (1986) Tooth mutilating and extraction practices amongst the peoples of South West Africa (Namibia). In: Singer R and Lundy JK (editors). Variation, culture and evolution in African populations: papers in honour of Dr Hertha de Villiers. Johannesburg: Witwatersrand University Press. Pp. 159-169.
- Vedder H (1938) South West Africa in early times: being the story of South West Africa up to the date of Maharero's death in 1890. In: Hall CG (editor). London, Humphrey Milford: Oxford University Press.
- Walker PL and Hewlett BS (1990) Dental health diet and social status among Central African foragers and farmers. American Anthropology 92:383-398.

- Walker RA and Lovejoy CO (1985) Radiographic changes in the clavicle and proximal femur and their use in the determination of skeletal age at death. American Journal of Physical Anthropology 68(1):67-78.
- Walker PL, Bathurst RR, Richman R, Gjerdrum T and Andrushko VA (2009) The causes of porotic hyperostosis and cribra orbitalia: a reappraisal of the iron-deficiency-anemia hypothesis. American Journal of Physical Anthropology 139:109-125.
- Walrath DE, Turner P, Bruzek J (2004) Reliability test of the visual assessment of cranial traits for sex determination. American Journal of Physical Anthropology 125:132-137.
- Wanek VL (2002) A qualitative analysis for sex determination in humans utilizing posterior and medial aspects of the distal humerus. PhD thesis, Portland State University.
- Weiss KM (1973) Demographic models for anthropology. American Antiquity 38(2): Part 2, Memoir 27.
- Weiss KM (1976) Demographic theory and anthropological inference. Annual Review of Anthropology 5:351-381.
- Wells C (1964) Bones, bodies and disease: evidence of disease and abnormality in early man. London: Thames and Hudson
- Weslager CA (1942) Ossuaries on the Delmarva Peninsula and exotic influences in the coastal aspect of the Woodland pattern. American Antiquity 8(2):142-151.
- Wesolowsky AB (1993) Book review: Prehistoric cannibalism at Mancos 5MTUMR-2346 by Tim D. White. Journal of Field Archaeology 20(2):242-246.
- White TD (1992) Prehistoric cannibalism at Mancos 5MTUMR-2346. Princeton, NJ: Princeton University Press.
- White TD (2000a) Chapter 17: Assessment of age, sex, stature, ancestry, and identity. In: Human osteology. 2nd ed. San Diego, California: Academic Press. Pp. 3337-379.
- White TD (2000b) Chapter 18: Osteological and dental pathology. In: Human osteology. 2nd ed. San Diego, California: Academic Press. Pp. 381-406.
- White TD (2000c) Chapter 19: Postmortem skeletal modifications. In: Human osteology. 2nd ed. San Diego, California: Academic Press. Pp. 407-408.
- White TD (2001) Once were cannibals. Scientific America 285(2):58-66.
- Wilson ML and Lundy JK (1994) Estimated living stature of dated Khoisan skeletons from the south-western coastal region of South Africa. South African Archaeological Bulletin 49:2-8.
- Wood JW, Milner GR, Harpending HC and Weiss KM (1992) The osteological paradox. Current Anthropology 33(4):343-370.

APPENDIX 1

A) Loan Agreement from the State Museum of Namibia to study the skeletal collection from Khoraxa-ams


STAATSMUSEUM STATE MUSEUM	
DEPARTEMENT VAN NASIONALE OPVOEDING - DEPARTMENT OF NATIONAL EDUCATION - ERZIEHUNGSDEPARTMENT	
P. O. BOX 1203 - WINDHOEK 9000 - SOUTH WEST AFRICA / NAMIBIA - TELEPHONE 34047	
LOAN INVOICE	LOAN NO: A 398
TO: <i>John Kinahan P.O. Box 22407 Windhoek</i>	The material listed below is sent as: <input type="checkbox"/> 1. A Gift <input checked="" type="checkbox"/> 2. A Loan at your request <input type="checkbox"/> 3. For identification at our request <input type="checkbox"/> 4. In Exchange
	By Authority of <i>Josy Kamumbo</i>
	Date of Dispatch <i>28 Aug 2007</i>
	Via <i>ROAD</i>
CONDITIONS OF LOAN:	
1. Specimens to be returned by <i>28 Aug 2008</i> (an extension of this period is permitted by arrangement)	
2. Holotypes arising from loans must be returned. Where series are available paratypes of duplicate specimens may be retained by definite arrangement.	
3. Reprints of publications based on this material would be appreciated.	
CATALOGUE NUMBER	DESCRIPTION OF MATERIAL
<i>B4108</i>	<i>5 BOXES HUMAN SKELETAL REMAINS</i>
	<i>J. Kinahan</i>
The loan was received in good order. The undersigned agrees to take care of the specimens, to return them in good condition and accept the loan conditions stated above.	
	Date <i>28 Aug 07</i>
PLEASE RETURN THE WHITE COPY ON RECEIPT OF THE LOAN AND RETAIN THE YELLOW COPY FOR RECORD PURPOSES	

B) Temporary Export Permit received from the National Heritage Council of Namibia for the transportation of the remains to Cape Town, South Africa

National Heritage Council of Namibia

52 Robert Mugabe Avenue
Private Bag 12043, Ausspannplatz
Windhoek - Namibia

Tel: (061) 244 375
Fax: (061) 246 872
Email: nmc@iway.na



Permit No: 20 of 2007

PERMIT

Issued under Section 52(1) of the National Heritage Act (Act 27 of 2004).

Permission is hereby given to:

Name of applicant:
Ms Lache Rossouw

Address of Applicant
87 Fourth Avenue, Grassy Park, Cape Town, 7941 RSA

for:
Temporary export to Cape Town, South Africa

of:
of human remains for research purposes as part of her Masters Degree.

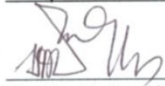
from:
Skeleton remains of 15 individuals are kept at National Museum of Namibia with an Accession Number: B 4108.

in accordance with
Permit application dated 23 July 2007


The following conditions apply to this permit:
(list any conditions that the Council may see fit to impose in terms of Section 52 (2) of the Act.

- a) An overall report must be submitted to the National Heritage Council of Namibia within 60 days of completion of the activities.
- b) Copies of all papers resulting from this work must be lodged with the National Heritage Council of Namibia.
- c) All human remains temporarily exported must be returned and deposited with the National Museum of Namibia in the same condition as taken.
- d) This permit does not exempt the applicant from any conditions that may be imposed by the Government of the Republic of South Africa, hosts or any other relevant authorities who have stake in this matter.

This permit will be valid from 13th August 2007 **to** 15th August 2008



Director: National Heritage Council



Permit 20 of 2007 Miss Lache' Rossouw

APPENDIX 2

Definitions of Biometric Landmarks on the Skull

As defined by De Villiers, 1968; and Buikstra and Ubelaker, 1994

ALARE (**al**): the most lateral points on the nasal aperture in a transverse plane.

ALVEOLON (**alv**): the point on the hard palate where a line drawn through the most posterior points of the alveolar ridges crosses the midline.

AURICULARE (**au**): defined as the point on the lateral aspect of the root of the zygomatic process at the deepest incurvature.

BASION (**ba**): the midpoint on the anterior margin of the foramen magnum.

BREGMA (**b**): the ectocranial midline point where the coronal and sagittal sutures intersect.

CONDYLION LATERALE (**cdl**): the most lateral point on the mandibular condyle

DACRYON (**d**): the point where the lacrimo-maxillary suture and the frontal bone intersect.

ECTOCONCHION (**ec**): the intersection of the most anterior surface of the lateral border of the orbit and a line bisecting the orbit along its long axis.

ECTOMALARE (**ecm**): the most lateral point on the outer surface of the alveolar borders of the maxilla.

EURYON (**eu**): the points on opposite sides of the skull that forms the termini of the line of the greatest cranial breadth.

FRONTOMALARE TEMPORALE (**fmt**): the most laterally projecting point on the fronto-zygomatic suture.

FRONTOTEMPORALE (**ft**): most medial point on temporal line of the frontal bone.

GLABELLA (**g**): the most prominent point between the superciliary arches in the median sagittal plane.

GNATHION (**gn**): the most inferior midline point on the mandible.

GONION (**go**): the most lateral external point on the junction between the

mandible body and the ascending ramus; gonial flare.

INFRADENTALE (id): the midline point at the superior tip of the septum between the mandibular central incisors.

LAMBDA (l): the ectocranial midline point where the sagittal and lambdoidal sutures intersect.

NASION (n): the point of intersection between the frontonasal suture and the midsagittal plane.

NASOSPINALE (ns): the point where a line drawn between the inferior most points of the piriform aperture crosses the midsagittal plane.

OPISTHION (o): the midline point at the posterior margin of the foramen magnum.

OPISTHOCRANION (op): the most posterior point of the skull not located on the occipital protuberance.

PROSTHION (pr): the anterior most point in the midline on the alveolar processes of the maxillae.

ZYGION (zy): the most lateral point on the zygomatic arch.

APPENDIX 3

Cranial measurements used for Principal Component Analysis:

Vault Measurements (16)	Face Measurements (18)	Mandibular Measurements (14)
Maximum Length of vault	Nasion-Basion Length	Maximum Breadth of Mandible
Maximum Breadth of vault	Prosthion-Basion Length	Bi-Coronoidal Breadth
Basibregmatic Height	Bi-Zygomatic Breadth	Bi-Gonial Breadth
Bi-Stephanic Breadth	Upper Facial Height	Bi-Mental Breadth
Bi-Asterion Breadth	Inner Bi-orbital Breadth	Condyle Length
Frontal Sagittal Arc	Outer Bi-orbital Breadth	Condyle Breadth
Parietal Sagittal Arc	Bi-Dacryon Breadth	Minimum Width of Ramus
Occipital Sagittal Arc	Orbital Breadth	Symphyseal Height
Transverse Arc	Orbital Height	Corpus Height at M2
Frontal Sagittal Chord	Nasal Breadth	Corpus Width at M2
Parietal Sagittal Chord	Nasal Height	Maximum Length of Mandible
Occipital Sagittal Chord	Least Nasal Breadth	Projected Height of Ramus
Foramen Magnum Length	Maximum Alveolar Length	Projected Height of Coronoid
Foramen Magnum Breadth	Maximum Alveolar Breadth	Mandibular Angle
Mastoid Height	Palatal Length	
Least Frontal Breadth	Palatal Breadth	
	Bi-Maxillary Breadth	

APPENDIX 4

Cranial measurements for the Khoraxa-ams sample:

	UCT1A	UCT1B	UCT1C	UCT1D	UCT1E	UCT1F	UCT1G	UCT1H	UCT1I	UCT1J	UCT1K	UCT1L
	H1:4,43	H1:7	H1:10	H1:5	H1:9	H1:8,15	H1:28,12,62	H1:2	H1:1,60	H1:44,63	H1:6	H1:3
Sex*	M	U	M	M	F	M	F	M	F	M	F	M
Age	40+	15.1-20	40+	40+	20.1-40	20.1-40	20.1-40	40+	40+	45+	40+	40+
Vault:												
Max Cranial Length	220.0	168.2	180.5	184.5	182.5	187.0	176.0	192.0	185.0	0	181.0	191.0
Max Cranial Breadth	132.0	119.5	139.5	132.2	122.0	126.0	115.0	134.0	122.2	0	132.0	126.0
Basi-Bregmatic Height	130.0	124.2	134.6	138.0	127.5	134.0	0	139.0	128.1	0	130.5	136.5
Bi-Stephanic Breadth	108.0	105.0	112.1	115.1	96.0	0	95.0	105.0	102.2	0	110.0	98.5
Bi-Asterionic Breadth	122.5	100.0	123.8	113.0	102.0	112.0	0	110.0	109.3	102.5	98.2	116.5
Bi-Mastoid Breadth	130.5	107.0	118.5	121.3	113.0	108.0	0	130.0	108.5	123.0	117.0	0
Bi-Temporal Breadth	125.5	106.0	126.5	121.0	111.0	112.0	0	107.5	113.5	0	116.5	112.0
Frontal Sagittal Arc	130.0	120.0	136.0	128.0	125.0	0	127.0	140.0	127.0	0	128.0	129.0
Frontal Sagittal Chord	113.0	101.5	114.8	110.5	109.0	0	109.0	124.0	111.5	0	113.5	110.0
Parietal Sagittal Arc	140.0	116.0	119.0	155.0	126.0	140.0	130.0	121.0	134.0	0	128.0	140.0
Parietal Sagittal Chord	127.4	107.5	117.0	135.1	113.0	124.0	116.5	110.0	120.0	0	119.0	126.0
Occipital Sagittal Arc	0	112.0	126.0	105.0	120.0	121.0	0	122.0	116.0	108.0	120.0	120.0
Occipital Sagittal Chord	105.5	97.5	103.0	94.5	100.0	100.0	0	100.0	96.0	94.0	98.0	100.2
Transverse Arc	295.0	270.0	306.0	305.0	298.0	305.0	0	306.0	286.0	0	290.0	302.0
Foramen Magnum Length	0	33.9	34.7	38.8	36.0	34.5	37.0	37.2	35.9	34.5	36.3	0
Foramen Magnum Breadth	0	28.2	29.5	27.6	28.5	25.0	26.0	29.0	26.2	31.0	26.9	0
Mastoid Height	30.0	24.2	29.5	27.6	28.5	25.0	26.0	29.0	26.2	31.0	26.9	0
Least Frontal Breadth	99.8	90.8	96.8	99.0	95.0	0	92.8	100.0	94.1	0	102.0	97.0
Nasion-Prosthion Height	80.5	54.0	70.0	67.9	67.5	0	60.5	0	63.4	0	73.2	0
Face:												
Bi-Frontal Breadth	107.5	95.0	110.8	109.2	96.8	0	98.8	0	96.2	0	105.0	106.0
Bi-Zygomatic Breadth	119.8	105.0	138.0	0	121.0	0	123.0	0	0	0	126.0	0
Bi-Maxillary Breadth	110.5	87.3	96.0	0	93.2	0	103.8	0	0	0	101.4	105.0
Bi-Auricular Breadth	123.0	102.9	121.0	115.5	112.0	111.5	0	124.0	112.1	0	115.0	111.2
Upper Facial Height	77.1	53.1	69.3	66.1	65.0	0	55.5	0	0	0	69.3	69.5

	UCT1A	UCT1B	UCT1C	UCT1D	UCT1E	UCT1F	UCT1G	UCT1H	UCT1I	UCT1J	UCT1K	UCT1L
--	-------	-------	-------	-------	-------	-------	-------	-------	-------	-------	-------	-------

	H1:4,43	H1:7	H1:10	H1:5	H1:9	H1:8,15	H1:28,12,62	H1:2	H1:1,60	H1:44,63	H1:6	H1:3
Sex*	M	U	M	M	F	M	F	M	F	M	F	M
Age	40+	15.1-20	40+	40+	20.1-40	20.1-40	20.1-40	40+	40+	45+	40+	40+
Upper Facial Breadth	0	97.9	112.2	108.2	0	0	0	0	104.1	0	112.1	0
Least Frontal Breadth	99.8	90.8	96.5	98.6	94.4	0	93.0	99.9	94.9	0	101.3	0
4Nasion-Basion Length	107.0	94.0	94.8	100.6	99.0	0	0	106.0	95.5	0	100.0	0
Prosthion-Basion Length	109.0	89.0	94.0	91.8	99.0	0	0	0	0	105.0	102.0	0
Inner Bi-Orbital Breadth	108.0	90.0	98.5	103.0	96.0	0	97.4	0	95.6	0	103.9	104.5
Outer Bi-Orbital Length	116.0	96.7	112.2	0	103.1	0	104.0	0	104.3	0	112.0	113.0
Bi-Dacryon Breadth	30.0	20.1	28.2	27.4	27.0	0	26.2	0	24.8	0	23.9	28.3
Maxillofrontale Breadth	16.1	8.9	14.0	21.3	17.5	0	11.4	14.2	15.4	0	13.6	16.0
Orbital Breadth	38.5	36.3	35.8	37.0	35.0	0	36.0	0	35.1	0	46.5	40.8
Orbital Height	36.0	31.8	34.3	35.4	35.5	0	33.0	0	33.7	0	33.4	40.5
Nasal Height	59.0	40.7	49.0	52.2	49.1	0	49.2	0	0	0	49.6	52.0
Nasal Breadth	30.2	22.1	25.9	27.3	24.0	0	29.0	0	0	23.9	28.1	29.9
Least Nasal Breadth	17.0	16.0	16.4	19.9	16.9	0	11.1	0	0	0	15.2	12.0
Maxillo-Alveolar Length	58.0	40.9	49.0	48.5	50.1	0	0	0	0	63.2	56.4	0
Maxillo-Alveolar Breadth	71.5	59.0	65.0	62.1	56.5	0	61.9	0	0	64.1	64.1	64.5
Palatal Length	41.6	34.9	45.0	44.2	28.0	0	28.7	0	0	37.8	48.5	0
Palatal Breadth	43.2	30.8	35.8	41.2	36.1	0	39.3	0	0	39.1	38.1	47.3
Mandible:												
Maximum Breadth	115.0	100.8	123.5	113.4	105.0	0	0	0	0	0	0	0
Bi-Coronoidal Breadth	97.8	81.5	99.2	95.0	83.0	0	0	0	0	0	0	0
Bi-Gonial Breadth	96.2	81.5	102.2	91.5	77.0	0	0	83.5	0	0	0	0
Bi-Mental Breadth	48.8	43.0	43.6	48.0	42.6	0	0	0	0	0	0	0
Projective Height Ramus	69.0	45.5	72.1	54.1	56.4	0	0	0	0	0	0	0
Projective Height Coronoid	70.8	47.9	71.5	61.0	55.9	0	0	0	0	0	0	0
Projective Length Mandible	86.0	69.0	88.0	76.1	81.0	0	0	0	0	0	0	0
Condyle Length	23.2	15.3	25.8	21.1	19.9	0	0	0	0	0	0	0
Condyle Breadth	11.9	7.8	16.2	9.0	10.2	0	0	0	0	0	0	0
Minimum Width Ramus	40.6	34.8	43.8	34.6	39.4	0	0	0	0	0	41.8	0
Symphyseal Height	36.5	25.4	29.8	33.8	29.5	0	0	0	0	0	0	0
Corpus Height M2	34.1	20.1	30.3	26.9	27.6	0	0	0	0	0	0	0
Corpus Width M2	14.1	15.0	12.9	12.8	12.8	0	0	0	0	0	0	0
Mandibular Angle	101 ^o	124 ^o	104 ^o	126 ^o	115 ^o	0	0	0	0	0	0	0

*M = Males; F = Females; U = Indeterminate Sex

University Of Cape Town